INFORMATION TO USERS

This material was produced from a microfilm copy of the original document. While the most advanced technological means to photograph and reproduce this document have been used, the quality is heavily dependent upon the quality of the original submitted.

The following explanation of techniques is provided to help you understand markings or patterns which may appear on this reproduction.

1. The sign or "target" for pages apparently lacking from the document photographed is "Missing Page(s)". If it was possible to obtain the missing page(s) or section, they are spliced into the film along with adjacent pages. This may have necessitated cutting thru an image and duplicating adjacent pages to insure you complete continuity.

2. When an image on the film is obliterated with a large round black mark, it is an indication that the photographer suspected that the copy may have moved during exposure and thus cause a blurred image. You will find a good image of the page in the adjacent frame.

3. When a map, drawing or chart, etc., was part of the material being photographed the photographer followed a definite method in "sectioning" the material. It is customary to begin photoing at the upper left hand corner of a large sheet and to continue photoing from left to right in equal sections with a small overlap. If necessary, sectioning is continued again — beginning below the first row and continuing on until complete.

4. The majority of users indicate that the textual content is of greatest value, however, a somewhat higher quality reproduction could be made from "photographs" if essential to the understanding of the dissertation. Silver prints of "photographs" may be ordered at additional charge by writing the Order Department, giving the catalog number, title, author and specific pages you wish reproduced.

5. PLEASE NOTE: Some pages may have indistinct print. Filmed as received.

Xerox University Microfilms
300 North Zeeb Road
Ann Arbor, Michigan 48106

THE UNIVERSITY OF OKLAHOMA

GRADUATE COLLEGE

SECULAR VARIATION OF THE INTENSITY OF THE GEOMAGNETIC FIELD DURING THE PAST 3,000 YEARS IN NORTH, CENTRAL, AND SOUTH AMERICA

A DISSERTATION

SUBMITTED TO THE GRADUATE FACULTY

in partial fulfillment of the requirement for the degree of

DOCTOR OF PHILOSOPHY

By

Sheng-shyong Lee

Norman, Oklahoma

1975

SECULAR VARIATION OF THE INTENSITY OF THE GEOMAGNETIC FIELD DURING THE PAST 3,000 YEARS IN NORTH, CENTRAL, AND SOUTH AMERICA

APPROVED BY

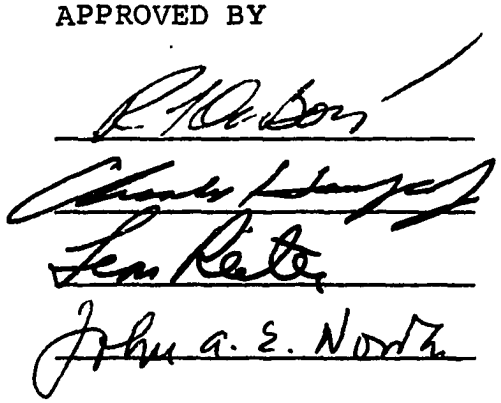

DISSERTATION COMMITTEE

DEDICATION

This work is dedicated to my parents, Mr. and Mrs. Ko-chau Lee, and to my wife, Fu-tze Lin Lee.

ACKNOWLEDGMENTS

The author wished to express his sincere appreciation to Dr. Robert L. DuBois for suggesting this topic and for providing invaluable help and encouragement. Dr. DuBois also provided the author with financial support from various National Science Foundation Research Grants. Some parts of this research are a continuation of some earlier works on archeomagnetic intensity done by my advisor.

The author is extremely grateful to Drs. Michael Fuller, Charles W.Harper, John A. Norden and Leon Reiter for reading the manuscript and providing many helpful suggestions. Thanks are due Mr. David Bradshaw for help in solving problems of instrumentation, and Mr. Chris Lintz for providing archeological information concerming the samples. The author also wishes to express his appreciation to Mr. Charles Lewis and Mr. Steve Wells for editing the dissertation.

The author wish to express his sincere appreciation to his wife, Fu-tze Lin, for providing much support and encouragement throughout this work and for typing the dissertation. The author also desire to thank his parents, Mr. and Mrs. Ko-chau Lee, and his in-laws, Dr. and Mrs. Chi Tsung Lin for their encouragement and for helping me an many different ways.

ABSTRACT

A total of 324 specimens from 100 samples of pottery and baked clays, associated with burnt rooms or hearths, collected from North, Central, and South America, have been used to investigate the intensity of the geomagnetic field during the past 3,000 years. In Thelliers' Stepwise Heating Method, the information on the changes of the orientation of the RNRM and the PTRM in each step help to identify the factors causing anomalous RNRM-PTRM curves, and also are an indication of the reliablity of the paleointensity data. Theoretical calculations, test experiments, and the actual measurements show that the results from Thelliers' Method are more reliable than those from other methods in archeomagnetic field intensity measurements. Statistical analysis suggests that the probability of obtaining a reliable result from a baked clay sample is about 1.6 times that from pottery or brick.

Maximum field intensity around 450 AD is indicated not only by the Central American data, but also by the data from South America. All of the archeomagnetic field intensity results for North, Central, and South America indicate that the intensities for 0 AD are nearly equal to the present intensities. The reliable archeomagnetic field intensity curve for Central America may be a new basis for an archeological chronology in this area

and perhaps developed, as well, for Southwest United States and South America.

TABLE OF CONTENTS

LIST OF TABLES

LIST OF FIGURES

Figure Page

SECULAR VARIATION OF THE INTENSITY OF THE GEOMAGNETIC FIELD DURING THE PAST 3,000 YEARS IN NORTH, CENTRAL, AND SOUTH AMERICA

CHAPTER I

INTRODUCTION

The earliest literature about the characteristics of the Earth's magnetic field is contained in Chinese historical writtings. King Hwang, about 2500 BC, used the south-seeking property of the magnet to tell direction when his army fought during an invasion from the North in a fog. Magnetic declination had been discovered by at least 1300 AD; and William Gilbert, approximately 1600 AD, was the first to have the idea that the magnetic field of the Earth could be approximated by that of a magnetic dipole (Gilbert, 1600).

Henry Gellibrand, an English professor, during 1634 AD noticed that magnetic declination changes with time (Gellibrand, 1935). He found that the magnetic declination in London had changed by 5^{o} in a 42-year period. Since then, continuous changes of declination have been measured in London. This time change in the geomagnetic field from one year to the next is known as

secular variation.

The magnetic field intensity had not been measured until 1804 AD when Alexander von Humboldt discovered an increase in the total magnetic field intensity from the equator to the poles. He measured the intensity of the field by observing the number of swings of a dip-needle in meridional planes for ten-minute periods in four northern hemisphere zones and in one southern hemisphere zone. The results of these measurements were expressed in relation to a standard station at Micuipampa in Peru on the magnetic equator where the intensity was arbitrarily taken as unity.

Later Gauss modified the method, using an auxiliary magnet of known moment, to determine an absolute value for horizontal field intensity H (Gauss, 1838). The base unit value used by Alexander von Humboldt was estimated to be equal to 34940 r (gamma) or 0.3494 oersted(or gauss) by Gauss. In addition to H, the declination was determined by astronomical observations using a compass, and the inclination, by a dipping needle, therefore, defining the complete vector field. Later, a number of magnetometers were developed using electric circuits and galvanometers or a magnetron tube as detectors. The fluxgate magnetometer, a more modern instrument, is useful for measuring time changes in the field with short periods.

Since the time of von Humboldt, changes in field intensity, declination, and inclination, have been measured at a few locations. Since the early part of this

century many efforts have been made to expand our knowledge of the magnetic field over the ocean and unexplored regions of the world in order to obtain a more precise description of the Earth's magnetic field and its secular variation. Recently, world maps plotting different magnetic elements, and their secular variation, have been published for the epochs 1955, 1965 and 1970 by the U.S. Naval Oceanographic Office.

Most of our knowledge about the geomagnetic field is derived from direct recordings at magnetic observatories. However, magnetic field records have only been made for the past 400 years; the earlier measurements were neither complete nor accurate. Fortunately, the information about the geomagnetic field, even back into the geological past, is accessible to geophysical investigation because the geomagnetic field leaves behind a trace of its history in the form of a remanent magnetization in rocks, pottery, or baked clays. Such investigations have been directed towards measuring the direction and intensity of the Natural Remanent Magnetization (NRM) of rocks or other materials, to indicate the intensity and direction of the geomagnetic field at the time when the materials were formed. We apply the term "Paleomagnetism" as a general term and usually relate it to investigations of geological materials of ancient age. When the work is concerned with variations of the geomagnetic field during historical and recent prehistorical time, using archeologically-related mate-

rials, the term "Archeomagnetism" is used. Archeomagnetic results to be useful must be of high precision. This study concerns the variation in archeomagnetic field intensity during the past 3,000 years in North, Central, and South America.

Since the introduction of the Stepwise Heating Method as proposed by E. Thellier and O. Thellier (Thellier and Thellier,1959), the secular variation of the total geomagnetic field has been studied by several authors. Burlatskaya and Rusakov have published results of samples from Russia(Burlatskaya, etc.,1969; Rusakov, etc., 1973). Nagata, DuBois, Kitazawa, and Bucha have published data on geomagnetic secular variation in America(Nagata, etc., 1962; DuBois, etc., 1965; Kitazawa, etc., 1968; Bucha, 1970). Nagata, Sasajima, and Kitazawa have published data from Japan(Nagata, etc., 1963; Sasajima, etc., 1966; Kitazawa, 1970) for this same subject. Thellier and Thellier, Bucha, and Kavacheva have published results from European materials(Thellier and Thellier, 1959; Bucha, 1967; Kovacheva, 1972). The data available from all these various sources are not generally in agreement. In many cases a single measurement of ancient field intensity was made for each sample instead of multiple determinations. A mean value could not be obtained in these cases not a statistical analysis made. Whereas some of the samples tested are well dated, many are not.

Wilson used the different heating method to measure the paleointensity from bakes laterites(Wilson,

1961). van Zijl used the Alternating Field Demagnetization Method to measure the paleointensity from the Stormberg lavas (van Zijl, 1962).

Recently Banerjee and Mellema proposed a new anhysteretic Remanent Magnetization (ARM) method for paleointensity determination and used it to measure lunar samples (Banerjee, etc., 1974a; Banerjee, etc., 1974b). Stephenson and Collinson used another ARM method to measure the paleointensity of several Apollo 11 and Apollo 16 samples (Stephenson, etc., 1974). These two methods can only be applied to lunar samples and are not useful for archeomagnetic studies. The reliability of the results from these methods does not seem to be as good as that from Thelliers' method. Their main advantage is that they avoid chemical changes due to heating.

Shaw used a new method to determine the paleointensity from five historic lavas and five archeological samples (Shaw, 1974). The method he used is similar to the Alternating Field (AF) Method, except a comparison of two ARMs created before and after heating can help select a temperature range within which the heating has not changed the magnetic properties of the sample.

In order to compare the results from Thelliers' Stepwise Heating Method with the other methods; i.e. the Alternating Field (AF) Demagnetization Method and Wilson's Heating Method, a few specimens were processed by all three methods. The results of the comparison suggest that Thelliers' Stepwise Heating Method is pro-

bably more reliable in archeomagnetic field intensity measurements*.

For the purpose of making sure that the method and apparatus used to measure the archeomagnetic field intensity are applicable do not introduce errors, a test experiment using artificial fields has been conducted by Thelliers' Method in the laboratory. The deviations among the actual magnetic field intensities and the measured field intensities from eight baked clay specimens range from 0.07 percent to 2.76 percent, and the deviation in one pottery specimen is 5.77 percent.

The remaining natural remanent magnetization - partial thermoremanent magnetization (RNRM-PTRM) curves of some of the specimens can be used to suggest ratios between ancient field intensities and artificial intensities where they approximate a straight line and the orientations of the NRM and the PTRM in each step are constant. A least squares method is used to calculate the slopes of the curves. The RNRM-PTRM curves for some specimens are anomalous, and these materials cannot be used to estimate ancient intensity values. Theoretical calculations and test experiments for the specimen which had been either reheated or struck by lightning, and the information on the change of the orientation of the

* Samples were not measured by Shaw's ARM Method, since this method is comparable to the AF Demagnetization Method.

RNRM and PTRM in each heating step, help to distinguish what types of factors caused the anomalous RNRM-PTRM curves. A new modified method for the determination of paleointensity from baked clays or pottery is used to minimize deviations in orientation and temperature.

A secular variation curve of the intensity of the geomagnetic field in Central America during the past 2,300 years was obtained from this study. Fourier Analysis revealed the dominant periods of variation of magnetic field intensities. The archeomagnetic field intensity data for North and South America are compared to the Central America curve.

CHAPTER II

DETERMINATION OF THE INTENSITY OF THE ANCIENT GEOMAGNETIC FIELD

A. THEORY

Magnetic Properties of the Samples

Almost all of the samples used in archeomagnetic field intensity studies are pottery and baked clays. The minerals which are the bearers of the magnetization occur as ferromagnetic grains, dispersed in a practically non-magnetic medium (Thellier and Thellier, 1959).

The predominant ferromagnetic mineral contained in the pottery from Mexico, Peru, and Bolivia are probably iron oxides of a spinel phase (such as magnetite or maghemite with some amount of titanium), since the samples show high saturation magnetization values (Nagata, 1962). Also, the ferromagnetic minerals contained in the Bolivian pottery are magnetite or maghemite with some impurities determined on the basis of a cubic spinel structure with the lattice constant a=8.32 A (Kitazawa, 1968). The same ferromagnetic minerals are also found in pottery from eastern Japan (Kitazawa, 1970).

Because the Curie temperatures of most of the samples in this study are from 500°C to 700°C and the blocking temperatures are from 100 °C to T_c (which will be shown in the following sections), this indicates that

the ferromagnetic minerals in our samples are mainly hematite and magnetite.

In order to determine the stablity of samples against heat treatment in air, the different authors (Nagata, 1952; Kitazawa, 1967) have used a quartzspring magnetic balance to measure the temperature variation of saturation magnetization of the pottery. They found that almost all of them are reversible during the heating-cooling cycle between room temperature (approximately 20°C) and 600°C, and the maximum deviation is approximately 20 percent.

Natural Remanent Magnetization and Thermoremanent Magnetization

All the measurable residual magnetization possessed by rocks, baked clays or pottery in situ have been called natural remanent magnetization or simply NRM (Nagata, 1961). From this definition, the NRM includes not only the magnetization which was impossed when the sample was formed but also the remanent magnetization of the sample caused by lightning or by other means after the sample was formed: the former is the original magnetization or primary magnetization and the latter is the secondary magnetization.

The thermoremanent magnetization (TRM) of a sample is defined as the remanent magnetization acquired by a sample which, after being heated to a temperature in excess of or equal to the highest Curie temperature T_c of the constituents of this sample, has been cooled to room temperature in a constant field. The partial thermoremanent magnetization (PTRM) is a remanent magnetization

which develops in a magnetic field which is applied only within the temperature range T_1 to T_2 ($T_2 < T_1 \leq T_c$), some portions of the cooling process can take place in a zero field in particular experiments.

The important relation, called the Addition Law of PTRM, was introduced by E. Thellier in 1938 and relates that the sum of the PTRMs from temperature T_i to temperature T_f is equal to the PTRM from T_i to T_f or

$$J^{T_i}_{T_{i+1}, H_{ex}}(T_o) + J^{T_{i+1}}_{T_{i+2}, H_{ex}}(T_o) + \ldots + J^{T_{f-1}}_{T_f, H_{ex}}(T_o) = J^{T_i}_{T_f, H_{ex}}(T_o) \qquad (2\text{-}1)$$

where $J^{T_i}_{T_{i+1}, H_{ex}}(T_o)$ is the PTRM acquired by cooling from temperature T_i to temperature T_{i+1} in an external magnetic field H_{ex} measured at room temperature T_o. T_i and T_f are temperatures within the range from room temperature T_o to the Curie temperature T_c.

The other important fact is that the PTRM $J^{T_1}_{T_2, H_{ex}}(T_o)$ is almost reversible with respect to temperature. This means that if the sample does not have any mineralogical change, then the PTRM $J^{T_1}_{T_2, H_{ex}}(T_o)$, which is the remanent magnetization acquired by the sample when the temperature decreases from T_1 to T_2 in a magnetic field H_{ex}, is equal to the amount of the remanent magnetization lost when the temperature decreases from T_1 to

T_2 in zero magnetic field.

The samples used in this study are baked clays and pottery which had been fired in ancient times at temperatures above their T_c ; thus, the original magnetization of these samples is TRM.

Secondary Magnetization

All of the samples used in this study are baked clays and pottery which were collected from various archeological sites. Because of the age of the samples, the effects from reheating, weathering, thermal cycling, and lightning, etc. cannot be neglected. The following types of remanent magnetizations are possibly secondary magnetizations of the samples:

(1) Viscous Remanent Magnetization (VRM) is the remanent magnetization acquired by a sample when the application of H_{ex} is of long duration and in different direction from that existing during the original cooling. Baked clays and pottery, having been in the geomagnetic field for hundreds of years, may have acquired some of this type of magnetization.

(2) Isothermal Remanent Magnetization (IRM) is the remanent magnetization produced in a sample by an applied field H_{ex} which decreases from some field intensity H_a to the intensity of the earth's field at constant temperature. The IRM of the sample of these experiment is probably due to lightning which will be discussed in more detail later*.

(3) Thermoremanent Magnetization (TRM) is the remanent magnetization acquired in cooling from T_c to T_o in

* see page 77.

the presence of an external magnetic field. The possibility of pottery having been reheated after its original firing is high. If the reheating temperature T_r is higher than the Curie temperature of the pottery, then a new TRM will completely replace the original NRM, whereas, if T_r is lower than the Curie temperature of the pottery than a PTRM will be superimposed on the NRM, which has been thermally demagnetized up to temperature T_r.

(4) Chemical Remanent Magnetization (CRM) is the remanent magnetization produced at a temperature below the Curie temperature when the ferromagnetic substance is chemical formed or has crystallized in the presence of a magnetic field. The sample may gain CRM by undergoing surface weathering involving oxidation or other chemical changes of the ferromagnetic substances in the Earth's magnetic field. During laboratory experiments, the sample may gain CRM due to chemical reactions caused by heating, in a non-original atmosphere.

(5) Anhysteretic Remanent Magnetization (ARM) is the remanent magnetization induced in a sample by the application of a small direct field on which is superimposed a much larger alternating magnetic field, with the amplitude of the field diminishing gradually with time. A few investigators suggested that the probable cause of the occurrence of ARM in nature is that the sample has been struck by lightning. Since lightning is considered to be an alternating current, the action of the geomagnetic field and the alternating field produced by lightning may magnetize the sample (Nagata,1961). This will be discussed later*.

* see page 79

The effects of secondary magnetization on the measurement of the ancient field intensity is the main problem in the development of field intensity studies.

Basis of Field Intensity Determination

The intensity of the thermal remanent magnetization induced in a specimen, by cooling it through its Curie point in a magnetic field H_{ex}, is proportional to the external magnetic field H_{ex}, provided that H_{ex} is smaller than one and one half oersted (Nagata, 1943); i.e.,

$$J_{T_o}^{T_c}, H_{ex}(T_o) \propto H_{ex} . \qquad (2\text{-}2)$$

Fig. 1 shows this relation for two igneous rocks. Assuming J_n, the natural remanent magnetization acquired by the specimen in an ancient field F, is TRM, and J_t is the artificial TRM acquired by the same specimen in a known magnetic field H, and since all the field intensity results published so far indicate that the Earth's field have been less than one oersted or so, then

$$\frac{F}{H} = \frac{J_n}{J_t} \qquad (2\text{-}3)$$

and the ancient field intensity F can be calculated from the above equation.

Thelliers' Stepwise Heating Method

Thermoremanent magnetization of a sample is given as $J_{T_2}^{T_1}, H_{ex}(T_o) = {}_{\Delta}J_T$, where T_1 and T_2 denote the temperatures at the beginning and end of the application of

a field H_{ex} on the sample during its cooling process, and T_o is room temperature. When the natural remanent magnetization of the sample is stable thermoremanent magnetization, then the intensity of the remanent magnetization is given as:

$$\Delta J_n = F \cdot K(T_1 , T_2 ; T_o) \qquad (2\text{-}4)$$

where F is the ancient magnetic field intensity in which the sample cooled and $K(T_1 , T_2 ; T_o)$ is a function of the temperature and also the magnetic properties of the sample and is independent of the field intensity F, if F is less than one oersted. It has been mentioned above that the partial thermoremanent magnetization is reversible with respect to temperature provided the magnetic properties of the sample do not change. The PTRM of the sample acquired when it cooled from T_1 to T_2 in an artificial magnetic field F' is:

$$\Delta J_T = F' \cdot K(T_1 , T_2 ; T_o), \qquad (2\text{-}5)$$

from equations (2-4) and (2-5), and the ancient field intensity F can be calculated if ΔJ_n , ΔJ_T , and F' are known. That is,

$$F = F' \cdot \frac{\Delta J_n}{\Delta J_T} \qquad (2\text{-}6)$$

The Thelliers have proposed a stepwise comparison, based on the Law of Addition of PTRM, between the loss of the natural remanent magnetization and the acquisition of the partial thermoremanent magnetization in the same sample (Thellier and Thellier, 1959).

A modified Thelliers' Stepwise Heating Method has been used in this study. The natural remanent magnetization was measured at room temperature T_o ; then the sample was put inside a non-magnetic oven in an artificial field F', heated to temperature T_i, and cooled to T_o. The remanent magnetization of the sample measured at T_o, $\vec{J}(T_i)$ is the vector sum of the residual natural remanent magnetization $\vec{J}_n(T_i)$ after the sample has been thermally demagnetized to temperature T_i and $_{\Delta}\vec{J}_T(T_i)$ is the PTRM acquired by the sample upon cooling from T_i to T_o in a magnetic field F'. The same heat treatment is repeated after rotating the sample 180 degrees. As shown in Fig. 2, the remaining natural remanent magnetization (RNRM), $\vec{J}_n(T_i)$, and the partial thermoremanent magnetization (PTRM), $_{\Delta}\vec{J}_T(T_i)$, can be calculated from the following two equations:

$$\vec{J}_N(T_i) = \tfrac{1}{2}(\vec{J}(T_i) + \vec{J}'(T_i))$$

$$_{\Delta}\vec{J}_T(T_i) = \tfrac{1}{2}(\vec{J}(T_i) - \vec{J}'(T_i)) \qquad (2\text{-}7)$$

where $\vec{J}(T_i)$ and $\vec{J}'(T_i)$ are the measurable remanent magnetization after the two heatings.

The same procedure was then repeated by increasing the temperature stepwise from T_1, T_2, $\cdots$, T_f, and cooling to T_o in each step. T_f is a temperature higher than the Curie temperature of the sample. From equations (2-1) and (2-5), the loss of NRM and the acquisition of PTRM in each temperature interval can be expressed as :

$$\begin{cases} J_N(T_o) - J_N(T_1) = F \cdot K(T_1, T_o; T_o) \\ {}_{\Delta}J_T(T_1) = F' \cdot K(T_1, T_o; T_o) \end{cases}$$

$$\left.\begin{aligned} J_N(T_1) - J_N(T_2) &= F \cdot K(T_2, T_1; T_o) \\ {}_{\Delta}J_T(T_2) - {}_{\Delta}J_T(T_1) &= F' \cdot K(T_2, T_1; T_o) \end{aligned}\right\} \quad \ldots$$

$$\left.\begin{aligned} J_N(T_{f-1}) - J_N(T_f) &= F \cdot K(T_f, T_{f-1}; T_o) \\ {}_{\Delta}J_T(T_f) - {}_{\Delta}J_T(T_{f-1}) &= F' \cdot K(T_f, T_{f-1}; T_o) \end{aligned}\right\} \quad (2\text{-}8)$$

Then the ancient field intensity F can be calculated from the slope of the line in $J_N(T_i) - {}_{\Delta}J_T(T_i)$ diagram as shown in Fig. 3

$$\frac{J_N(T_o) - J_N(T_1)}{{}_{\Delta}J_T(T_1)} = \frac{J_N(T_1) - J_N(T_2)}{{}_{\Delta}J_T(T_2) - {}_{\Delta}J_T(T_1)} =$$

$$\ldots = \frac{J_N(T_{f-1}) - J_N(T_f)}{{}_{\Delta}J_T(T_f) - {}_{\Delta}J_T(T_{f-1})} = \frac{F}{F'} = \left|\text{slope of line}\right| . \quad (2\text{-}9)$$

Alternating Field Demagnetization Method

Owing to the fact that some of the samples from the Stormberg lavas have abnormally high NRMs which may consist of IRMs acquired from lightning or VRMs by exposure for a long period of time in the Earth's magnetic field, van Zijl used the AF Demagnetization Method to measure the paleointensity. This method involves applying an alternating magnetic field which decreases gradually from a certain peak field magnitude to zero by decreasing the current of the field coil for both the NRM and TRM of

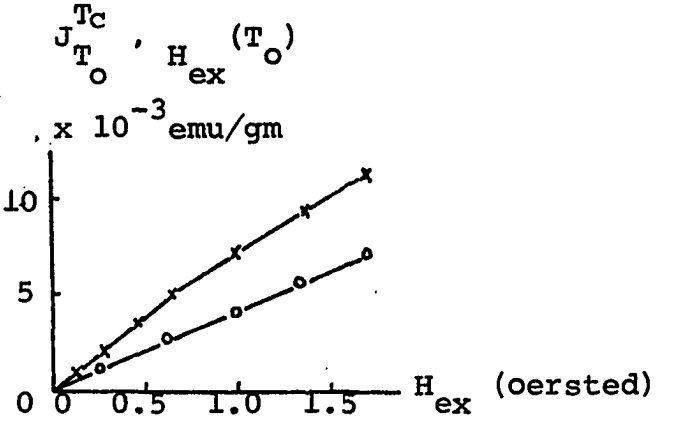

Fig. 1 Examples of field dependence of total TRM of two igneous rocks in a weak field range. Redrawn from Nagata (1961).

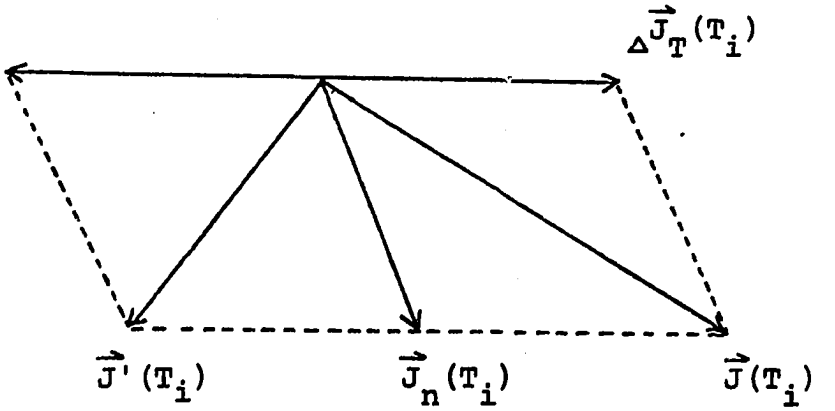

Fig. 2 Relation between RNRM $\vec{J}_n(T_i)$ and PTRM $\Delta\vec{J}_T(T_i)$ after double heating.

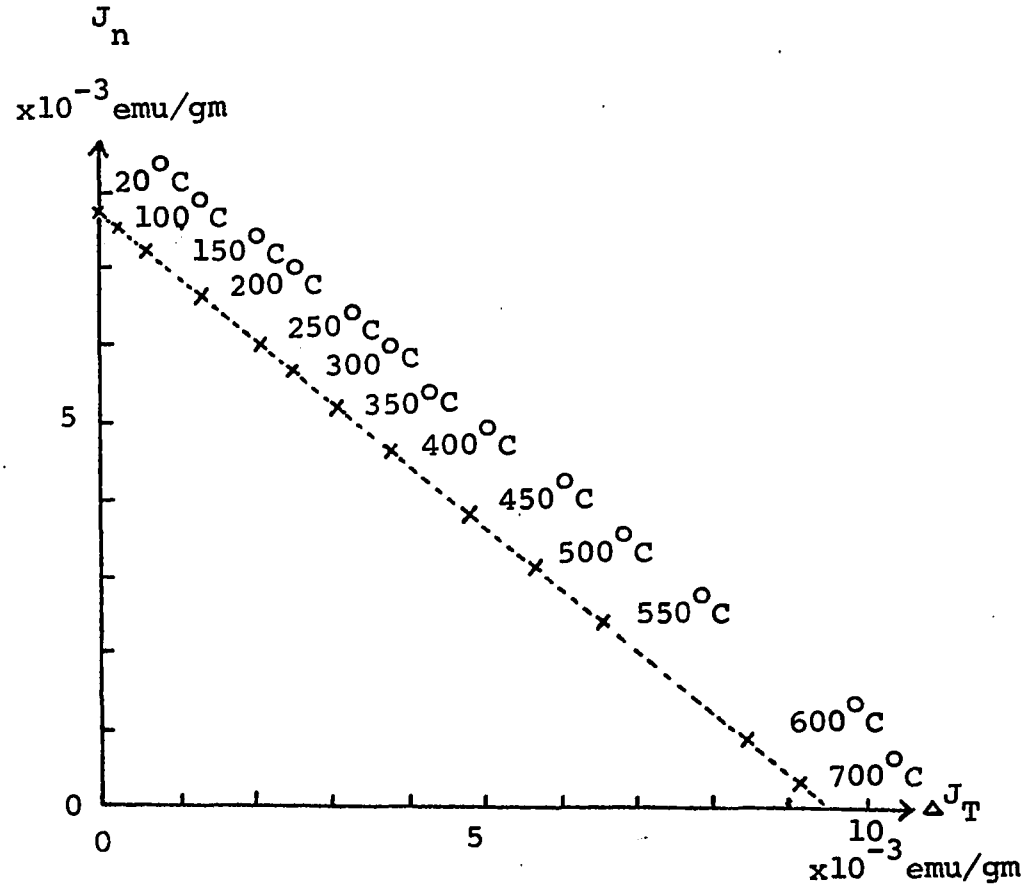

Fig. 3 RNRM J_n - PTRM ΔJ_T diagram.

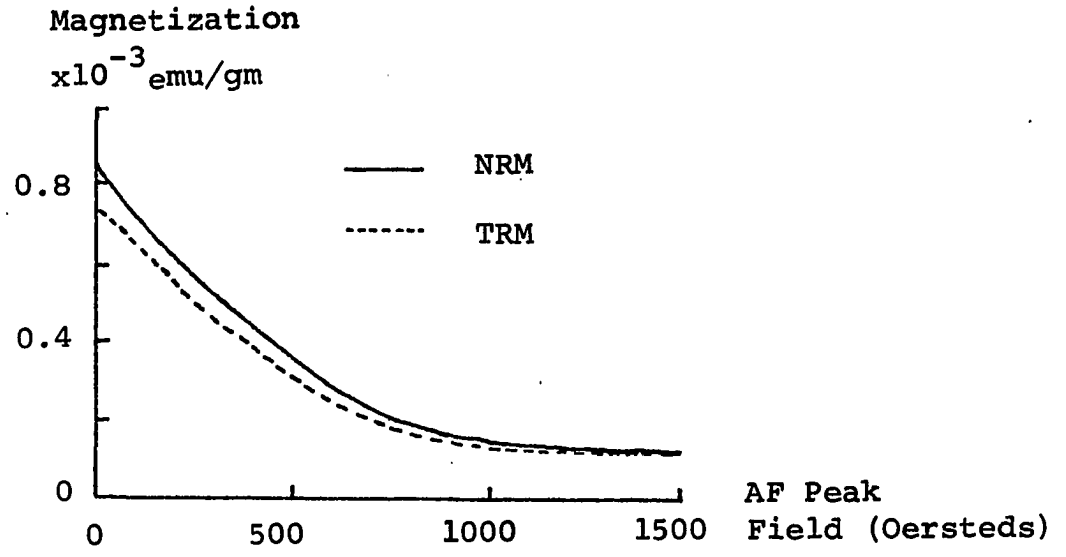

(a)

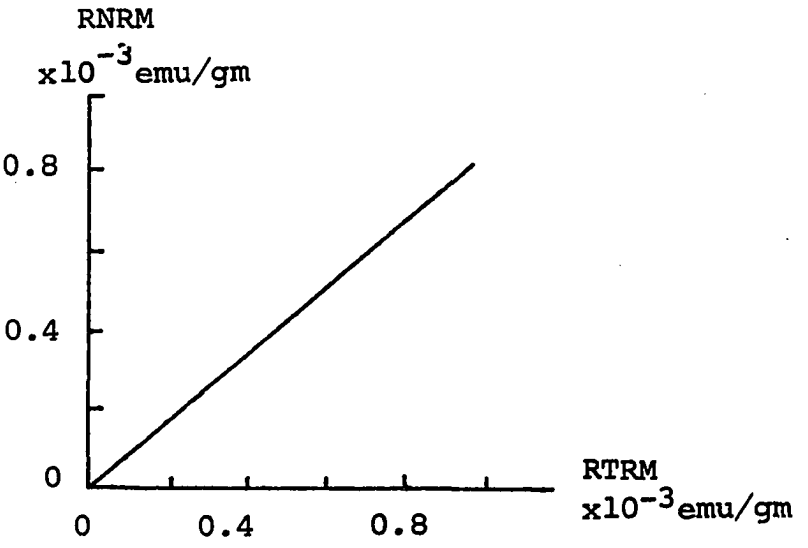

(b)

Fig. 4 (a) AF demagnetization curves of NRM and TRM.
(b) RNRM-RTRM curve

each sample (van Zijl, 1962). Instead of the ratio of NRM/TRM, he calculated the ancient field intensity from the ratio of $(NRM/TRM)_{219\ oe}$, which is the ratio of remaining natural remanent magnetization to remaining thermoremanent magnetization (RNRM/RTRM) after 219 oersteds AF demagnetization. This method was employed since IRM and VRM are very unstable to AF demagnetization. They are almost completely eliminated when the peak field is 219 oersteds, whereas the TRM is very stable to AF demagnetization.

Theoretically, if the NRM of the sample is only original TRM, and also, the phase of the sample did not change since it formed, then the AF demagnetization curve of the NRM will be similar in shape to that of the TRM which is induced in a known magnetic field F'. This relation is shown in Fig. 4(a). If we plot the RNRM and RTRM values of each peak field in the RNRM-RTRM diagram, then all of the points fall in a straight line which passes through the origin, as shown in Fig. 4(b). The slope of the straight line will be equal to the ratio of the ancient field intensity F to the known magnetic field intensity F'.

Anhysteretic Remanent Magnetization Method

Banerjee and Mellema proposed a new " ARM Method" for paleointensity determination from the ARM properties of rocks, based on a modification of a thermodynamic theory of a grain interaction proposed by W. F. Jeap (Banerjee and Mellema, 1974). The new expression between ARM and TRM is:

$$\frac{P_{ARM}}{P_{TRM}} = \left(\frac{M_{sb}}{M_s}\right)^2 \left(\frac{T}{T_b}\right)^{\frac{1}{2}} \left(\frac{\lambda_b + KT_b/M_{sb}}{\lambda + KT/M_s}\right) \frac{H_d}{H} \qquad (2\text{-}10)$$

Here P_{TRM} and P_{ARM} are the values of the normalized TRM and ARM (normalized by dividing by saturation IRM), M_{sb} and M_s are the saturation magnetizations at blocking temperature T_b and room temperature T, respectively, λ is the interaction constant, K is Boltzmann's constant, H_d and H are the DC inducing fields for ARM and TRM, respectively. In a paleointensity experiment, H is the unknown parameter to be determind, Banerjee and Mellema used this method to measure the three Apollo 15 crystalline rocks (Banerjee and Mellema, 1974). Using the approximation that $KT_b/M_{sb} < \lambda$ and $KT_b/M_{sb} < \lambda_b$, both KT_b/M_{sb} will be negligible, and $\lambda = \lambda_b$, then equation (2-10) becomes:

$$H = \left(\frac{M_{sb}}{M_s}\right)^2 \left(\frac{T}{T_b}\right)^{\frac{1}{2}} \left(\frac{P_{TRM}}{P_{ARM}}\right) H_d \quad . \qquad (2\text{-}11)$$

The major advantage of this method is that the lunar sample must be heated only once to determine the blocking temperature of the sample. The values of equation (2-11) are measurable, so the paleointensity H can be determined. This method has the following two disadvantages: (1) making the approximation $\lambda_b = \lambda$ may produce an error of 15 percent in the deduced H, and (2) owing to the fact that KT/M_s is negligible, then the deduced H is only the upper limit of the actual ancient field intensity.

Stephenson and Collinson used the other ARM Method

to measure the paleointensity of several Apollo 11 and Apollo 16 samples (Stephenson and Collinson, 1974). The relation between the change of TRM and ARM with variation of the peak field H in AF demagnetization is :

$$\frac{1}{h_T}\frac{\partial(TRM)}{\partial H} = f'\frac{1}{h_A}\frac{\partial(ARM)}{\partial H} \quad , \qquad (2\text{-}12)$$

where h_T and h_A are the DC field values in which the TRM and ARM of the sample is acquired, f' is an average value of (M_s/M_{sb}) taken over the sample's blocking temperature distribution and is thus greater than unity. Values of f' have to be determined experimentally. Two samples have been measured for the value of f': 1.28 was obtained for an iron grain, and 1.40 for one of the lunar samples. an average value of 1.34 is used in paleointensity determinations of lunar samples. The main advantage of this method is that it can avoid chemical change due to heating. However, this method has two disadvantages. (1) In lunar rocks, since the remanence is carried only by the iron grains, the average value f'=1.34 used in lunar samples is still accurate probably only to a few ten percent, whereas in terrestrial rocks or archeomagnetic samples, a much greater variation in f' is to be expected because the Ferromagnetites responsible for the remanence have lower Curie points; therefore, this method is difficult to use in archeomagnetic field intensity studies. (2) The average value of f' has to be determined from heating, so it has the same disadvantage as the AF demagnetization method.

Recently, Shaw used a new method to determine the

paleomagnetic field intensity from five historic lavas and five archeological samples (Shaw, 1974). The method he used was almost exactly the same as the AF Demagnetization Method. By the comparison of two ARMs (the same DC induced field) created before and after heating, this method can select a coercive force region within which the heating has not changed the magnetic properties of the sample. Then the AF Demagnetization Method can be used to calculate the paleointensity from the points in the region where there are no changes in magnetic properties. The results of this study show that some samples may have variation in magnetic properties from one specimen to another. Using two specimens (one for the comparison of the two ARMs and the other for calculation of the ratio of RNRM to RTRM) for the one calculation may produce an inaccurate result.

Wilson's Heating Method

Wilson first used this method to measure the paleointensity from baked laterites (Wilson, 1961). The method is very similar to Thelliers' Method: the sample is heated to progressively higher temperatures , from room temperature T_o to Curie temperature T_c , and cooled to T_o in zero field. RNRM is measured at each elevated temperature. Then a total TRM is imparted by cooling from T_c to T_o in a known field F_o , and the above thermal demagnetization procedure is repeated. The paleointensity can be calculated from the ratios of the RNRM to RTRM in each thermal demagnetization step. The method has also been modified to include prior AF cleaning (Doell and Smith, 1969).

B. EXPERIMENTAL METHODS

Thelliers' Stepwise Heating Method

A vibrating sample magnetometer (PAR model FM-1) was used to measure the remanent magnetization, isothermal remanent magnetization, and saturation magnetization of the samples. The samples were cooled from 400°C and 700°C to room temperature in 0.8 oersted magnetic field and then rotated at angles of 90°, 180°, and 270° on the magnetometer for each measurement. The results from Sample No.1 and Sample No. 2 are shown in Table 1. The results show that the remanent magnetization, isothermal remanent magnetization, and saturation magnetization are essentially the same not only before and after heating but also for the different orientations as well. This indicates that the samples are stable against heat treatment in air and also that the effects of anisotropy are very small. One must remember that all the above tests are conducted in strong field intensities (approximately one thousand oersteds or above). The Earth's magnetic field, however, is a weak magnetic field (less than one oersted), and all the measurements for the ancient field intensity studies are done in a weak magnetic field.

For the purpose of measuring the ancient field intensity from the sample using Thelliers' Stepwise Heating Method, three pairs of Helmholtz coils are used to cancel the North-South, East-West, and Vertical components of the Earth's magnetic field. Inside the coils there is zero field, and the fourth pair of Helmholtz coils is used to produce artificial magnetic fields of

various intensities. The Helmholtz controller is so precise that the drift of the magnetic field is no more than ± 25 gamma. In the center of the Helmholtz coils, there is a non-magnetic oven. The temperature inside the oven is read by a thermocouple meter and an integrating digital multimeter is used to read the DC voltage of the thermocouple. Thus, the temperature in the oven can be controlled within the range of $\pm 1^{o}C$. The magnetizations of the samples are measured by the PAR(Princeton Applied Research) Model 2 Spinner Magnetometer, which can measure a magnetization as weak as 10^{-5} emu. The direction of the magnetization of the sample is given in spherical coordinates, as shown in Fig. 8, where θ (theta) is the longitudinal or azimuthal angle and ∅ (phi) is the colatitude.

Almost all of the samples in this study are measured by Thelliers' Stepwise Heating Method. In order to have more reliable results, procedures and calculations have been progressively improved from Method D to Method A (see below).

(1) Method D : The samples are cut into specimens of circular discs with one inch diameters and various thicknesses. The specimens are heated in an oven from $100^{o}C$ to $700^{o}C$ in $100^{o}C$ intervals. The temperature inside the oven is read by the thermocouple meter, so the temperature can be controlled within the range of $\pm 5^{o}C$. The ancient field intensity is calculated by drawing a best-fitting straight line in the RNRM-PTRM diagram. Fig. 9 shows the results of the measurements of the two specimens from Sample No.3.

(2) Method C : The procedures of this method are

similar to those of Method D, except there are two additional calculations in this method: (a) the information concerning the changes in orientation of the RNRM and PTRM in each step aid in the interpretation of results; (b) the slope of the curve in the RNRM-PTRM diagrams is calculated by the least squares method. All of the calculations are done by computer. Fig. 7 shows the result of the two specimens from Sample No.50. In Fig. 7(a), the points in the RNRM-PTRM diagram are not in a straight line, also the orientation of the RNRM is not constant. These indicate Spec. No.50.1 underwent a chemical or mineralogical change during measurement, so the result from this specimen is not reliable. In Fig. 7(b), the points from 100°C to 500°C are almost in a straight line; also, the orientation of the RNRM is very stable in this range of temperature, which indicates that Spec. No.50.2 is stable during heating up to 500°C, and the result from this specimens is reliable.

(3) Method B : In this method, an integrating digital multimeter is used to read the DC voltage of the thermocouple, so the temperature inside the oven can be controlled within the range of $\pm$ 1°C. In order to have a more reliable result, heating in 100°C intervals is replaced by heating in intervals of 50°C. IBM 1130 plotter subroutines are used to plot the RNRM-PTRM diagrams, thermal demagnetization curves, remagnetization curves, and the changes of the orientations of RNRM and PTRM. The reliability of the RNRM may be less than that of the PTRM at low temperatures because of the secondary magnetization of the sample, and the reliability of the PTRM may be less

Table 1 Dependence of J_s , J_i , and J on different heating temperatures and orientations.

Sample No. 1						
Orientation		0^o	90^o	180^o	270^o	Average
Original	J_s ($\times 10^{-4}$ emu/gm)	242	247	241	240	242.5
	J_i ($\times 10^{-4}$ emu/gm)	55	55	59	53	55.5
	J ($\times 10^{-4}$ emu/gm)	11	12	11	12	11.5
After	J_s ($\times 10^{-4}$ emu/gm)	251	253	251	252	252
heating	J_i ($\times 10^{-4}$ emu/gm)	60	57	61	58	59
to 400^oC	J ($\times 10^{-4}$ emu/gm)	13	13	12	13	13
After	J_s ($\times 10^{-4}$ emu/gm)	245	252	244	248	247
heating	J_i ($\times 10^{-4}$ emu/gm)	60	57	58	56	58
to 700^oC	J ($\times 10^{-4}$ emu/gm)	14	13	13	14	13.5
Sample No. 2						
Orientation		0^o	90^o	180^o	270^o	Average
Original	J_s ($\times 10^{-3}$ emu/gm)	93	91	94	90	92
	J_i ($\times 10^{-3}$ emu/gm)	32	30	32	31	31
	J ($\times 10^{-3}$ emu/gm)	5	6	5	6	5.5
After	J_s ($\times 10^{-3}$ emu/gm)	94	93	92	92	93
heating	J_i ($\times 10^{-3}$ emu/gm)	31	31	31	31	31
to 400^oC	J ($\times 10^{-3}$ emu/gm)	5	6	5	6	5.5
After	J_s ($\times 10^{-3}$ emu/gm)	87	89	86	86	87
heating	J_i ($\times 10^{-3}$ emu/gm)	30	29	29	28	29
to 700^oC	J ($\times 10^{-3}$ emu/gm)	6	6	5	6	6

J_s = Saturation magnetization

J_i = Isothermal remanent magnetization

J = Remanent magnetization

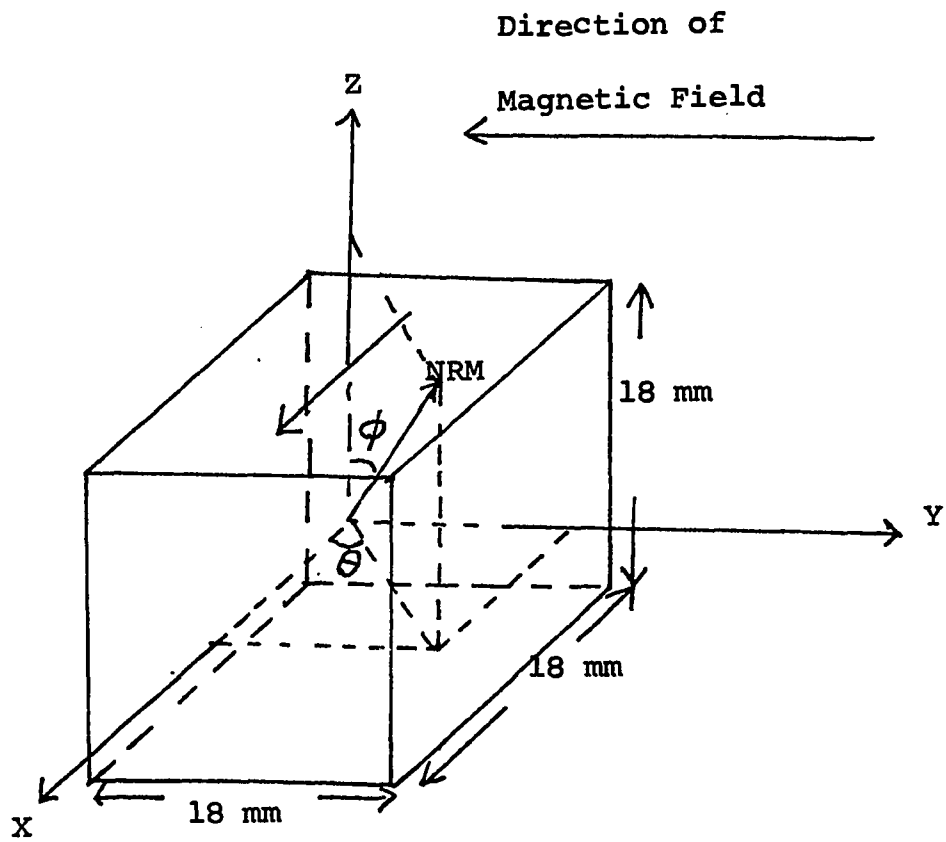

Fig. 5 Direction of magnetization of a sample in spherical coordinates.

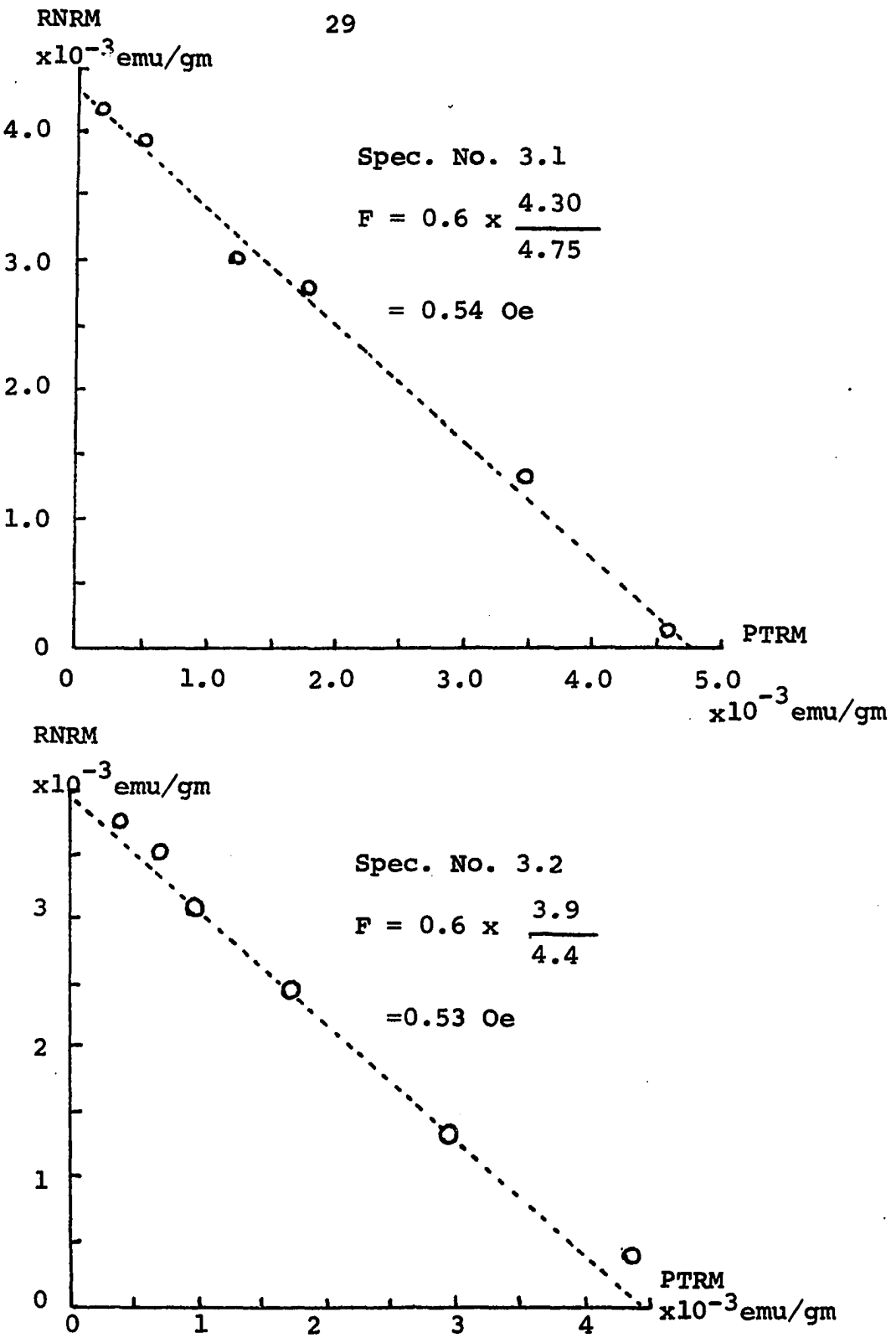

Fig. 6 RNRM-PTRM curves from Sample No.3 obtained by Thelliers' Method (D).

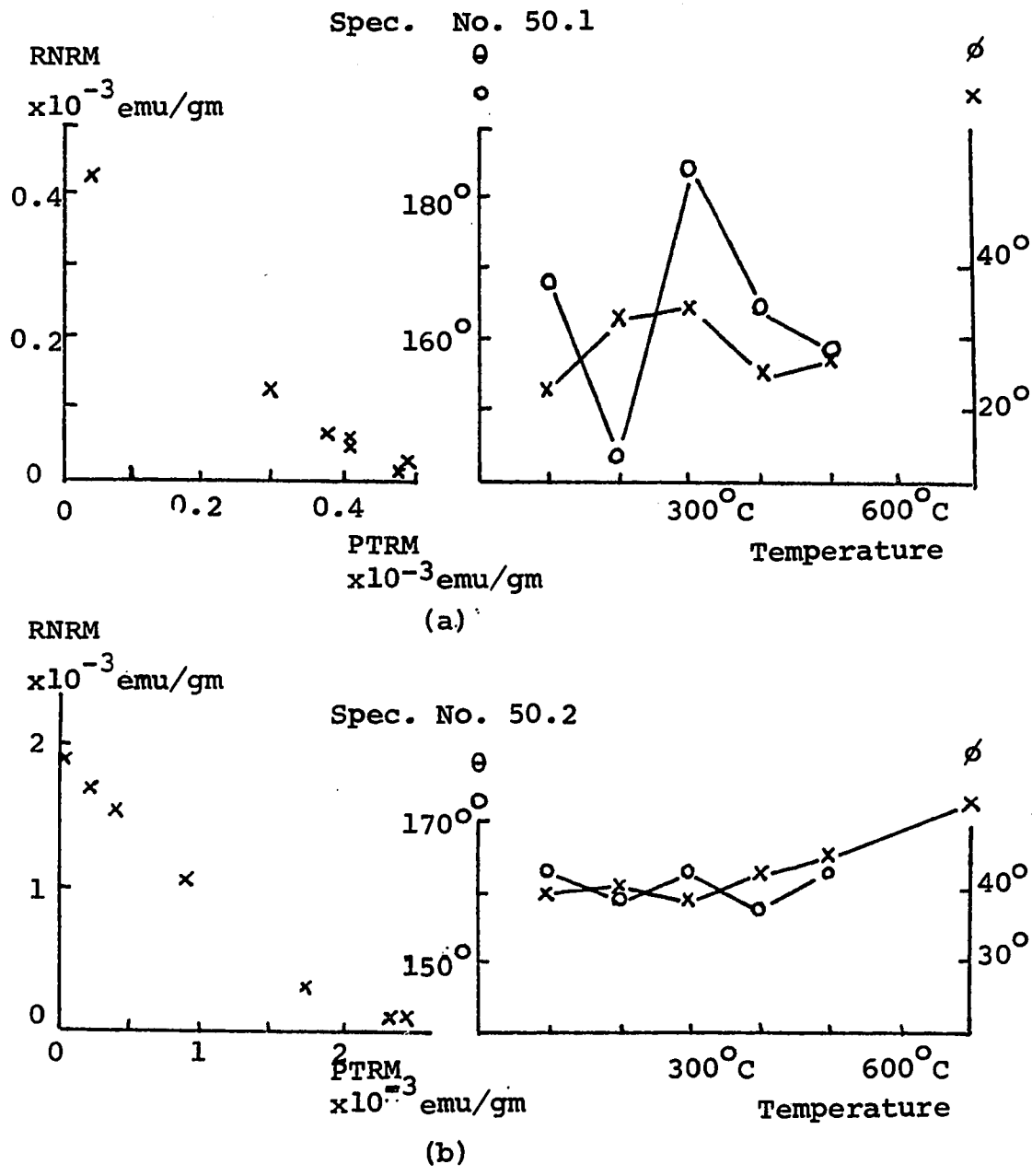

Fig. 7 Results of Spec. Nos. 50.1 and 50.2 obtained by Thelliers' Method (C).

than that of RNRM at high temperatures because of chemical reactions. In addition to the least squares method, the least squares cubic method is used to calculate the results (York, 1966 and 1967).

Because all the points in the RNRM-PTRM diagram which were used to calculate the ancient field intensity have been checked with the information from the changes of the orientations of RNRM and PTRM, to make sure the points are not affected by secondary magnetization or chemical reactions, and if the appropriate weights in the least squares cubic method are chosen, then the results calculated from the least squares cubic method are very close to those from the least squares method. The results of the four specimens from Sample No.59, which will be decribed in detail later*, are 0.51 oersted, 0.47 oersted, 0.48 oersted, and 0.48 oersted, repectively, if calculated by the least squares method; they are 0.51 oersted, 0.48 oersted, 0.48 oersted, and 0.48 oersted respectively, if calculated by the least squares cubic method. Since the two above-mentioned methods give approximately the same results, the table in the results list the values calculated only from the least squares method, although the values have also been calculated by the least squares cubic method.

(4) Method A : In the above methods, the samples are cut into circular discs and orientation lines are drawn with heat resistant ink. Difficulties lie in rotating the sample exactly 180° in the opposite direction in

* See page 66.

the oven and in placing the sample into the sample holder in exactly the same position during each measurement. It has been theoretically calculated that if the difference in the direction is 2^{o}, then the deviations between the actual RNRM, PTRM values and the measured RNRM, PTRM values are approximately two percent. Of course, it depends on the individual sample. In order to avoid the above deviation, the baked clays are cut into 18 mm cubes and the pottery are cut into square discs. The samples are placed on top of a non-magnetic brick which is placed in oven horizontally. On the top of the brick are 6 parallel slots which have been cut, and into which 2 plastic rulers can be inserted to maintain a constant orientation of the sample. The sample holder is also cut into a shape which has three mutually perpendicular surfaces inside: this allows the sample to be placed in the same orientation in each step as it was in the oven. The procedures and calculations in this method are exactly the same as those in Method B. The results of the measurements of Spec. No.66.5 from the outputs of the computer programs are shown from Table 2 to Table 5. Table 2 shows the measured values of the magnetizations of the specimen from the Spinner Magnetometer at each step. Table 3 shows the magnitudes and directions of RNRM and PTRM at each step. Fig. 8 shows the diagrams of RNRM-PTRM, thermal demagnetization curve, remagnetization curve, and the changes of the orientations of the RNRM and PTRM. Table 4 shows the result of the calculation from the least squares method; the points in the calculation are from 100^{o}C to 500^{o}C.

Because the NRM usually includes some soft second-

ary magnetizations and also some soft components that decay with time, the NRM point was not put into the calculation. In Table 3 and Fig. 8, it is obvious that the orientation of the RNRM moved rapidly at 550°C, so the points above 550°C were not put into the calculation. The ancient geomagnetic field intensity F is 0.4284 oersted, the standard deviation of F is 0.0025 oersted, and the 95 percent confidence interval of F is from 0.4225 oersted to 0.4343 oersted. These values indicate that the value of F is very reliable. The present geomagnetic field intensity in site F=0.4150 oersted is calculated from the map of the total intensity of the Earth's magnetic force at epoch 1965 published by the U.S. Naval Oceanographic Office. The ratio of the ancient field intensity to the present field intensity is 1.0323. Table 5, which shows a result of 0.4290 oersted for the ancient geomagnetic field intensity, is calculated by the least square cubic method. This result (0.4290 oersted) is very close to the result from the least squares method (0.4284 oersted).

The reliability of the results from the methods A,B,C, or D are quite different from one another. This can be explained by the results of Sample No.53, which is a well-fired baked clay from Chachi, Mexico. Spec. Nos.53.1 and 53.2 are measured by Method C; the RNRM-PTRM diagrams and the changes of orientations of RNRM are shown in Fig. 9 . Because Method C uses 100°C intervals, there are only seven points in the diagram and these approximate a straight line. The ancient field intensities from these two specimens are 0.2882 oersted and 0.3452 oersted, respectively and the results seem reliable. Spec. Nos. 53.3

and 53.4 are measured by Method B: the results are shown in Fig. 10 and Fig. 11 respectively, since both specimens are unstable against heating, the results are unreliable.

Spec. Nos. 53.5, 53.6, 53.7 and 53.8 are measured by Method A: the results are shown from Fig. 12 to Fig. 15 and Table 6. Spec. Nos. 53.5 and 53.7 are unstable upon heating, and Spec. Nos. 53.6 and 53.8 are very stable, so the results from Spec. Nos. 53.6 and 53.8, which indicated the ancient field intensities are 0.4043 oersted and 0.4137 oersted, are very reliable.

Comparing the changes of the orientations of RNRM in Fig. 9 and Fig. 13, it is obvious that the change in Spec. Nos. 53.1 and 53.2 are quite large compared to those in Spec. No. 53.6. This indicates that either Spec. Nos. 53.1 and 53.2 are unstable during heating or the small deviations of the orientation of the specimen and the temperature in the oven caused the change of the orientation of RNRM. By this comparison, the results from Spec. Nos. 53.1 and 53.2 are not considered reliable. If only two specimens had been measured by Method C, then the results would indicate the ancient field intensity for this sample is 0.3167 oersted instead of the more reliable results from Method A, which indicate the ancient field intensity is 0.4040 oersted.

Alternating Field Demagnetization Method

Because the samples in this study are baked clays and pottery, their original NRMs are TRMs. The AF Demagnetization Method can be used to measure the ancient field intensity. The AF Demagentization Method has the advantage of requiring less time than Thelliers' Method, and the

Table 2 Measured values of the magnetization of Spec. No.66.5 from the Spinner Magnetometer at each heating step in Thelliers' Method.

THELLIER HEATING METHOD FOR ARCHEOMAGNETIC INTENSITY

TEM.	20.0 DEGREE C	WT.	8.09GM	JN	0.3358E-02EMU/GM	JT	0.0 EMU/GM	SPEC.NO 66.5
	X1	0.5940E-02		Y1	-0.2545E-01		Z1 0.7520E-02	
	X2	0.6140E-02		Y2	-0.2558E-01		Z2 0.7720E-02	
	X3	0.6580E-02		Y3	-0.2508E-01		Z3 0.7540E-02	
	X4	0.6270E-02		Y4	-0.2513E-01		Z4 0.7860E-02	
		0.6232E-02			-0.2531E-01		0.7660E-02	
	XP1	0.5940E-02		YP1	-0.2545E-01		ZP1 0.7520E-02	
	XP2	0.6140E-02		YP2	-0.2558E-01		ZP2 0.7720E-02	
	XP3	0.6580E-02		YP3	-0.2508E-01		ZP3 0.7540E-02	
	XP4	0.6270E-02		YP4	-0.2513E-01		ZP4 0.7860E-02	
		0.6232E-02			-0.2531E-01		0.7660E-02	
TEM.	100.0 DEGREE C	WT.	8.09GM	JN	0.3295E-02EMU/GM	JT	0.9335E-04EMU/GM	SPEC.NO 66.5
	X1	0.5770E-02		Y1	-0.2571E-01		Z1 0.7440E-02	
	X2	0.5930E-02		Y2	-0.2584E-01		Z2 0.7660E-02	
	X3	0.5970E-02		Y3	-0.2548E-01		Z3 0.7650E-02	
	X4	0.5810E-02		Y4	-0.2552E-01		Z4 0.7390E-02	
		0.5870E-02			-0.2564E-01		0.7535E-02	
	XP1	0.5790E-02		YP1	-0.2419E-01		ZP1 0.7450E-02	
	XP2	0.5970E-02		YP2	-0.2430E-01		ZP2 0.7610E-02	
	XP3	0.5990E-02		YP3	-0.2399E-01		ZP3 0.7600E-02	
	XP4	0.5860E-02		YP4	-0.2403E-01		ZP4 0.7420E-02	
		0.5902E-02			-0.2413E-01		0.7520E-02	
TEM.	150.0 DEGREE C	WT.	8.09GM	JN	0.3217E-02EMU/GM	JT	0.1868E-03EMU/GM	SPEC.NO 66.5
	X1	0.5650E-02		Y1	-0.2586E-01		Z1 0.7260E-02	
	X2	0.5780E-02		Y2	-0.2600E-01		Z2 0.7470E-02	
	X3	0.6020E-02		Y3	-0.2564E-01		Z3 0.7220E-02	
	X4	0.5800E-02		Y4	-0.2573E-01		Z4 0.7360E-02	
		0.5812E-02			-0.2581E-01		0.7327E-02	
	XP1	0.5620E-02		YP1	-0.2284E-01		ZP1 0.7300E-02	
	XP2	0.5830E-02		YP2	-0.2296E-01		ZP2 0.7400E-02	
	XP3	0.5750E-02		YP3	-0.2263E-01		ZP3 0.7420E-02	
	XP4	0.5640E-02		YP4	-0.2272E-01		ZP4 0.7260E-02	
		0.5710E-02			-0.2279E-01		0.7345E-02	

Table 2 (Continued)

TEM.	200.0	DEGREE C	WT.	8.09GM	JN	0.3121E-02EMU/GM	JT	0.2942E-03EMU/GM	SPEC.NO	66.5	
	X1	0.5480E-02			Y1	-0.2600E-01		Z1	0.7220E-02		
	X2	0.5720E-02			Y2	-0.2612E-01		Z2	0.7280E-02		
	X3	0.5670E-02			Y3	-0.2576E-01		Z3	0.7290E-02		
	X4	0.5580E-02			Y4	-0.2585E-01		Z4	0.7170E-02		
		0.5612E-02				-0.2593E-01			0.7240E-02		
	XP1	0.5450E-02			YP1	-0.2122E-01		ZP1	0.7060E-02		
	XP2	0.5590E-02			YP2	-0.2133E-01		ZP2	0.7210E-02		
	XP3	0.5580E-02			YP3	-0.2103E-01		ZP3	0.7240E-02		
	XP4	0.5490E-02			YP4	-0.2112E-01		ZP4	0.7010E-02		
		0.5527E-02				-0.2117E-01			0.7130E-02		
TEM.	250.0	DEGREE C	WT.	8.09GM	JN	0.2991E-02EMU/GM	JT	0.4402E-03EMU/GM	SPEC.NO	66.5	
	X1	0.5210E-02			Y1	-0.2625E-01		Z1	0.6880E-02		
	X2	0.5470E-02			Y2	-0.2628E-01		Z2	0.7020E-02		
	X3	0.5420E-02			Y3	-0.2598E-01		Z3	0.7050E-02		
	X4	0.5390E-02			Y4	-0.2608E-01		Z4	0.6790E-02		
		0.5372E-02				-0.2615E-01			0.6935E-02		
	XP1	0.5160E-02			YP1	-0.1906E-01		ZP1	0.6750E-02		
	XP2	0.5250E-02			YP2	-0.1920E-01		ZP2	0.6860E-02		
	XP3	0.5370E-02			YP3	-0.1890E-01		ZP3	0.6840E-02		
	XP4	0.5230E-02			YP4	-0.1895E-01		ZP4	0.6790E-02		
		0.5252E-02				-0.1903E-01			0.6810E-02		
TEM.	300.0	DEGREE C	WT.	8.09GM	JN	0.2820E-02EMU/GM	JT	0.5838E-03EMU/GM	SPEC.NO	66.5	
	X1	0.5050E-02			Y1	-0.2607E-01		Z1	0.6370E-02		
	X2	0.5130E-02			Y2	-0.2621E-01		Z2	0.6630E-02		
	X3	0.5240E-02			Y3	-0.2569E-01		Z3	0.6590E-02		
	X4	0.5100E-02			Y4	-0.2592E-01		Z4	0.6390E-02		
		0.5130E-02				-0.2602E-01			0.6495E-02		
	XP1	0.4800E-02			YP1	-0.1660E-01		ZP1	0.6370E-02		
	XP2	0.4920E-02			YP2	-0.1670E-01		ZP2	0.6480E-02		
	XP3	0.4950E-02			YP3	-0.1649E-01		ZP3	0.6440E-02		
	XP4	0.4860E-02			YP4	-0.1653E-01		ZP4	0.6300E-02		
		0.4882E-02				-0.1658E-01			0.6397E-02		

Table 2 (Continued)

TEM.	350.0 DEGREE C	WT.	8.09GM	JN	0.2556E-02EMU/GM	JT	0.8611E-03EMU/GM	SPEC.NO	66.5
	X1	0.4720E-02		Y1	-0.2622E-01		Z1	0.5800E-02	
	X2	0.4770E-02		Y2	-0.2643E-01		Z2	0.6150E-02	
	X3	0.4930E-02		Y3	-0.2611E-01		Z3	0.6020E-02	
	X4	0.4790E-02		Y4	-0.2612E-01		Z4	0.5830E-02	
		0.4802E-02			-0.2624E-01			0.5950E-02	
	XP1	0.4380E-02		YP1	-0.1232E-01		ZP1	0.5770E-02	
	XP2	0.4460E-02		YP2	-0.1244E-01		ZP2	0.5880E-02	
	XP3	0.4560E-02		YP3	-0.1225E-01		ZP3	0.5790E-02	
	XP4	0.4420E-02		YP4	-0.1226E-01		ZP4	0.5740E-02	
		0.4455E-02			-0.1232E-01			0.5795E-02	

TEM.	400.0 DEGREE C	WT.	8.09GM	JN	0.2215E-02EMU/GM	JT	0.1216E-02EMU/GM	SPEC.NO	66.5
	X1	0.3930E-02		Y1	-0.2668E-01		Z1	0.5040E-02	
	X2	0.4010E-02		Y2	-0.2675E-01		Z2	0.5260E-02	
	X3	0.4090E-02		Y3	-0.2644E-01		Z3	0.5230E-02	
	X4	0.3970E-02		Y4	-0.2644E-01		Z4	0.4970E-02	
		0.4000E-02			-0.2658E-01			0.5125E-02	
	XP1	0.3590E-02		YP1	-0.6910E-02		ZP1	0.5130E-02	
	XP2	0.3770E-02		YP2	-0.6970E-02		ZP2	0.5090E-02	
	XP3	0.3650E-02		YP3	-0.6830E-02		ZP3	0.5130E-02	
	XP4	0.3650E-02		YP4	-0.6890E-02		ZP4	0.5070E-02	
		0.3665E-02			-0.6900E-02			0.5105E-02	

TEM.	450.0 DEGREE C	WT.	8.09GM	JN	0.1553E-02EMU/GM	JT	0.1934E-02EMU/GM	SPEC.NO	66.5
	X1	0.2930E-02		Y1	-0.2721E-01		Z1	0.3810E-02	
	X2	0.3120E-02		Y2	-0.2749E-01		Z2	0.4140E-02	
	X3	0.3090E-02		Y3	-0.2713E-01		Z3	0.4120E-02	
	X4	0.3050E-02		Y4	-0.2718E-01		Z4	0.3840E-02	
		0.3047E-02			-0.2725E-01			0.3977E-02	
	XP1	0.2580E-02		YP1	0.4080E-02		ZP1	0.3820E-02	
	XP2	0.2710E-02		YP2	0.4030E-02		ZP2	0.3690E-02	
	XP3	0.2650E-02		YP3	0.4050E-02		ZP3	0.3740E-02	
	XP4	0.2640E-02		YP4	0.4000E-02		ZP4	0.3770E-02	
		0.2645E-02			0.4040E-02			0.3755E-02	

Table 2 (Continued)

TEM.	500.0 DEGREE C	WT.	8.09GM	JN	0.7881E-03EMU/GM	JT	0.2739E-02EMU/GM	SPEC.NO 66.5
	X1	0.1780E-02		Y1	-0.2808E-01		Z1	0.2330E-02
	X2	0.1930E-02		Y2	-0.2810E-01		Z2	0.2530E-02
	X3	0.1850E-02		Y3	-0.2778E-01		Z3	0.2520E-02
	X4	0.1830E-02		Y4	-0.2782E-01		Z4	0.2210E-02
		0.1847E-02			-0.2794E-01			0.2397E-02
	XP1	0.6300E-03		YP1	0.1644E-01		ZP1	0.2400E-02
	XP2	0.7300E-03		YP2	0.1643E-01		ZP2	0.2160E-02
	XP3	0.6900E-03		YP3	0.1631E-01		ZP3	0.2190E-02
	XP4	0.7300E-03		YP4	0.1625E-01		ZP4	0.2330E-02
		0.7075E-03			0.1636E-01			0.2270E-02
TEM.	550.0 DEGREE C	WT.	8.09GM	JN	0.2338E-03EMU/GM	JT	0.3276E-02EMU/GM	SPEC.NO 66.5
	X1	0.6500E-03		Y1	-0.2804E-01		Z1	0.1160E-02
	X2	0.8100E-03		Y2	-0.2812E-01		Z2	0.1350E-02
	X3	0.6400E-03		Y3	-0.2781E-01		Z3	0.1340E-02
	X4	0.6200E-03		Y4	-0.2783E-01		Z4	0.1110E-02
		0.6600E-03			-0.2795E-01			0.1240E-02
	XP1	-0.3000E-03		YP1	0.2517E-01		ZP1	0.1370E-02
	XP2	-0.1100E-03		YP2	0.2518E-01		ZP2	0.8800E-03
	XP3	-0.2900E-03		YP3	0.2492E-01		ZP3	0.1040E-02
	XP4	-0.2100E-03		YP4	0.2492E-01		ZP4	0.1280E-02
		-0.2275E-03			0.2505E-01			0.1142E-02
TEM.	600.0 DEGREE C	WT.	8.09GM	JN	0.1208E-03EMU/GM	JT	0.3402E-02EMU/GM	SPEC.NO 66.5
	X1	0.5300E-03		Y1	-0.2775E-01		Z1	0.6800E-03
	X2	0.4900E-03		Y2	-0.2733E-01		Z2	0.1140E-02
	X3	0.4900E-03		Y3	-0.2747E-01		Z3	0.1100E-02
	X4	0.6100E-03		Y4	-0.2746E-01		Z4	0.8200E-03
		0.5275E-03			-0.2755E-01			0.9350E-03
	XP1	-0.4800E-03		YP1	0.2752E-01		ZP1	0.1240E-02
	XP2	-0.3100E-03		YP2	0.2750E-01		ZP2	0.7400E-03
	XP3	-0.3900E-03		YP3	0.2728E-01		ZP3	0.8700E-03

Table 2 (Continued)

XP4	-0.3900E-03	YP4	0.2726E-01	ZP4	0.1140E-02
	-0.3925E-03		0.2739E-01		0.9975E-03

TEM. 700.0 DEGREE C WT. 8.09GM JN 0.1144E-03EMU/GM JT 0.3409E-02EMU/GM SPEC.NO 66.5

X1	0.4100E-03	Y1	-0.2774E-01	Z1	0.6900E-03
X2	0.3900E-03	Y2	-0.2773E-01	Z2	0.1060E-02
X3	0.4100E-03	Y3	-0.2737E-01	Z3	0.1020E-02
X4	0.3800E-03	Y4	-0.2740E-01	Z4	0.6800E-03
	0.3975E-03		-0.2756E-01		0.8625E-03
XP1	-0.5500E-03	YP1	0.2770E-01	ZP1	0.1250E-02
XP2	-0.4400E-03	YP2	0.2767E-01	ZP2	0.7200E-03
XP3	-0.5600E-03	YP3	0.2750E-01	ZP3	0.8800E-03
XP4	-0.5200E-03	YP4	0.2748E-01	ZP4	0.1090E-02
	-0.5175E-03		0.2759E-01		0.9850E-03

Table 3 Magnitudes and directions of RNRM and PTRM of Spec.No.66.5 at each step in Thelliers' Method.

RESIDUAL NATURAL REMANENT MAGNETIZATION				PARTIAL THERMOREMANENT MAGNETIZATION SPEC.NO 66.5		
TEMPERATURE		SITA	PHI		SITA	PHI
	EMU/GM	DEGREE	DEGREE	EMU/GM	DEGREE	DEGREE
NRM	0.3358E-02	-76.17	73.62	0.0	0.0	0.0
100.0 DEGREE C	0.3295E-02	-76.69	73.60	0.9335E-04	-91.23	89.43
150.0 DEGREE C	0.3217E-02	-76.66	73.63	0.1868E-03	-88.06	90.33
200.0 DEGREE C	0.3121E-02	-76.69	73.47	0.2942E-03	-88.98	88.68
250.0 DEGREE C	0.2991E-02	-76.76	73.50	0.4402E-03	-89.03	88.99
300.0 DEGREE C	0.2820E-02	-76.77	73.59	0.5838E-03	-88.50	89.41
350.0 DEGREE C	0.2556E-02	-76.50	73.50	0.8611E-03	-88.57	89.36
400.0 DEGREE C	0.2215E-02	-77.10	73.41	0.1216E-02	-89.02	89.94
450.0 DEGREE C	0.1553E-02	-76.22	72.07	0.1934E-02	-89.26	89.59
500.0 DEGREE C	0.7881E-03	-77.57	68.53	0.2739E-02	-88.53	89.83
550.0 DEGREE C	0.2338E-03	-81.14	50.96	0.3276E-02	-89.02	89.89
600.0 DEGREE C	0.1208E-03	-62.78	8.68	0.3402E-02	-89.04	90.06
700.0 DEGREE C	0.1144E-03	167.10	3.81	0.3409E-02	-89.05	90.13

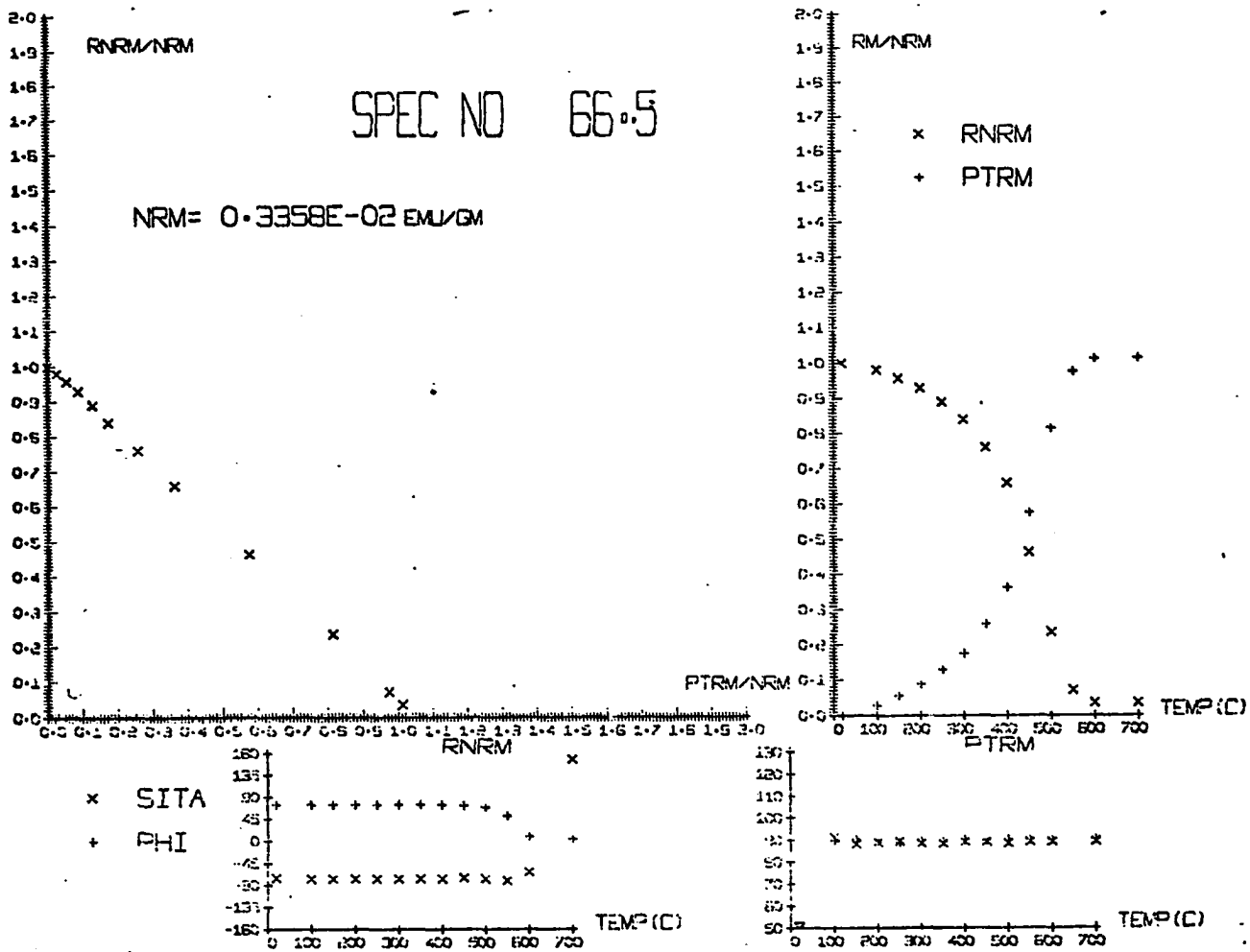

Fig. 8 Results of Spec. No.66.5 obtained by Thelliers' Method (A).

Table 4 Results of calculation of Spec.No.66.5 by the least squares method.

CALCULATED BY THE LEAST SQUARE METHOD

SPEC. NO 66.5

POINTS IN LEAST SQUARE METHOD	9	FROM 100.0 DEG. C	TO 500.0 DEG. C		
ARTIFICIAL MAGNETIC FIELD INTENSITY			0.4500		GAUSS
SLOPE OF RESIDUAL NRM VS PARTIAL TRM			-0.9520		
STANDARD DEVIATION OF THE SLOPE			0.0055		
THE ANCIENT GEOMAGNETIC FIELD INTENSITY			0.4284		GAUSS
STANDARD DEVIATION OF THE ANCIENT GEOMAGNETIC FIELD INTENSITY			0.0025		GAUSS
THE 95 PERCENT CONFIDENCE INTERVAL OF THE ANCIENT GEOMAGNETIC FIELD INTENSITY			0.4225	0.4343	GAUSS
THE PRESENT GEOMAGNETIC FIELD INTENSITY IN SITE		0.4150		GAUSS	
THE RATIO OF THE ANCIENT / PRESENT GEOMAGGETIC FIELD INTENSITY		1.0323			

Table 5 Results of calculations of Spec. No.66.5 by the least squares cubic method.

LEAST SQUARES CUBIC METHOD FOR ARCHEOMAGNETIC INTENSITY SPEC. NO 66.5

	RESIDUAL NATURAL REMANENT MAGNETIZATION		PARTIAL THERMOREMANENT MAGNETIZATION	
	EMU/CC	WEIGHT	EMU/CC	WEIGHT
100.0 DEGREE C	0.3295E-02	20.0	0.9335E-04	120.0
150.0 DEGREE C	0.3217E-02	30.0	0.1868E-03	110.0
200.0 DEGREE C	0.3121E-02	40.0	0.2942E-03	100.0
250.0 DEGREE C	0.2991E-02	50.0	0.4402E-03	90.0
300.0 DEGREE C	0.2820E-02	60.0	0.5838E-03	80.0
350.0 DEGREE C	0.2556E-02	70.0	0.8611E-03	70.0
400.0 DEGREE C	0.2219E-02	80.0	0.1216E-02	60.0
450.0 DEGREE C	0.1553E-02	90.0	0.1934E-02	50.0
500.0 DEGREE C	0.7881E-03	100.0	0.2739E-02	40.0

ARTIFICIAL MAGNETIC FIELD INTENSITY	0.4500	GAUSS
APPROXIMATE VALUE FOR SLOPE	-1.1000	
SLOPE OF RESIDUAL NRM VS PARTIAL TRM	-0.9533	
THE ANCIENT GEOMAGNETIC FIELD INTENSITY	0.4290	GAUSS
A EQUAL TO	0.5213	
THE PRESENT GEOMAGNETIC FIELD INTENSITY IN SITE	0.4150	GAUSS
THE RATIO OF THE ANCIENT / PRESENT GEOMAGNETIC FIELD INTENSITY	1.0337	

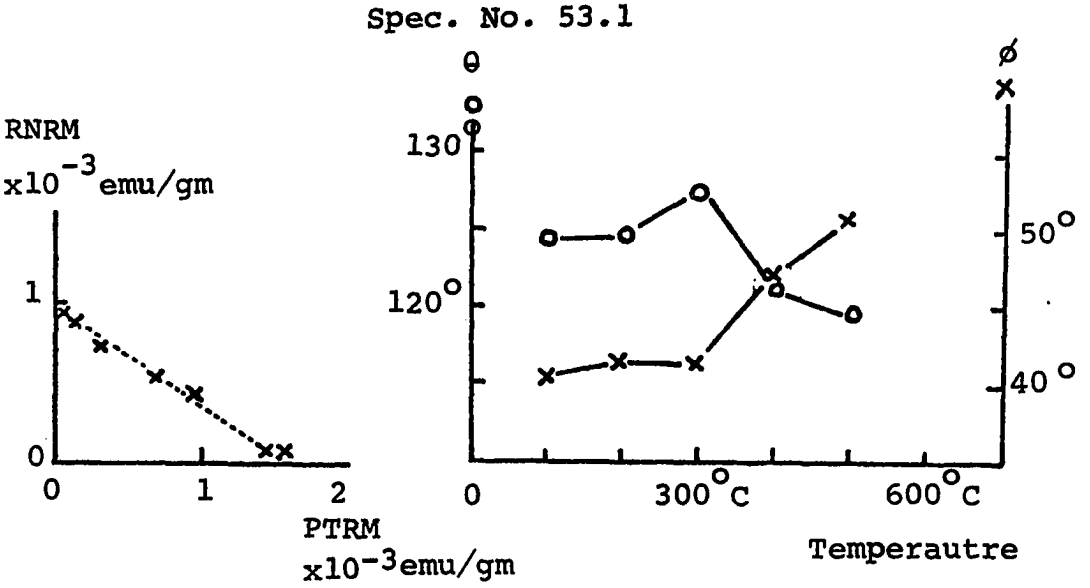

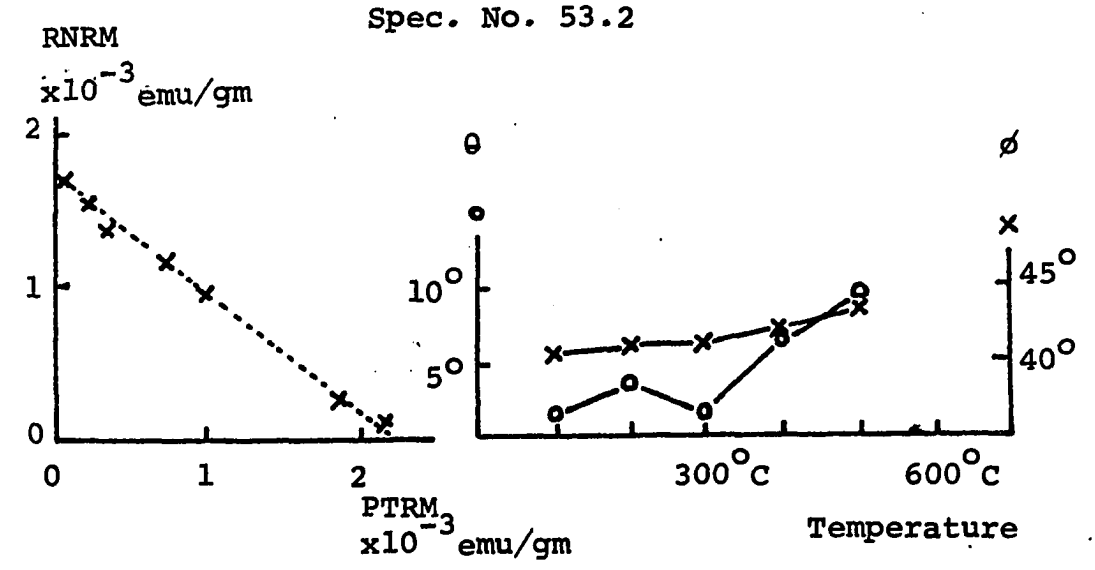

Fig. 9 Results of Spec. Nos. 53.1 and 53.2 obtained by Thelliers' Method (C).

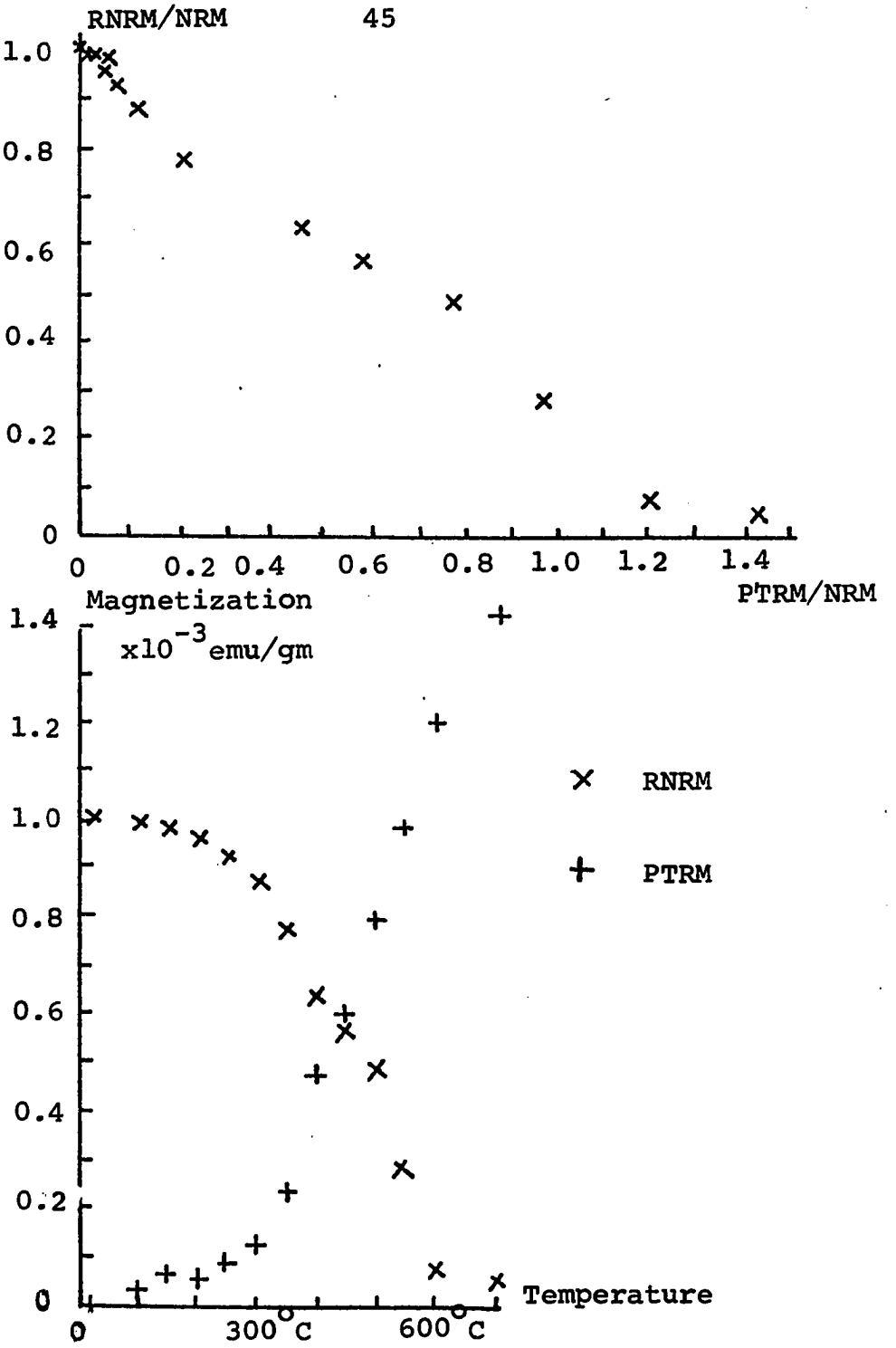

Fig. 10 Results of Spec. No. 53.3 obtained by Thelliers' Method (B).

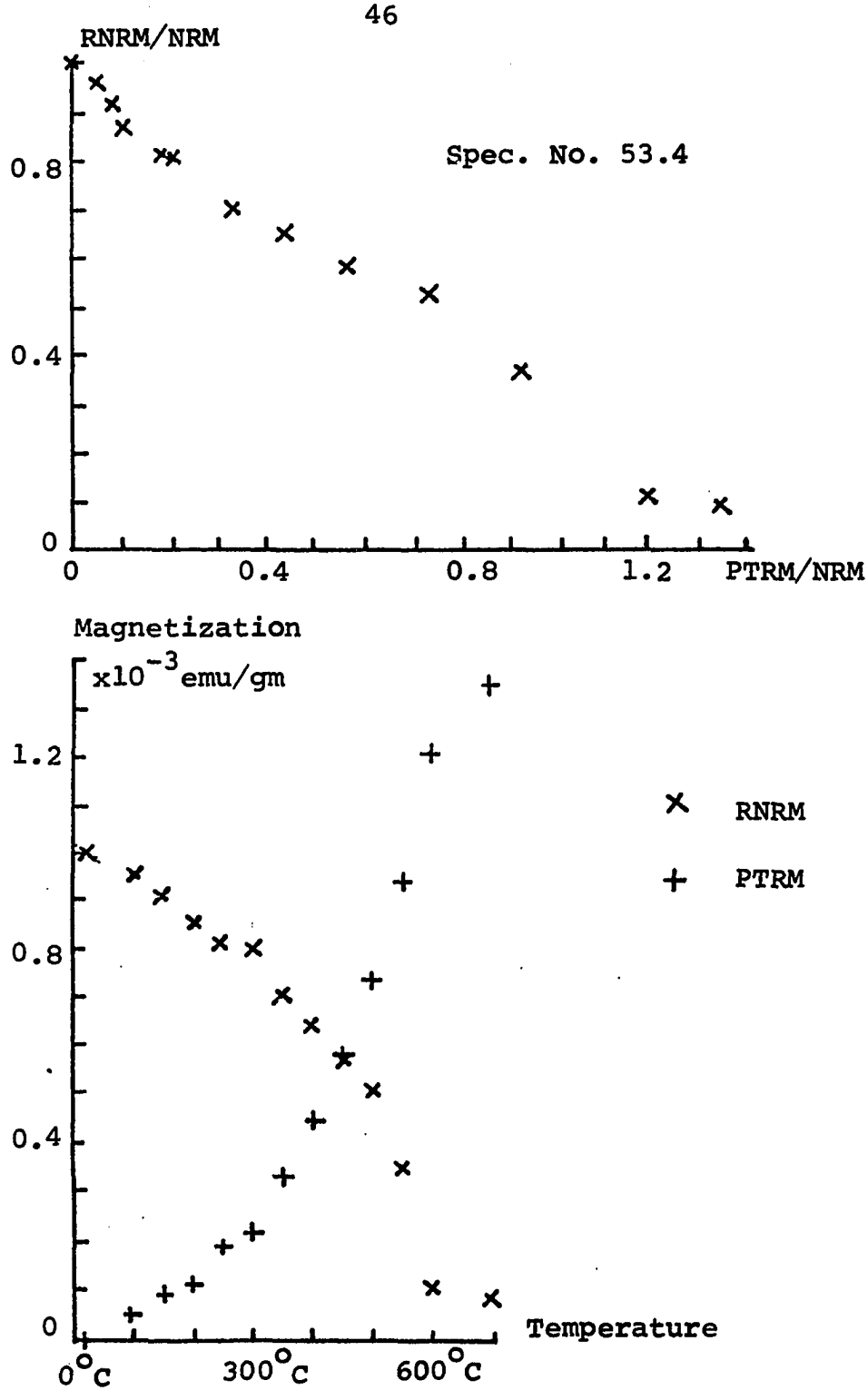

Fig. 11 Results of Spec. No. 53.4 obtained by Thelliers' Method (B).

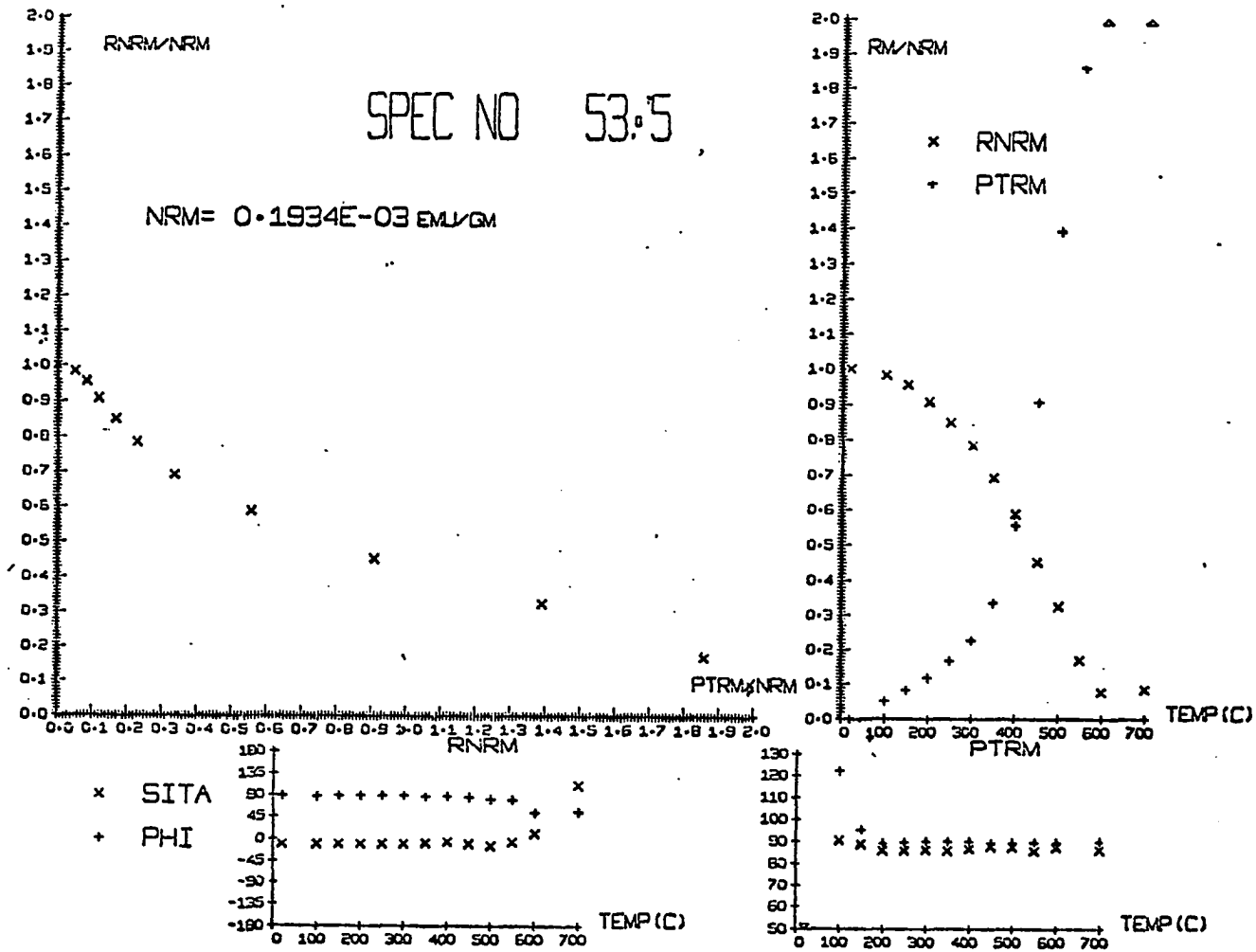

Fig. 12 Results of Spec. No. 53.5 obtained by Thelliers' Method (A).

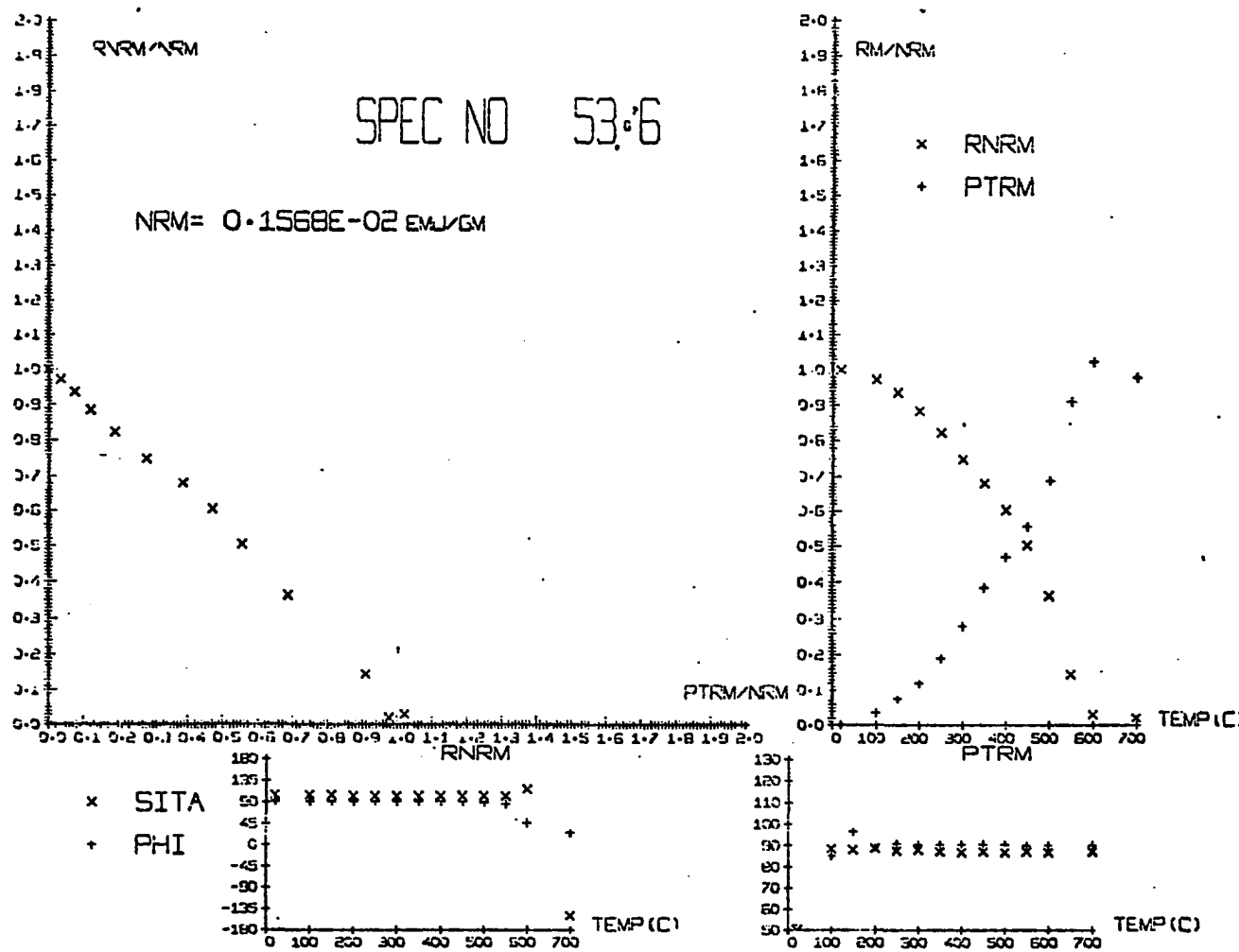

Fig. 13 Result of Spec. No. 53.6 obtained by Thelliers' Method (A).

Table 6 Magnitudes and directions of RNRM and PTRM of Spec. No. 53.6 at each heating step in Thelliers' Method.

RESIDUAL NATURAL REMANENT MAGNETIZATION				PARTIAL THERMOREMANENT MAGNETIZATION SPEC.NO 53.6		
TEMPERATURE		SITA	PHI		SITA	PHI
	EMU/GM	DEGREE	DEGREE	EMU/GM	DEGREE	DEGREE
NRM	0.1568E-02	103.94	92.65	0.0	0.0	0.0
100.0 DEGREE C	0.1523E-02	103.54	91.64	0.5395E-04	-88.25	85.04
150.0 DEGREE C	0.1467E-02	103.53	91.38	0.1173E-03	-87.84	96.31
200.0 DEGREE C	0.1388E-02	103.33	92.60	0.1889E-03	-88.67	89.33
250.0 DEGREE C	0.1288E-02	103.05	92.59	0.2985E-03	-87.68	90.84
300.0 DEGREE C	0.1174E-02	102.76	92.29	0.4405E-03	-87.97	90.46
350.0 DEGREE C	0.1067E-02	102.81	92.43	0.6030E-03	-87.34	90.23
400.0 DEGREE C	0.9450E-03	102.66	92.29	0.7361E-03	-86.86	90.51
450.0 DEGREE C	0.7882E-03	102.66	91.77	0.8694E-03	-87.25	90.23
500.0 DEGREE C	0.5681E-03	102.65	90.80	0.1078E-02	-86.97	90.36
550.0 DEGREE C	0.2290E-03	103.25	85.68	0.1425E-02	-87.17	89.99
600.0 DEGREE C	0.4799E-04	117.57	46.73	0.1603E-02	-86.77	90.06
700.0 DEGREE C	0.2950E-04	-149.04	25.63	0.1534E-02	-87.09	90.11

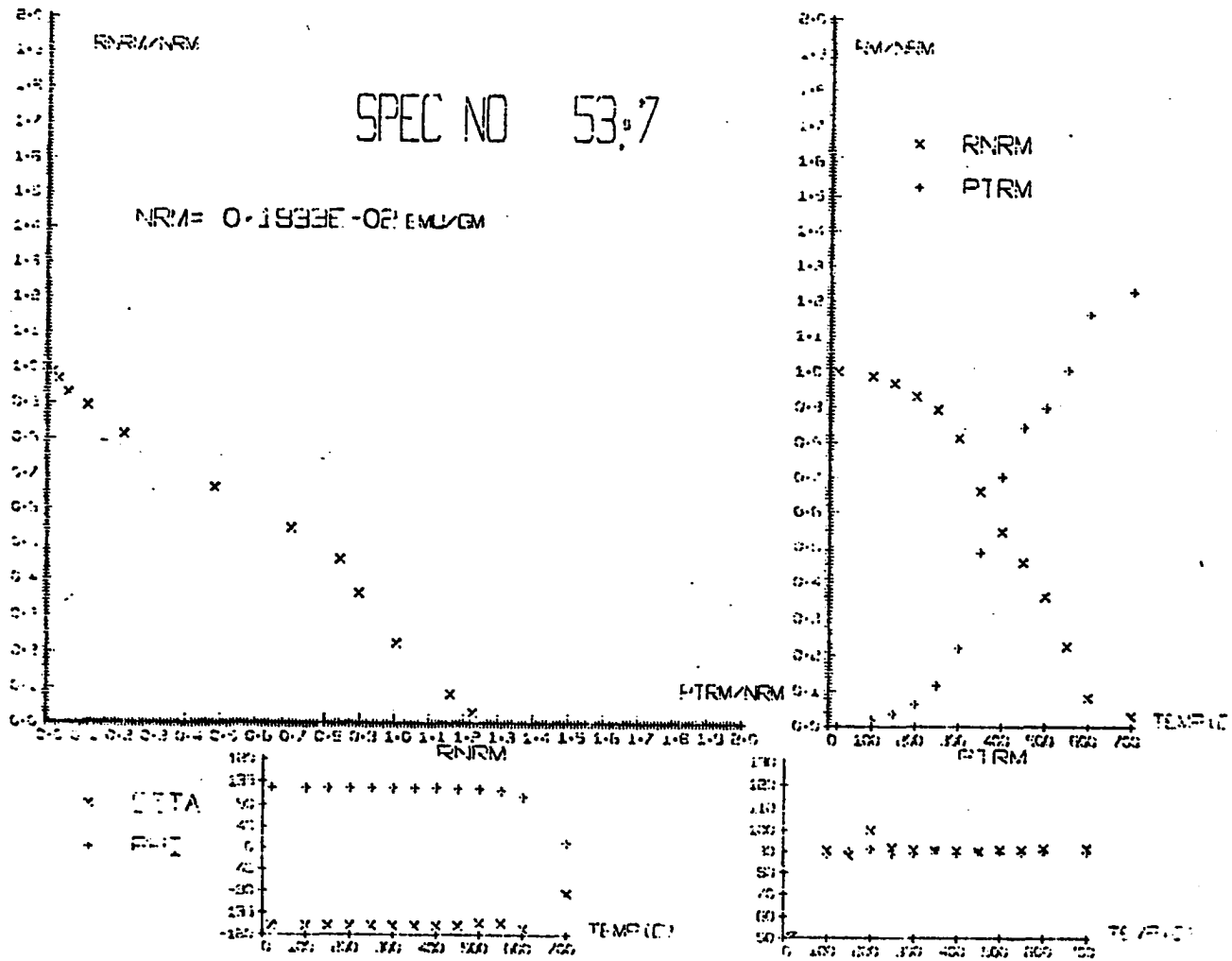

Fig. 14 Results of Spec. No. 53.7 obtained by Thelliers' Method (A).

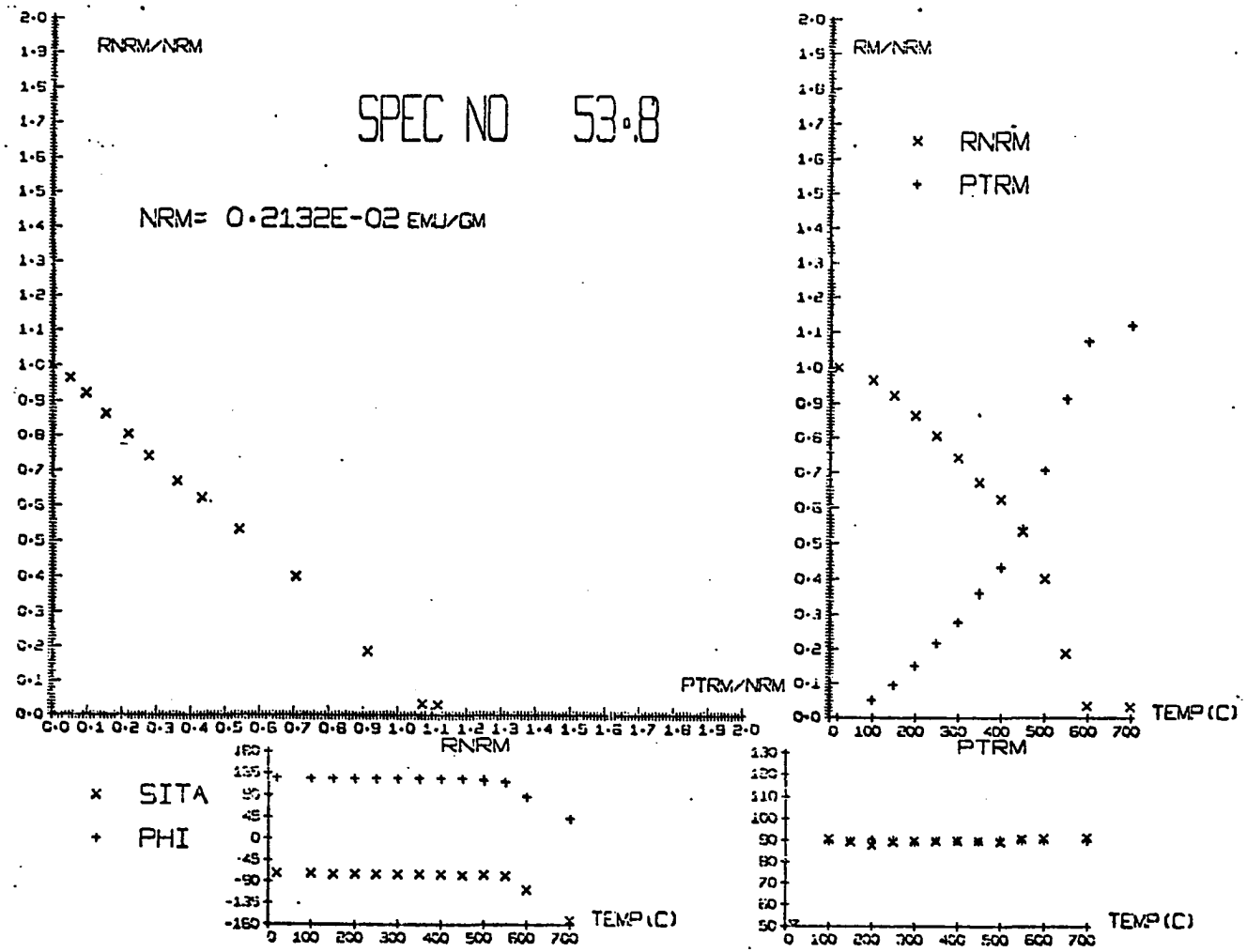

Fig. 15 Results of Spec. No. 53.8 obtained by Thelliers' Method (A).

origin in the RNRM-RTRM diagram (RTRM is the remaining TRM after AF demagnetization) can serve as the reference point because the curve (a straight line) passes through the origin. Eleven specimens from six samples were carefully measured by the AF Demagnetization Method in this study. The results suggest that some of the curves in the RNRM-RTRM diagrams are not exactly straight lines and most of the curves do not exactly pass through the origin.

The results of Spec. No.66.9 are shown in Fig. 16. The change of the orientations of the RNRM shows that this sample is very stable, the curve in the RNRM-RTRM diagram is almost a straight line but slightly concave downward, and does not pass through the origin. Because the points of zero oersted and 100 oersteds field may be affected by VRM, a least squares method to calculate the slope of the points from 150 oersteds to 1500 oersteds is used; the results show that the ancient field intensity is 0.47 oersted. Comparing this value with 0.45 oersted, which is the average value of Sample No.66, measured by Thelliers' Method, the result from the AF Method is reliable for this specimen.

The main difference between Thelliers' Method and the other three methods(which are the AF Method, ARM Method, and Wilson's Method) is that in Thelliers' Method the TRM is imparted as several PTRMs from room temperature up to the Curie point, step by step, whereas in the other three methods it is imparted continuously from the Curie point to room temperature. If the specimen has chemical or mineralogical changes during the heating from room temperature up to the Curie point, then Thelliers' Method can

demonstrate this change and give more reliable results, but the other methods cannot demonstrate these changes and have completely biased results. This will be discussed in more detail later*.

Wilson's Heating Method

Ten specimens from six samples were measured by Wilson's Method. Fig. 17 shows the results from Spec. Nos. 61.9 and 61.10; the points for 400°C, 500°C, and 600°C are almost in straight lines which pass through the origins, and it also indicates that this sample may have been reheated up to approximately 300°C. The ancient field intensities are 0.38 oersted and 0.39 oersted, respectively. Taking into account that the sample has been reheated after the original firing, the average ancient field intensity obtained by Wilson's Method is 0.39 oersted. Results from Sample No.61 as obtained by Thelliers' Method, will be shown in Fig. 53 also indicates that the sample has been reheated and the average field intensity is 0.36 oersted. Therefore, the two methods give essentially the same results for samples which have reheated after the original firing. If the sample has chemical or mineralogical changes at high temperatures, then the results of the measurements by this method will be totally incorrect.

The results of the two specimens from Sample No. 3 which are shown in Fig. 18, measured by Thelliers' Method, indicate that the sample underwent oxidation at a temperature of 700°C. The results of the three specimens from the same sample, measured by Wilson's Method, are

* See page 112.

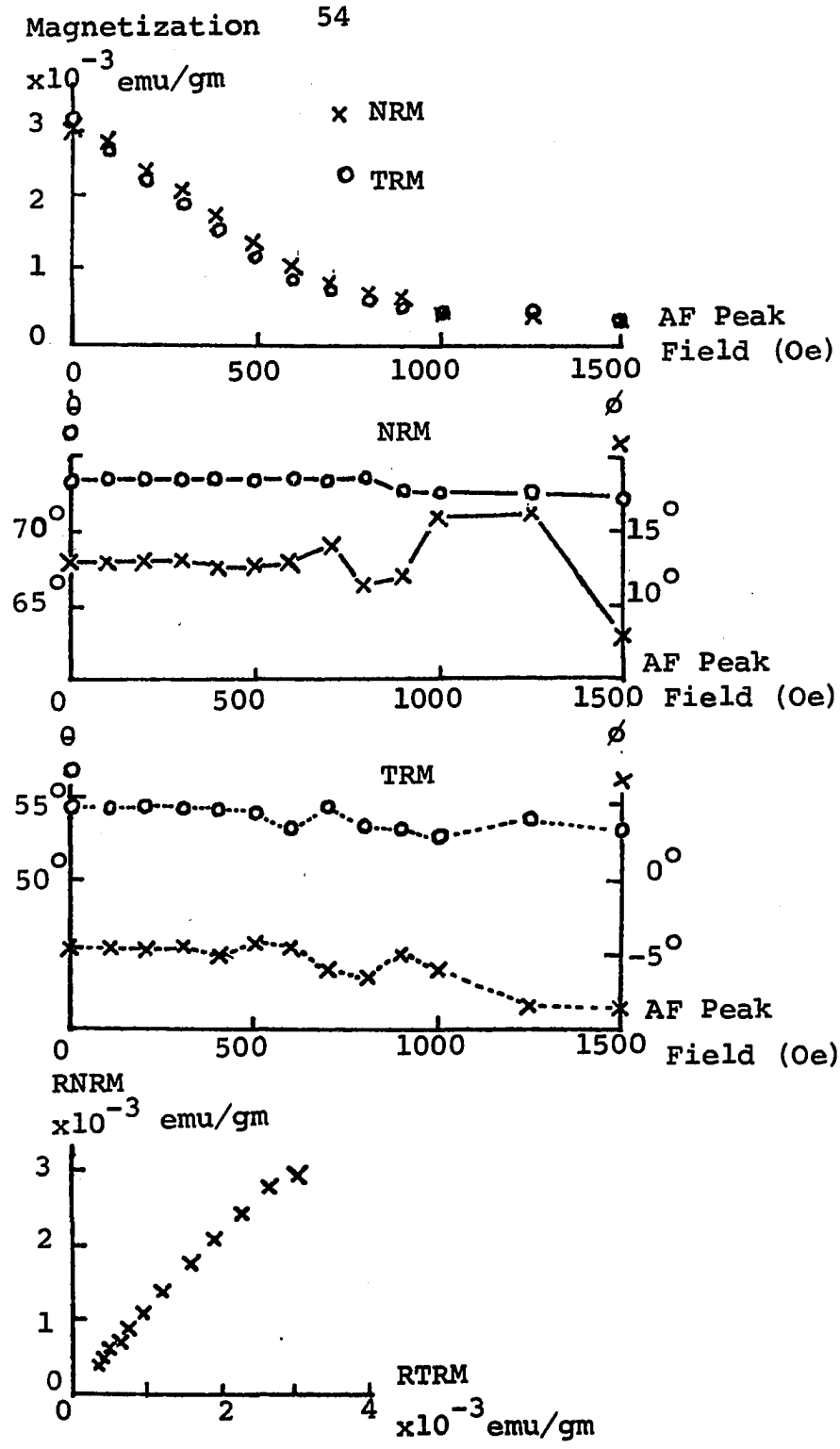

Fig. 16 Results of Spec. No.66.9 obtained by the AF Demagnetization Method.

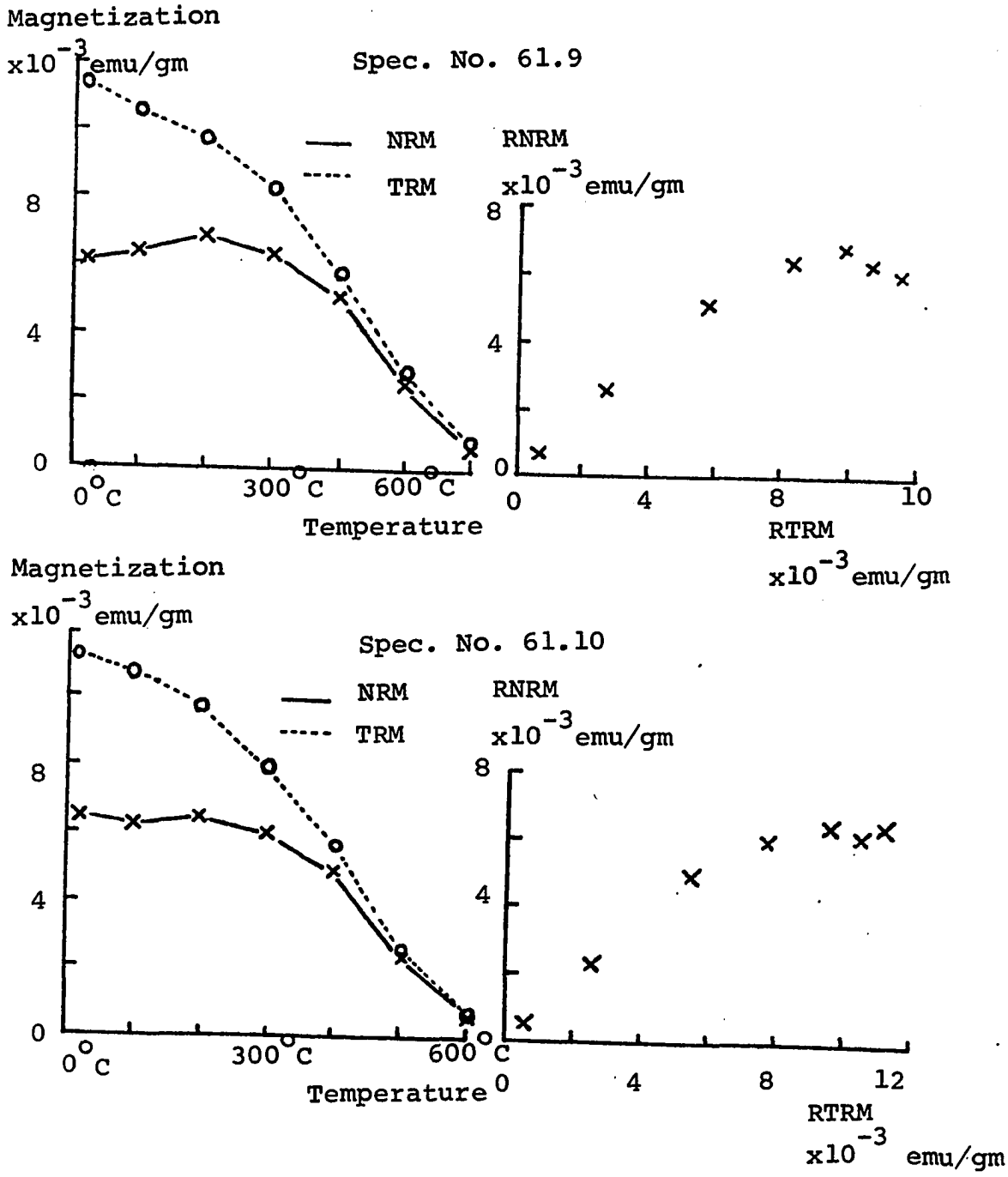

Fig. 17 Results of Sample No.61, obtained by Wilson's Method.

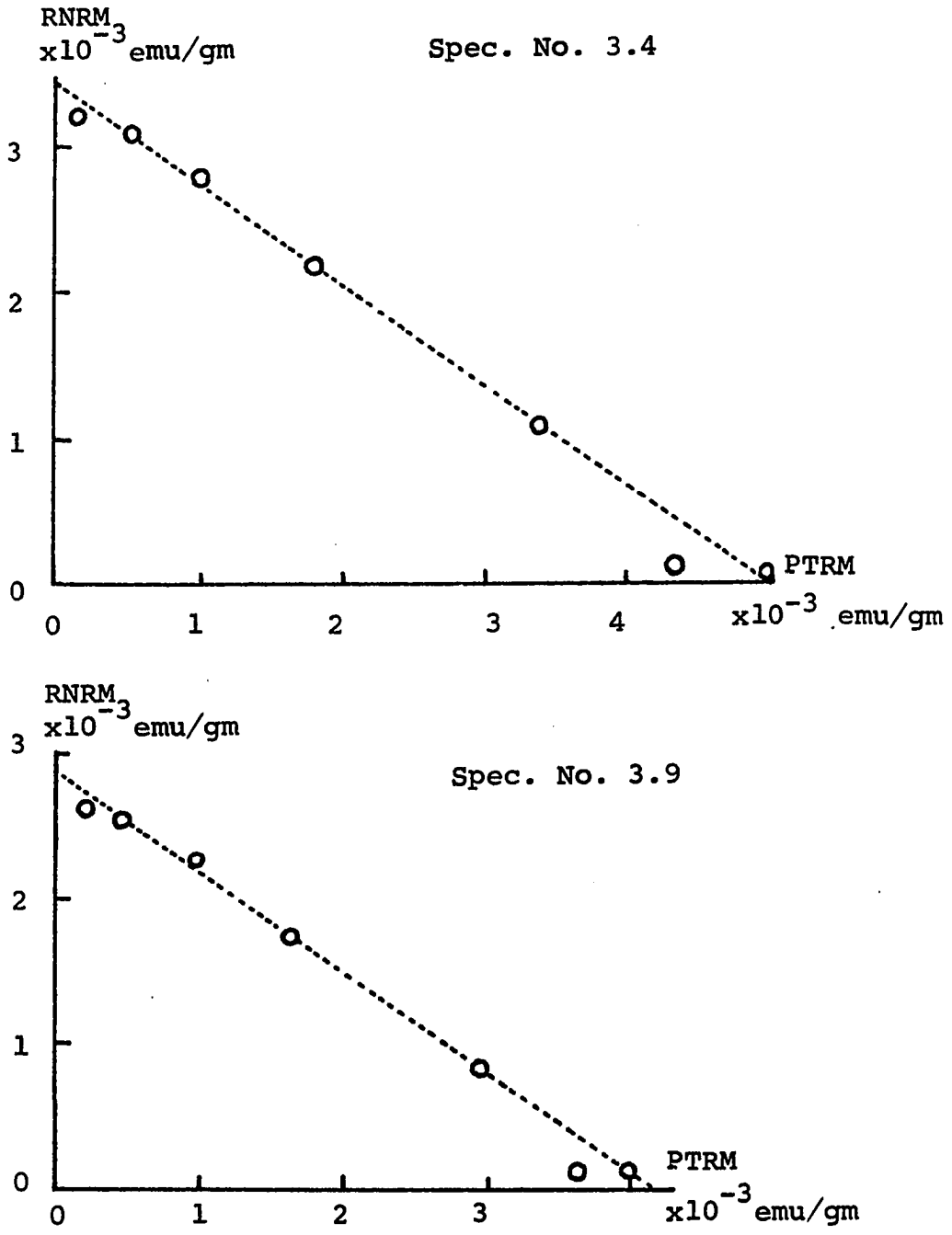

Fig. 18 Results of Spec. Nos.3.4 and 3.9, obtained by Thelliers' Method (C).

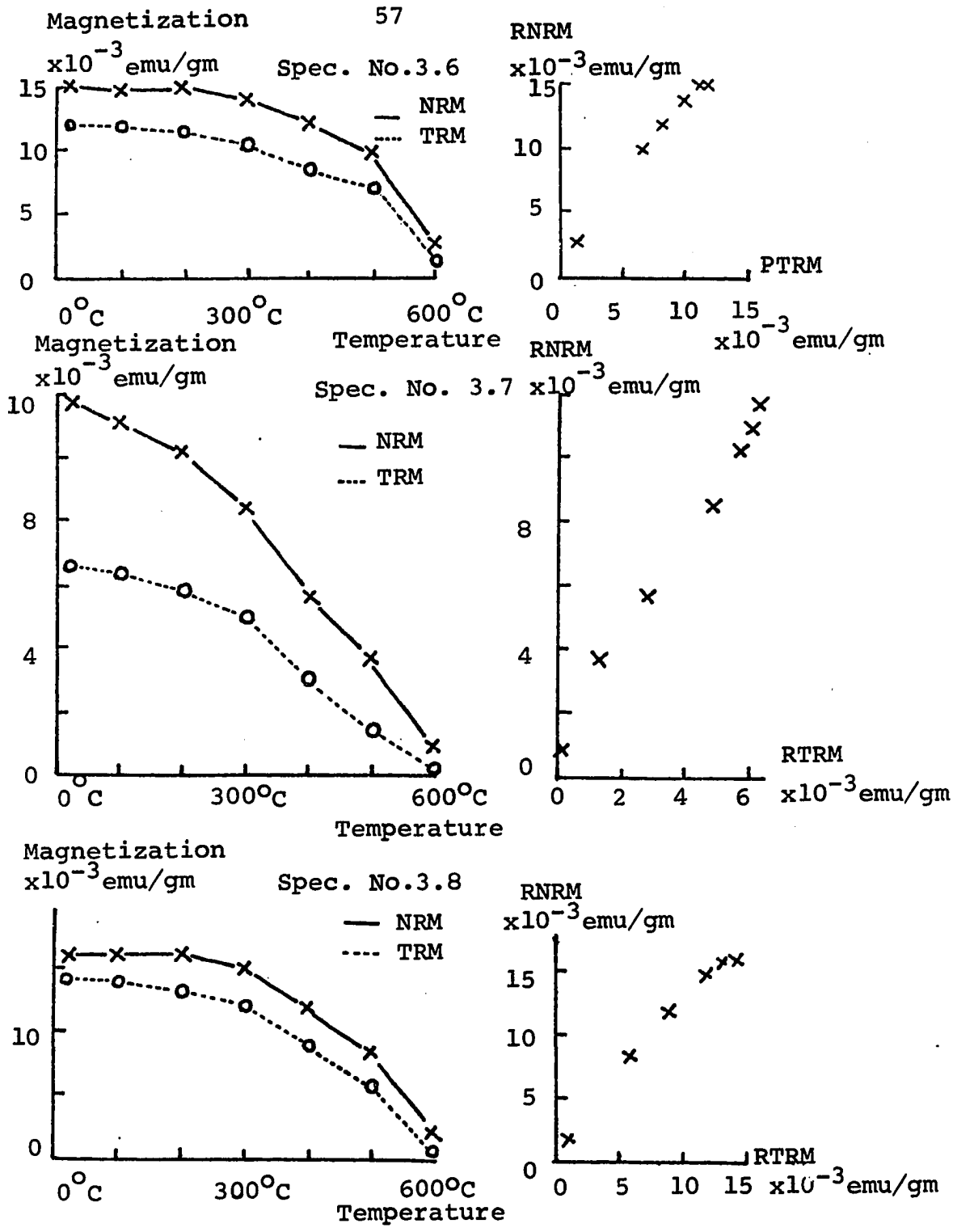

Fig. 19 Results of Spec. Nos. 3.6, 3.7, and 3.8, obtained by Wilson's Method.

shown in Fig. 19: the ancient field intensities are 0.65 oersted, 0.79 oersted, and 0.60 oersted, respectively, compared with the average ancient field intensity of 0.55 oersted from Thelliers' Method. This shows that these values are too high. This is due to oxidation; the artificial TRM of the sample is much lower than expected.

From the above discussion, it is concluded that Wilson's Method and the AF Demagnetization Method have similar drawbacks. The discussion that follows will give a comparison between Thelliers' and the AF Demagnetization Methods.

C. EXPERIMENTAL TESTING AND EVALUATION OF METHODS

Test Results by Thelliers' Method

Eight specimens from different baked clay samples were cut into 1.8 cm cubes, and one specimen from the pottery sample was cut into 1.8 cm square disk. These nine specimens were fired up to 750°C in different artificial magnetic field intensities and in different orientations relative to the artificial magnetic fields (Table 7). Then using the Thelliers' Stepwise Heating Method, these nine specimen were measured in 0.45 oersted artificial field. The RNRM-PTRM diagrams of the nine specimens are shown in Fig. 20. All the points can generally be fitted to a straight line.

The results of the calculations of all the nine specimens are shown in Table 7. Among the baked clay samples, the largest deviation between the actual magnetic field intensity and the measured field intensity is +2.76 percent, and the smallest one is only -0.07 percent.

The deviation of the pottery specimen is +5.77 percent. The results of this test experiment indicate the following: (1) Thelliers' Stepwise Heating Method is valuable in determining archeomagnetic field intensity; (2) the instruments and the calculations used in this method are correct; and (3) the results from the baked clays are more reliable than the results from the pottery.

Test Results for Reheated Samples by Thelliers' Method

The results of the measurements of the samples show that some of these samples seem to have been reheated after their original production, especially the pottery. In order to get more reliable results from the measurements by the Stepwise Heating Method, theoretical calculations and test experiments for the samples which have been reheated are necessary.

The thermal demagnetization curve of Spec. No.89.3 has been used in this theoretical calculation, because of the "almost straight line" obtained in the RNRM-PTRM curve for this specimen. Assume that the specimens had been fired in 0.45 oersted field. Using the Stepwise Heating Method the archeomagnetic field intensity is measured in the 0.44 oersted artificial magnetic field. Assume this specimen had been reheated to $400^{\circ}C$ in 0.48 oersted magnetic field. The angle between the directions of the NRM of the specimen and the 0.48 oersted magnetic field is γ. Then the NRM after reheating is :

$$\vec{OR} = \vec{ON} - \vec{OD}(400^{\circ}C) + \vec{OT}(400^{\circ}C) \qquad (2\text{-}13)$$

Table 7 Results for nine specimens in the Test Experiment of Thelliers' Method.

Spec. No.	Material	Artificial Magnetic Field Intensity F_o (Oersted)	Field Intensity Sample measured F' (Oersted)	Angle between F_o & F' (degree)	Result from measure-ment L.S.M. F (Oersted)	$\frac{F}{F_o}$	Deviation (percent)
66.40	baked clay	0.547	0.450	90	0.5491	1.0039	+ 0.39
66.50	baked clay	0.460	0.450	0	0.4597	0.9993	- 0.07
66.60	baked clay	0.547	0.450	0	0.5611	1.0276	+ 2.76
71.60	baked clay	0.350	0.450	45	0.3575	1.0215	+ 2.15
92.30	baked clay	0.350	0.450	0	0.3140	0.9744	- 2.56
111.60	baked clay	0.350	0.450	90	0.3567	1.0191	+ 1.91
112.50	baked clay	0.460	0.450	45	0.4626	1.0057	+ 0.57
112.60	baked clay	0.460	0.450	90	0.4650	1.0108	+ 1.08
61.30	pottery	0.547	0.450	45	0.5786	1.0577	+ 5.77

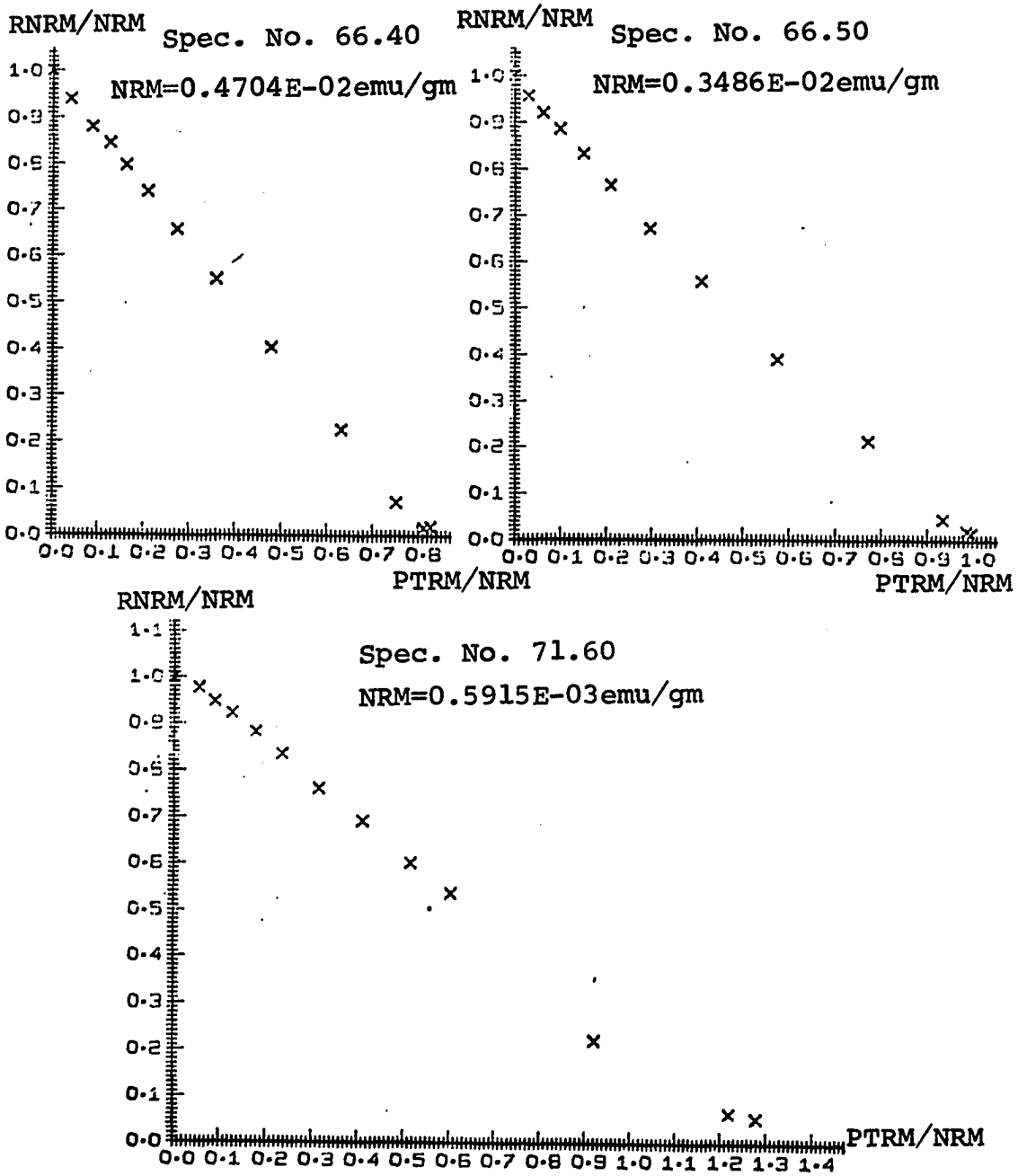

Fig. 20 Normalized (divided by NRM) RNRM-PTRM curves for the nine specimens in the Test Experiment of Thelliers' Method.

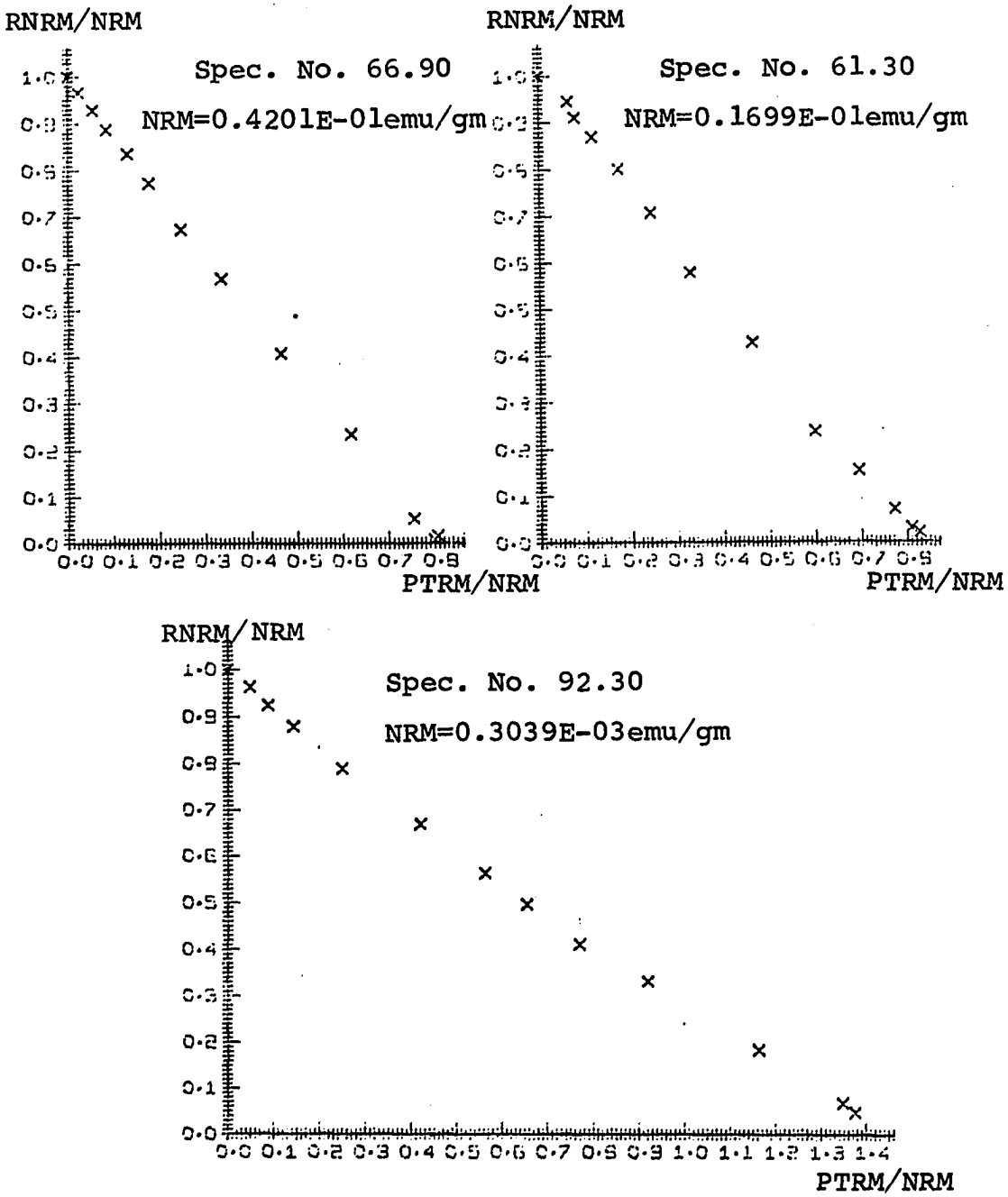

Fig. 20 (Continued)

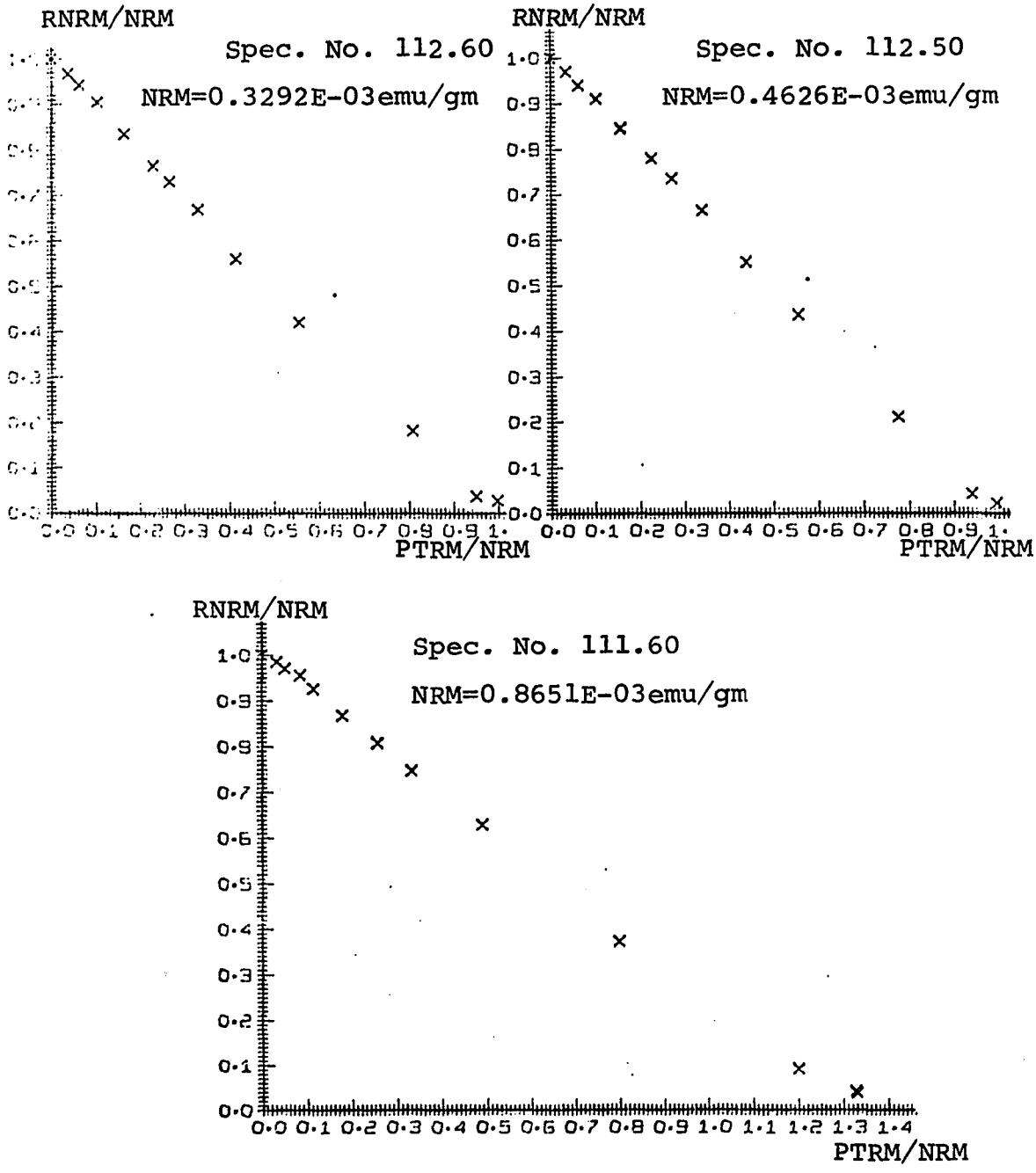

Fig. 20 (Continued)

as shown in Fig. 22. $\overrightarrow{OR}$ is the NRM after reheating; $\overrightarrow{ON}$ is the NRM before reheating; $\overrightarrow{OD}(400^{\circ}C)$ is the PTRM of the specimen cooling from $400^{\circ}C$ to room temperature in 0.45 oersted field; and $\overrightarrow{OT}(400^{\circ}C)$ is the PTRM of the specimen cooling from $400^{\circ}C$ to room temperature in 0.48 gauss field. The magnitude and the direction of $\overrightarrow{OR}$ are:

$$|\overrightarrow{OR}| = \left[\left\{ON - OD(400^{\circ}C) + OT(400^{\circ}C)\cos\gamma\right\}^2 + \left\{OT(400^{\circ}C)\sin\gamma\right\}^2\right]^{\frac{1}{2}}$$

$$\phi = \tan^{-1}\left[\frac{OT(400^{\circ}C)\sin\gamma}{ON - OD(400^{\circ}C) + OT(400^{\circ}C)\cos\gamma}\right]$$

(2-14)

Thus, using the Stepwise Heating Method to measure this specimen, the NRM after heating up to $100^{\circ}C$ will be $\overrightarrow{OR}(100^{\circ}C)$ as shown in Fig. 23:

$$\overrightarrow{OR}(100^{\circ}C) = \overrightarrow{ON} - \overrightarrow{OD}(400^{\circ}C) + \overrightarrow{OT}(400^{\circ}C) - \overrightarrow{OH}(100^{\circ}C)$$

(2-15)

$\overrightarrow{OH}(100^{\circ}C)$ is the PTRM of the specimen that has cooled from $100^{\circ}C$ to room temperature in 0.48 oersted field. The magnitude and the direction of $\overrightarrow{OR}(100^{\circ}C)$ are:

$$|\overrightarrow{OR}(100^{\circ}C)| = \left[\left\{ON - OD(400^{\circ}C) + OT(400^{\circ}C) - OH(100^{\circ}C)\cos\gamma\right\}^2 + \left\{OT(400^{\circ}C) - OH(100^{\circ}C)\sin\gamma\right\}^2\right]^{\frac{1}{2}}$$

$$\phi = \tan^{-1}\left[\frac{\left\{OT(400^{\circ}C) - OH(100^{\circ}C)\right\}\sin\gamma}{ON - OD(400^{\circ}C) + \left\{OT(400^{\circ}C) - OH(100^{\circ}C)\right\}\sin\gamma}\right]$$

(2-16)

For 100°C up to 350°C, the RNRM values, i.e. $\overrightarrow{OR}$ are calculated from equations (2-15) and (2-16), and $\overrightarrow{OH}$(100°C) is replaced by $\overrightarrow{OH}$(150°C), $\overrightarrow{OH}$(200°C), ··· , $\overrightarrow{OH}$(350°C), respectively. From 400°C to 700°C, the RNRM values are equal to the RNRM values in which the sample had not been reheated, since for temperatures higher than 400°C, the reheating component $\overrightarrow{OT}$(400°C) will be completely thermally demagnetized. Fig. 24 shows the graphic change of the RNRM of a sample, which had been reheated, during the measurement by the Stepwise Heating Method.

Assume the sample had been reheated in the different temperatures 250°C, 400°C, and 550°C, and the angle between the directions of the original NRM and the Earth magnetic field during the reheating is 0°, 30°, 60°, 90°, 120°, 150°, and 180°. All these different conditions have been calculated by the computer according to the theoretical basis, and the results of the theoretical RNRM-PTRM curves and the change of the orientation of the RNRM are shown in Fig. 25.

Specimens Nos. 66.30 and 111.40 were heated to 750°C and then cooled in 0.46 oersted magnetic field. These two specimens are reheated to 400°C, then cooled in the 0.48 oersted magnetic field. The orientation of Spec. No.66.30 is γ=180°, i.e., the direction of the NRM from the original firing is opposite to the reheated magnetic field, and the orientation of the Spec. No. 111.40 is γ=90°, i.e., the direction of the NRM from the original heating is perpendicular to the reheated magnetic field. Using Thelliers' Stepwise Heating Method to measure these two specimens in 0.45 gauss artificial field, the following results are obtained

(Fig. 26 and Fig. 27).

Comparing the results of Spec. No.66.30 in Fig. 26 with the theoretical RNRM-PTRM curves and the change of the orientation of the RNRM in Fig. 25, it shows that the result of specimen No.66.30 is similar in shape to the result of T_r =400°C and γ =180° in Fig. 25. The points of NRM, 600°C, and 700°C in the curve of the change of the orientation of RNRM in Spec. No.66.30 deviated from the straight line, due to low magnetization. The result of Spec. No.111.40 is also similar in shape to the result of T_r =400°C and γ =90°(Fig. 25). By using the least squares method to calculate the slopes of RNRM-PTRM curves above 400°C, the measured field intensities of the Spec. No.66.30 and No. 111.40 are 0.4433 oersted and 0.4464 oersted, respectively. Compared with the actual magnetic field intensity, 0.46 oersted, the deviations are only 3.62 and 2.96 percents. This result shows that Thelliers' Stepwise Heating Method is reliable even when the sample has been reheated in low temperatures.

The results of the measurements in this study show that quite a few samples, especially the pottery, have been reheated after their original firing. Sample No.59 is a typical one which had been reheated. Fig. 28 shows the result of Spec. No.59.5; the RNRM-PTRM curve and the change of the orientation of RNRM of Spec. No.59.5 are similar to that of the theoretical calculation of T_r =250°C and γ=90° in Fig. 25. The change of the orientation of RNRM of Spec. No.59.5 is not as much as that of the theoretical calculation. This is due to fact that the PTRM of Spec. No.59.5 from room temperature to 250°C is only one fourteenth of

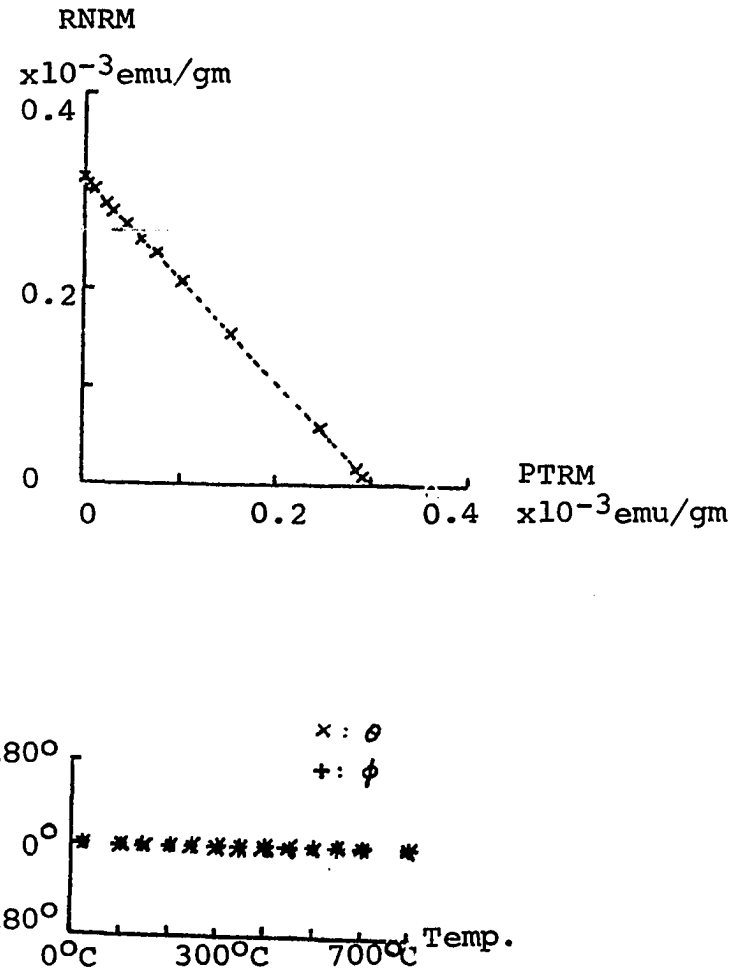

Fig. 21 RNRM-PTRM curve and the change of the orientation of RNRM of Spec. No.89.3 from theoretical calculations assuming that the ancient field is 0.45 oersted, and measured in 0.44 oersted magnetic field.

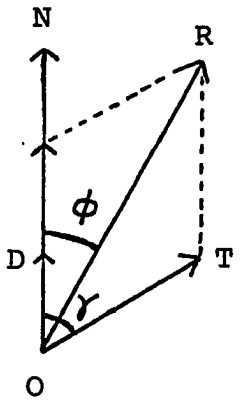

Fig. 22 $\overrightarrow{ON}$: NRM before reheating
$\overrightarrow{OR}$: NRM after reheating

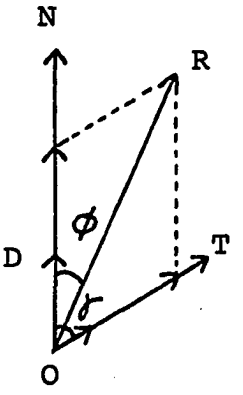

Fig. 23 The RNRM of a reheated sample after 100°C thermal demagnetization.

RNRM in Stepwise Heating Method

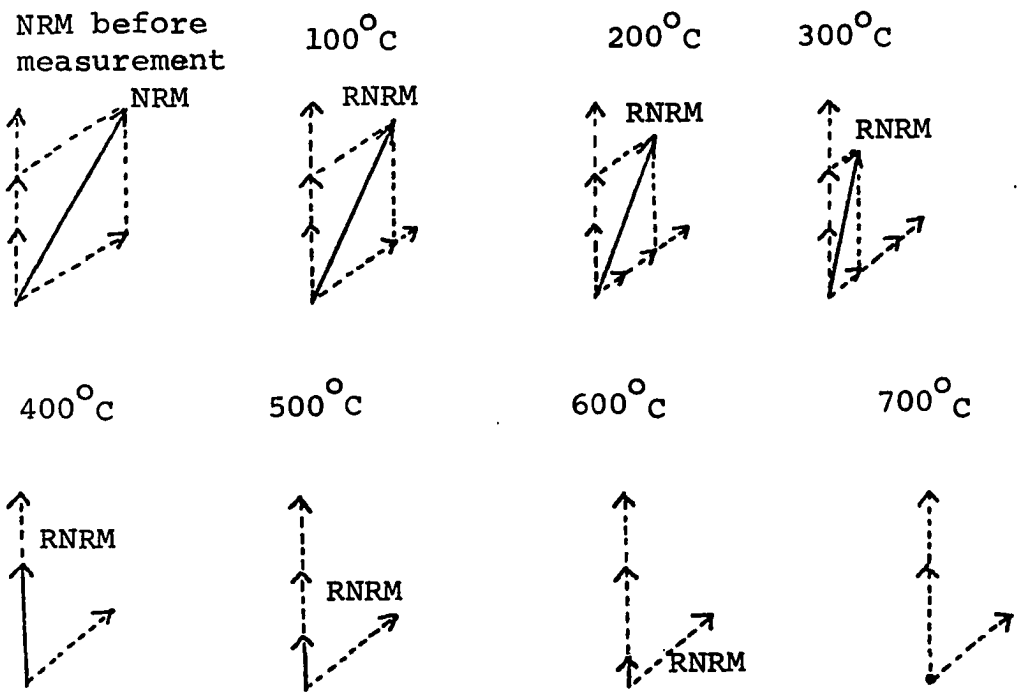

Fig. 24 The graphic change of the RNRM of a sample, which had been reheated, during the measurement by the Stepwise Heating Method.

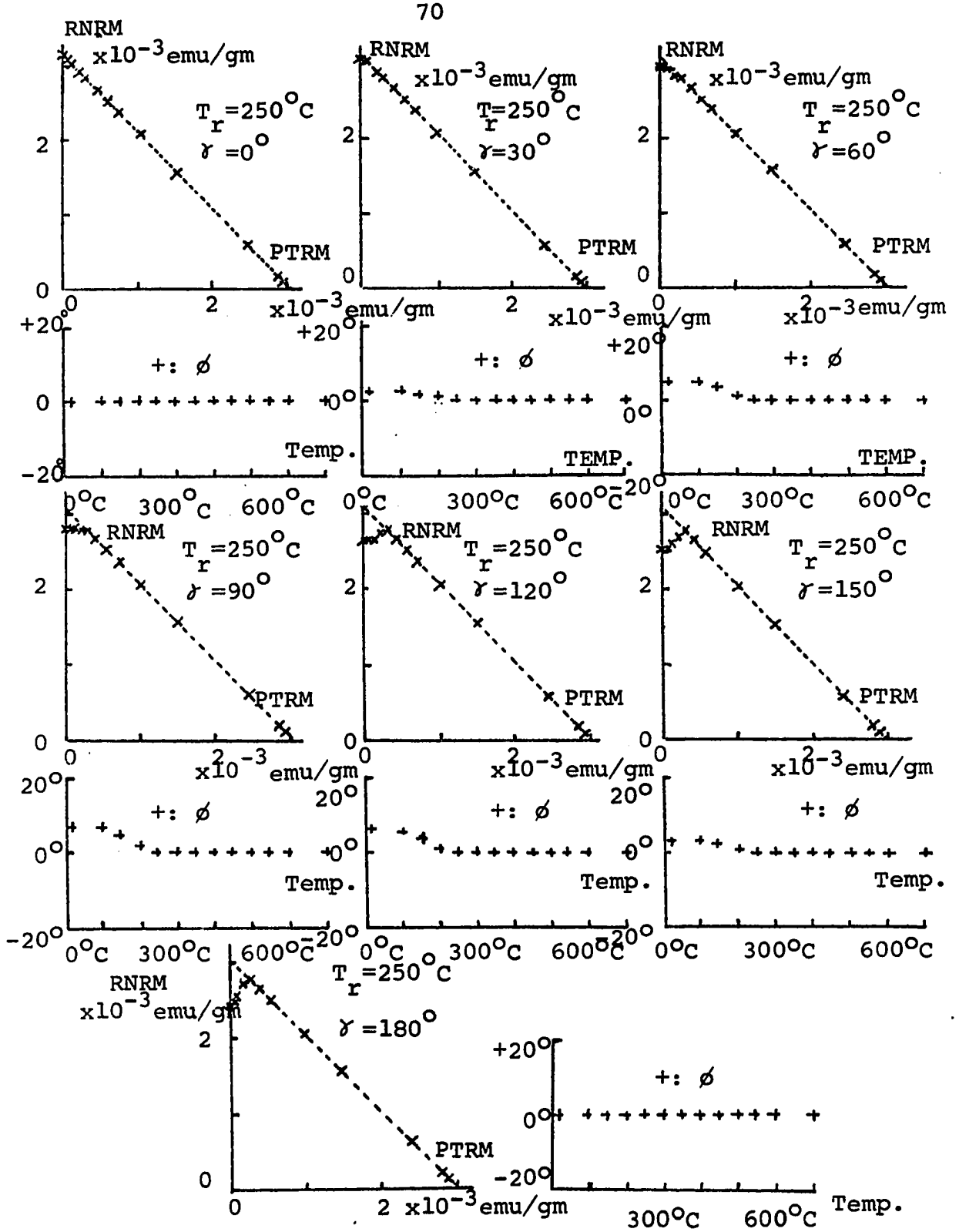

Fig. 25 Theoretical RNRM-PTRM curves and the change of the orientations of the RNRM of a reheated sample.

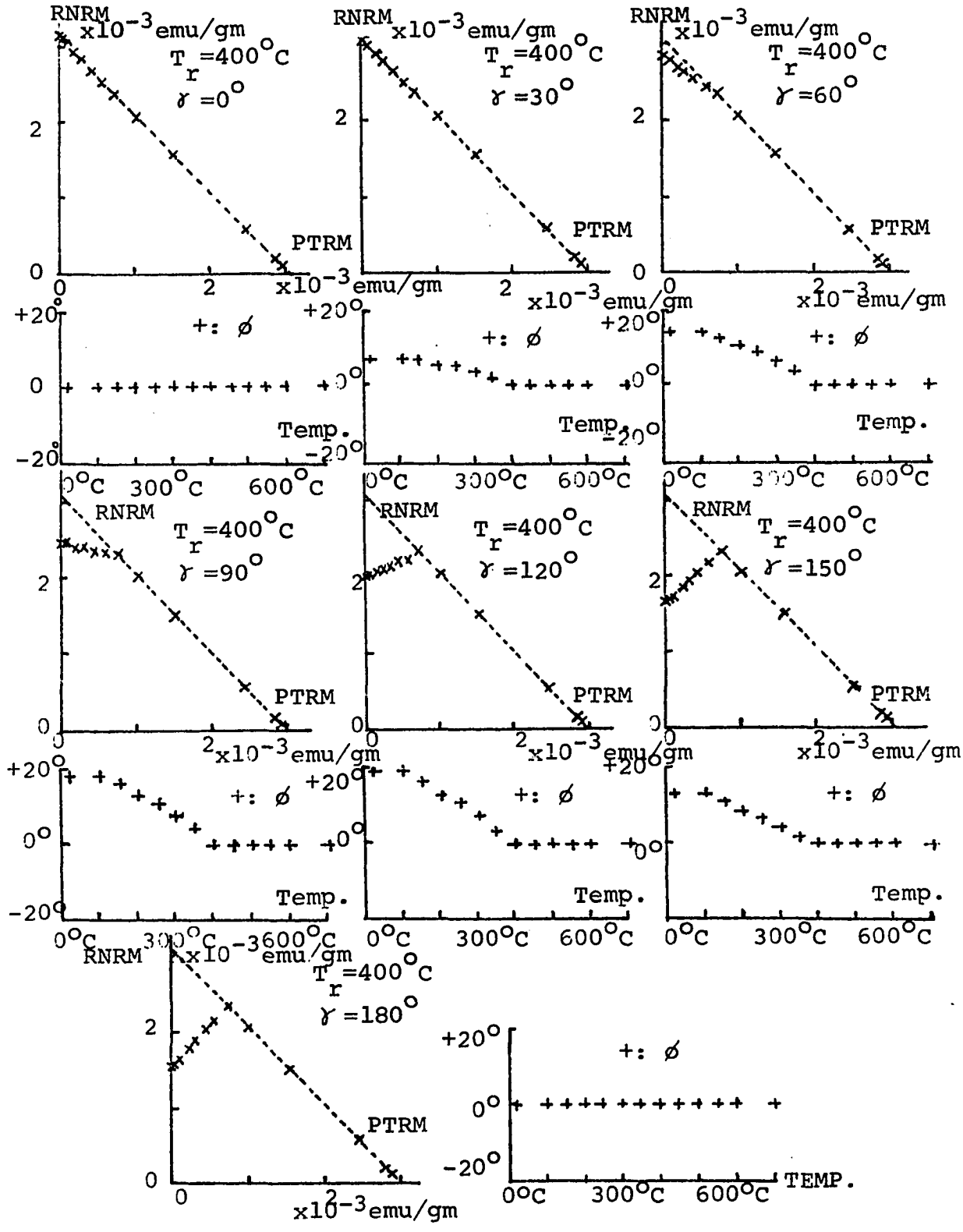

Fig. 25 (Continued)

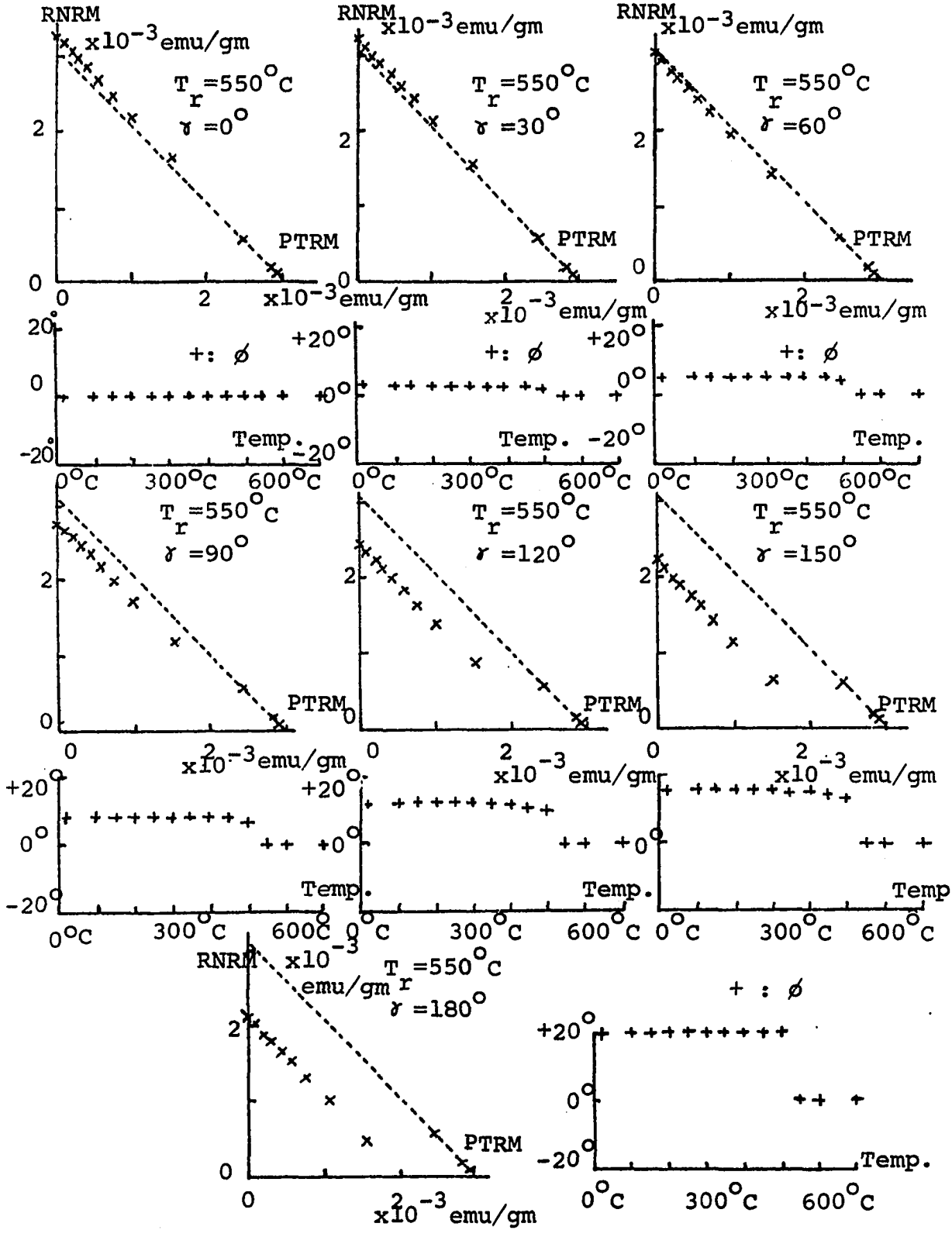

Fig. 25 (Continued)

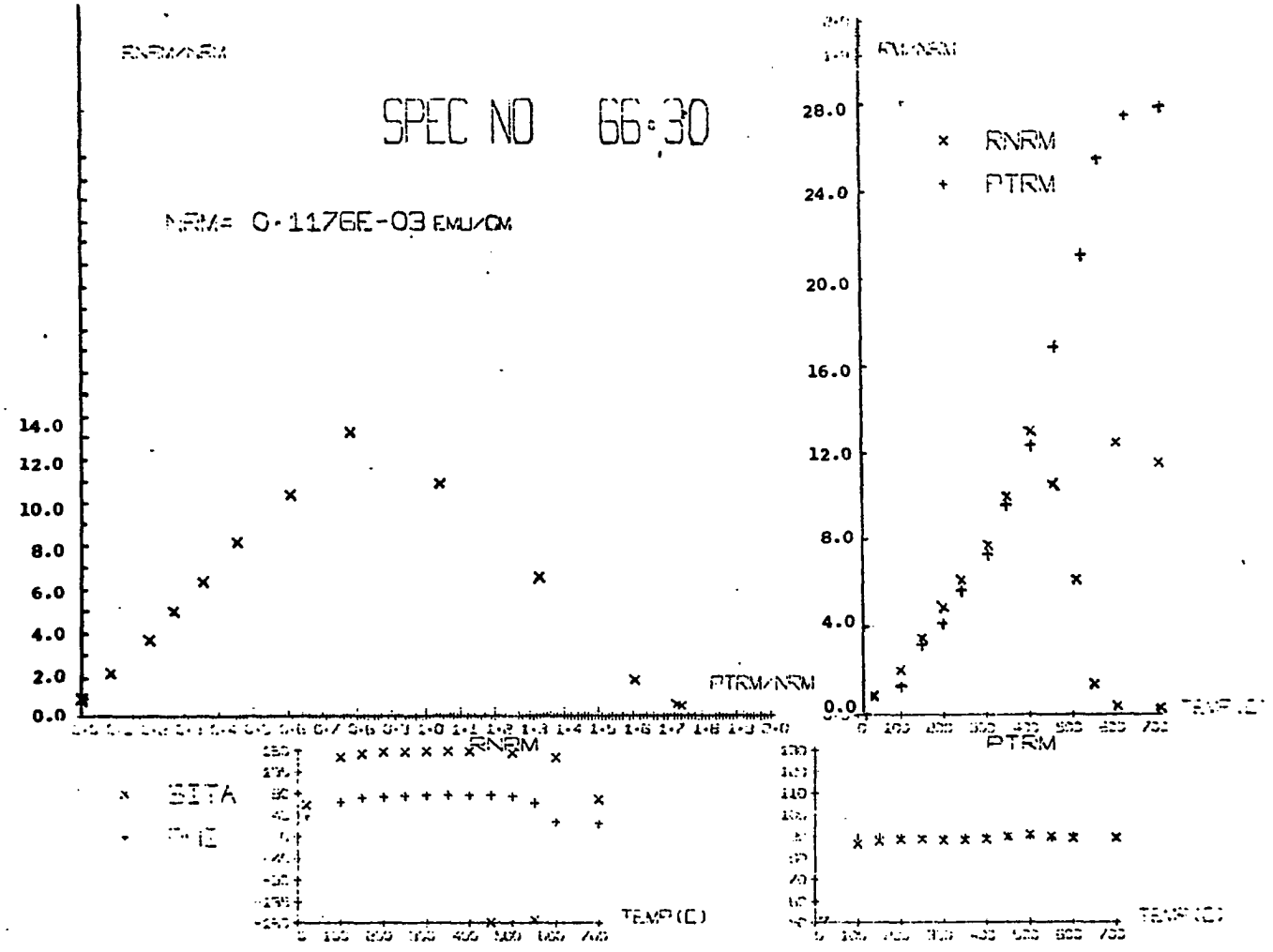

Fig. 26 Results of Spec. N0.66.30 obtained by Thelliers' Method (A).

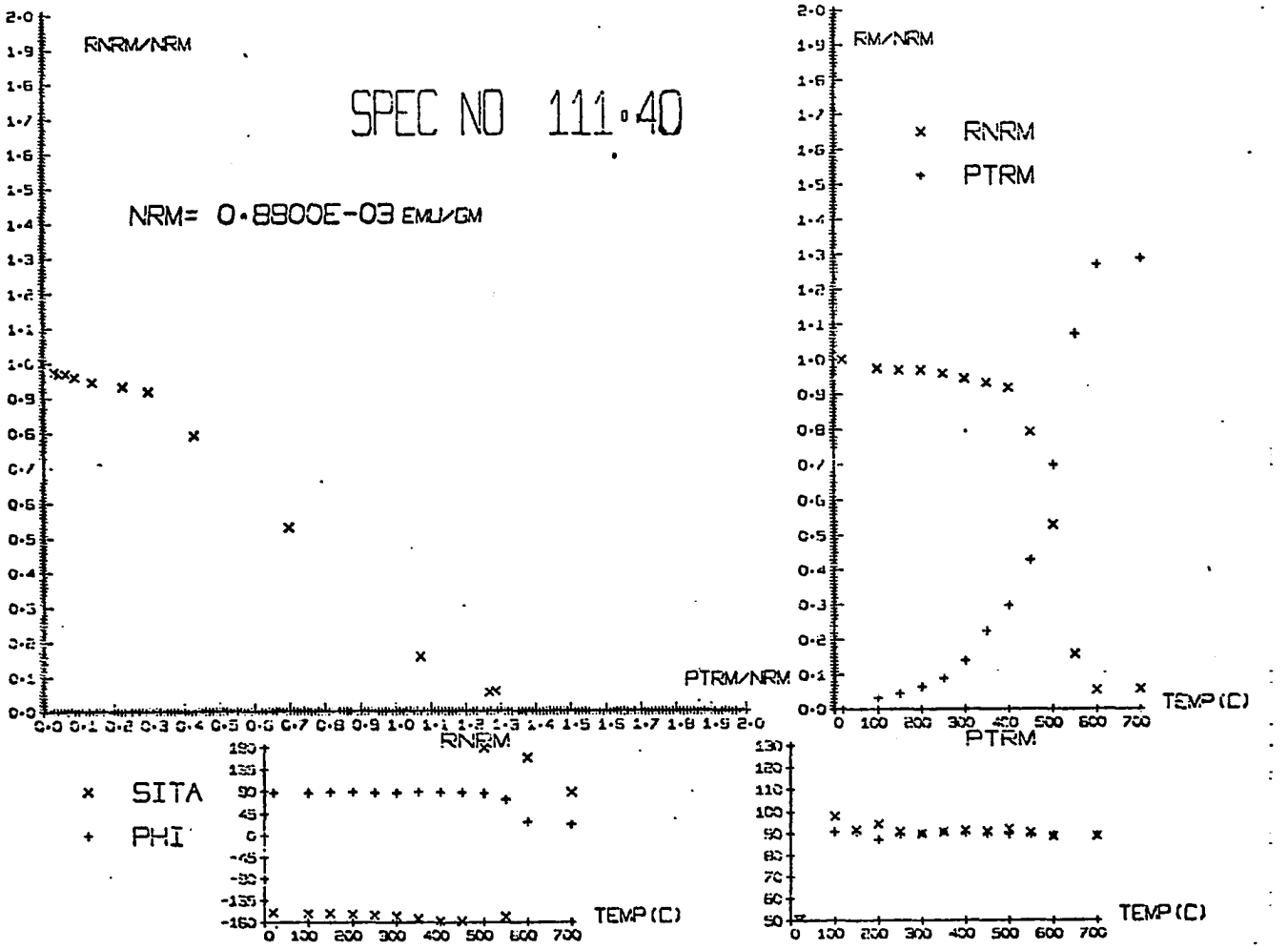

Fig. 27 Results of Spec. No.111.40 obtained by Thelliers' Method (A).

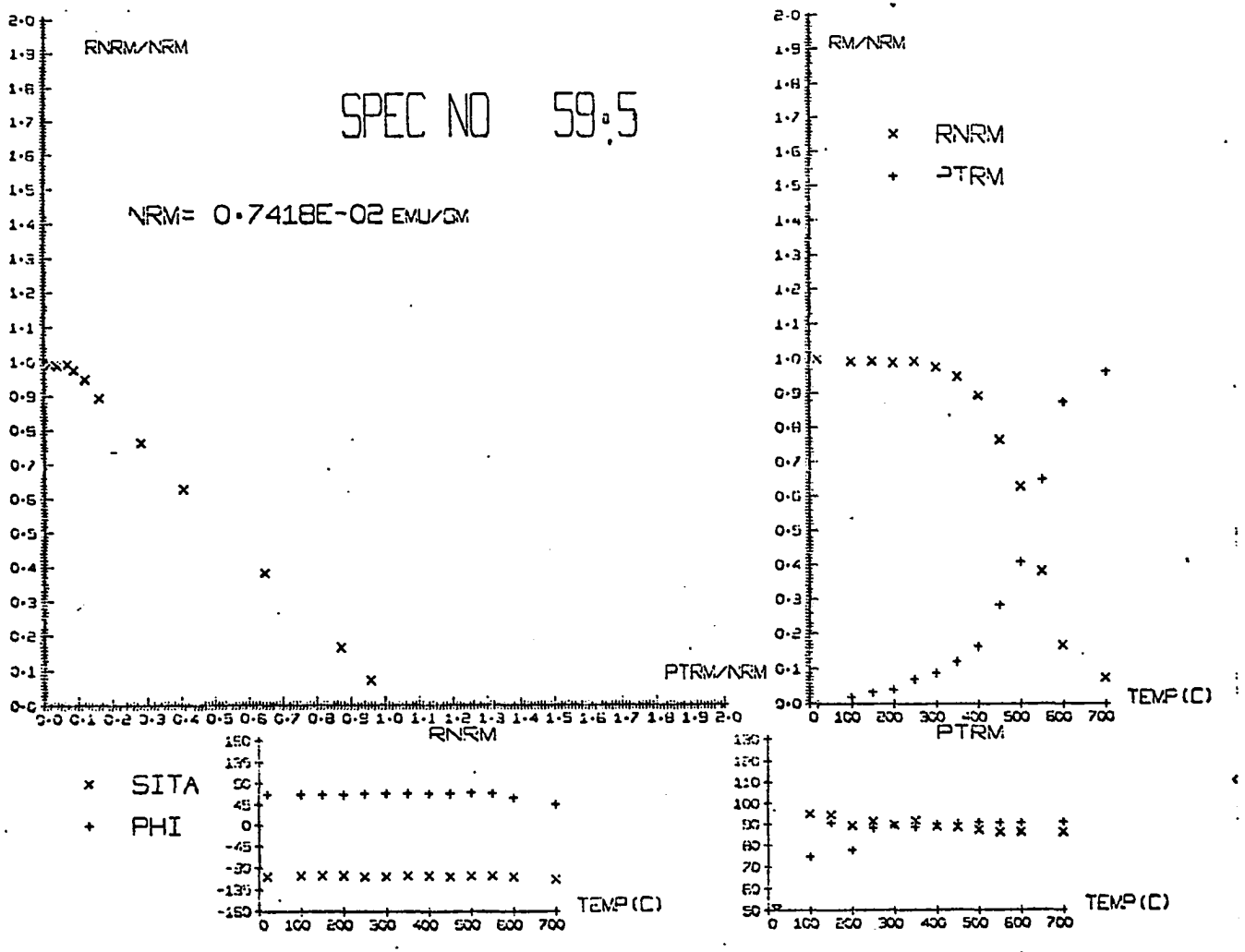

Fig. 28 Results of Spec. No.59.5 obtained by Thelliers' Method (A).

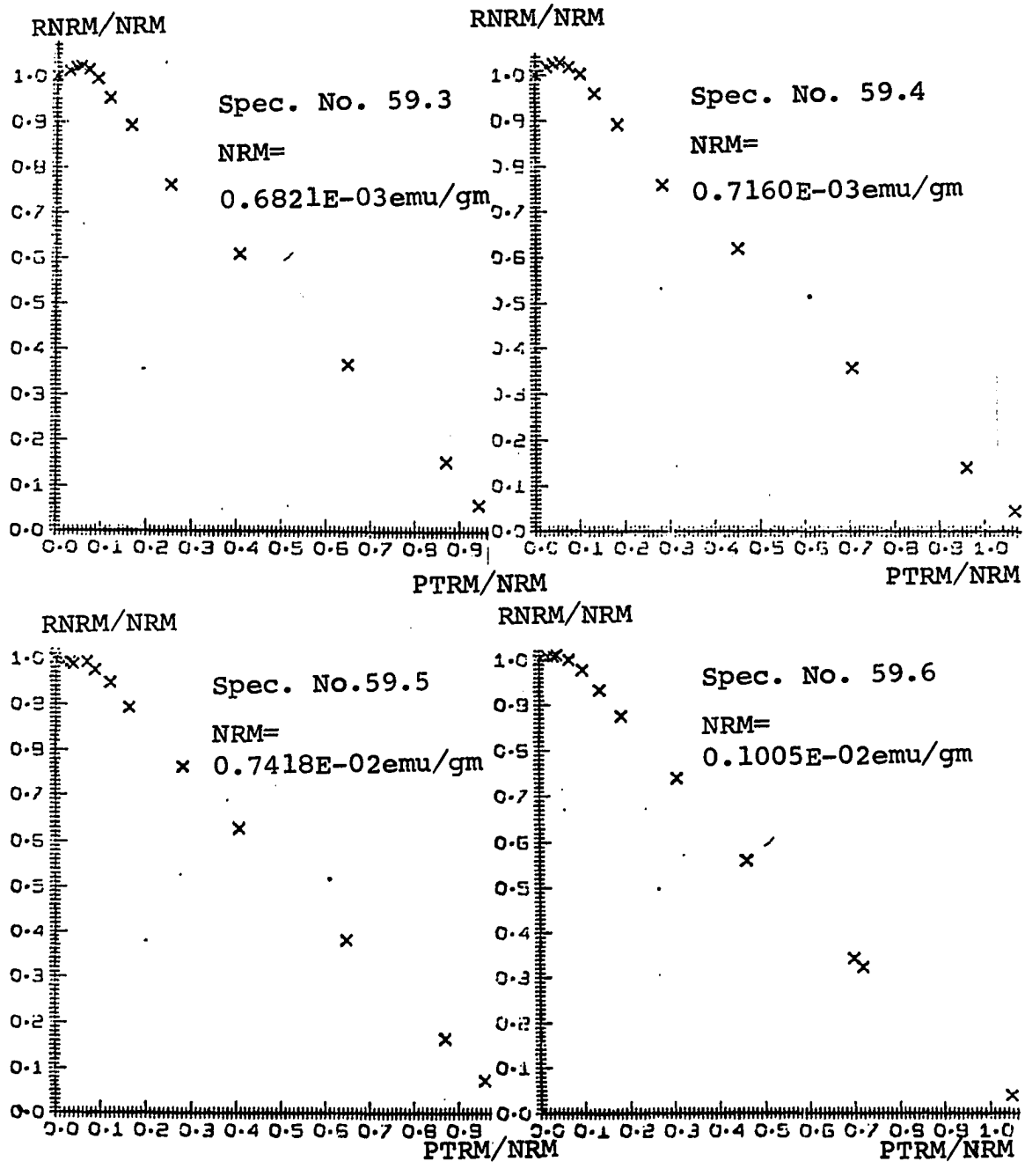

Fig. 29 Normalized RNRM-PTRM curves of four specimens from Sample No.59.

the TRM and in theoretical calculations this value is around one tenth of the TRM.

Four specimens from Sample No.59 have been carefully studied by using Method A. Fig. 29 shows the RNRM-PTRM curves and it indicates that all four specimens had been reheated up to 250°C. Using the least squares method to calculate the slope of the points between 250°C and 550°C, the results show that the ancient field intensity for these four specimens are 0.51 oersted, 0.49 oersted, 0.48 oersted, and 0.48 oersted. These four numbers are approximately equal, so the average value 0.49 oersted is a very reliable ancient field intensity for this sample.

Experimental Studies of Lightning-Struck Samples by Thelliers' Method

Samples of this study are pottery and baked clays associated with burnt rooms or hearths collected from archeological sites, and all of them have been near the surface for a long time, so the disturbing effect of lightning on the intensity measurements needs careful study.

Hallimond and Herroun (1933) first pointed out that lightning can re-magnetize a rock and disturb paleomagnetic observations. They suggested that the samples used in paleomagnetic observations shoud be taken from 50ft or more beneath the surface. Gough (1956) worked on outcrops of the Robinson dykes of the Pilansberg System in South Africa. The direction of the first group of samples, drilled from surface outcrops, showed almost random scatter with intensities of NRM ranging from 2.2×10^{-2} emu/cm^3 to 4×10^{-1} emu/cm^3 as shown in Fig. 30. The directions of the

samples from underground workings in the mining areas showed extremely good consistency with the mean intensity of magnetization of 2.8×10^{-3} emu/cm^3.

Fig. 31 shows the demagnetization curves measured by Graham (1961) for specimens probably magnetized by natural lightning, the specimens magnetized by a DC field, and the specimens magnetized by an artificial spark discharge. Graham pointed out that the demagnetization curves for the specimens thought to be magnetized by lightning begin with a gentle slope which increases to a point where the curves becomes nearly linear. The curves for the specimens magnetized by a DC field (duration from 15 sec. to 28 hrs.) do not show this initial gentle slope, and the curves for specimens magnetized by the field due to an artificial spark discharge (duration from 1.4 sec. to 10 sec.) resemble the curves for the specimens magnetized by natural lightning.

Actually all the three types of curves are quite similar. The initial gentle slope of the AC demagnetization curves of the specimens, which were probably magnetized by lightning, may be caused from the fact that some soft component of magnetization had been demagnetized by the effects of thermal fluctuations, weathering, etc. for geological periods of time. Graham pointed out that the pattern of the direct remanent magnetic observation represented in Fig. 30 is consistent with one that would be produced by an electric current flowing along a single straight conductor passing perpendicularly into the plane of the section at the point marked by C. So the magnetization occuring in rocks struck by lightning seems likely

to be IRM.

Recently Banerjee and Mellema (1974) measured AF demagnetization curves of 1 oersted ARM and TRM for a sample containing 1 % of magnetic, single-domain CrO_2 powder. It was seen that after normalization the above curves were identical for every value of H_{AF} (Alternating magnetic field intensity), indicating that the mechanism of ARM is very similar to that of TRM.

TRM is very resistant to AF demagnetization, whereas IRM can usually be destroyed by an AF field of similar magnitude as that of the original magnetizations of Sample Nos. 15 and 111 which, described later*, will confirm that the remanent magnetization of the rocks struck by lightning is not ARM, though a few investigators belive it seem likely to be ARM (Nagata, 1961).

The thermal demagnetization curve of Spec. No. 89.3 has been used in this theoretical calculation. The intensity and the characteristics of the IRM added to the sample struck by lightning depend upon the strength of the lightning and the distance from the sample to the lightning.

Roquet (1954) measured the thermal demagnetization curves (for dispersed magnetite powder) for TRM and IRM produced in various magnetic field, as shown in Fig. 32. The thermal demagnetization curve of IRM produced in an 88 oersted magnetic field has been used as a basis for calculation, and we assumed that the intensity of the IRM is half that of the NRM (TRM). Fig.33 (a) shows the ideal result of RNRM-PTRM curve for Spec. No.89.3, provided the sample has not

* see page 81.

been struck by lightning. Fig. 33(b) represents the thermal demagnetization curves of TRM and IRM. In Fig. 33(c), γ represents the angle between TRM and IRM. Assuming γ equal to 0^{o}, 30^{o}, 60^{o}, 90^{o}, 120^{o}, 150^{o}, and 180^{o}(all these different conditions have been calculated by the computer, according to the theoretical basis), the results of the theoretical RNRM-PTRM curves and the changes of the orientation of RNRM are shown in Fig. 34.

This theoretical calculation shows that the IRM from lightning will bias the results in ancient field intensity measurements if the results are calculated only from the slope of the RNRM-PTRM curve. Fig. 35 shows the results of Spec. Nos. 15.1 and 111.6, respectively. The RNRM-PTRM curves and the changes of the orientations of RNRMs of both Spec. Nos. 15.1 and 111.6 are similar to that of the theoretical calculations using $\gamma = 30^{o}$ (Fig.34). This means that both Samples Nos. 15 and 111 had been struck by lightning after their original firing. The RNRM-PTRM curves of Spec. Nos. 15.1 and 111.6 are much steeper than that of the theoretical calculation. This phenomenon is due to the fact that the IRM is almost six times greater than the TRM in Spec. No.15.1, and the IRM is almost equal to the TRM in Spec. No.111.6, which be described later*, but in the theoretical calculation, it is assumed that the IRM is only half of the TRM.

In order to confirm that Sample No.15 and 111 had been struck by lightning and acquired IRM, the AF demagnetization has been run for Spec. Nos .15.3 and 111.7. The results are shown in Fig. 36 and Fig. 37. The AF demag-

* See page 81.

netization curve of the NRM of Spec. No.15.3 declines rapidly as shown in Fig. 36(a), a typical AF demagnetization curve of IRM. Spec. No.15.3 has been fired up to 750°C, then cooled down to room temperature in a 0.45 oersted magnetic field. The residual magnetization thus acquired is TRM, which is then demagnetized by the AF method. The AF demagnetization curve of the TRM is also shown in Fig. 36(a). It decreases with a gentle slope which indicates that the TRM has a high degree of stability. The magnetization of the NRM is almost seven times that of TRM, the former is 0.1156×10^{-1} emu/gm and the latter is 0.1639×10^{-2} emu/gm. This means that the IRM from the natural lightning is around six times that of the original NRM (TRM).

Comparing these two curves, it shows that the IRM is almost reduced to zero upon AF demagnetization of 300 oersteds. After 300 oersteds, the AF demagnetization curve of the NRM is almost equal to that of the original NRM (TRM) which has not been struck by lightning. This fact is one of the advantages, of the AF Demagnetization Method as we shall see later*. Fig. 36(b) shows the normalized AF demagnetization curves for NRM and TRM. Fig. 36(c) presents the changes of the orientations of NRM during AF demagnetization; Fig. 36 (d) shows the orientation of the TRM is very stable during AF demagnetization.

Fig. 37 shows the results of AF demagnetization of Spec. No.111.7. It is quite similar to Fig. 36 except for the two following facts: (1) The magnetization of the NRM

* See page 112.

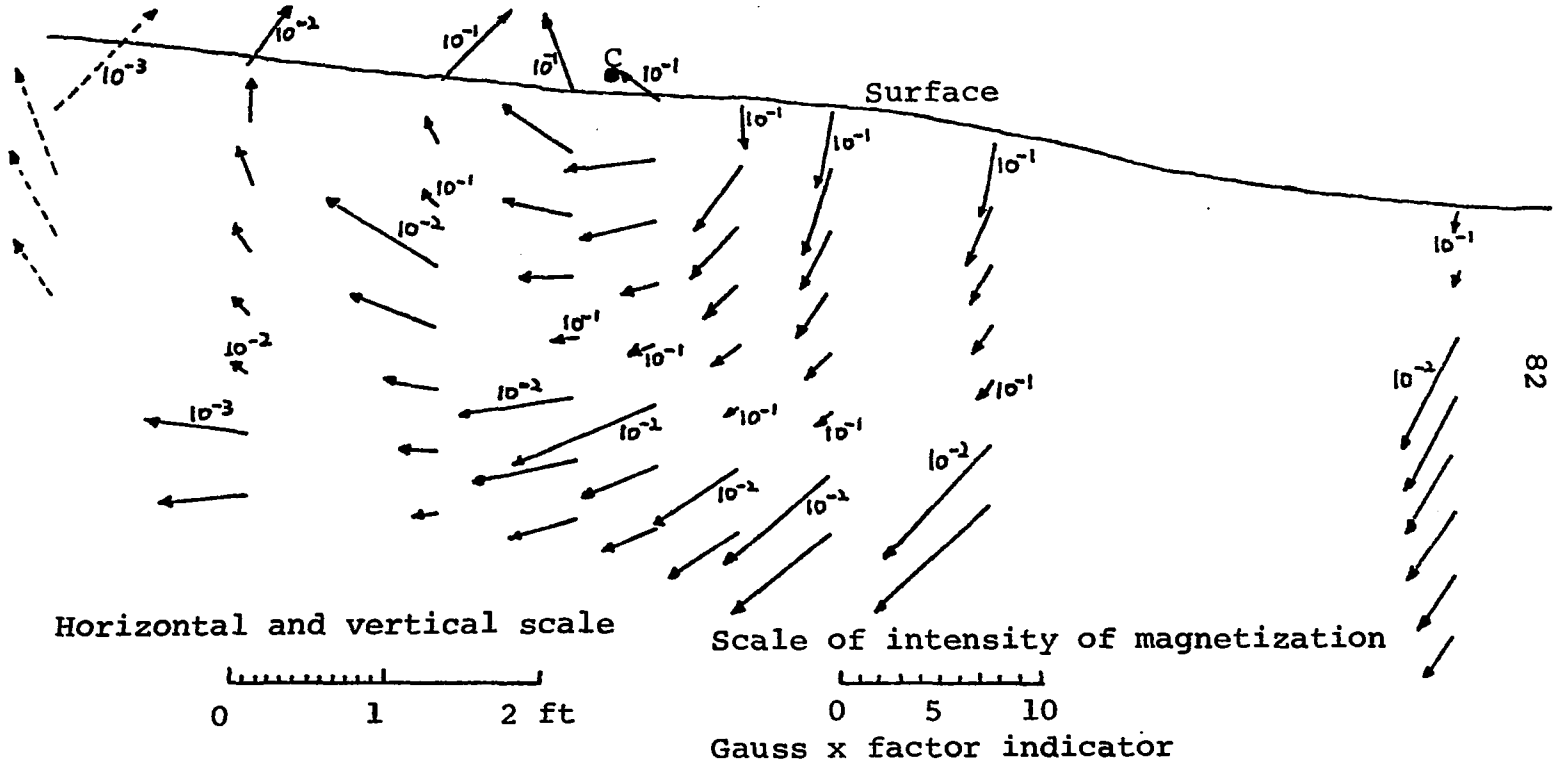

Fig. 30 Section in NE/SW plane, through an outcrop of the Robinson dike showing the variations of the direction and intensity of magnetization , about 5×10^4 amp current at C. Redrawn from Graham (1961).

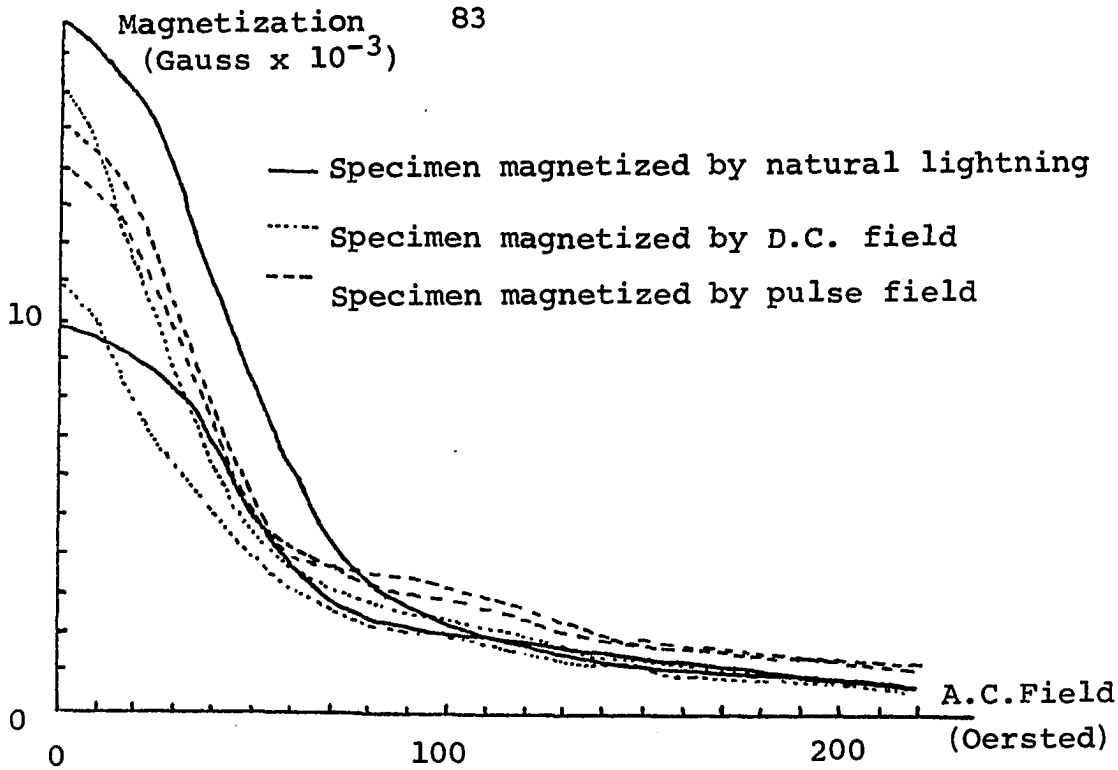

Fig. 31 The demagnetization curves for the three different kinds of specimens. Redrawn from Graham (1961).

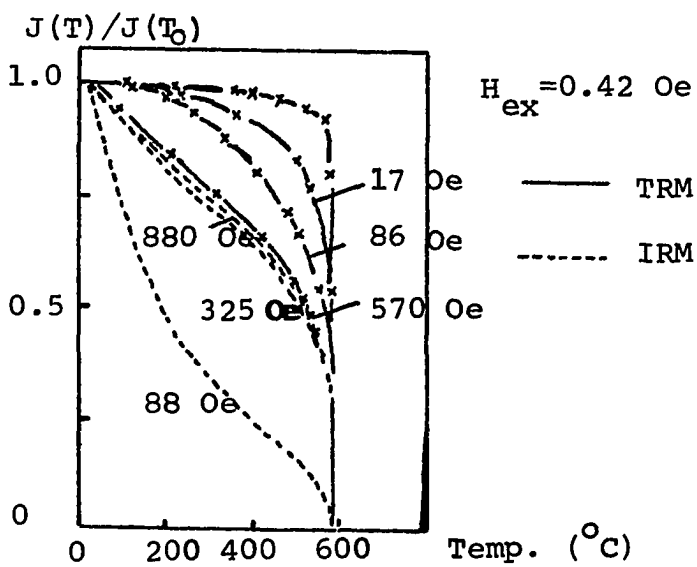

Fig. 32 Thermal demagnetization of TRM and IRM, produced in various H_{ex}. Sample: dispersed powder of magnetite. Redrawn from Roquet (1954).

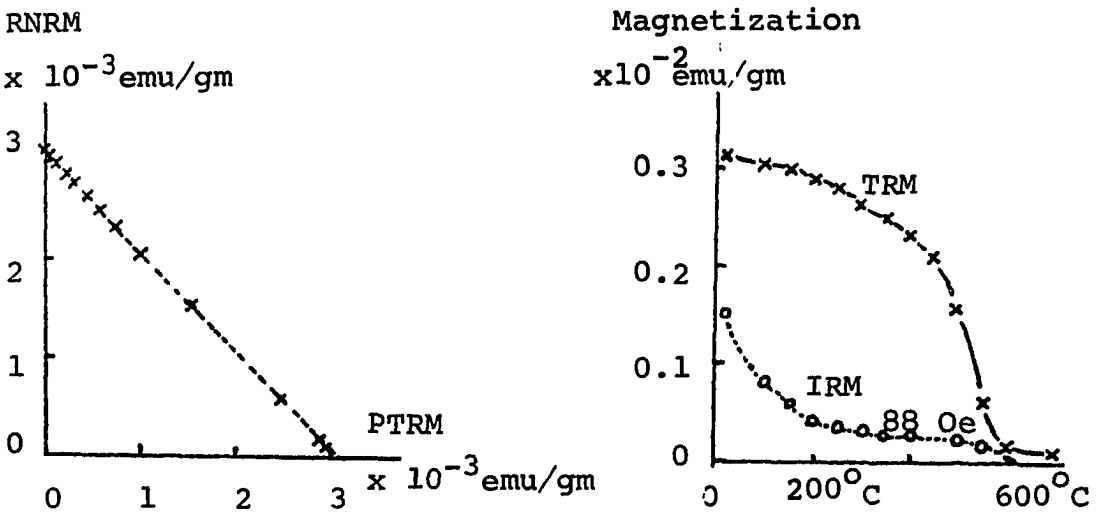

(a) (b)

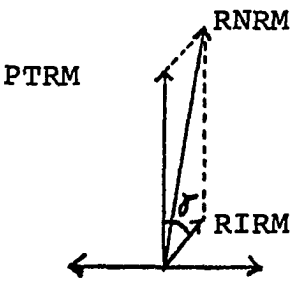

(c)

Fig. 33 (a) RNRM curve for Spec. No.39.3 (no lightning effect).
(b) Thermal demagnetization curves of TRM and IRM.
(c) Relation between PTRM and RIRM during measurement.

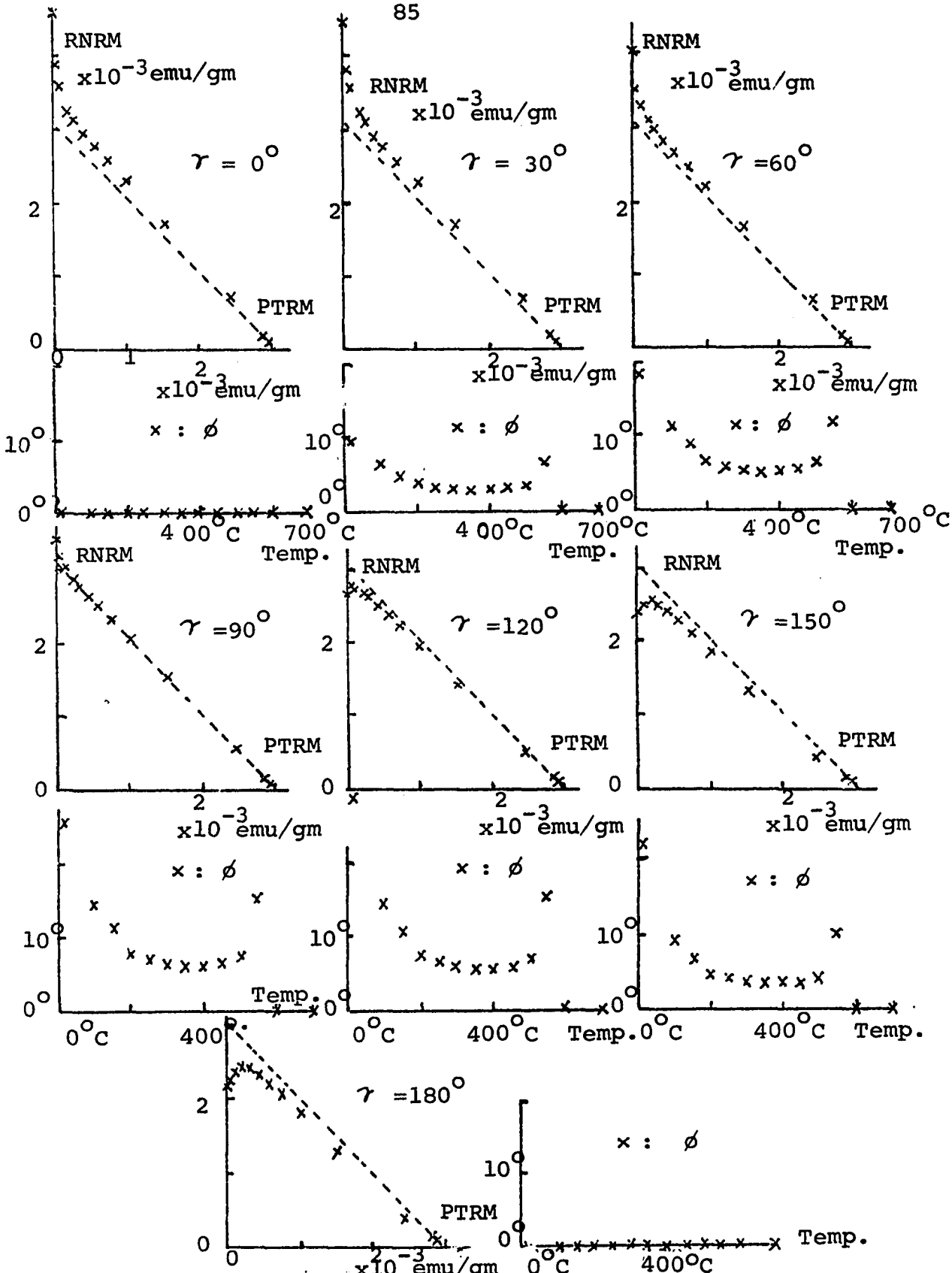

Fig. 34 Calculated RNRM-PTRM curves and change of orientation of RNRM with isothermal remanent magnetization.

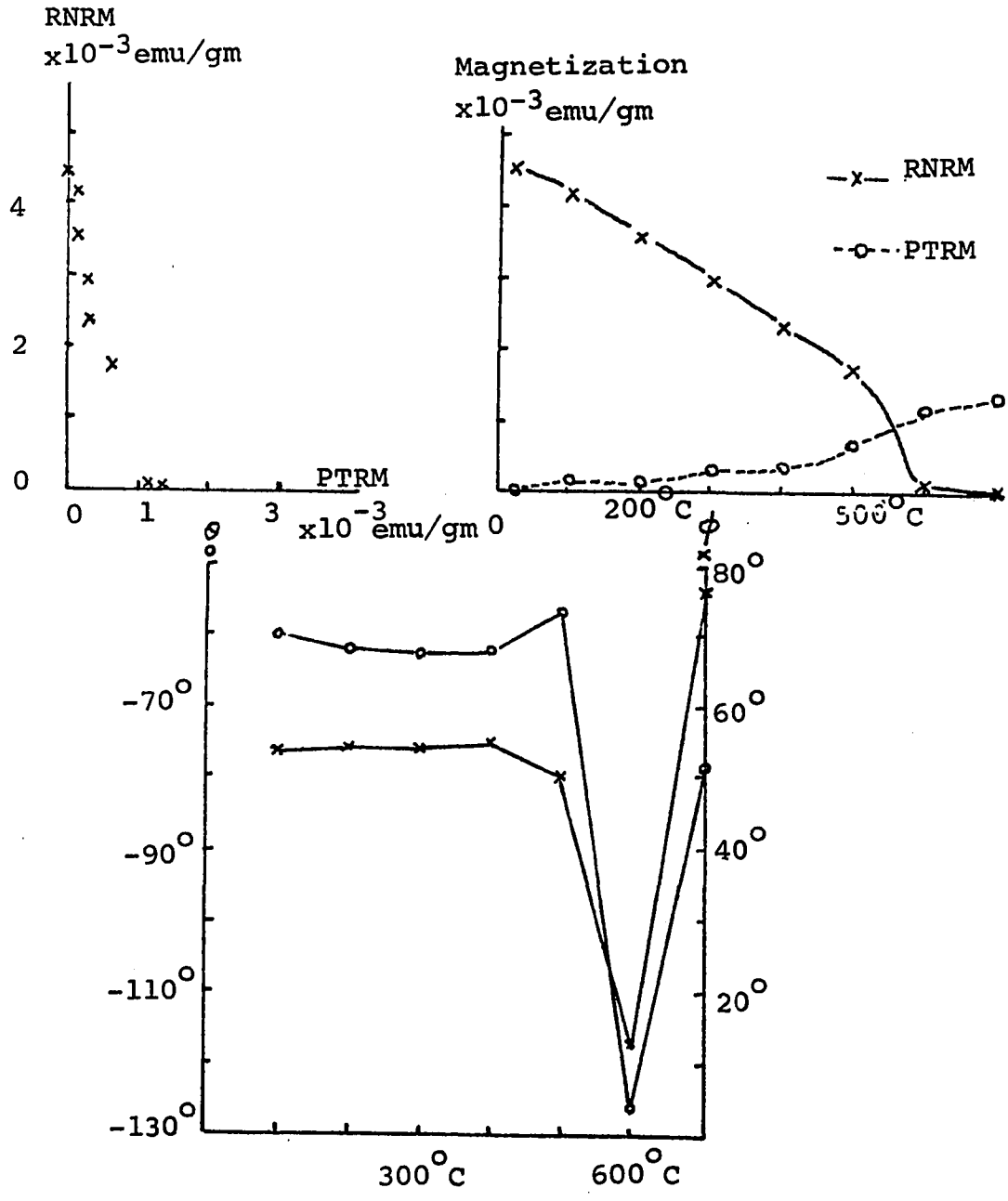

(a)

Fig. 35 (a) Results of Spec. No.15.1 .
(b) Results of Spec. No.111.6 obtained by Thelliers Method (A).

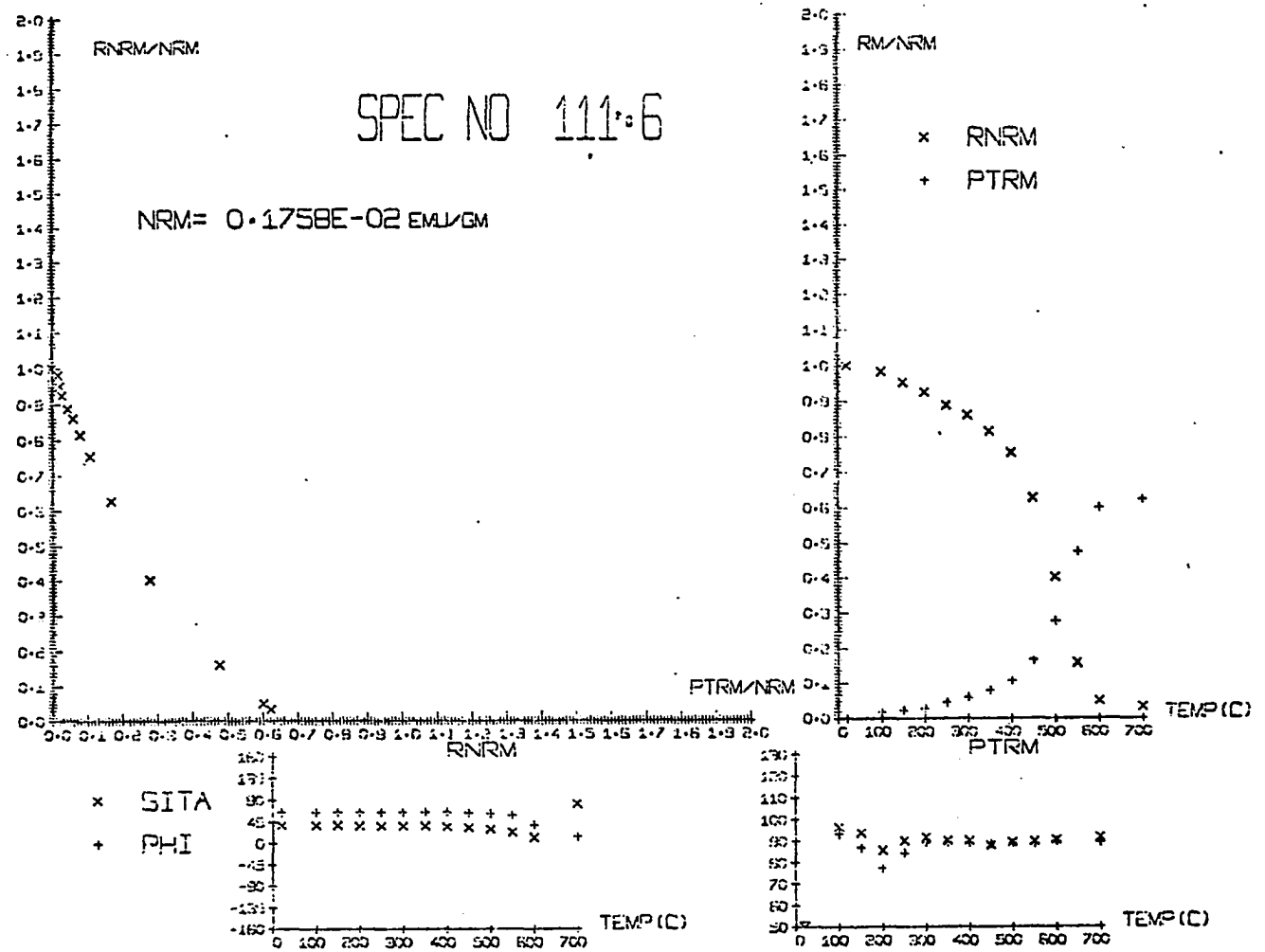

(b)

Fig. 35 (Continued)

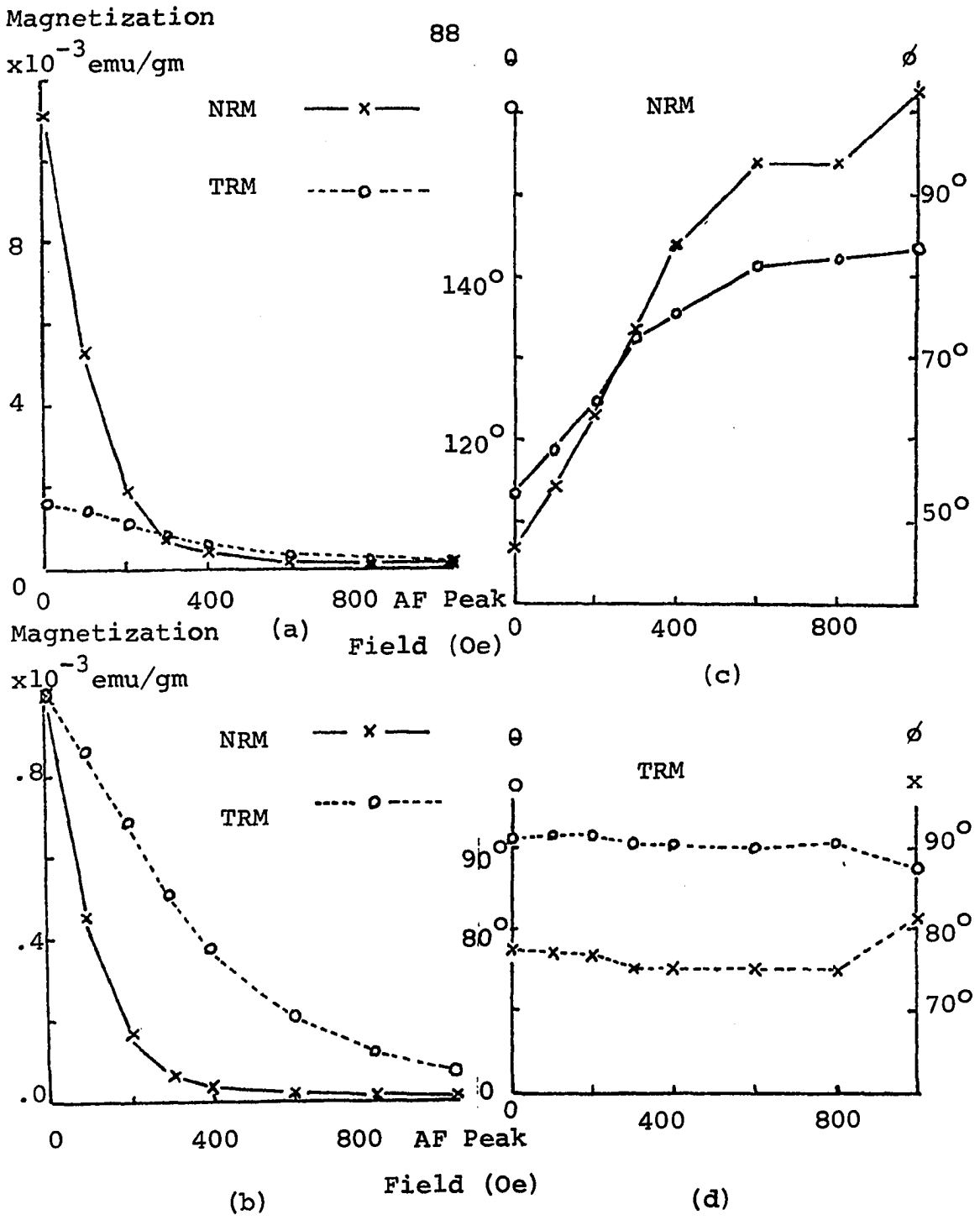

Fig. 36 AF demagnetization of Spec. No. 15.3
(a) AF demagnetizations of NRM and TRM (in 0.45 Oersted field)
(b) Normalized curves in (a)
(c) Change of the orientations of RNRM
(d) Change of the orientation of PTRM

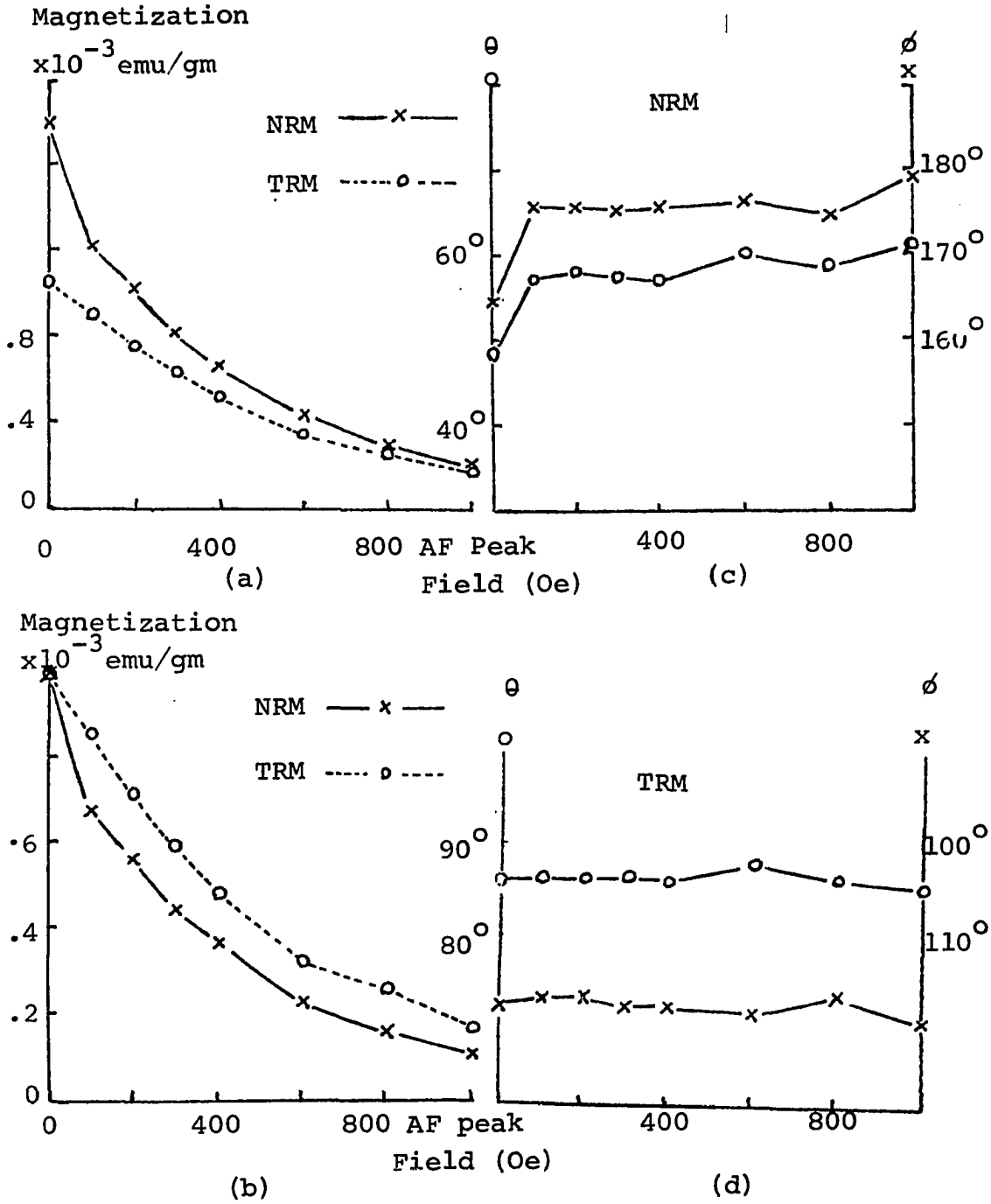

Fig. 37 AF demagnetization of Spec. No. 111.7
(a) Af demagnetization of NRM and TRM (in 0.45 Oersted field)
(b) Normalized curves in (a)
(c) Change of the orientation of RNRM
(d) Change of the orientation of PTRM

is 0.1828×10^{-2} emu/gm and that of TRM is 0.1074×10^{-2} emu/gm; this means that the magnetization of the IRM from the lightning is almost equal to that of the original NRM (TRM); (2) in Fig. 37(c), the orientation of the NRM only shifts at 100 oersteds AF demagnetization, after that it becomes very stable, indicating that the IRM has almost been eliminated at 100 oersteds AF demagnetization. These facts show that either the lightning which struck Sample No.15 was much stronger than the one that struck Sample No.111 or Sample No.15 was much closer to the center of the lightning than Sample No.111.

Test Results by the AF Demagnetization Method

The three pairs of Helmholtz coils, which are used to eliminate the Earth's magnetic field, are exactly like those used in Thelliers' Stepwise Heating Method. In the center of the Helmholtz coils is a large field coil used to generate an alternating magnetic field. The field coil is controlled by an inductor voltage regular control, the frequency is 60 cycles per second, the speed of increase is 70 oersted/sec., the speed of decrease is 20 oersted/sec., and the time delay is 8 seconds. In the center of the field coil is a sample holder. In order to apply the alternating magnetic field to the different directions of a sample, the sample holder is designed to rotate along two perpendicular axes. The essential procedure of alternating field demagnetization is to apply to the specimen an alternating magnetic field which decreases gradually from a certain peak field magnitude to

zero by decreasing the current in the field coil. There is a pick-up coil in one end of the axis of the field coil. An integrating digital multimeter is used to read the AC voltage of the pick-up coil, so that the peak field in the center of the field coil can be controlled within the range of $\pm$ 2 oersted.

Seven specimens from three different baked clay samples and two specimens from one pottery sample were cut into arbitrary shapes. These nine specimens were fired to 750^{o}C in different artificial magnetic field intensities for different orientations. Then, using the AF Demagnetization Method, these nine specimens, were measured in 0.45 oersted artificial magnetic field. The RNRM-RTRM diagrams of the nine specimens are shown in Fig. 38. Table 8 presents the results of the calculations of the nine specimens.

In baked clay samples, the RNRM-RTRM curves of Spec. Nos.51.60, 51.70, 66.70, 66.80, and 66.90 are all straight lines; also all of these straight lines pass through the origin. These are coincidental with the results from theoretical calculations. The deviations between the actual magnetic field intensities and the measured field intensities in these five specimens range from 0.93 to 4.99 percents. The change in orientation of these five specimens is very small and the AF demagnetization curves "drop gently", as shown in Fig. 39 and Fig. 40, compared with the AF demagnetization curves of the IRM which decline rapidly as shown in Fig. 36.

The RNRM-RTRM curves of Spec. Nos. 53.90 and 53.100, as shown in Fig. 38, are slightly concave down-

ward and the extensions of the curves do not pass through the origin. These indicate that the AF demagnetization curves of the TRM of Sample No.53 do not follow theoretical predictions Fig. 41 and Fig. 42 show the AF demagnetization curves of the TRM and the change of the orientation of the TRM during the AF demagnetization in Spec. Nos. 53.90 and 53.100, respectively. The results as shown in Fig. 42 suggest that the TRM of Spec.No.53.100,which has been induced in a 0.393 oersted field, is more stable than that induced in a 0.45 oersted field during AF demagnetization. The two AF demagnetization curves intersect at a value of 300 oersteds As shown in Table 8, using the least squares method to calculate the slopes of the points from zero to 1500 oersteds, the deviations between the actual magnetic field intensities and the measured field intensities in Spec. Nos. 53.90 and 53.100 are only 0.34 and 0.33 percent, respectively. If the least squares method is used to calculate the slopes of the best-fitted straight lines which pass through the origins, then the deviations between the actual magnetic field intensities and the measured field intensities in Spec. Nos. 53.90 and 53.100 are 14.54 and 18.90 percent, respectively.

The above two results show that the best-fitted straight lines do not necessarily pass through the origins. This is due to the fact that the mineralogical compositions after the two successive heating are slightly different, so the slopes of the two AF demagnetization curves are not completely similar. From the above results, the calculations in the AF demagnetization method in this study

were based only on the least squares method to calculate the slopes of the best fitting straight lines, and these lines do not necessarily pass through the origins.

The points in the RNRM-RTRM diagrams of Spec. Nos. 61.70 and 61.80, as shown in Fig. 38, are very scattered compared with that of other specimens. The AF demagnetization curves and the changes of the orientations during the AF demagnetization of Spec. Nos.61.70 and 61.80 are shown in Fig. 43 and Fig. 44, respectively. The AF demagnetization curves of the TRMs for these specimens drop very steeply and the curves are not smooth in the range from 500 oersted to 1000 oersteds; also, the orientations are very scattered. Compared with the typical AF demagnetization of the TRM as shown in Fig. 39 and Fig. 40, it shows that the TRM in Sample No. 61 is very unstable to AF demagnetization. Using the least squares method to calculate the slope of the points from zero to 1500 oersteds, the deviations between the actual magnetic field intensities and the measured field intensities in Spec. Nos.61.90 and 61.100, strange to say, are only 0.04 and 4.75 percent, respectively, as shown in Table 8, even though the points in the RNRM-RTRM diagrams are very scattered.

From the above test experiment, the results of the measurements by the AF Demagnetization Method for most samples are reliable. It must be remembered that the samples in this test experiment are ideal samples; that means the samples must meet the following conditions : (1) The temperature of the original firing must be above the Curie point (approximately 700^{o}C) of the sample ; (2) there must not be any change or reheating between the orig-

inal firing and the measurement; and (3) there must be no chemical change when firing up to 700°C in the laboratory. Actually most of the samples cannot meet all these conditions.

Test Results for Reheated Samples by the AF Demagnetization Method

Fig 45 shows the AF demagnetization curve of the PTRM of the Spec. No. 66.900 which had been thermally demagnetized to 700°C and heated up to 450°C and then cooled to room temperature in 0.45 oersted magnetic field. Fig. 45 also shows the AF demagnetization curve of the TRM of Spec. No. 66.900. The comparison of the two curves shows that the AF demagnetization curve of the PTRM drops more steeply than that of the TRM, but neither of these two curves show any abrupt decrease in the magnetization in any particular peak field during the AF demagnetization and both show some remaining magnetization. This means that it is impossible to remove all of the PTRM without entirely removing the TRM, and it is different from thermal demagnetization which can remove the PTRM at a certain temperature without removing all of the TRM.

The above discussion shows it is impossible to use the AF method to measure a sample which has been reheated after original firing. Spec. Nos. 66.700 and 66.800 are used an additional test experiment. The field in both the original firing and the reheating are 0.45 oersted, the reheating temperature is 450°C, the angles between the original TRM and the reheated magnetic field are 90° and 180°, respectively. The results of the measurements are shown in Fig. 46 and Fig. 47. It is easy to tell from the shape of the AF demagnetization curve of the NRM and the change

Table 8 Results from measurements of nine specimens used in the Test Experiment of the AF Demagnetization Method.

Spec. No.	Material	Artificial Magnetic Field Intensity F_o (Oersted)	Field Intensity Sample Measured F' (Oersted)	Resule from Measurement L.S.M. F (Oersted) (from NRM to 1500 Oe)	$\frac{F}{F_o}$	Deviation (percent)
51.60	baked clay	0.540	0.45	0.5457	1.0106	+ 1.06
51.70	baked clay	0.393	0.45	0.3735	0.9503	- 4.97
53.90	baked clay	0.540	0.45	0.5382	0.9966	- 0.34
53.100	baked clay	0.393	0.45	0.3956	1.0067	+ 0.33
66.70	baked clay	0.540	0.45	0.5196	0.9623	- 3.77
66.80	baked clay	0.393	0.45	0.3893	0.9907	- 0.93
66.90	baked clay	0.393	0.45	0.3734	0.9501	- 4.99
61.70	pottery	0.540	0.45	0.5402	1.0004	+ 0.04
61.80	pottery	0.393	0.45	0.4117	1.0475	+ 4.75

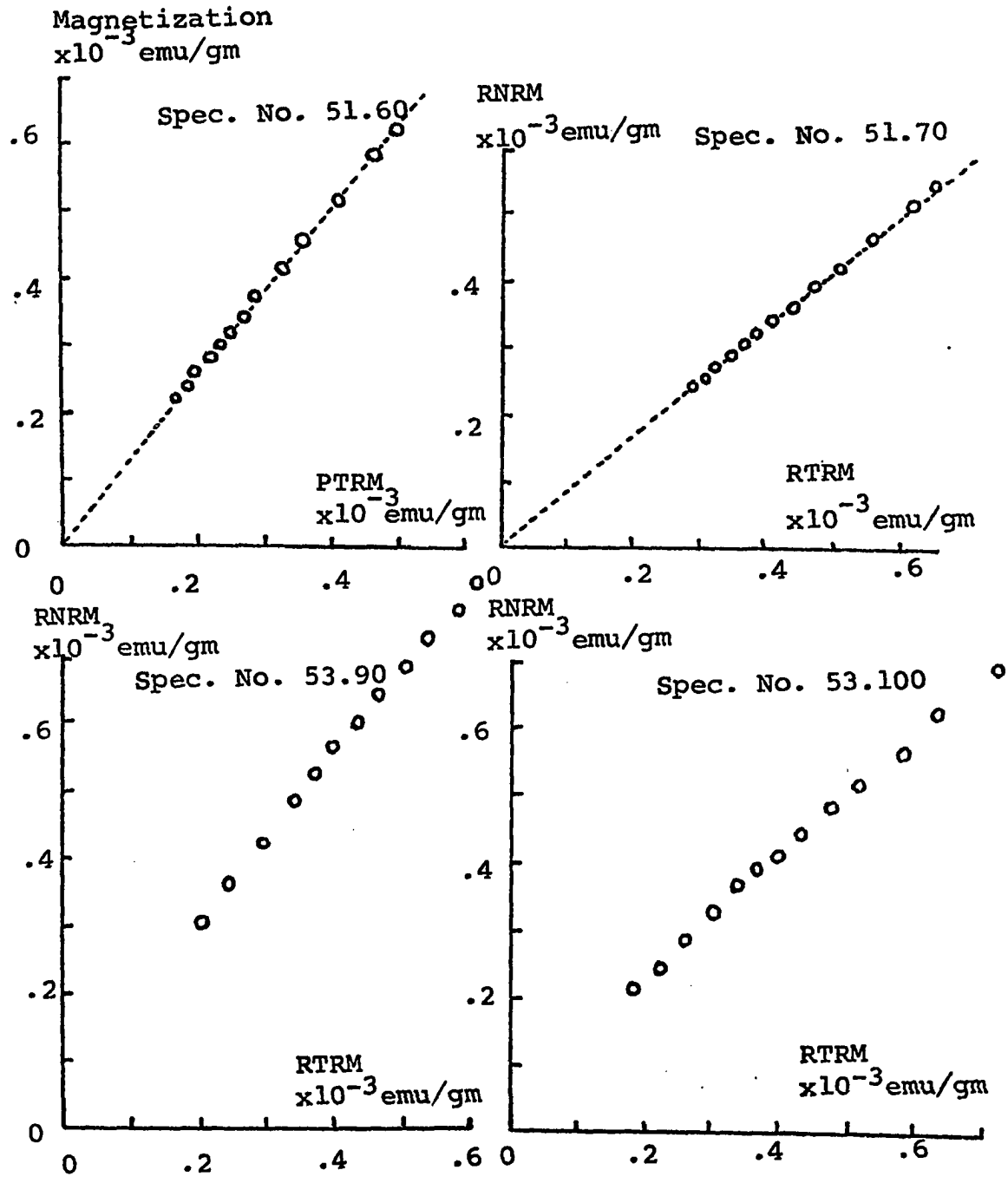

Fig. 38 RNRM-RTRM curves of nine specimens in the Test Experiment for the AF Demagnetization Method.

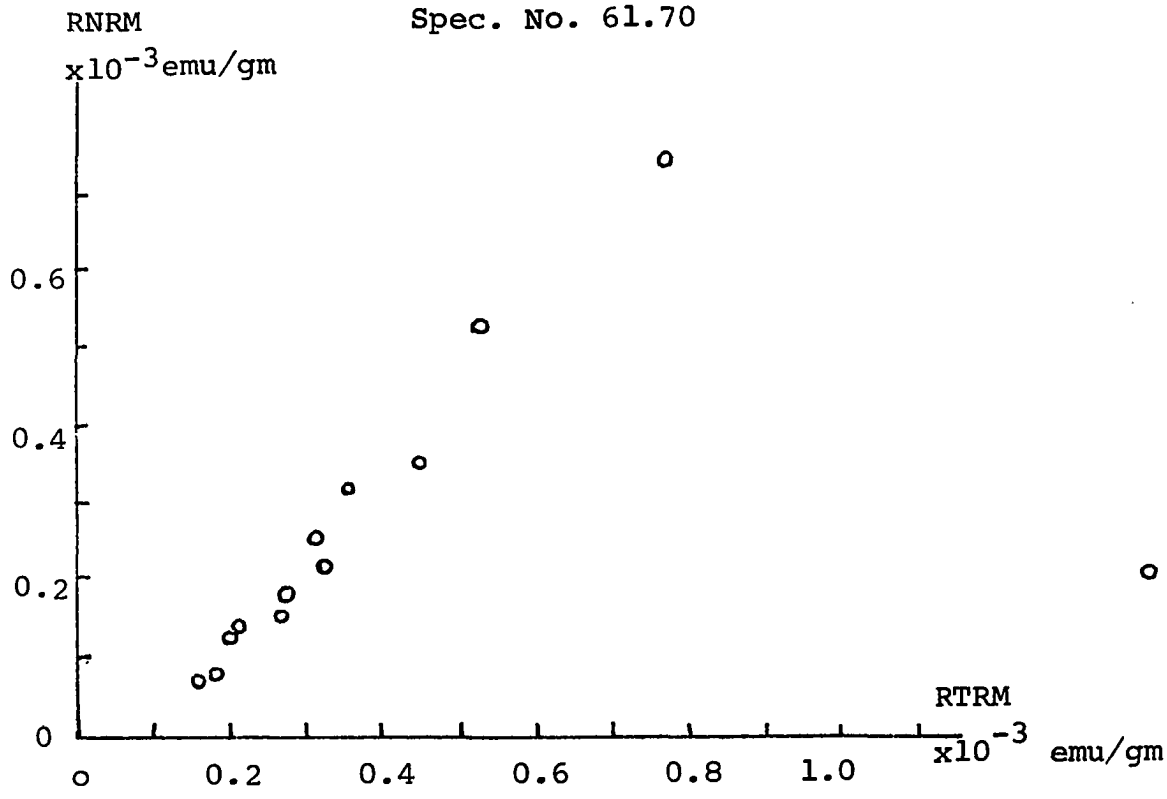

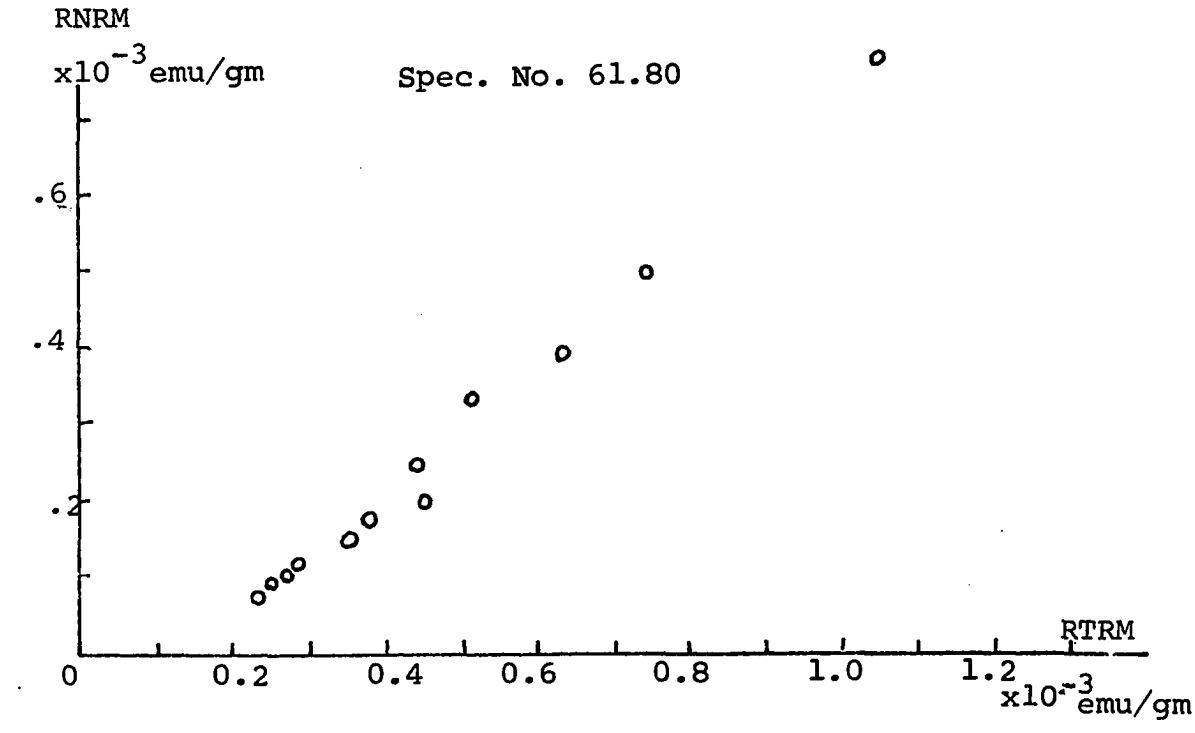

Fig. 38 (Continued)

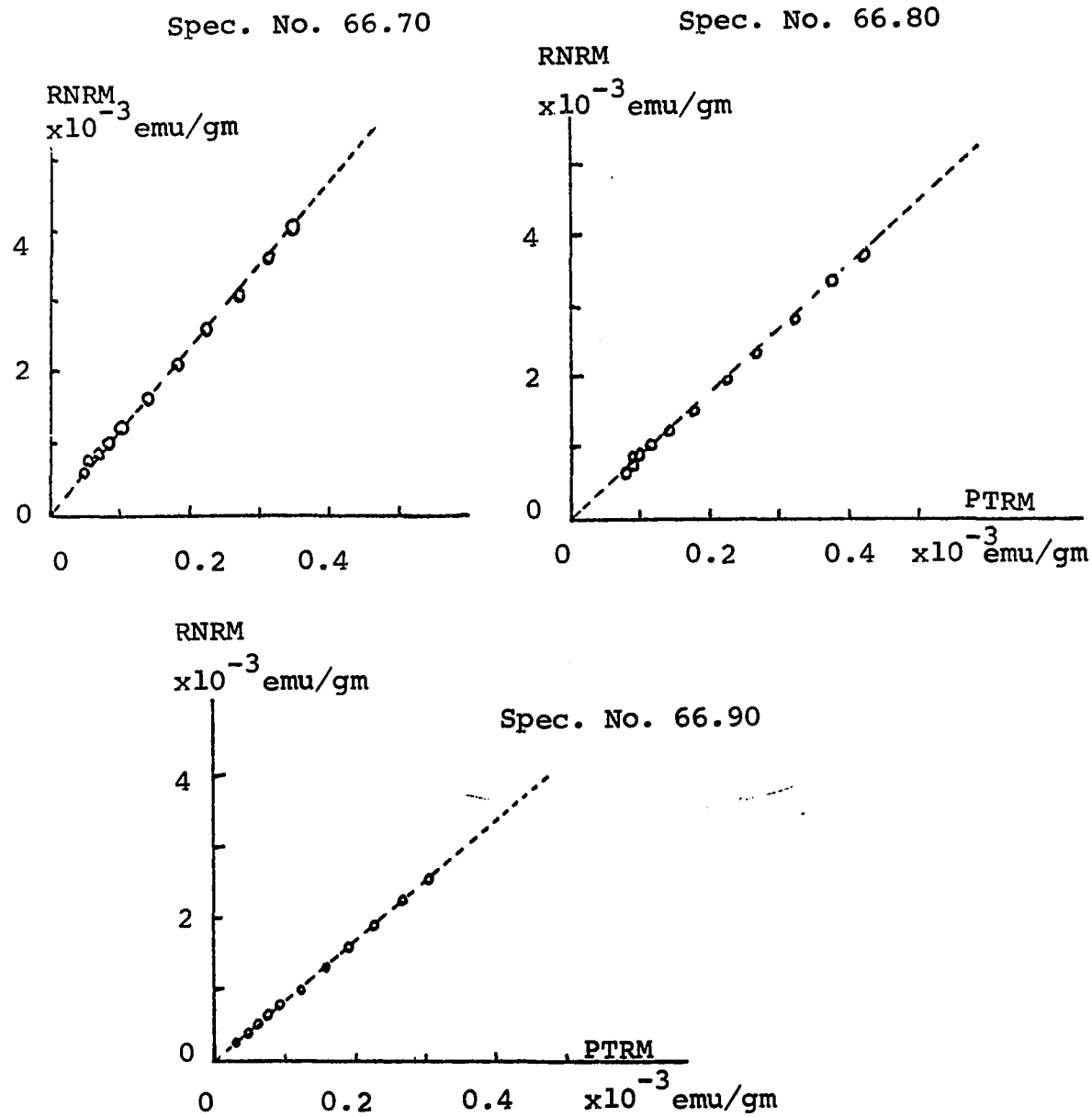

Fig. 38 (Continued)

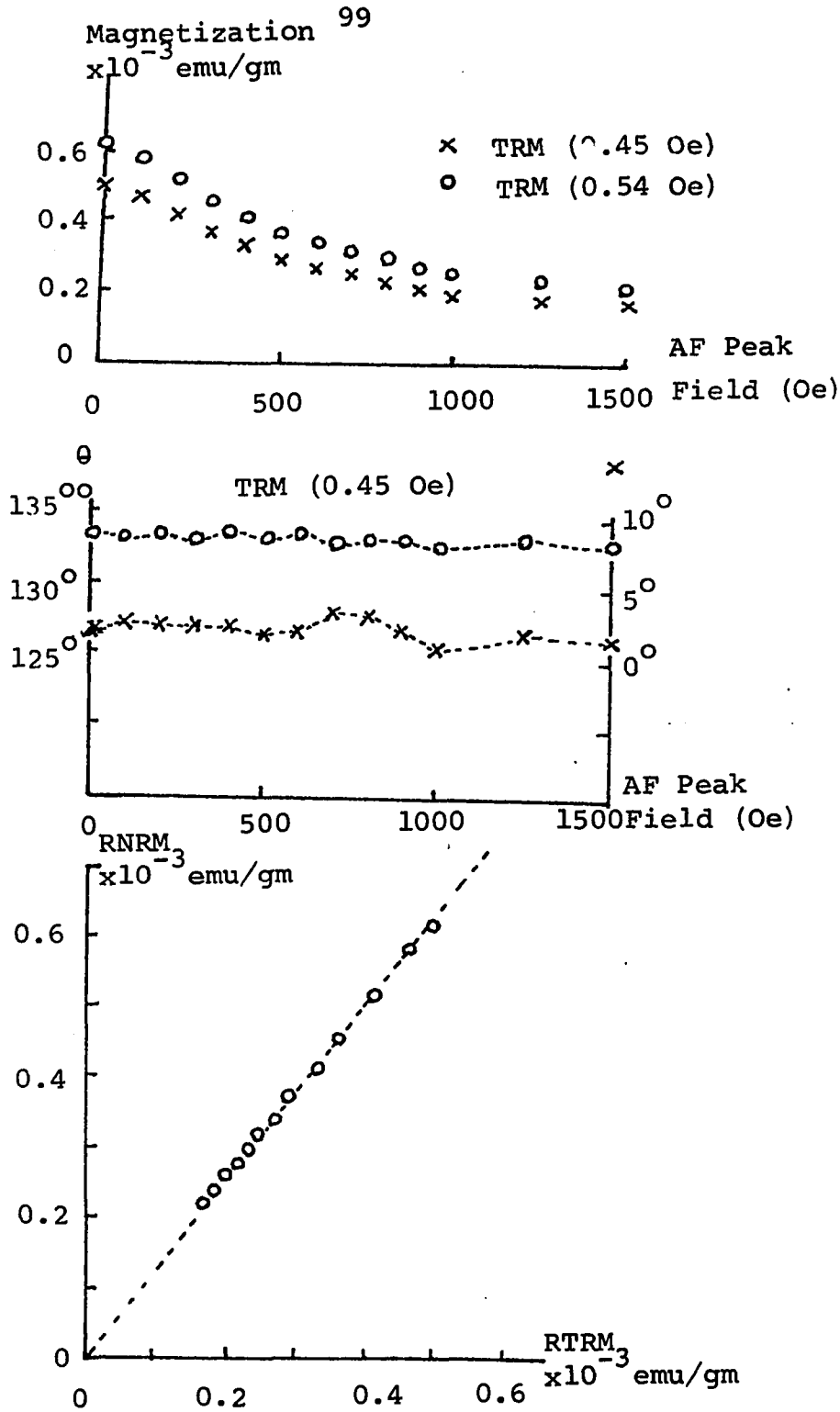

Fig. 39 Results of Spec. No.51.60 in the Test Experiment for the AF Demagnetization Method.

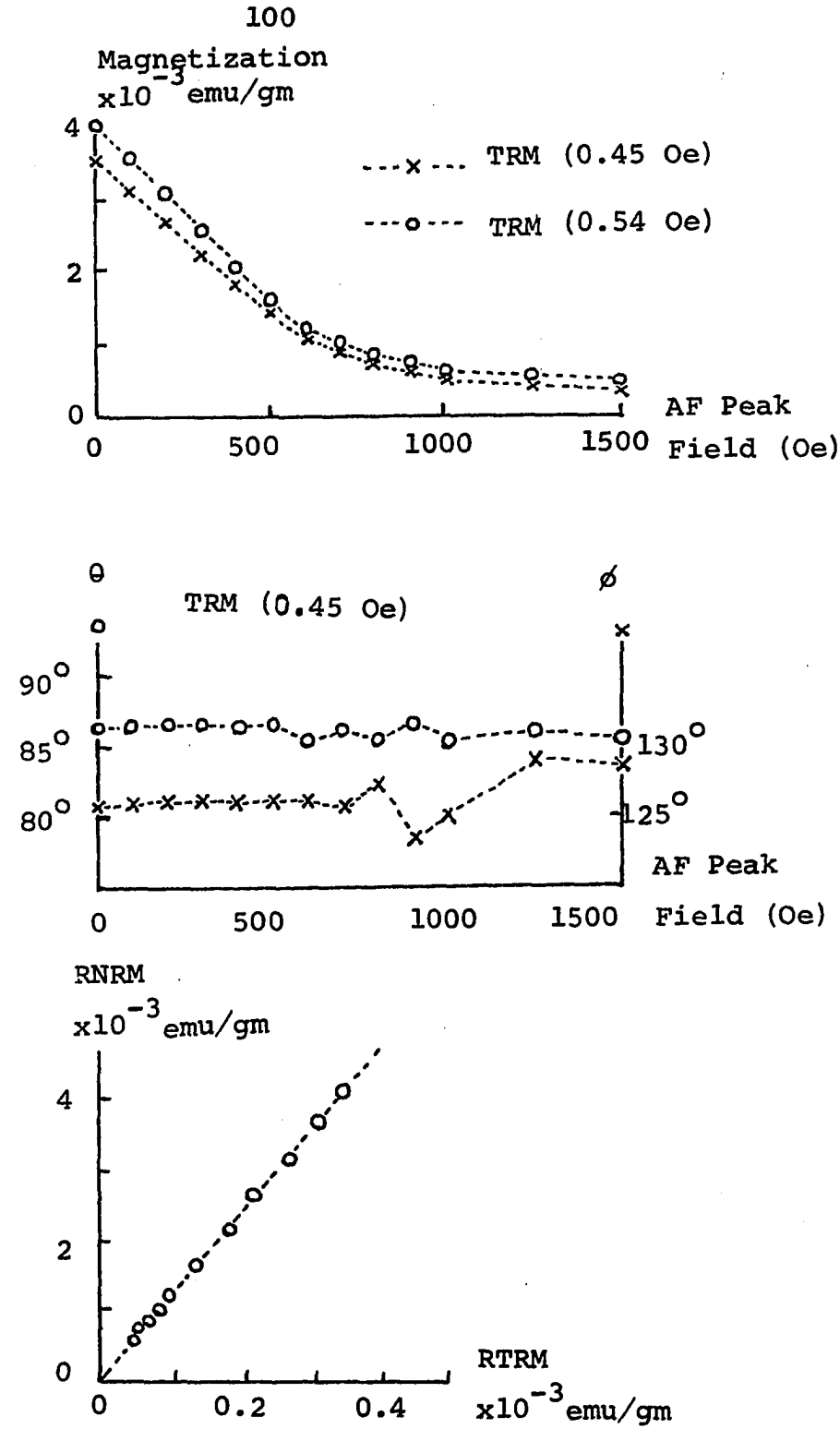

Fig. 40 Results of Spec. No.66.70 in the Test Experiment for the AF Demagnetization Method.

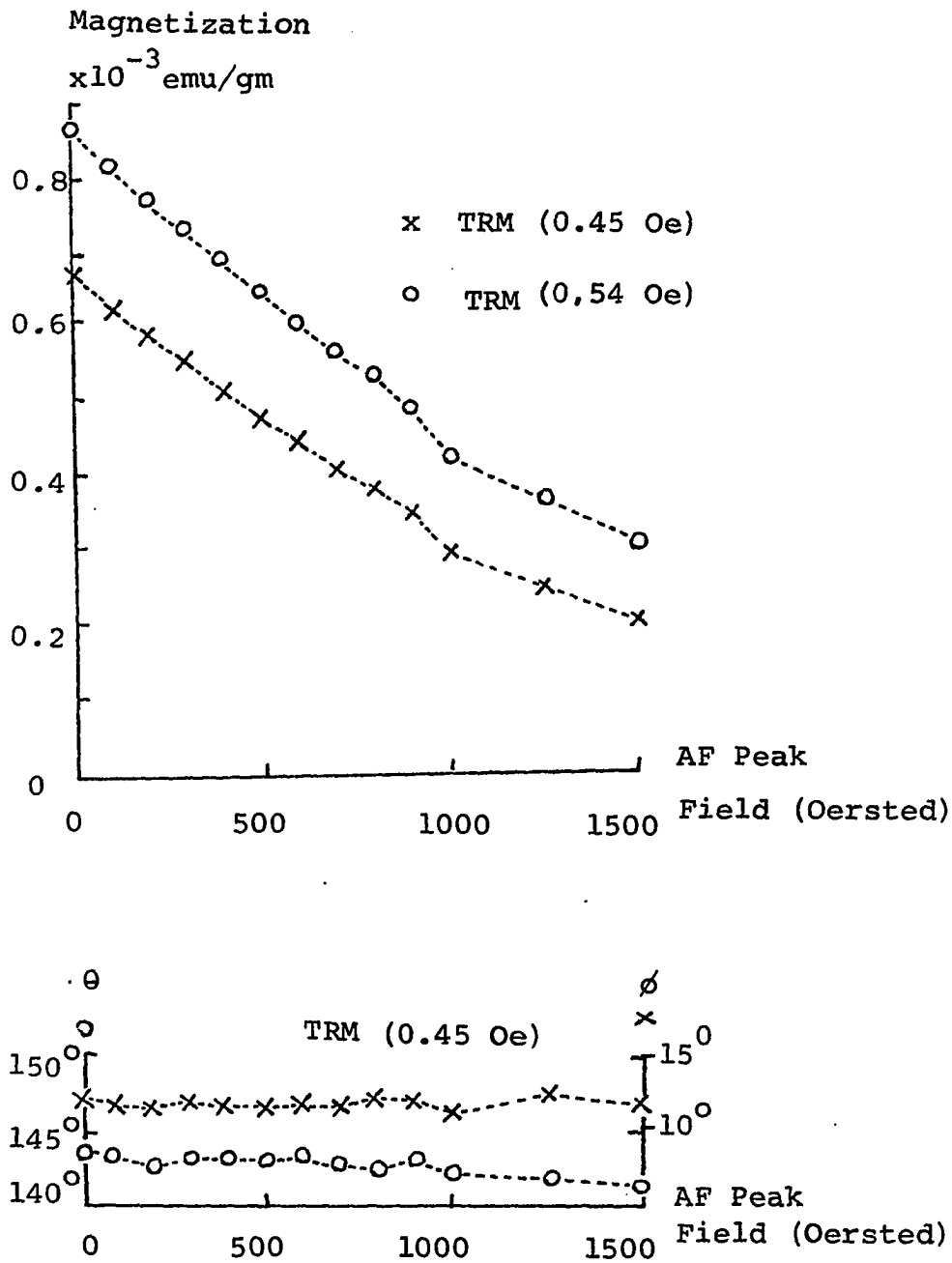

Fig. 41 Results of Spec. No.53.90 in the Test Experiment for the AF Demagnetization Method.

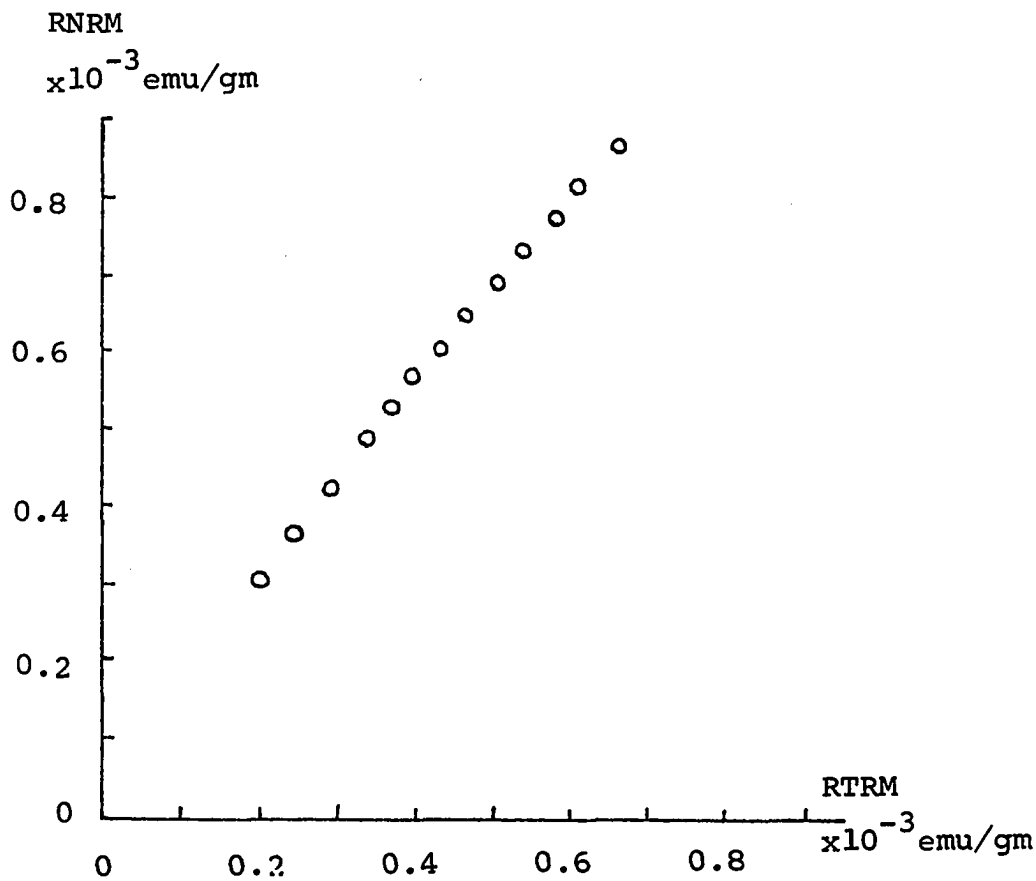

Fig. 41 (Continued)

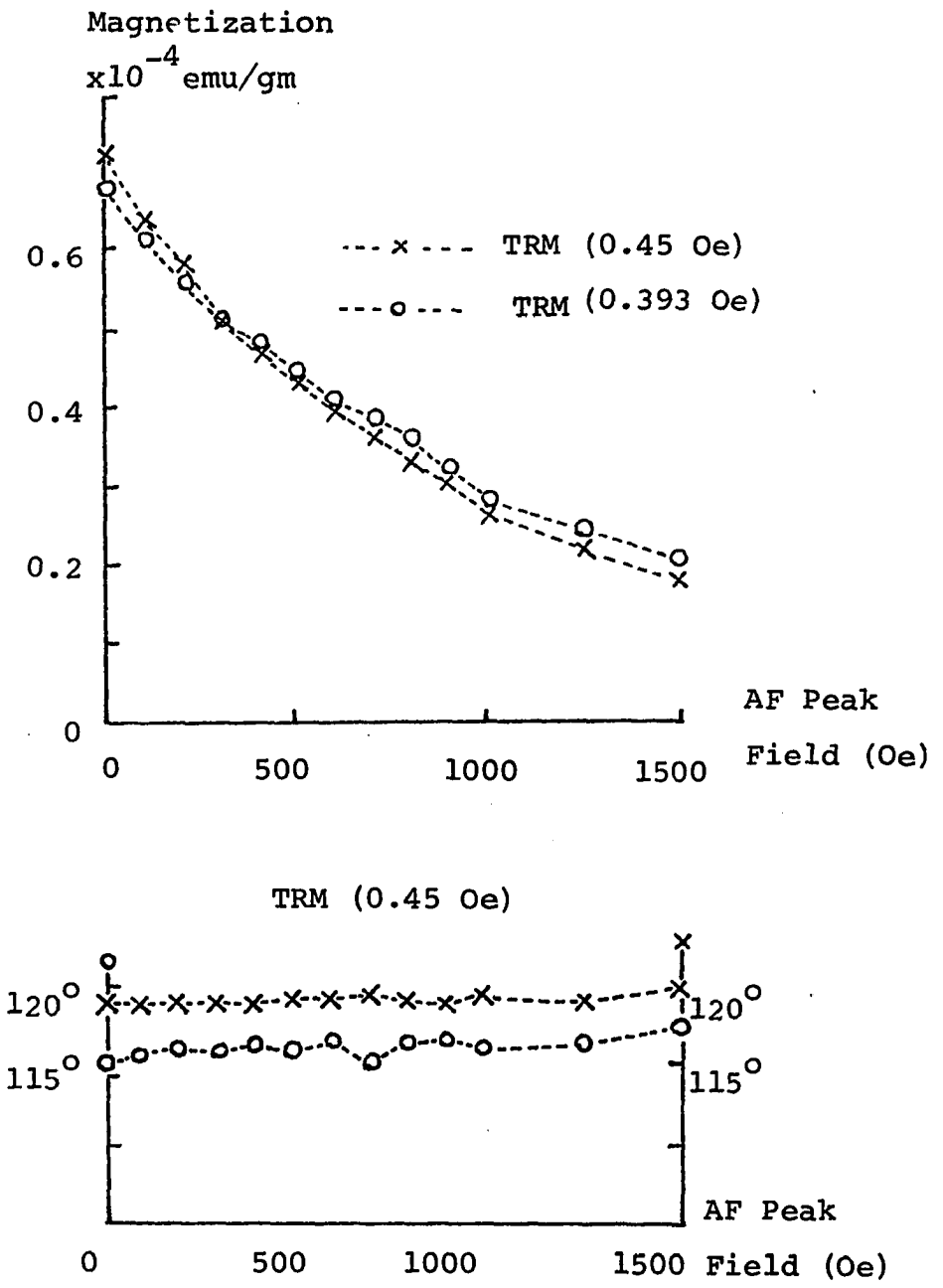

Fig. 42 Results of Spec. No.53.100 in the Test Experiment for the AF Demagnetization Method.

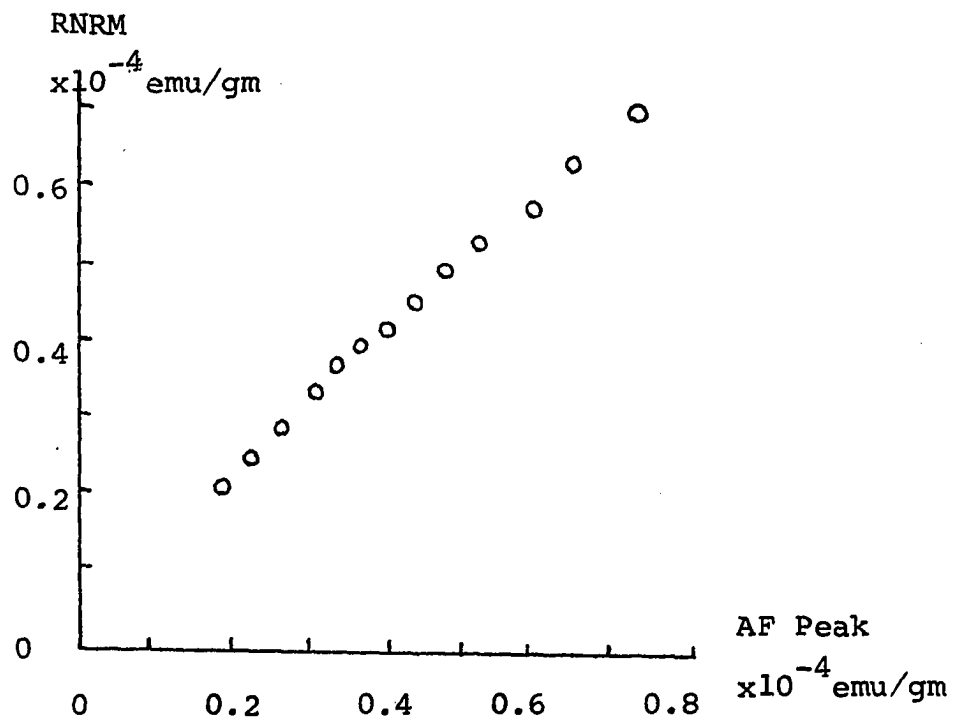

Fig. 42 (Continued)

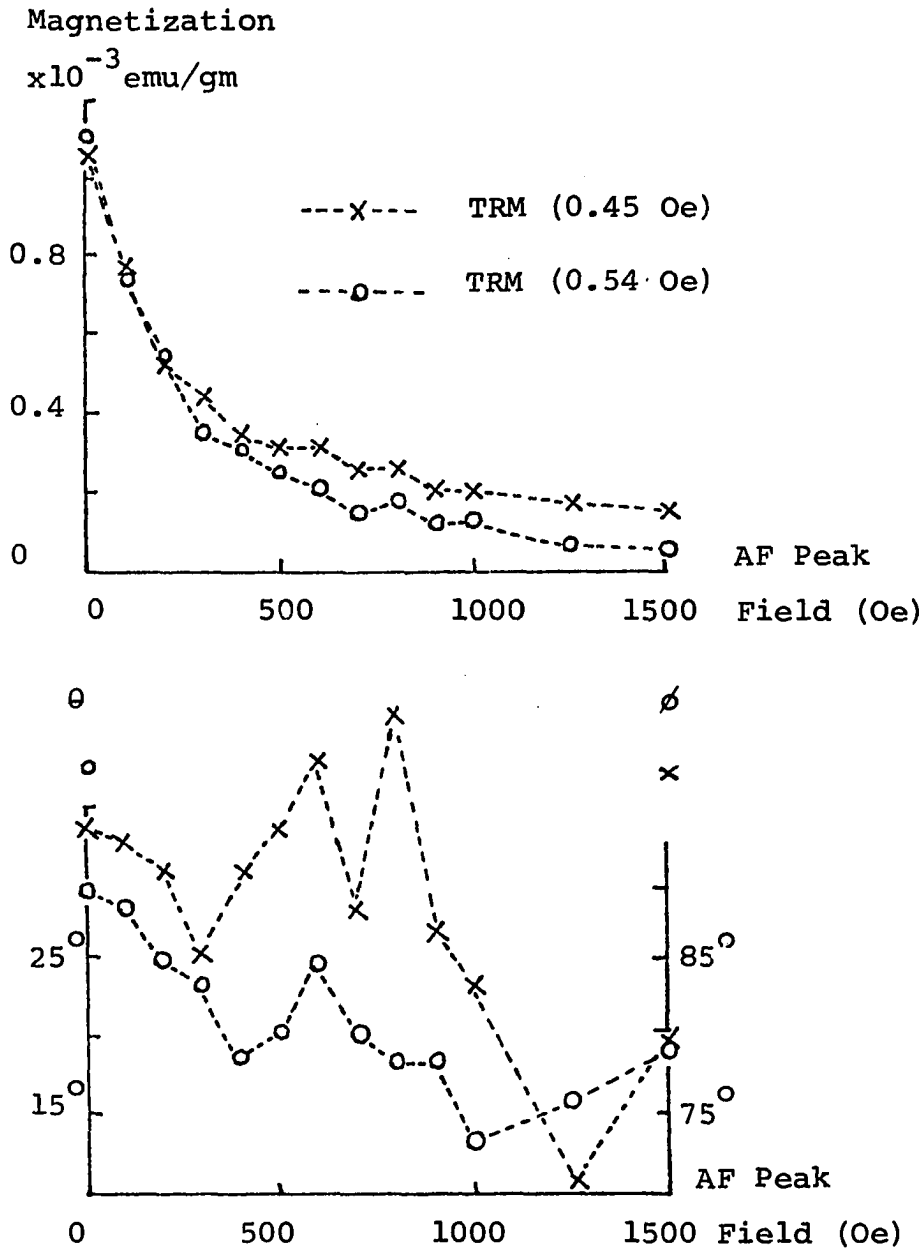

Fig. 43 Results of Spec. No.61.70 in the Test Experiment for the AF Demagnetization Method.

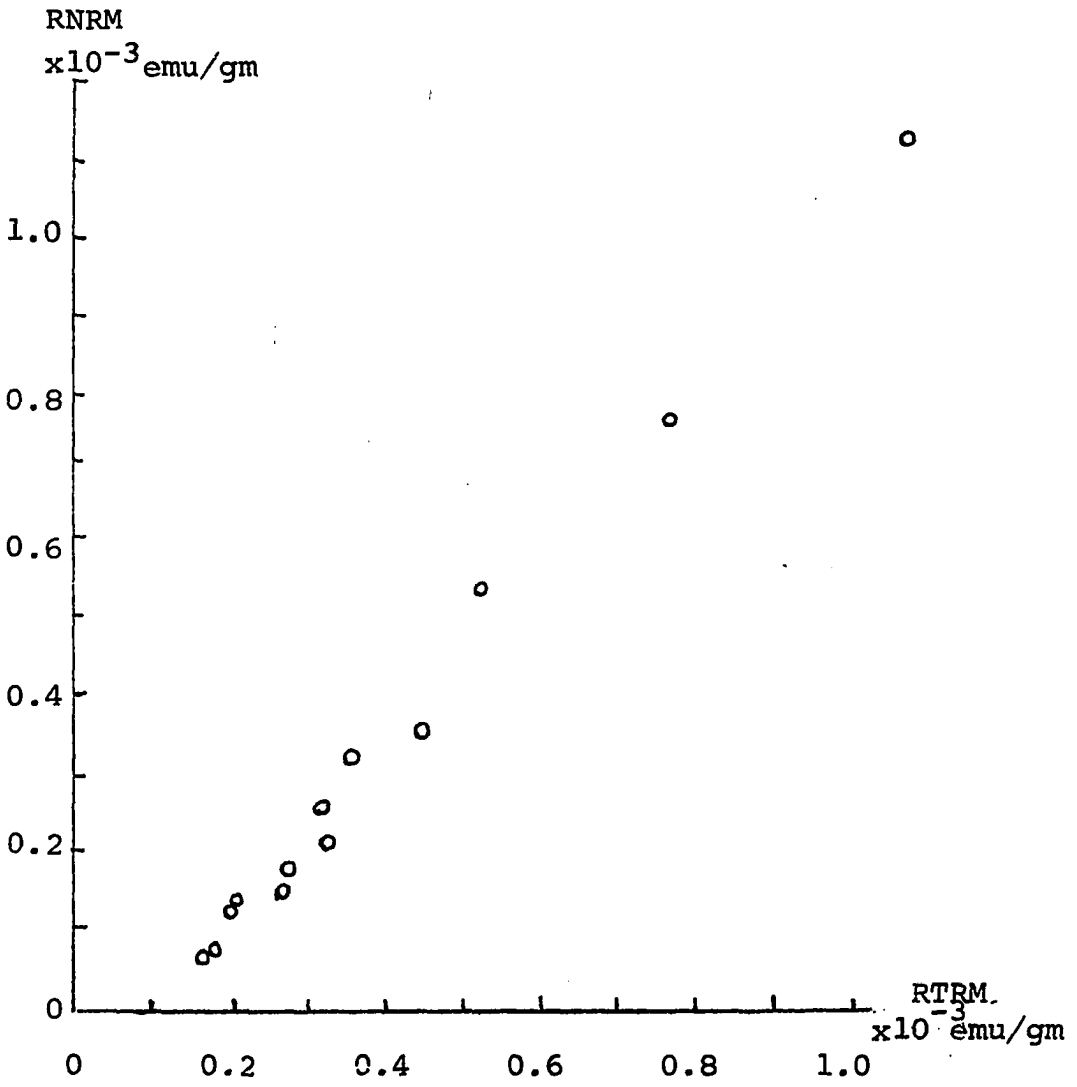

Fig. 43 (Continued)

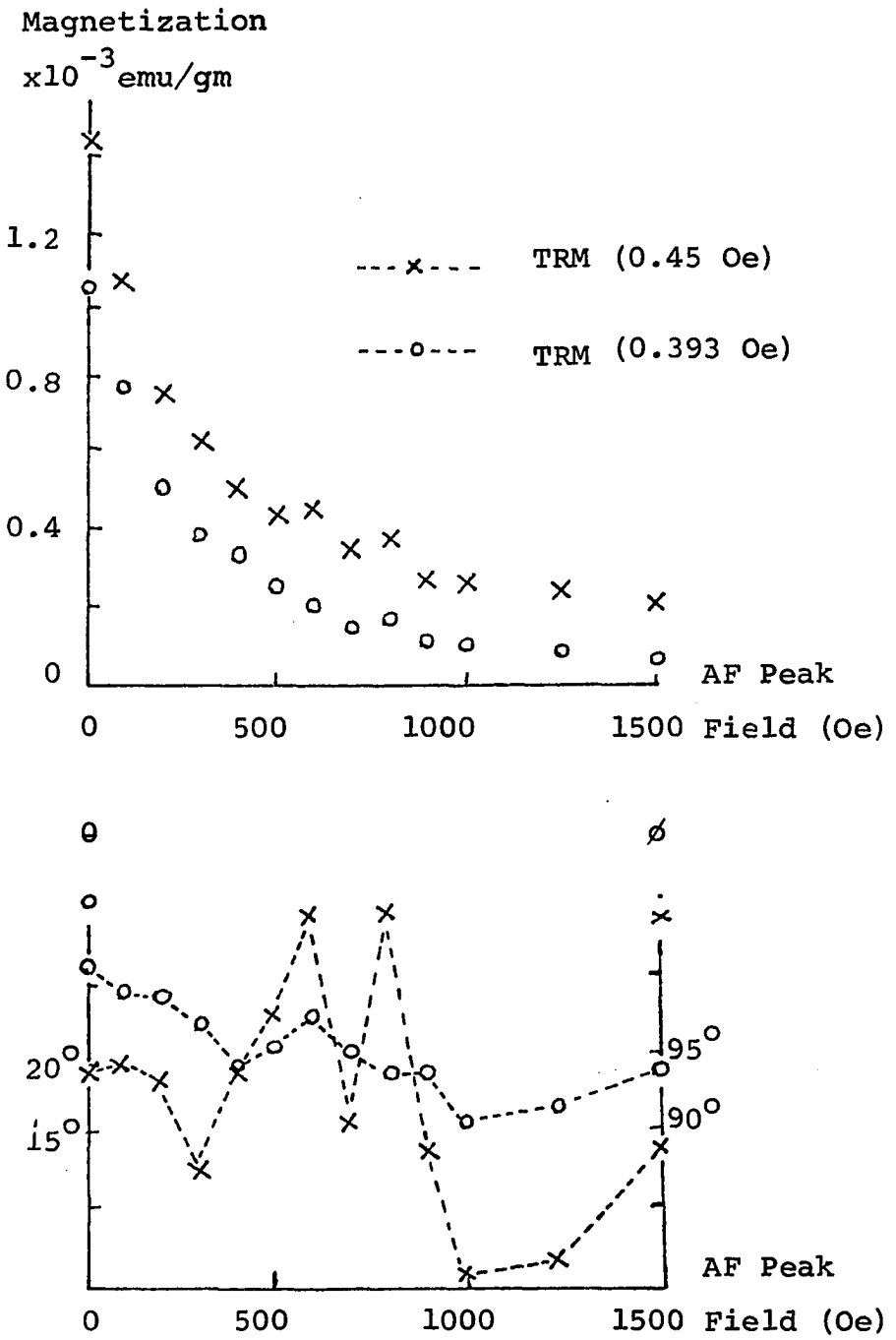

Fig. 44 Results of Spec. No.61.80 in the Test Experiment for the AF Demagnetization Method.

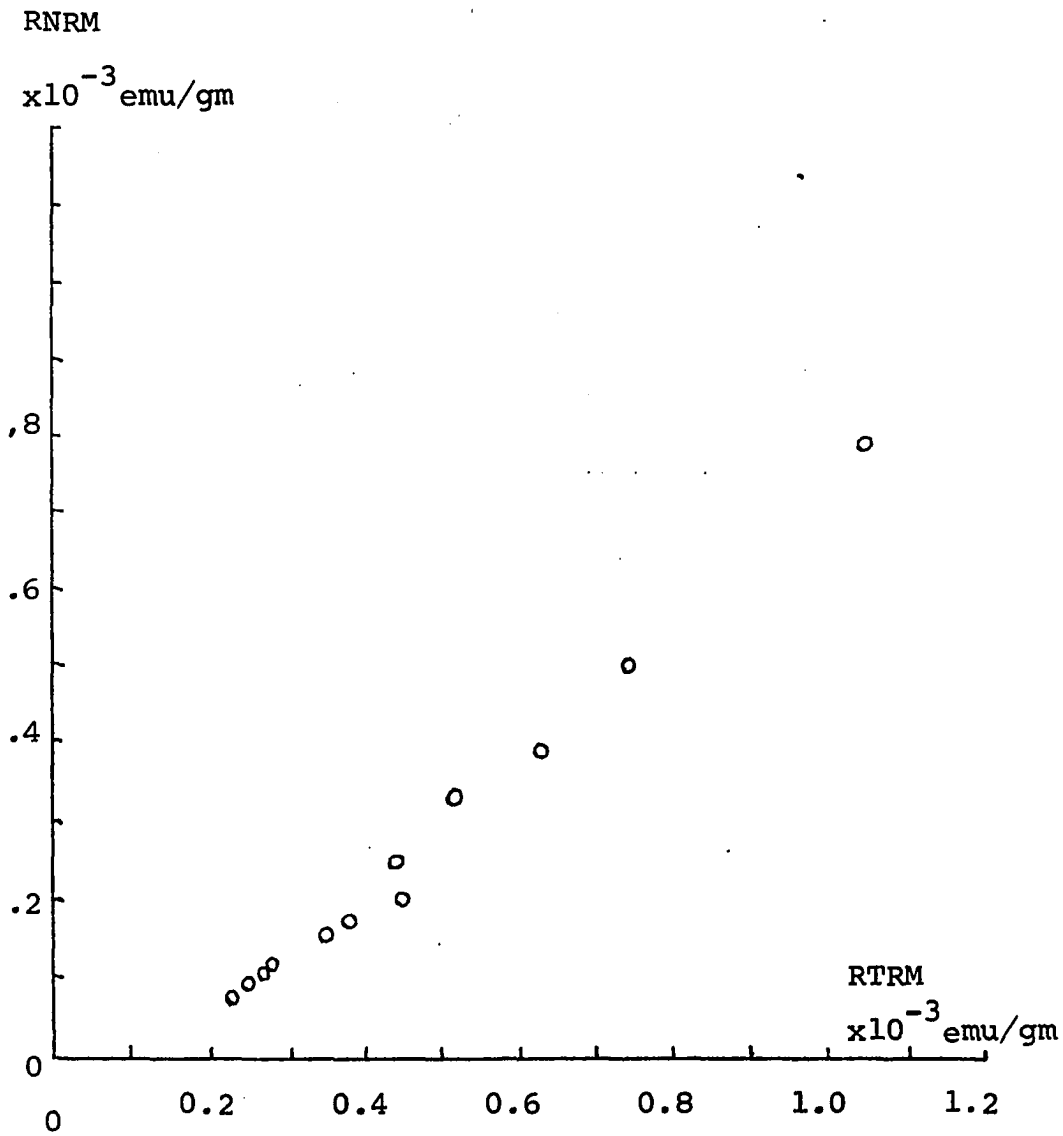

Fig. 44 (Continued)

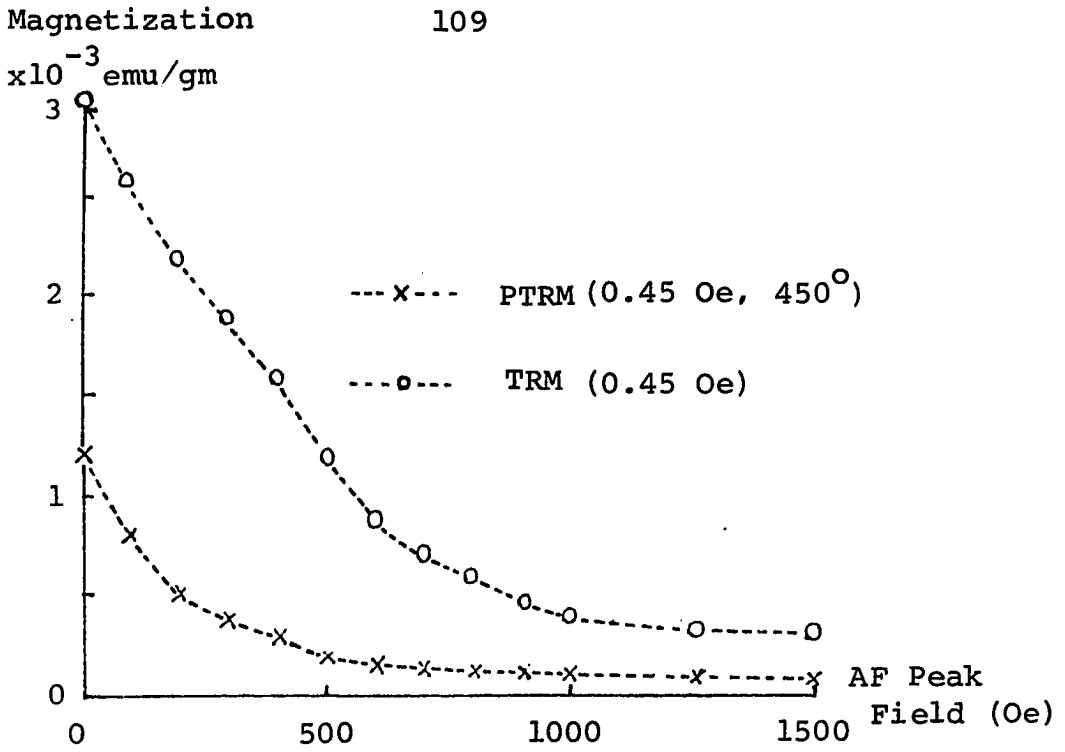

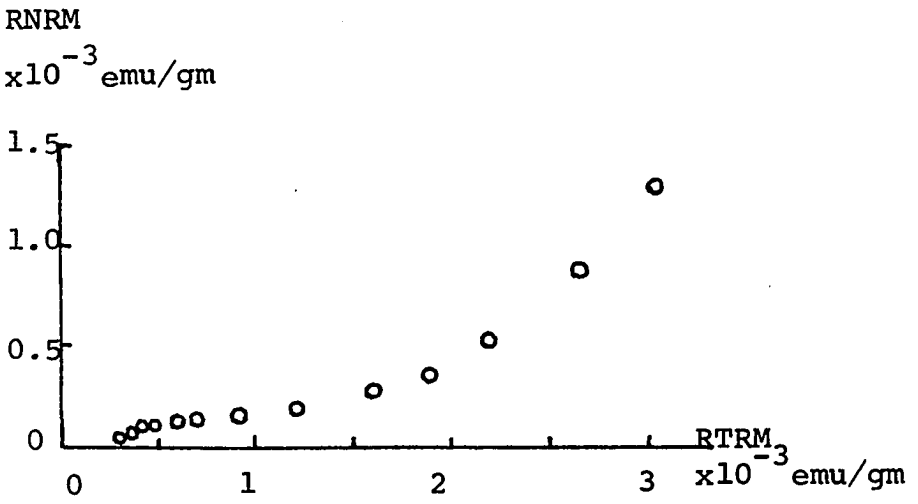

Fig. 45 Results of Spec. No.66,900, which was only heated to 450°C in 0.45 oersted field, in the Test Experiment for the AF Demagnetization Method.

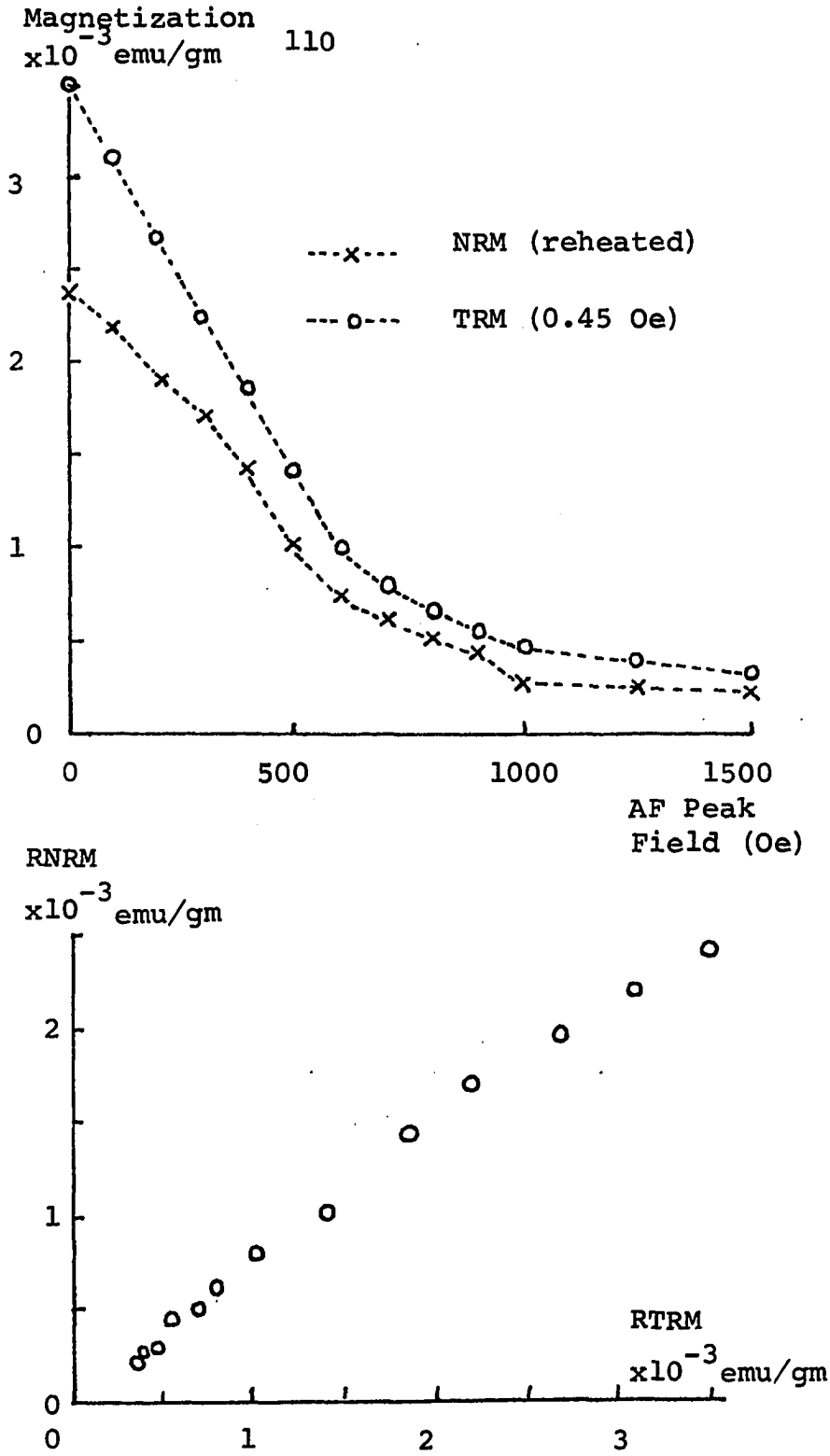

Fig. 46 Results of Spec. No.66.700, which has been reheated $\gamma=90^{o}$ and $T_r=450^{o}$ in the Test Experiment for the AF Demagnetization Method.

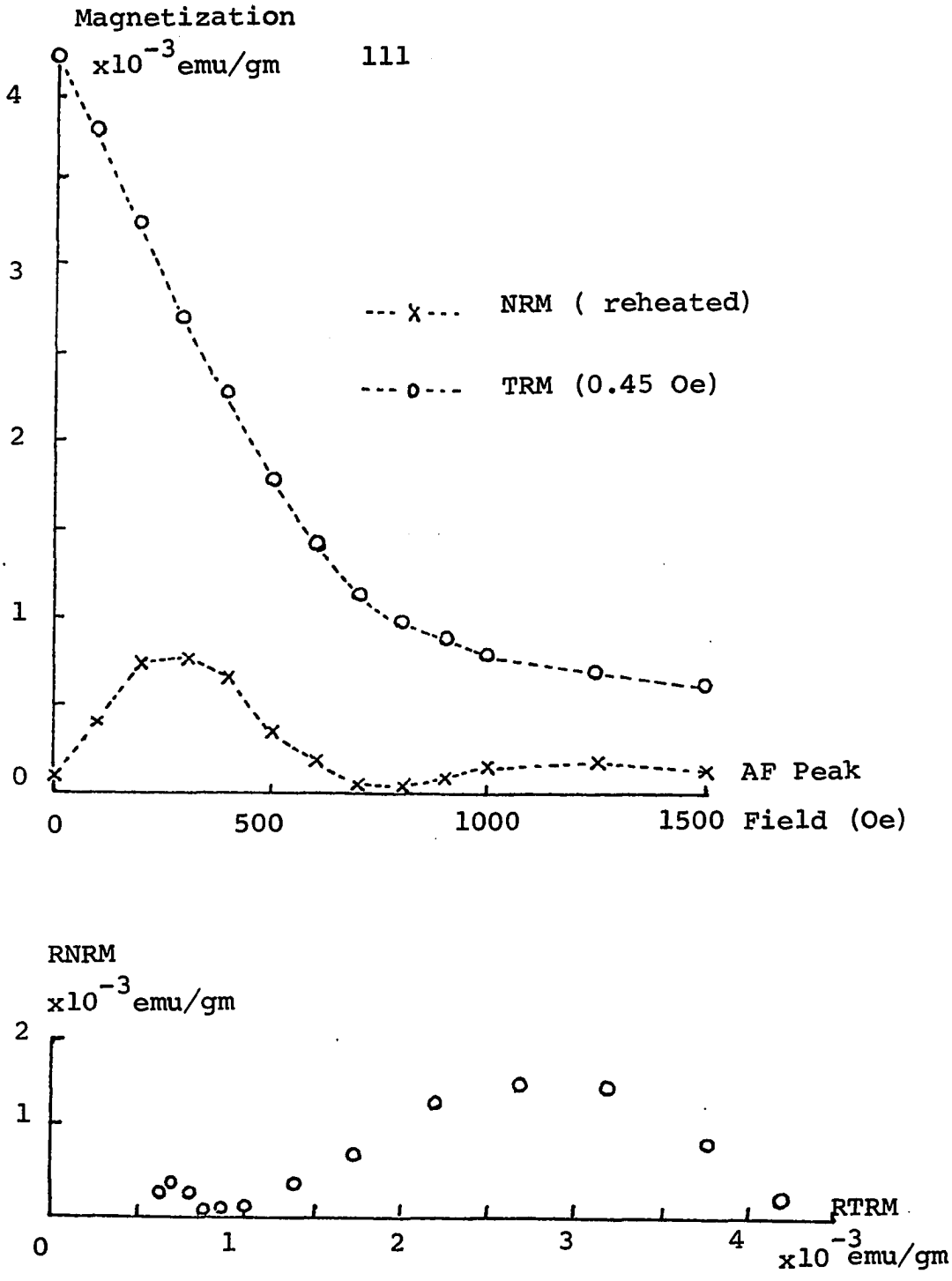

Fig. 47 Results of Spec. No.66.800, which has been reheated $\gamma=180^{\circ}$, and $T_r=450^{\circ}C$ in 0.45 oersted, in the Test Experiment for the AF Demagnetization Method.

of the orientation of the RNRM that the sample has been reheated after its original firing(Fig. 46 and Fig. 47).

D. COMPARISON OF METHODS

Comparison of Results from Thelliers' Method and the AF Demagnetization Method

In order to compare the Thelliers' Stepwise Heating Method with the AF Demagnetization Method, nine samples including six baked clays, Sample Nos.15, 51, 53, 66, 111, 185 and three pottery, Sample Nos.61, 96, 151 were chosen.

Four specimens from Sample No.66 have been run by Thelliers' Method (A). The result of one of the specimens, Spec. No.66.3, is shown in Fig. 48. The RNRM-PTRM diagrams of four specimens are shown in Fig. 49, all the points lie almost in a straight line. This is an ideal sample for archeomagnetic field intensity studies.

The results of the measurements from these four specimens show that the field intensities, are very similar, 0.47 oersted, 0.46 oersted, 0.43 oersted, and 0.46 oersted, respectively. Three specimens of Sample No.66 have been measured by the AF Demagnetization Method. The RNRM-RTRM diagrams of these specimens are shown in Fig. 50. The three curves are slightly concave downward. This shows that the results from the AF Demagnetization Method are not as reliable as those from Thelliers' Method, although the results of these three specimens, which are 0.47 oersted, 0.51 oersted, and 0.47 oersted, are very close to the results from Thelliers' Method.

From Sample No.95, a pottery sample, three speci-

mens have been measured by Thelliers' Method; the RNRM-PTRM diagrams are shown in Fig. 51. In all three diagrams, the slopes of the curves begin almost horizontally and geadually become steeper, finally decreasing to approximate a straight line. The orientation of the RNRM are very stable from room temperature up to 350°C. This may be due to exposure and magnetic relaxation, that is, some soft components of magnetization had undergone relaxation during the time expoed at the site. The ancient field intensities measured from these specimens are 0.53 oersted, 0.51 oersted, and 0.53 oersted respectively.

Comparing the above results with the 0.53 oersted from AF Demagnetization Method measurements of Spec. No. 95.4, which is shown in Fig. 52, we find that both methods are reliable in measuring this sample. The similarity of the AF demagnetization curves of both NRM and TRM after 200 oersted demagnetization suggests low temperature relaxation of the magnetism then stablity above 200 gauss.

Fig. 53 shows the RNRM-PTRM diagrams of four specimens from Sample No. 61 using Thelliers' Method. Comparing this result with the theoretical RNRM-PTRM diagrams in Fig. 25, it shows that the sample had been reheated up to approximately 250°C. The orientations of the RNRM changes gradually from room temperature up to 250°C. This also indicates that the sample had been reheated. The ancient field intensities measured from the above four specimens are 0.36 oersted, 0.37 oersted, 0.37 oersted, and 0.36 oersted. The average value of 0.36 oersted is used for this sample and it is reliable. Spec. Nos. 61.7 and 61.8 are measured by the AF Demagnetization Method. The results

in Fig. 55, show that Sample No. 61 is very unstable to AF demagnetization for the following reasons : (1) The orientations of both RNRM and RTRM change rapidly in both specimens; (2) the AF demagnetization curve of the NRM of Spec. No. 61.8 is not smooth; (3) the AF demagnetization curves of the TRM of both specimens are not smooth and drop very sharply; and (4) the points in RNRM-RTRM diagrams are very scattered. The results of the measurements from these two specimens show that the ancient field intensities are 0.32 oersted and 0.21 oersted. From the above discussions, we conclude that the results from the AF Demagnetization Method are unreliable in this sample.

Three specimens from Sample No. 151 were measured by Thelliers' Method. Fig. 56 shows the RNRM-PTRM diagrams of these specimens and the change of the orientations of Spec. No. 151.3. The peaked points in the RNRM-PTRM diagrams are 300°C points and the orientations of RNRM become stable after 300°C. All these indicate that the sample has been reheated to 300°C. The results of the measurements from these three specimens show that the ancient field intensities are 0.60 oersted, 0.52 oersted, and 0.55 oersted. The average of 0.56 oersted is used for this sample and it is reliable. The AF demagnetization curves of both NRM and TRM of Spec. No. 151.4 and the RNRM-RTRM diagram from AF Demagnetization Method are shown in Fig. 57. It shows that both the NRM and TRM of this sample have very hagh resistance to AF demagnetization; even the 3,500 oersted peak field removed only one third of the TRM. The AF Demagnetization Method is not valid for this sample.

Four specimens from Sample No. 51 were measured by

Thelliers' Stepwise Heating Method. The RNRM-PTRM diagrams for these specimens are shown in Fig. 58. All of the four diagrams show a sharp drop begining at 600°C. This indicates that oxidation has occurred when the sample was heated to 600°C in the oven during measurements. The results of the measurements from these four specimens show that the ancient field intensities are 0.69 oersted, 0.61 oersted, 0.63 oersted, and 0.68 oersted. The average value of 0.65 oersted is used for this sample and it is reliable.

The AF Demagnetization Method has been used to measure Spec. Nos. 51.6 and 51.7. As shown in Fig. 59 and Fig. 60, the change of the orientations of RNRM are very slight and the points in the RNRM-RTRM diagrams are almost along a straight line. The results of 0.82 oersted and 0.88 oersted would seem to be reliable, but actually they are not. From Thelliers' Method, we know that this sample will undergo oxidation if it is fired to 600°C, and the TRM of this sample was gived by firing up to 750°C and cooling to room temperature in 0.45 oersted magnetic field. Owing to the oxidation, the actual TRM is weaker than that in the theoretical calculation. So the results are much higher than the actual ancient magnetic field intensity.

Fig 61 shows the results of the four specimens from Sample No. 53 by Thelliers' Method. The RNRM-PTRM diagrams of Spec. Nos. 53.5 and 53.7 indicate that the reduction occurred when the two specimens were heated to 400°C. Spec. Nos. 53.6 and 53.8 do not show any chemical reactions during the heating. The results from Spec, Nos. 53.6 and 53.8 are 0.40 oersted and 0.41 oersted, respect-

ively. The average value is 0.41 oersted and it is reliable.

Using the AF Demagnetization Method to measure Spec. Nos. 53.9 and 53.10, the RNRM-RTRM diagrams are shown in Fig. 62. The result from Spec. No.53.9 is 0.39 oersted, which is very close to the result from Thelliers' Method, and this means that the specimen does not have any oxidation when it is fired to 750°C. The result from Spec. No. 53.10 is 0.30 oersted, which is much lower than that from Thelliers' Method. This means that reduction occurred when the specimen was heated to 750°C, and the actual TRM is much stronger than that in the theoretical calculations.

The above results of Sample Nos.51 and 53 show that if only the AF Demagnetization Method is used to measure the samples which have chemical reaction when heated up to 750°C, then the measured field intensities are quite different from the actual ancient magnetic field intensities.

In order to study archeomagnetism, a test experiment has been done in front of the building of the Archeomagnetism Laboratory, University of Oklahoma. The ground was fired and the temperature was measured by thermocouples. Sample No.185 was collected from this site, and this sample has heated above 750°C for three hours. The sample is very fragile, so it is impossible to use Thelliers' Method to measure this sample. Using the AF Demagnetization Method to measure Spec. Nos.185.1 and 185.2, the RNRM-RTRM diagrams are shown in Fig. 63. The results show that the field intensities are 0.56 oersted and 0.57 oersted, respectively. These results, compared

with the actual magnetic field of 0.54 oersted measured by the fluxgate magnetometer, are very close.

Samples Nos.15 and 111 have been struck by lightning. Fig. 64 shows the results of Spec. Nos.15.1 and 15.2 measured by Thelliers' Method. The points in the RNRM-PTRM diagrams drop very sharply; and it is impossible to measure the ancient field intensity. As shown in Fig. 36, the IRM from lightning has been almost totally eliminated by an AF demagnetization peak field of 300 oersteds. The RNRM-RTRM diagrams are shown in Fig. 65. The AF Demagnetization Method was used to calculate the point above 300 oersteds. The result shows that the ancient field intensity (F) is 0.41 oersted. compared with the present field intensity (F_o) of 0.42 oersted in the site, the ratio (F/F_o) is 0.97.

The archeological data for Sample No.15 is from 600 AD to 900 AD. The curve of the secular variation of the geomagnetic field intensity in Mexico and Guatemala*, which was obtained from this work, indicates a trough around 800 AD. Although the result of the AF Method is not very reliable, it is still consistent with the secular variation curve.

Four specimens from Sample No.111 have been measured by Thelliers' Method. The results shown in Fig. 66, indicate that only the points in Spec. No.111.5 lie almost in a straight line, while the others are concave upward. The orientations of the RNRM of Spec. No.111.5 are very

* See page 159.

stable from NRM up to 400°C. This means that the specimen has not been affected by lightning.

Sample No.111 includes several pieces of baked clay. The distances between each piece may be far enough so that some pieces might be affected by lightning and some piece might not, especially if the lightning was weak. The result from Spec. No.111.5 is 0.6498 oersted. Fig. 37 shows that the IRM here is eliminated at a peak field of 100 oersted. The RNRM-RTRM diagrams for Spec. No.111.7 is shown in Fig. 67. The points from 100 oersted to 1,000 oersted lie almost in a straight line. The result of the measurement by the AF Demagnetization Method is 0.6623 oersted, which is close to the result obtained from Thelliers' Method.

Summarization of Comparison

The results may now be summarized. (1) The result from Thelliers' Stepwise Heating Method is more reliable than that from the AF demagnetization method, although the former is a laborious work compared with the latter. (2) If the sample has been reheated after its original firing, or it has chemical reaction during measurement, the temperature of the reheating or the temperature of chemical reaction can be determined by Thelliers' Method, and the actual ancient field intensity can be obtained. However, the AF Demagnetization Method will give an erroneous result. (3) Because IRM is more resistant to thermal demagnetization than to AF demagnetization, some samples, which have been struck by lightning, can be measured more efficiently by the AF Demagnetization Method than by Thelliers' Method. (4) A few samples too fragile to be measured by

Thelliers' Method, can be measured by the AF Deamgnetization Method. (5) The TRMs of some samples have high resistance to AF demagnetization. It is impossible to used the AF Demagnetization Method to measure these samples, but Thelliers' Method can be used. (6) The TRMs of some samples are unstable to AF demagnetization, i.e., the AF demagnetization curves are not smooth and the orientation of TRM, changes greatly during AF demagnetization. This kind of sample can only be measured by Thelliers'Method. (7) Theoretically, all the points in the RNRM-RTRM diagram in the AF Demagnetization Method lie on a straight line which must pass through the origin; but actually, almost all of the straight lines of the samples do not pass through the origin, which means that even a small mineralogical change incurred through heating will completely change the shape of the AF demagnetization curve. The test experiments also showed that the deviation between the calculated field intensity and the actual field intensity would become larger if one calculated only the points which, in the higher peak alternating field, would fit a straight line passing through the origin. (8) In the Anhysteretic Remanent Magnetization Method (ARM Method), the measurement of the AF demagnetization curves of both NRM and TRM are necessary. This method, therefore, has the same problem as the AF Demagnetization Method. The ARM Method can detect a mineralogical change by heating during the measurements. (9) The above discussion indicates that Thelliers' Method is the most reliable method to measure the ancient field intensity since the results

from Thelliers' Method tell whether or not the sample has been reheated. It also can tell whether or not the sample has undergone chemical reaction during measurement. If this is so, Thelliers' Method can also tell the temperature at which the sample has been reheated or that which the chemical reaction has occurred.

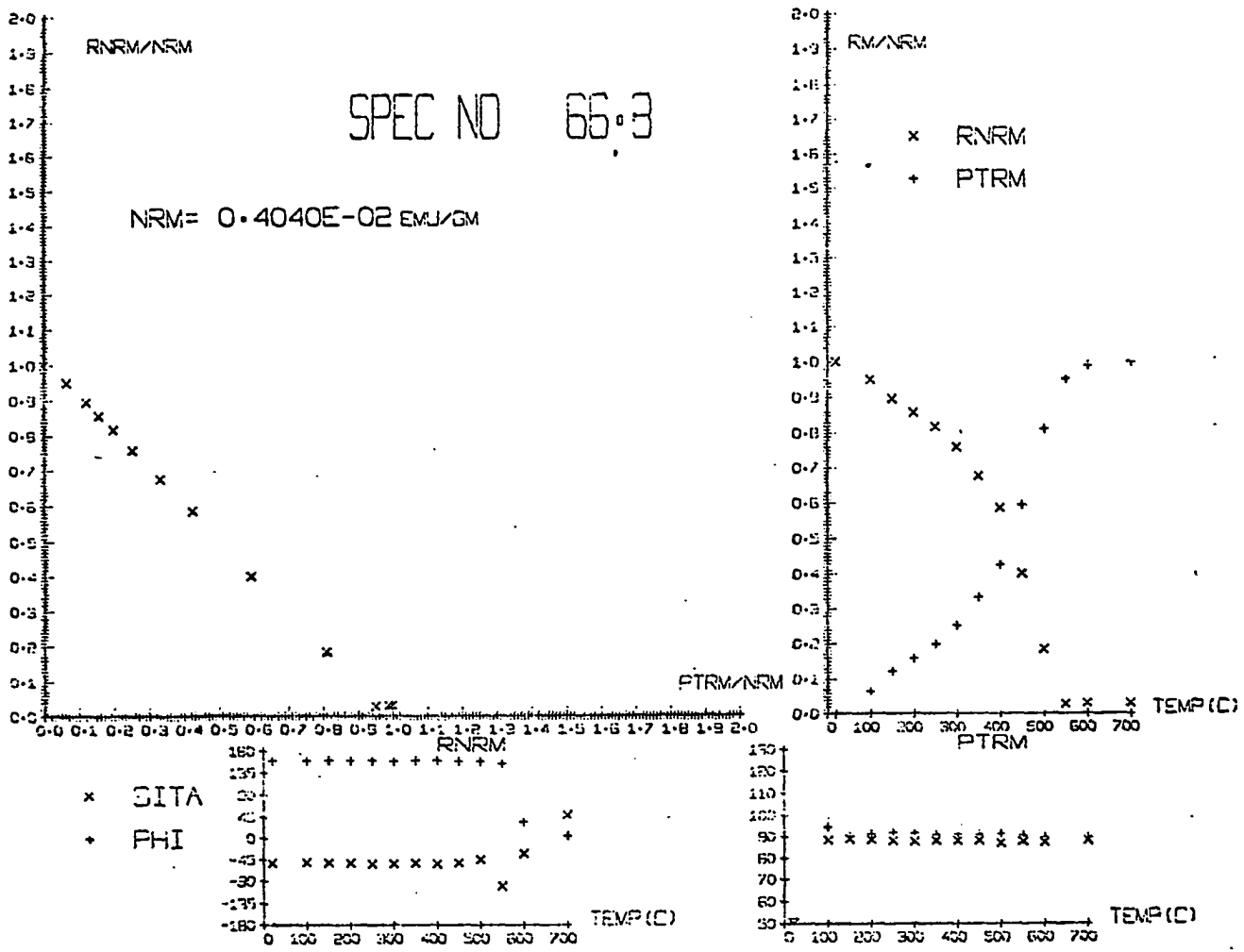

Fig. 48 Results of Spec. No.66.3 obtained by Thelliers' Method (A).

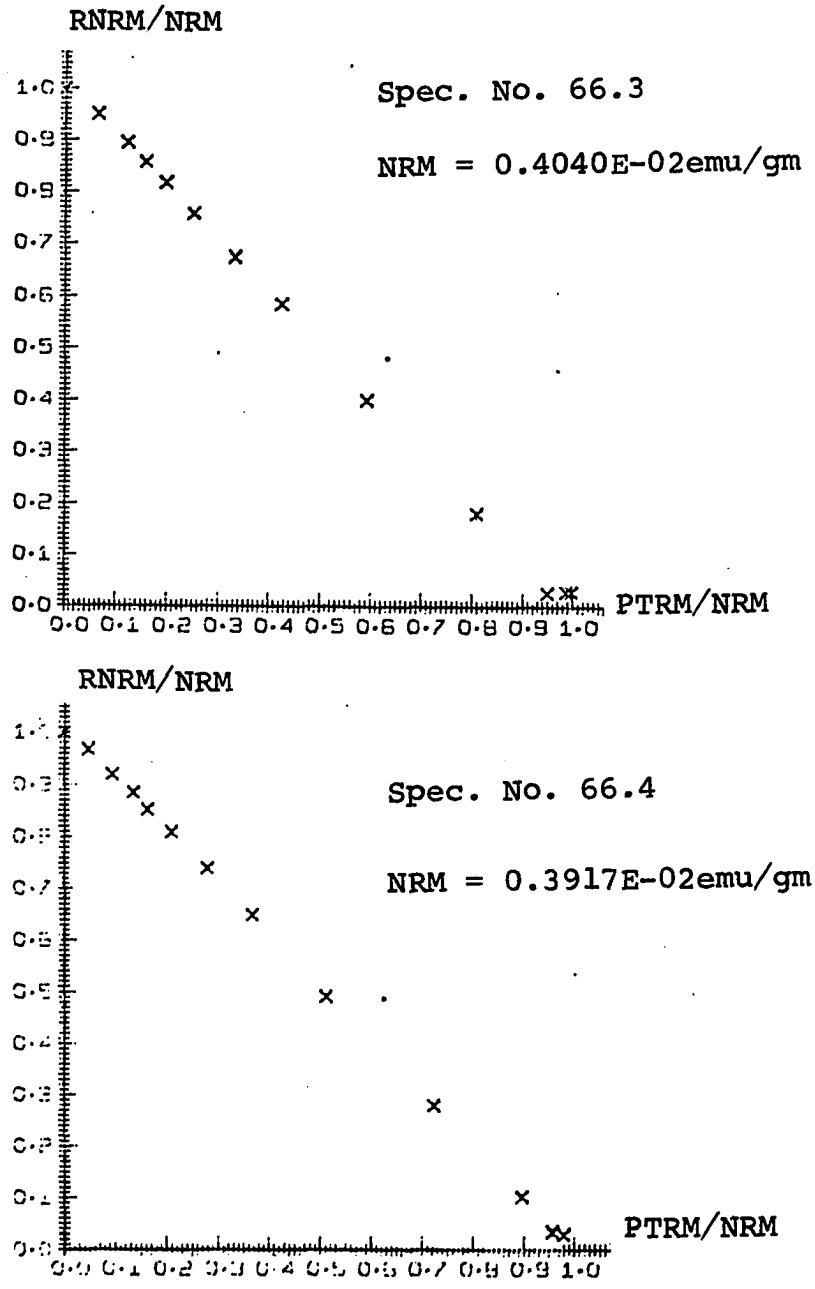

Fig. 49 Normalized RNRM-PTRM curves from Sample No.66 obtained Thelliers' Method.

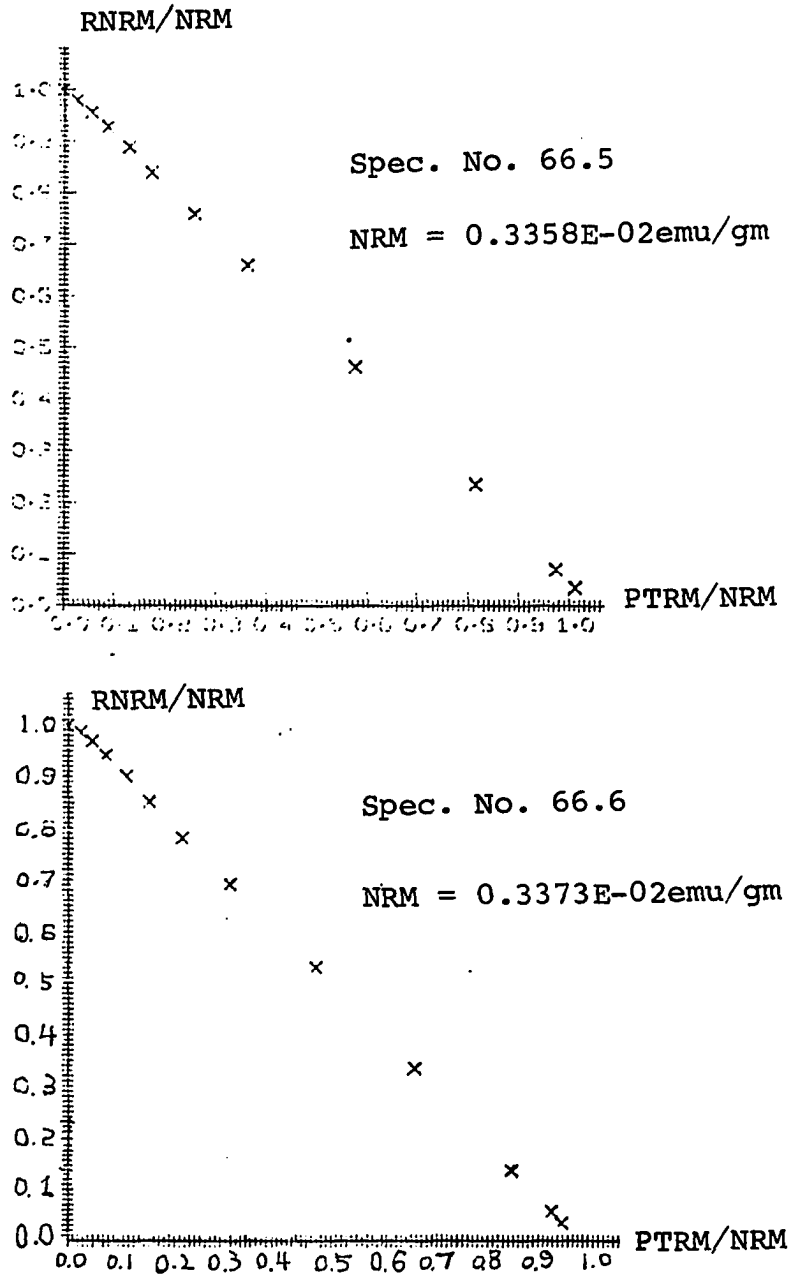

Fig. 49 (Continued)

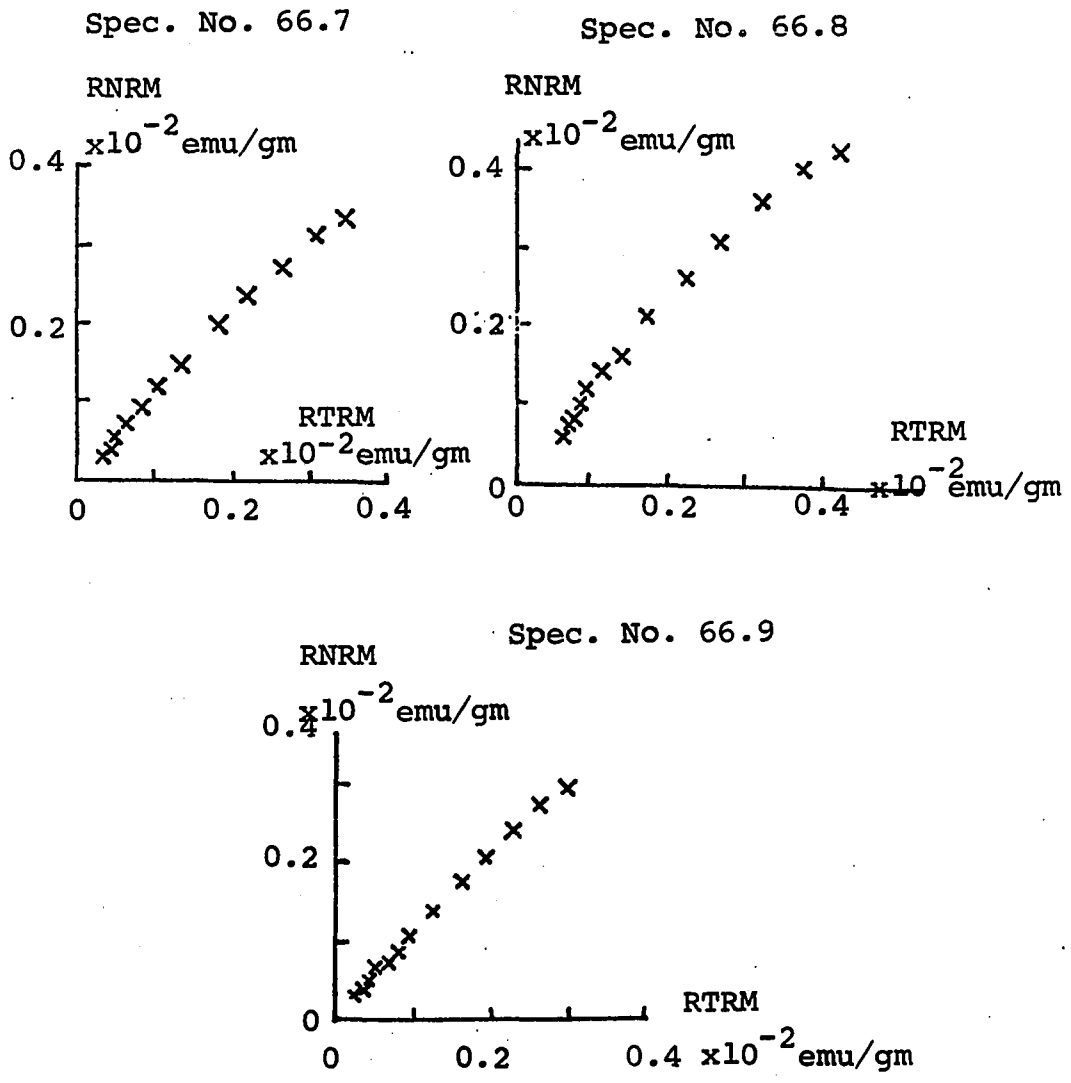

Fig. 50 RNRM-RTRM curves from Sample No.66 by the AF Demagnetization Method.

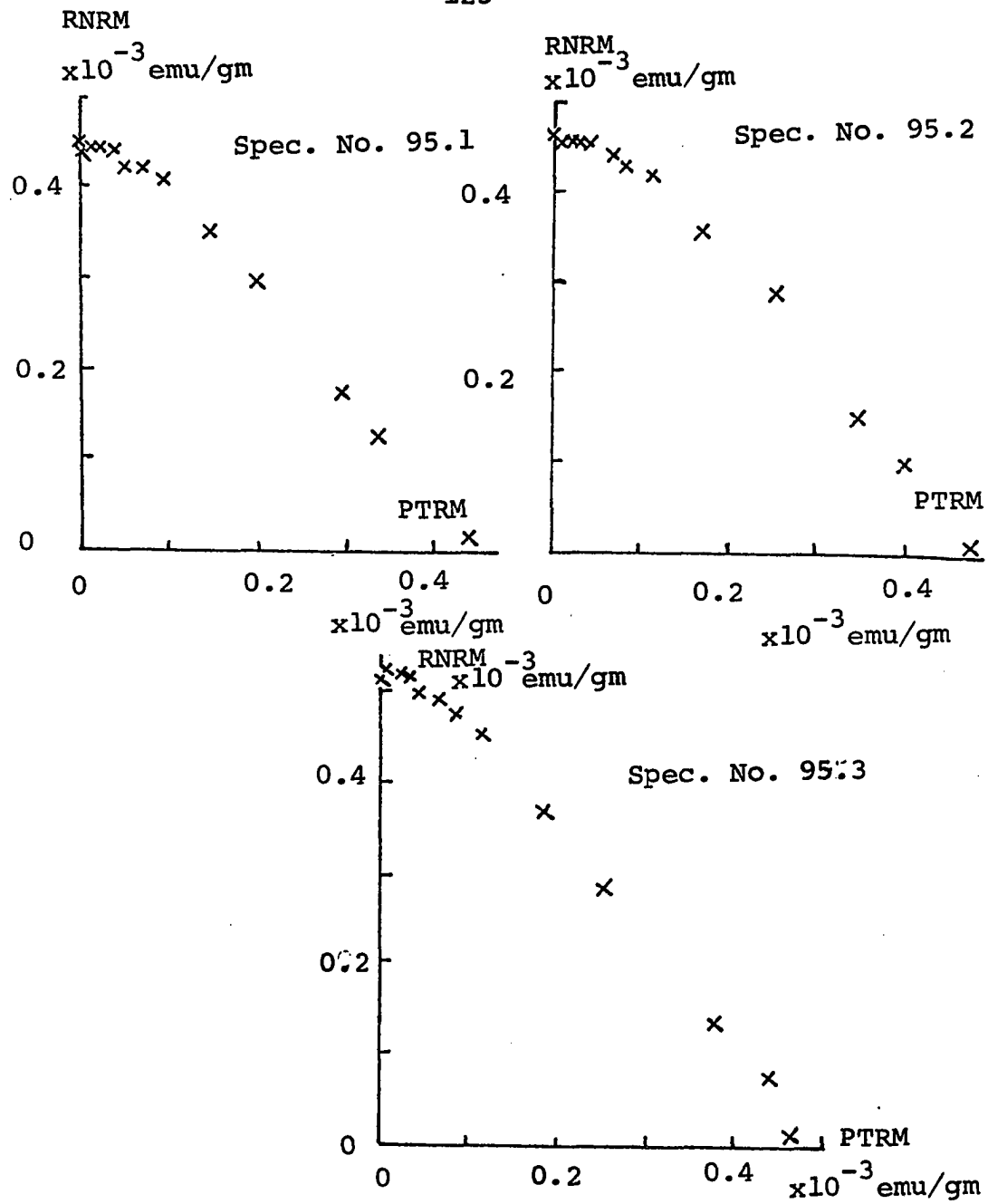

Fig. 51 RNRM-PTRM curves from Sample No.95 obtained by Thelliers' Method.

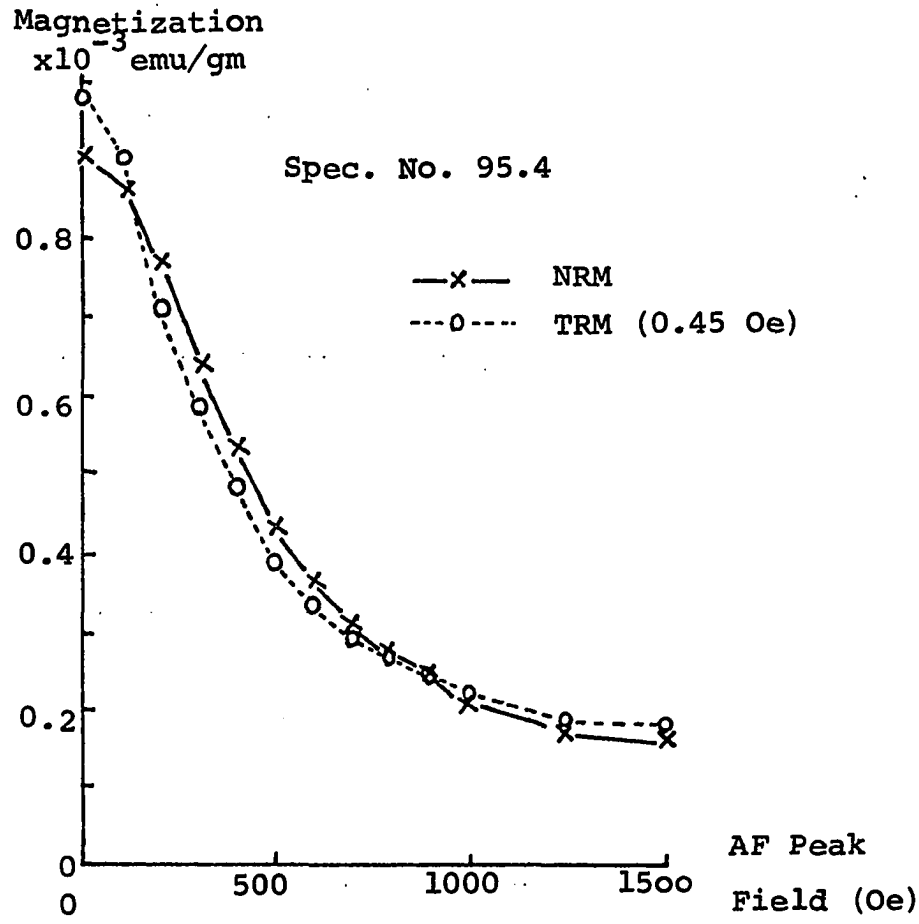

Fig. 52 Results of Spec. No.95.4 obtained by the AF Demagnetization Method.

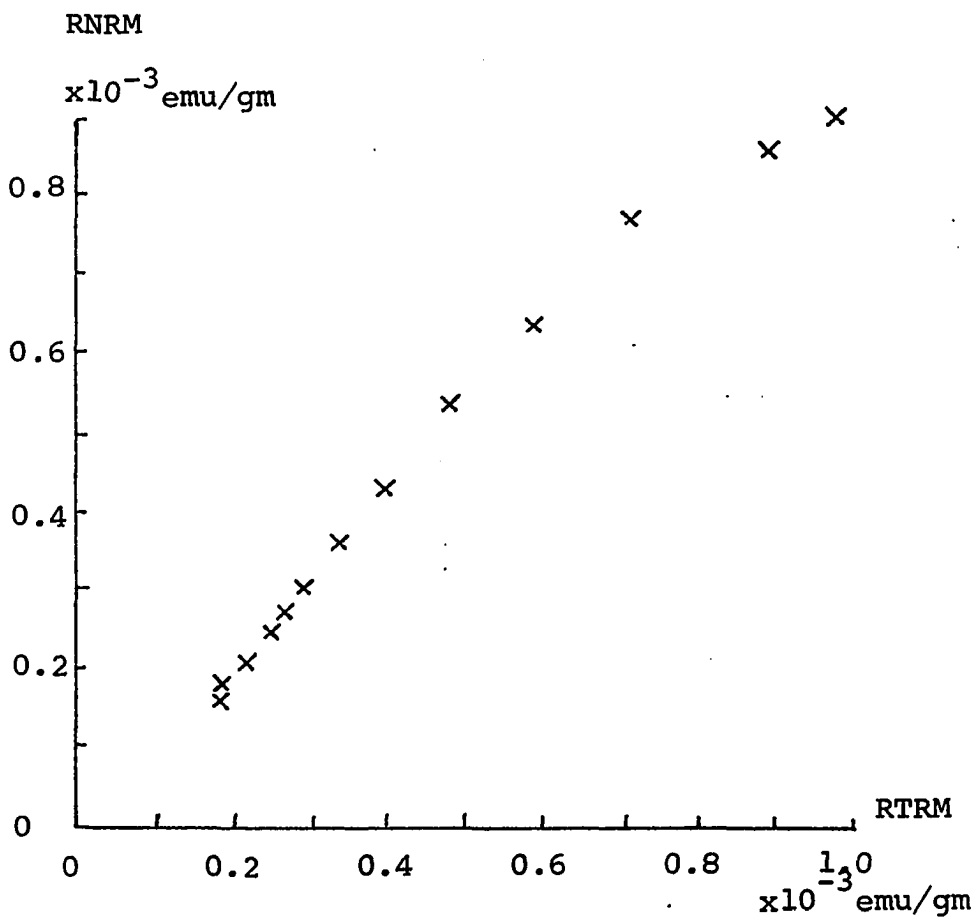

Fig. 52 (Continued)

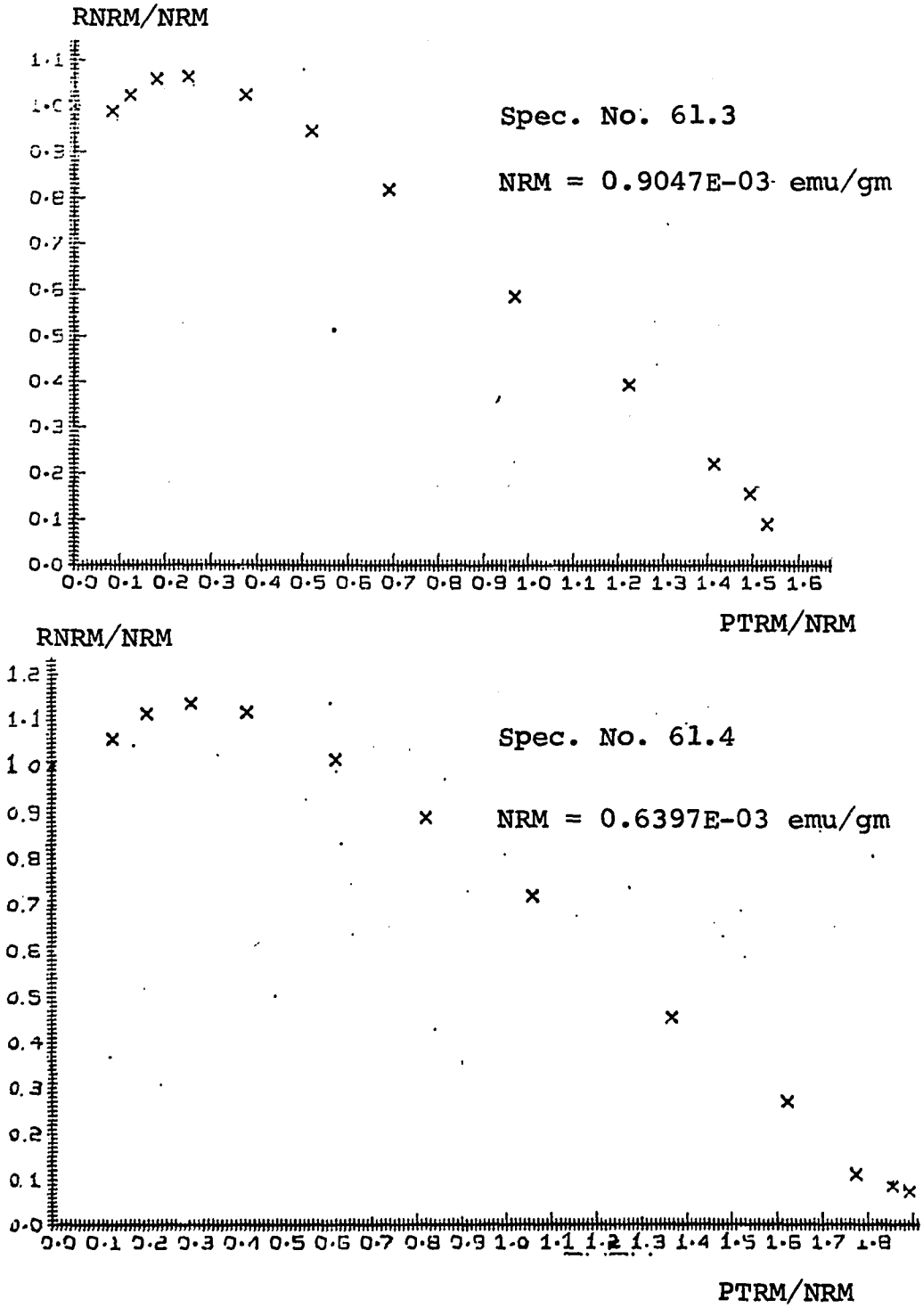

Fig. 53 Normalized RNRM-PTRM curves from Sample No.61 obtained by Thelliers' Method.

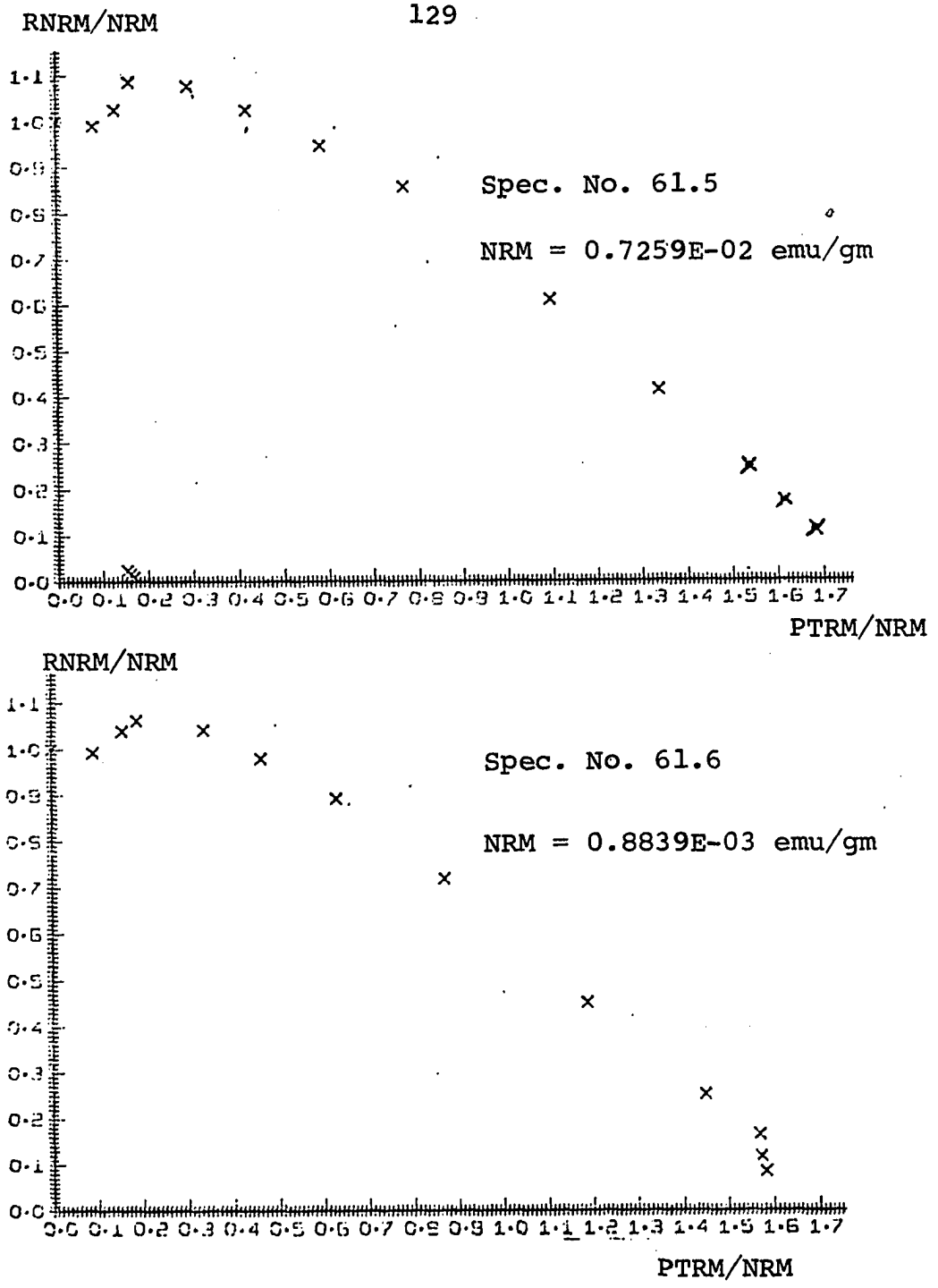

Fig. 53 (Continued)

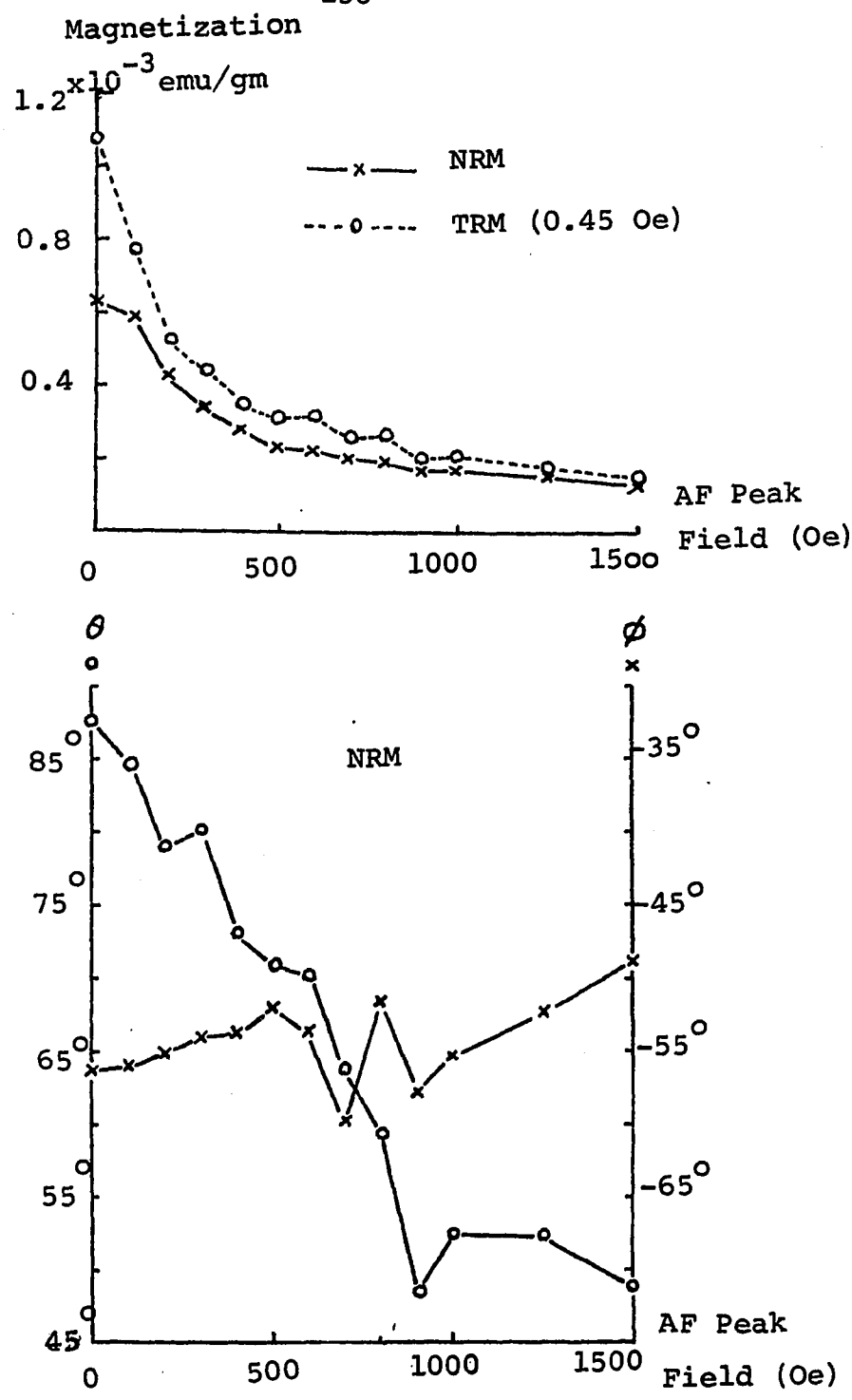

Fig. 54 Results of Spec. No.61.7 obtained by the AF Demagnetization Method.

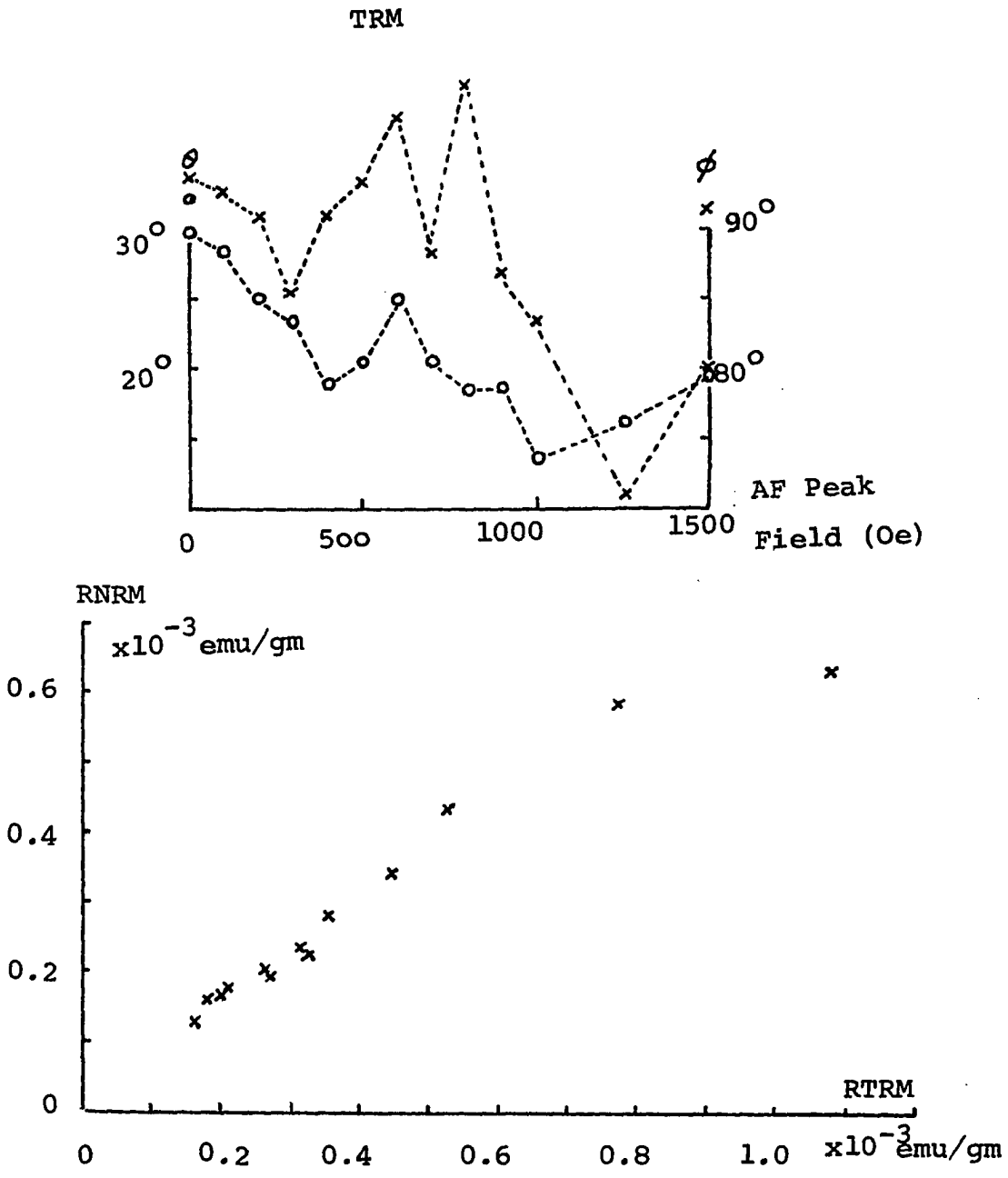

Fig. 54 (Continued)

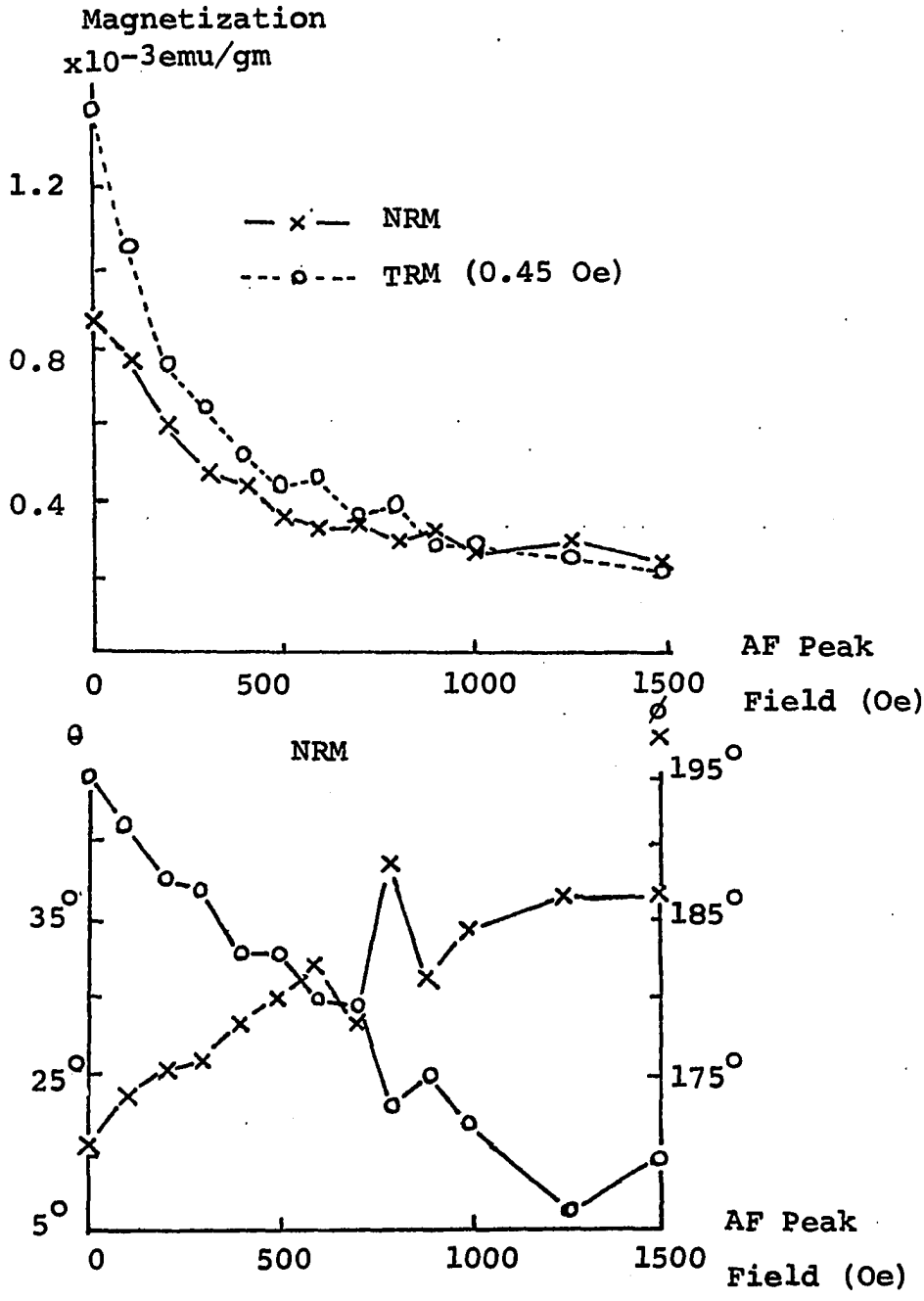

Fig. 55 Results of Spec. No.61.8 obtained by the AF Demagnetization Method.

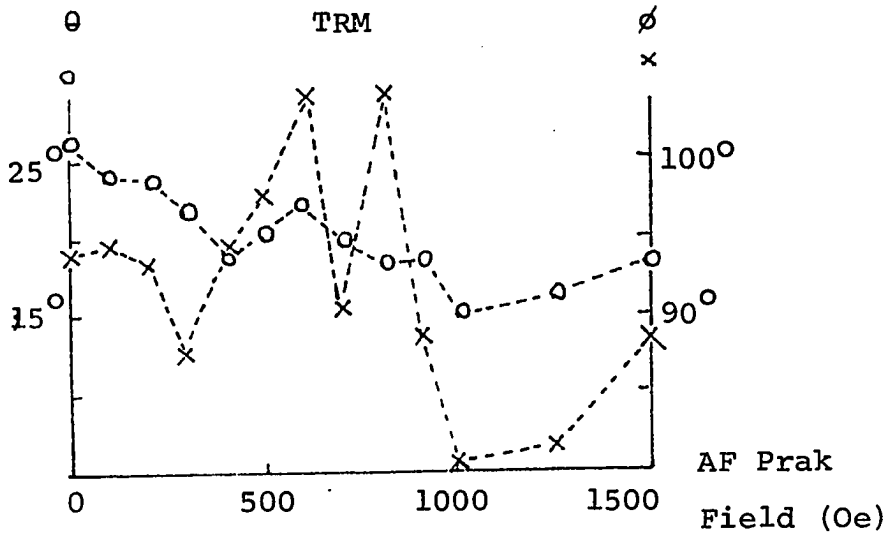

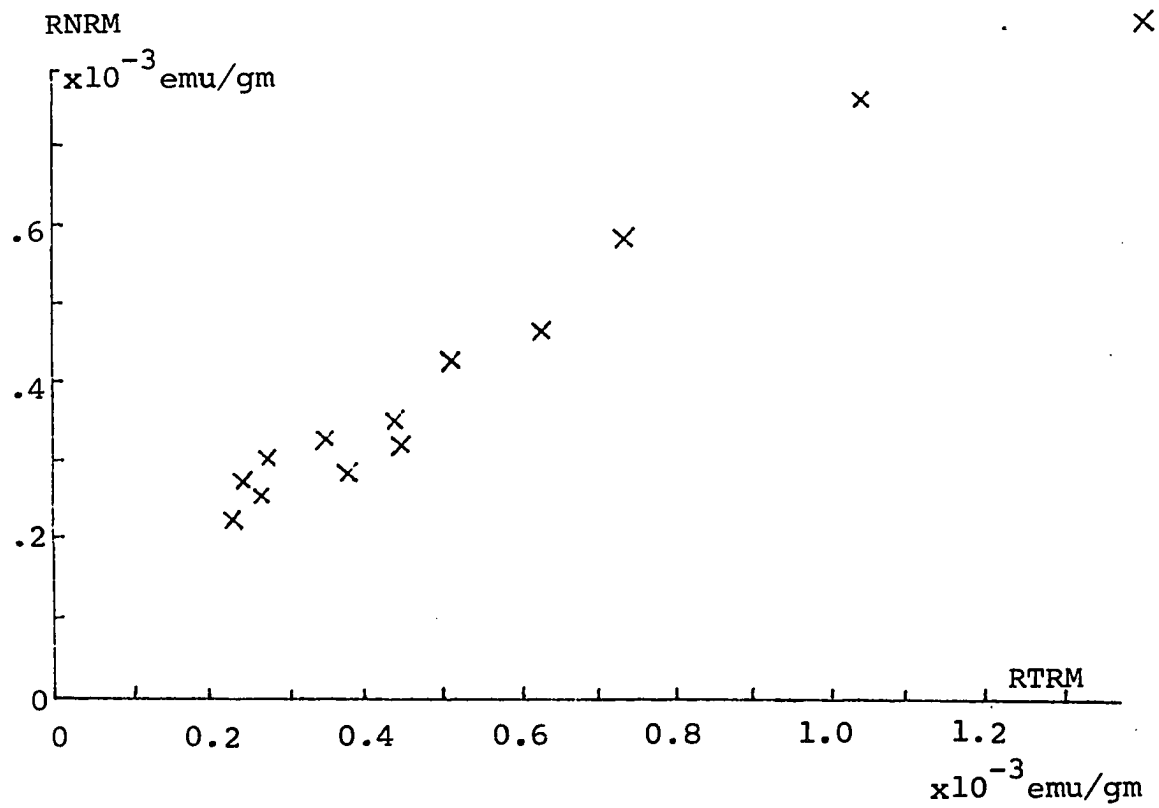

Fig. 55 (Continued)

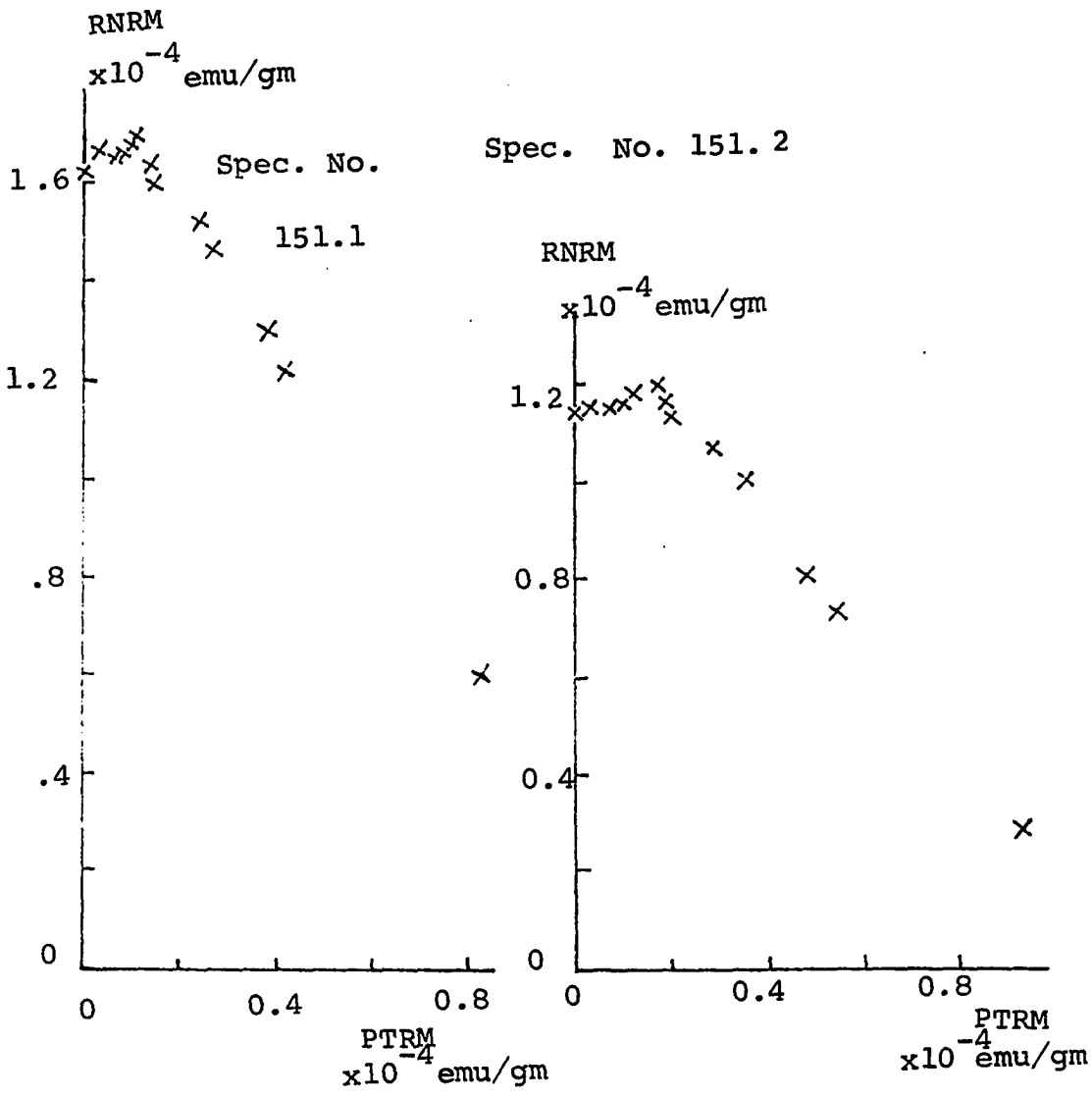

Fig. 56 RNRM-PTRM curves from Sample No.151 and the change of the orientation of Spec. No.151.3 obtained by Thelliers' Method.

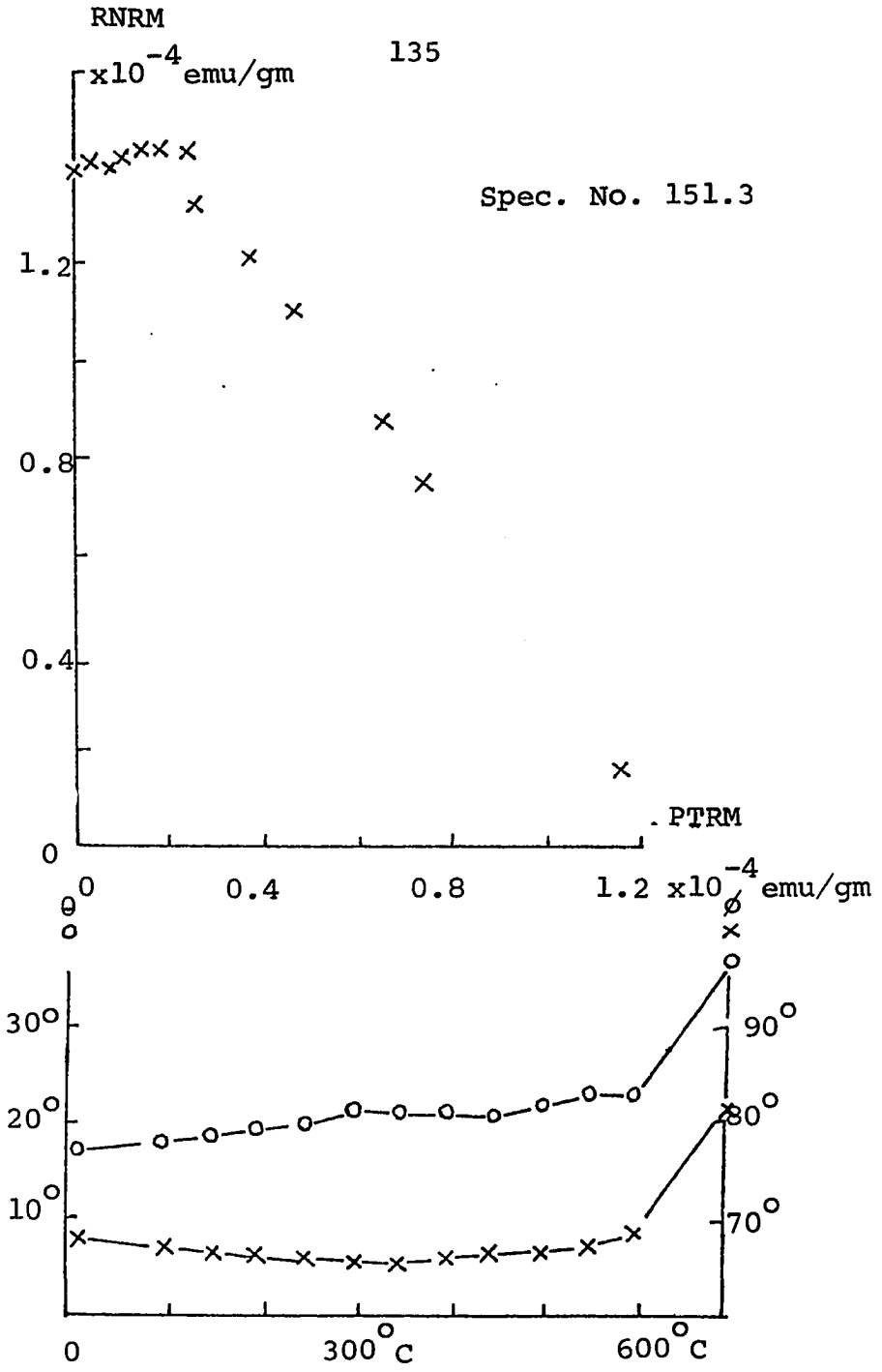

Fig. 56 (Continued)

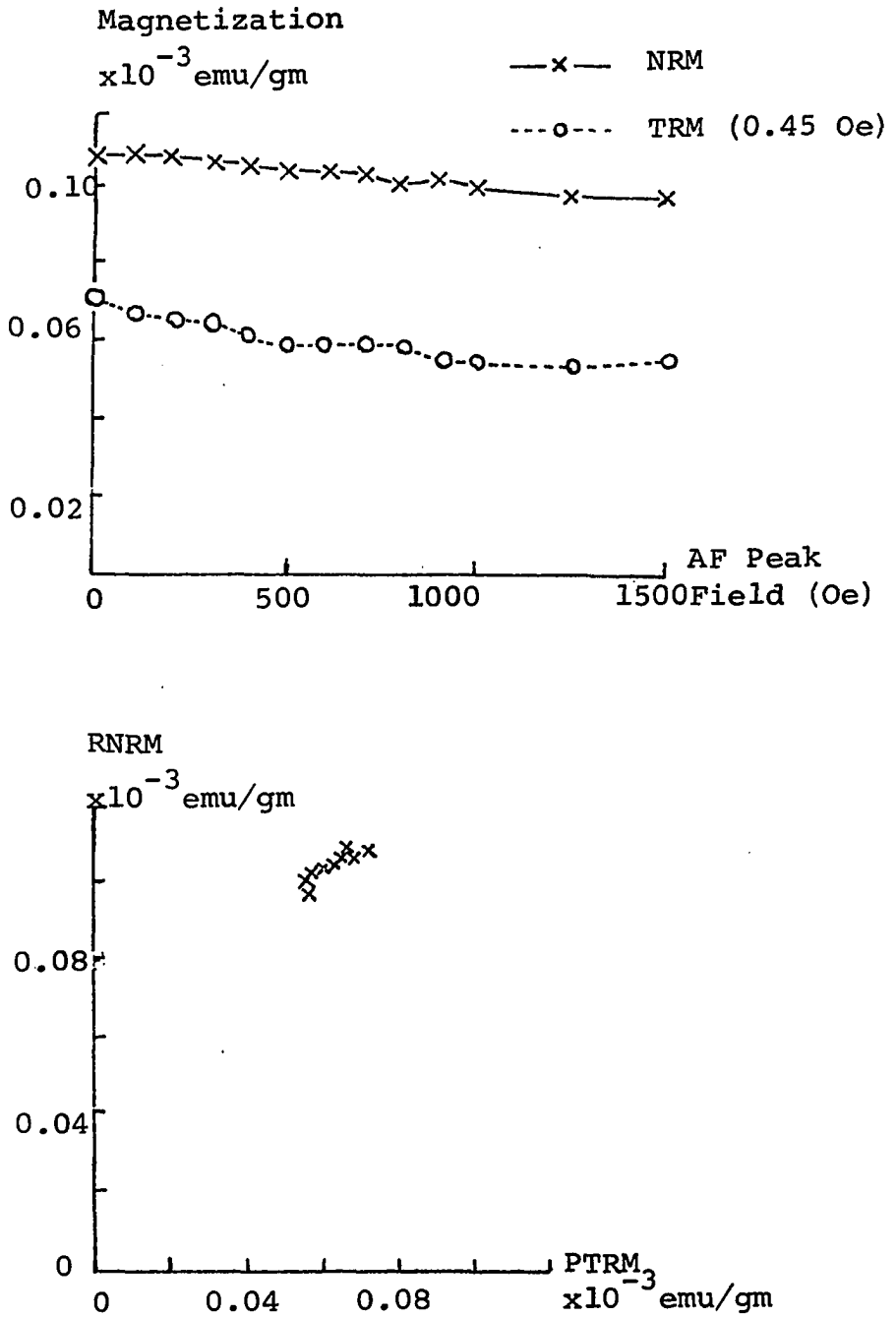

Fig. 57 Results of Spec. No.151.4 obtained by the AF Demagnetization Method.

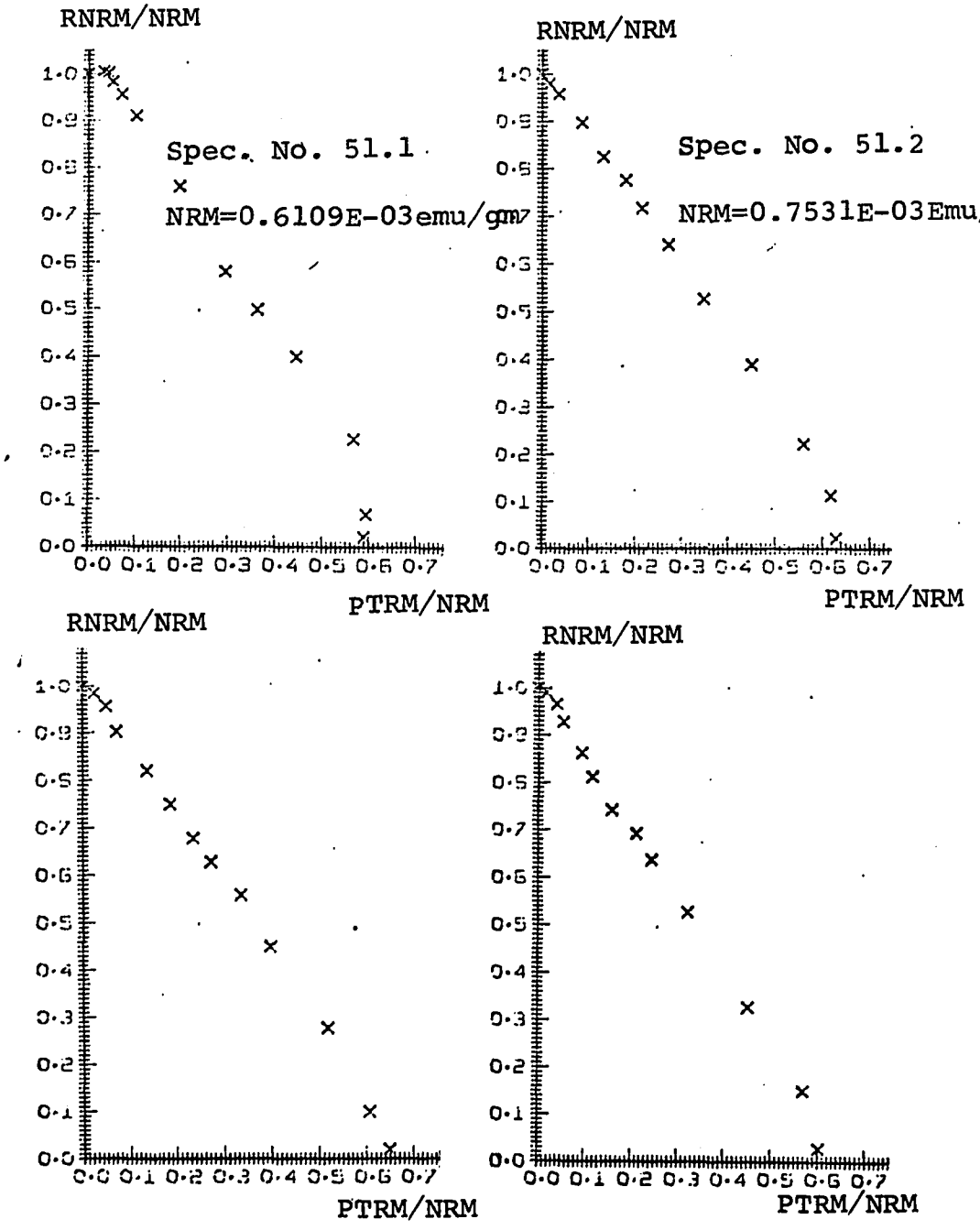

Fig. 58 Normalized RNRM-PTRM curves from Sample No.51 obtained by Thelliers' Method.

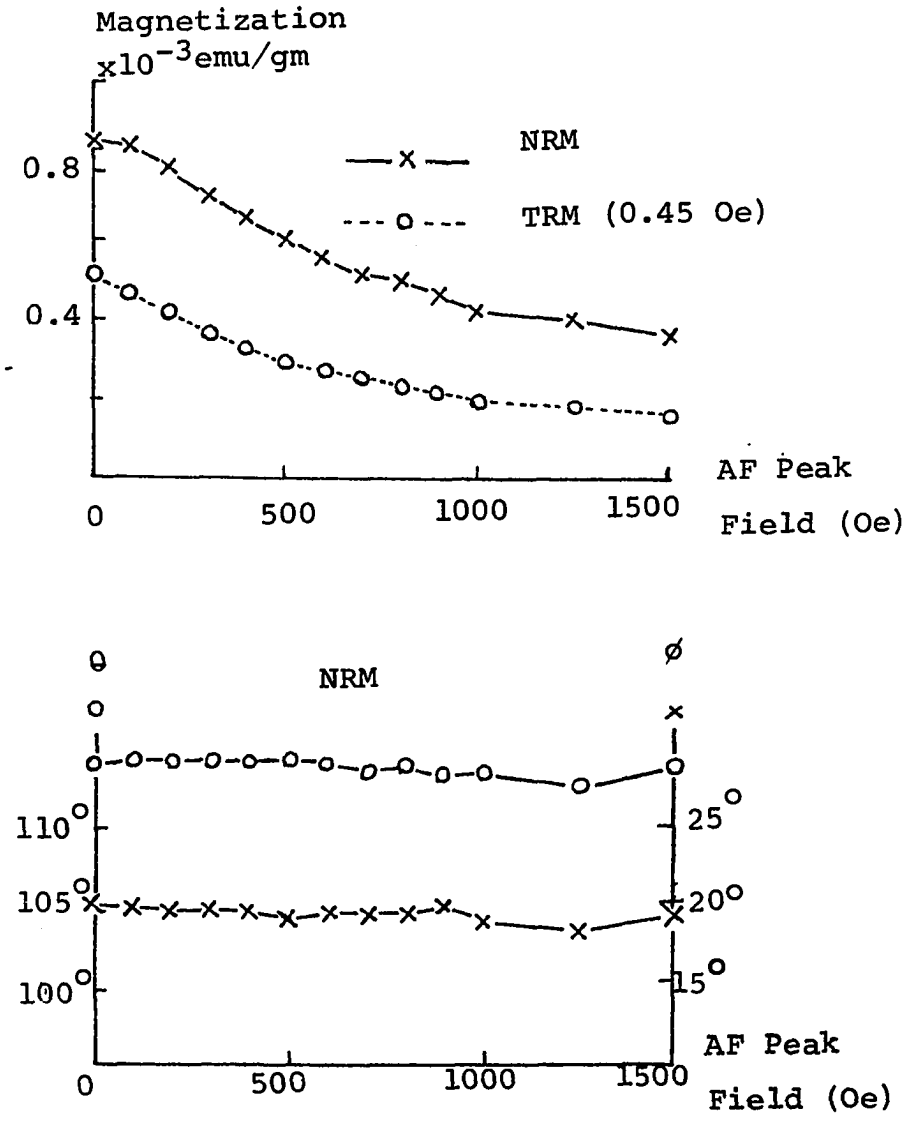

Fig. 59 Results of Spec. No.51.6 obtained by the AF Demagnetization Method.

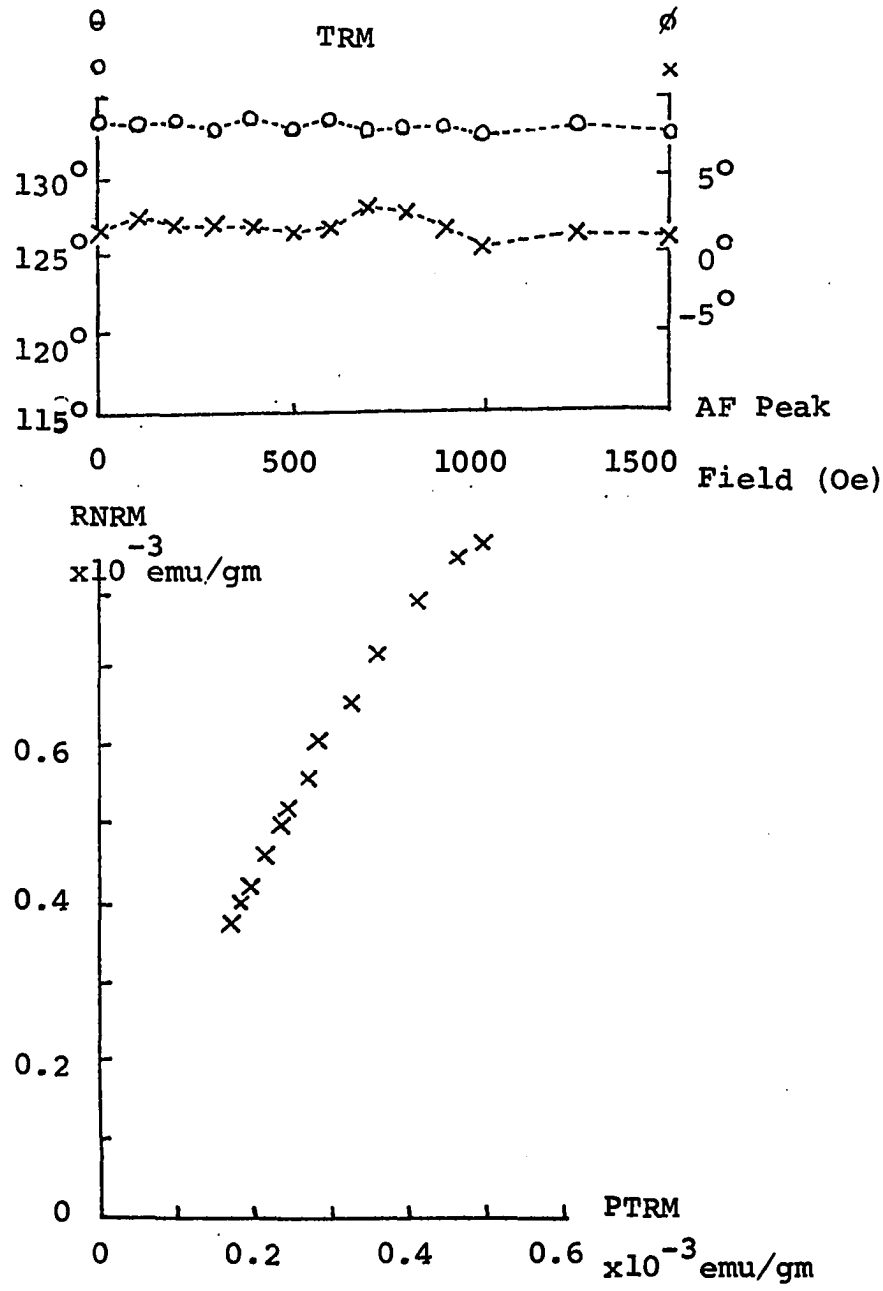

Fig. 59 (Continued)

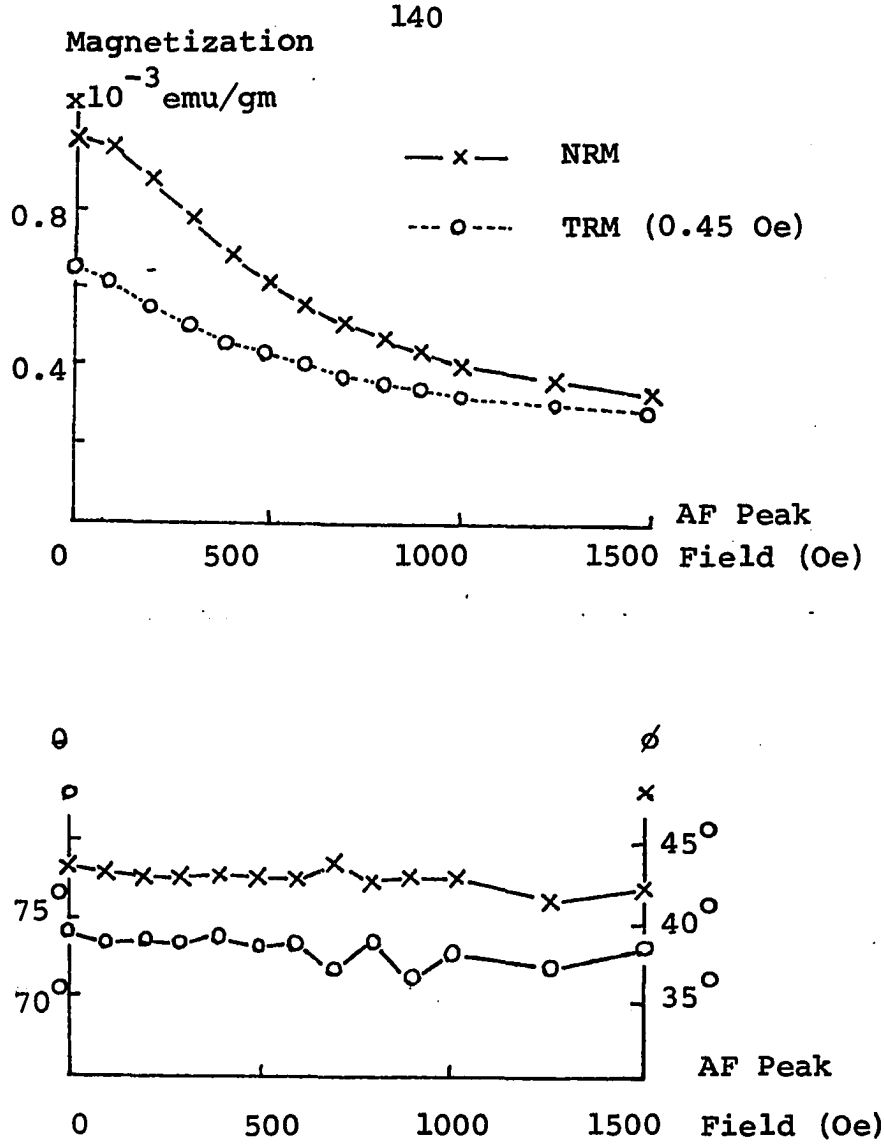

Fig. 60 Results of Spec. No. 51.7 obtained by the AF Demagnetization Method.

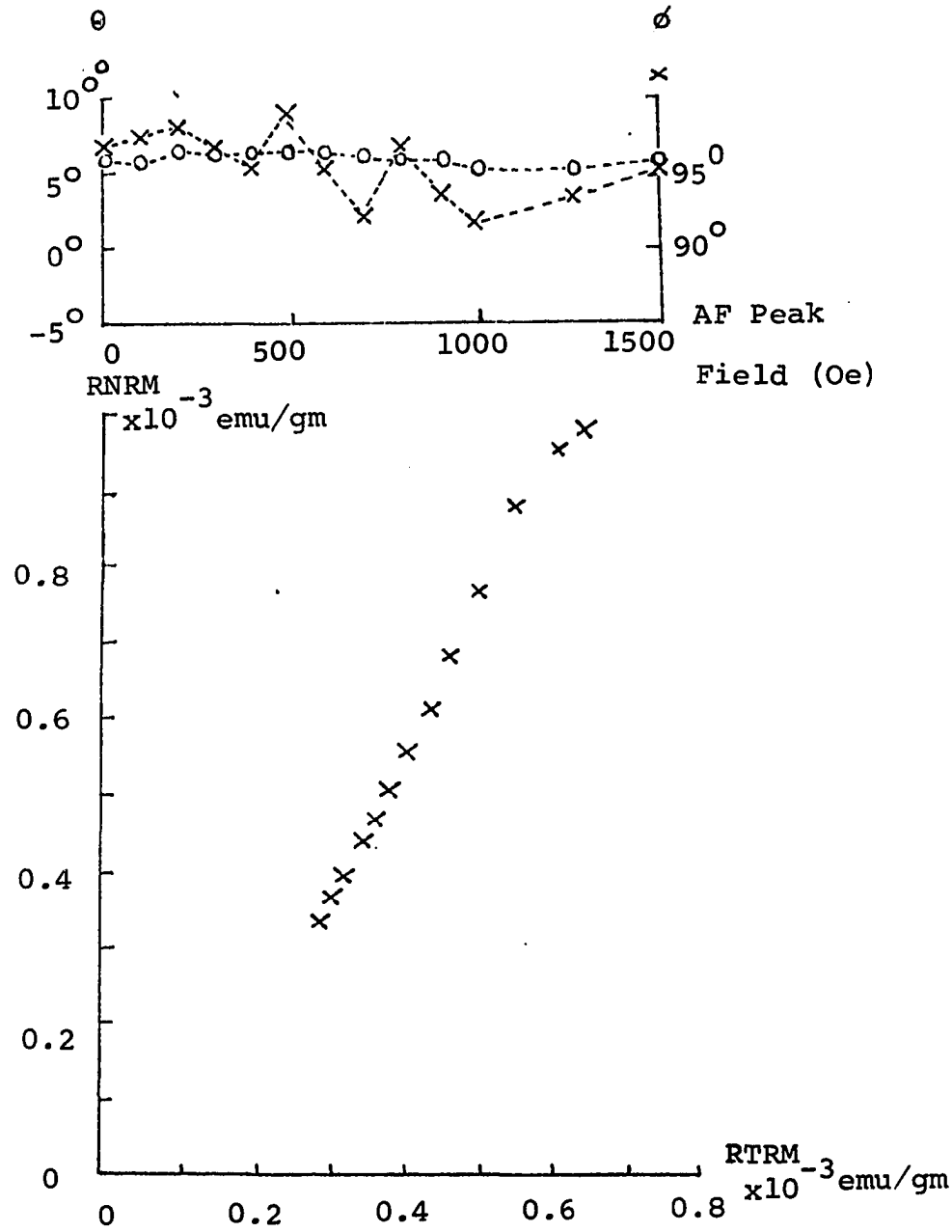

Fig. 60 (Continued)

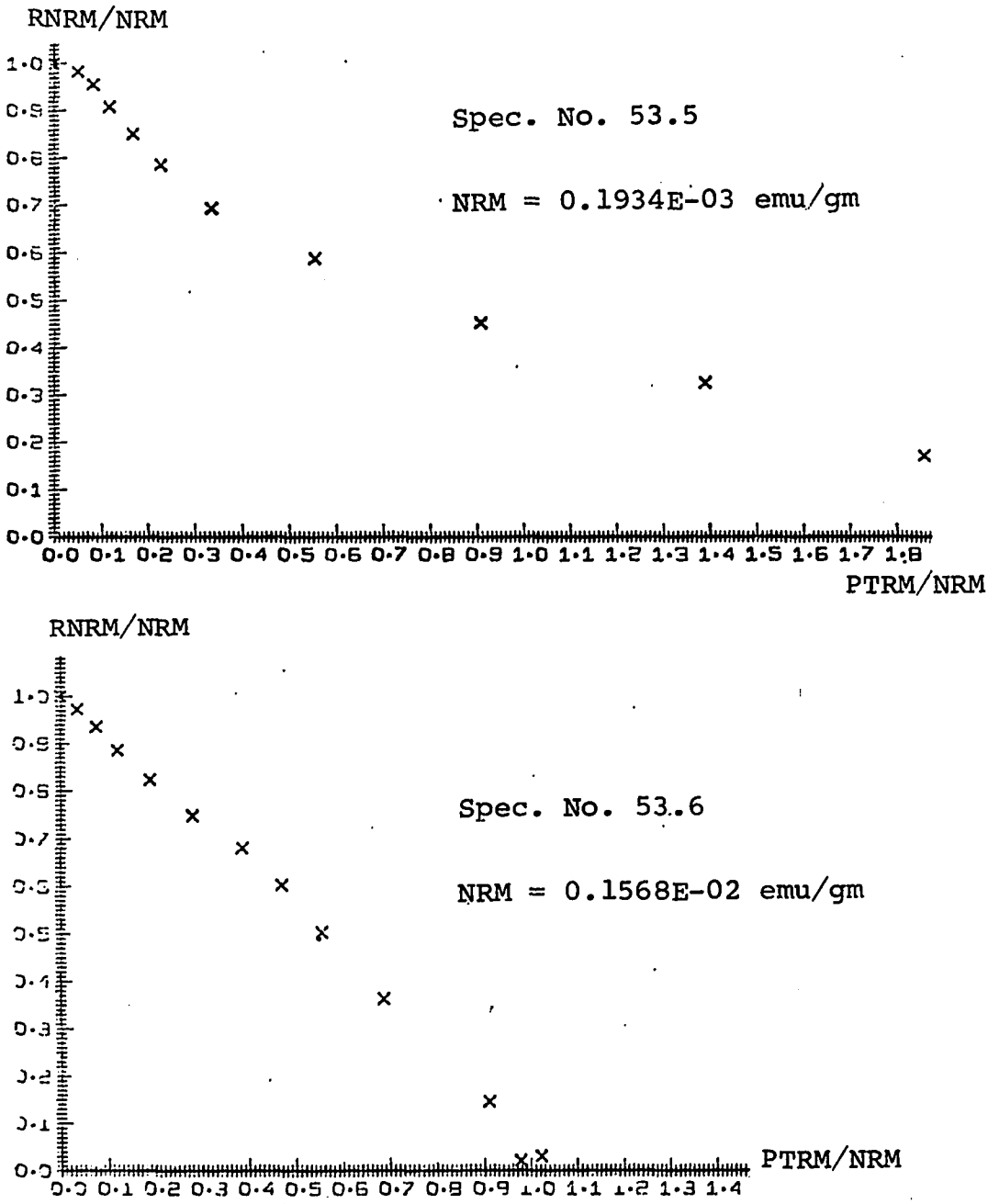

Fig. 61 Normalized RNRM-PTRM curves from Sample No.53 obtained by Thelliers' Method.

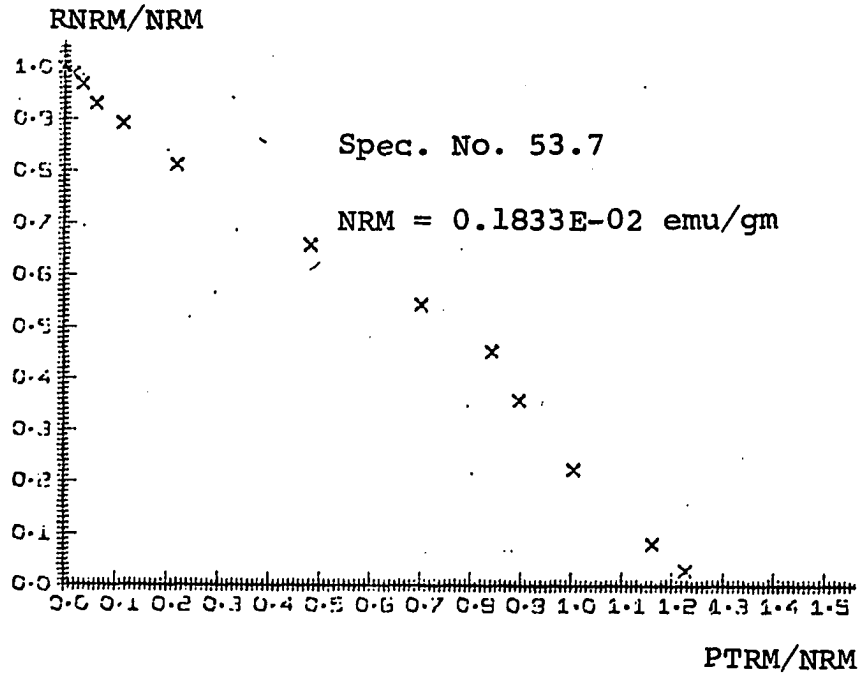

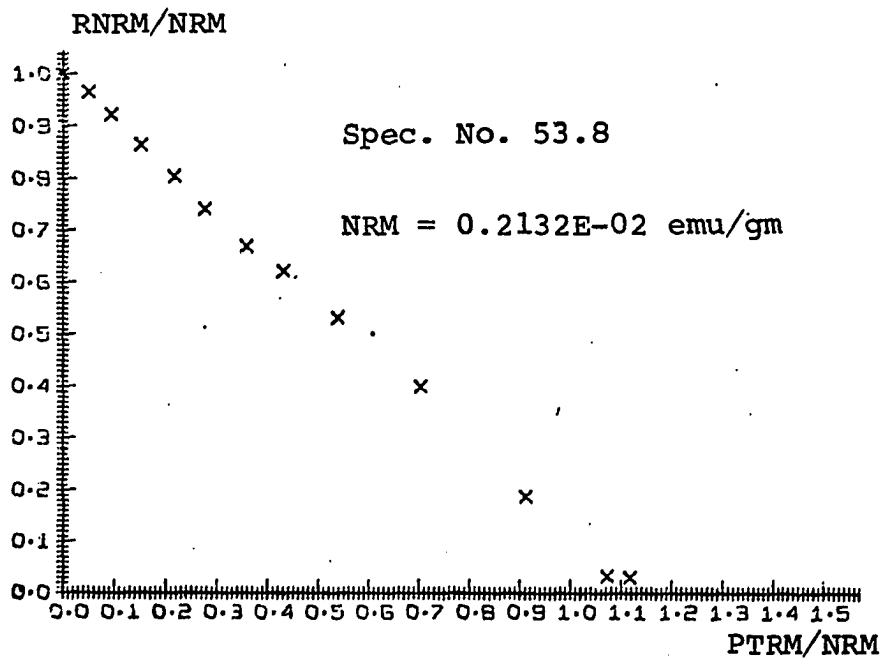

Fig. 61 (Continued)

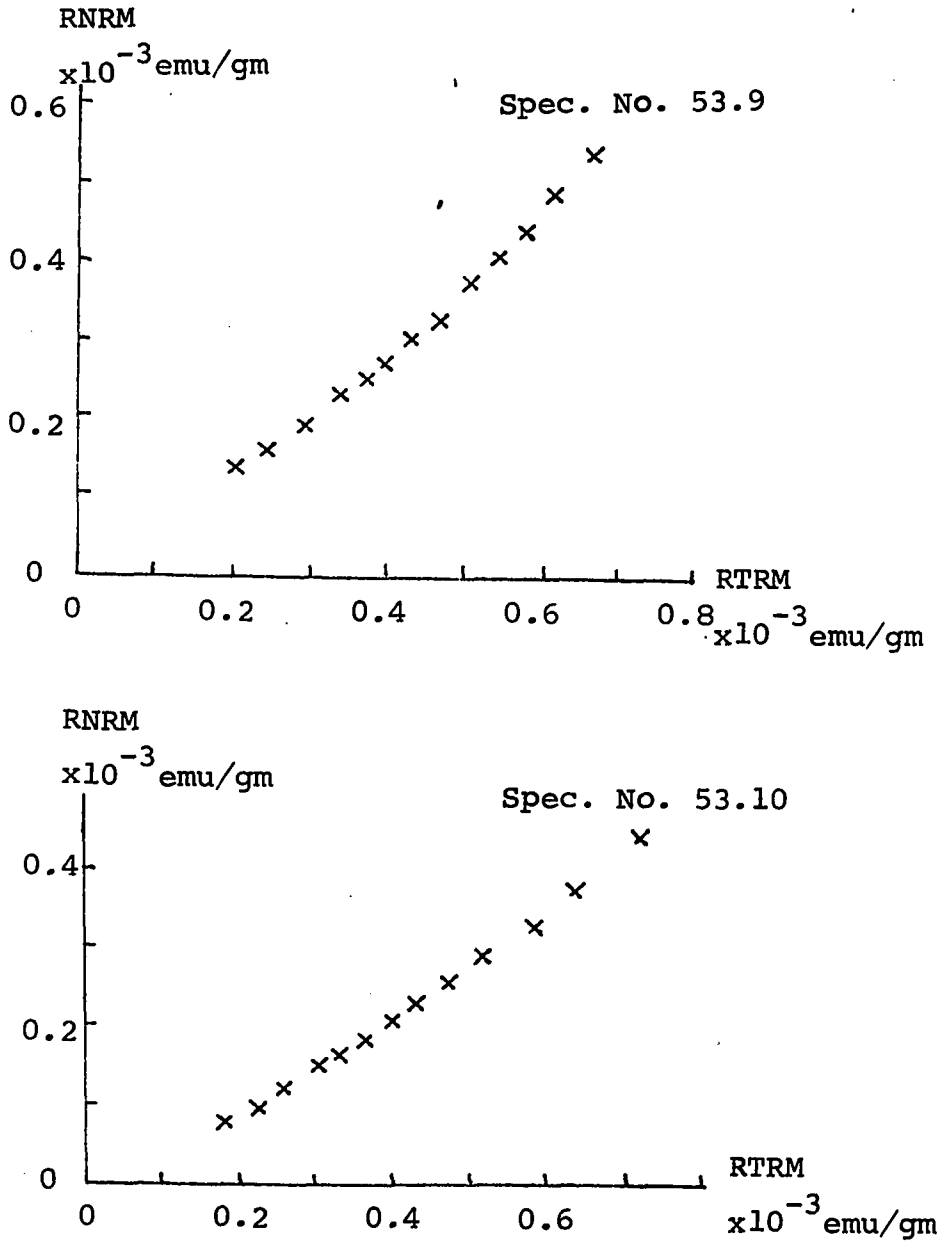

Fig. 62 RNRM-RTRM curves from Sample No.53 obtained by the AF Demagnetization Method.

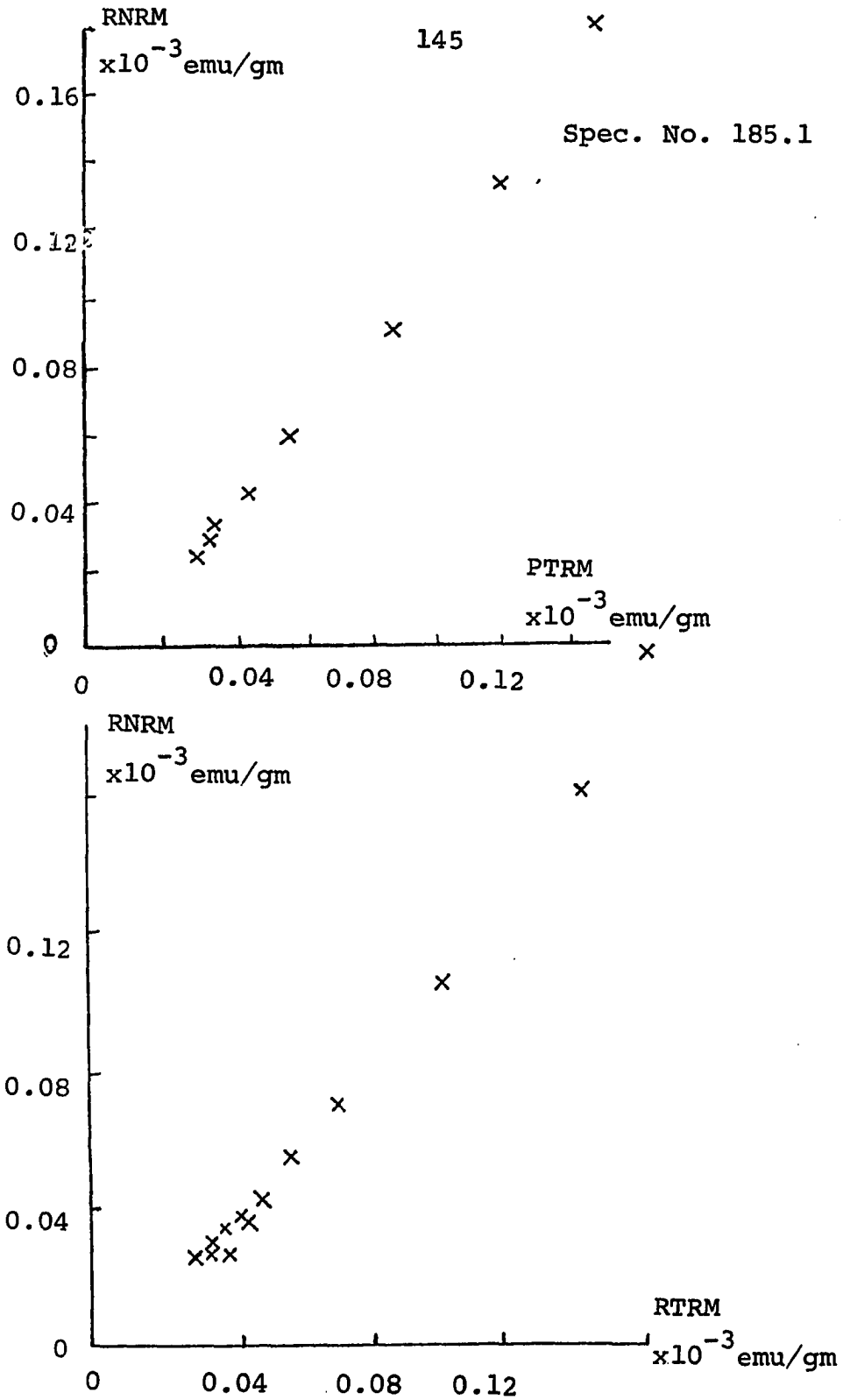

Fig. 63 RNRM-RTRM curves from Sample No.185 obtained by the AF Demagnetization Method.

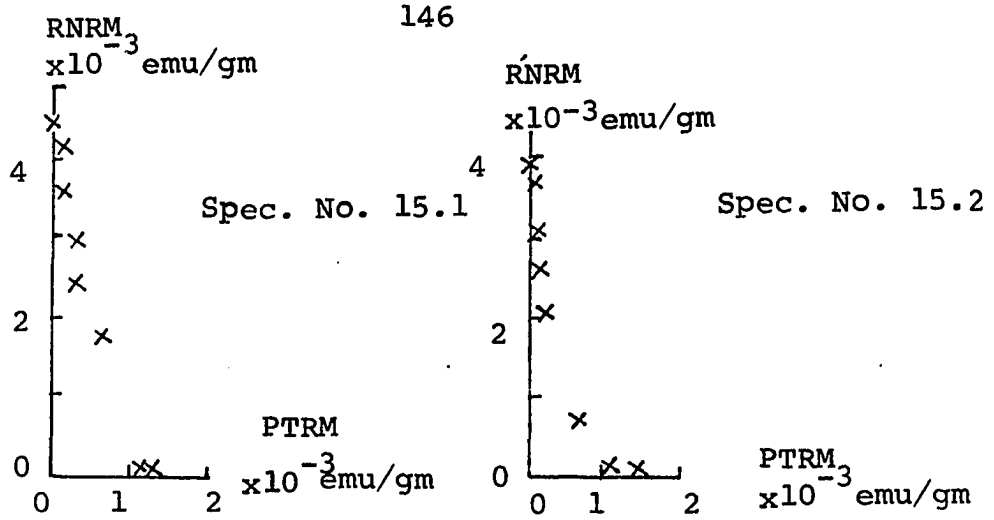

Fig. 64 RNRM-PTRM curves of Spec. Nos.15.1 and 15.2 obtained by Thelliers' Method.

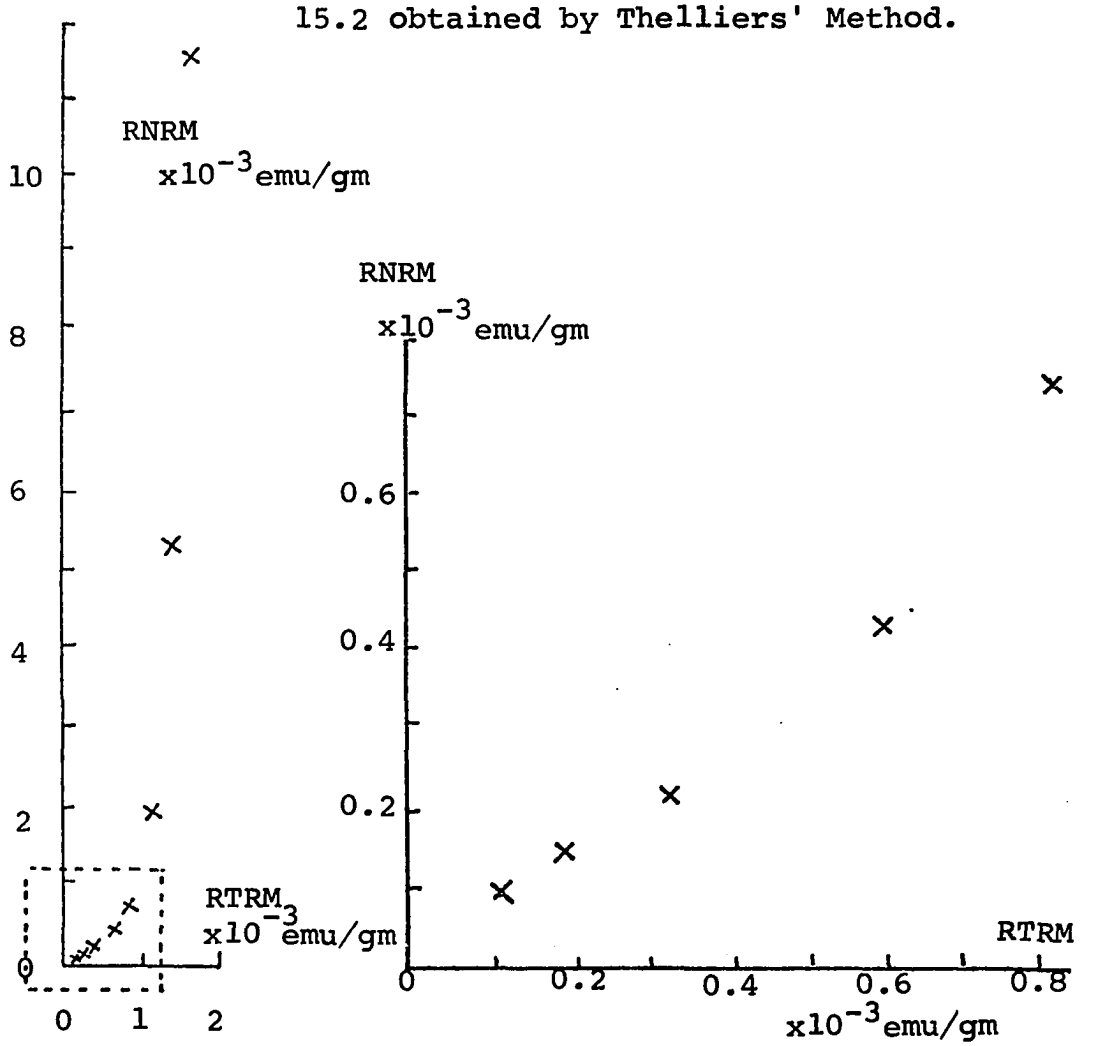

Fig. 65 RNRM-RTRM curves of Spec. No.15.3 obtained by the AF Demagnetization Method.

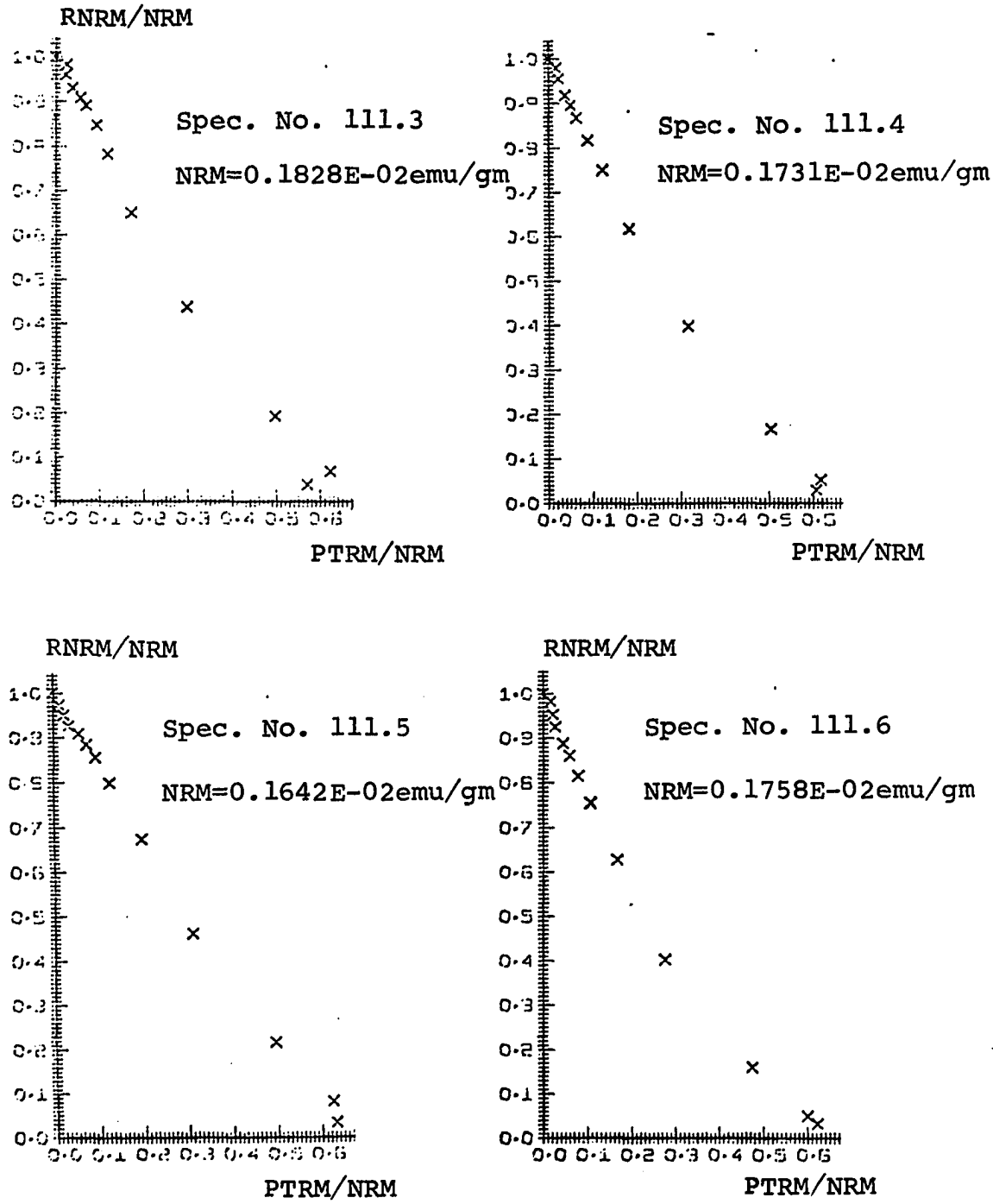

Fig. 66 Normalized RNRM-PTRM curves from Sample No.111 obtained by Thelliers' Method.

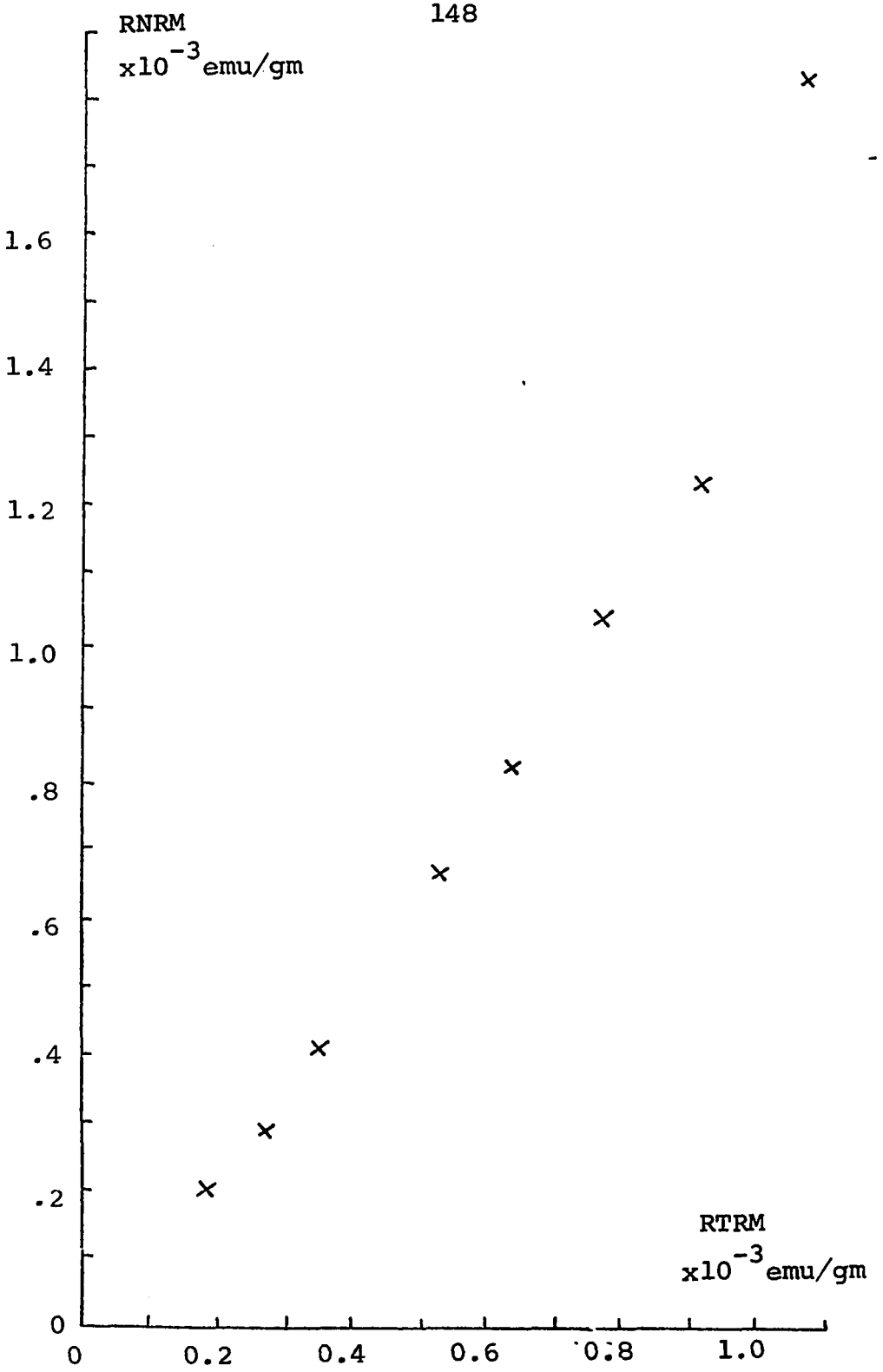

Fig. 67 RNRM-RTRM curve of Spec. No.111.7 obtained by the AF Demagnetization Method.

CHAPTER III

PRESENTATION OF ANCIENT FIELD INTENSITY DATA

Sampling Site Localities

A total of 324 specimens were cut from 100 samples of pottery and baked clays associated with burnt rooms or hearths and collected from North, Central, and South America. Almost all the specimens were used to investigate geomagnetic field intensity using Thelliers' Stepwise Heating Method. The geographic locations of sampling sites in these regions are shown in Fig. 68, Fig. 69, and Fig. 70, respectively. The ages of the samples were determined by historical dating, Carbon 14 dating, or by archeomagnetic methods.

Data from Samples from Central America

Two hundred and twenty-four specimens from sixty-five samples, which were collected from Mexico and Guatemala as shown in Fig. 69, have been carefully measured in this study. Most of the specimens are measured by Thelliers' Method, and a few specimens measured by the AF Demagnetization Method or Wilson's Method. The results of the measurements are listed in the appendix in Table 9. In Table 9, the abbreviations "Th(A)", "Th(B)", "Th(C)", "Th(D)", indicate the specimens were measured by

Method A, Method B, Method C, and Method D, respectively, by Thelliers' Method, which was described in chapter II. "AF" indicates the specimens were measured by the AF Demagnetization Method, and "W" indicates that the specimens were measured by Wilson's Method. F_o is the present geomagnetization field intensity in the site, and F is the ancient field intensity measured from the specimen. The abbreviation "VR" indicates the result of the measurement from this specimen is very reliable because it shows, (a) that there is almost no chemical change acquired during the measurement; (b) the specimen had not been reheated after its original firing; (c) the orientations of both the RNRM and PTRM are very stable; and (d) the points in the RNRM-PTRM diagrams lie almost in a straight line. If the results of the measurements show that the specimens have secondary magnetization and the results are still reliable, then the abbreviation "R" is used to indicate, (a) that the specimens may have VRM, or (b) the specimens have chemical reactions upon heating during measurement, or (c) the sample may have been struck by lightning and gained IRM. "P" means that it is impossible to get reliable results because of either the large scattering of measured points in the RNRM-PTRM diagrams or the orientations of RNRM and PTRM are unstable.

The previous chapter indicates that the results from Thelliers' Method are more reliable than those from the other methods, and Thelliers' Method (A) is more reliable than Thelliers' Method (B), (C), and (D). In cases where some of the specimens from a sample are measured by the various Thelliers' Method (A, B,C,D), it is only ne-

cessary to consider those results from Thelliers' Method (A) in order to obtain a more reliable average ancient field intensity value for each sample. If the results of the different specimens from the same sample include the different reliabilities "VR" and "R", then it is only necessary to count those which are "VR". F/F_o is the ratio of the ancient field intensity to the present field intensity in the site.

The secular variation curve of the intensity of the geomagnetic field in Central America obtained from this study is shown in Fig. 71. This hand-drawn curve is preferred over a mathematically determinal one because of the existence of a wide age range in dating for each sample. The curve implies that the intensities of the geomagnetic field in Central America at about 1150 AD and 450 AD were 1.5 times as large as the present field intensity, and at about 300 BC was 1.25 times. There are two minimun values at 100 AD and 800 AD. The field intensities were 0.84 and 0.94 times as large as the present field intensity.

Fourier Analysis is applied to the secular variation curve of the intensity of the geomagnetic field in Central America during the past 2,300 years. A function f(t) of the independent variable t (time) when expressed as a Fourier series is :

$$f(t) = \frac{a_o}{2} + \sum_{n=1}^{\infty} (a_n \cos n\omega_1 t + b_n \sin n\omega_1 t), \quad (3\text{-}1)$$

where ω_1 is the fundamental angular frequency which is related to the period T_1 of the function by the formula $T_1 = 2\pi/\omega_1$. The constant a_o and the coefficients a_n and b_n

for the cosine and sine series, respectively, are given by the integrals :

$$a_n = \frac{2}{T_1} \int_{-T_1/2}^{T_1/2} f(t) \cos n\omega_1 t \, dt \quad \text{for } n=0,1,2,\ldots \tag{3-2}$$

$$b_n = \frac{2}{T_1} \int_{-T_1/2}^{T_1/2} f(t) \sin n\omega_1 t \, dt \quad \text{for } n=1,2,\ldots \tag{3-3}$$

The expression of the Fourier series (3-1) and the coefficients (3-2), and (3-3) in the exponential forms (3-4) and (3-5) is a great convenience in analysis.

$$f(t) = \sum_{n=-\infty}^{\infty} F(n) \, e^{in\omega_1 t} \tag{3-4}$$

in which $F(n) = \frac{1}{2}(a_n - ib_n)$ for $n=0,\pm1,\pm2,\cdots$ (3-5)

By combining (3-2) and (3-3) according to (3-5) we find that

$$F(n) = \frac{1}{T_1} \int_{-T_1/2}^{T_1/2} f(t) \, e^{-in\omega_1 t} \, dt \quad \text{for } n=0,\pm1,\pm2,\ldots \tag{3-6}$$

Equation (3-6) is known as the Fourier transform of the function f(t); it is a function of the harmonic order n and is a representation of the time function in the frequency domain. We denote the absolute value of F(n) as a

function of n by $|F(n)|$, that is

$$|F(n)| = \frac{1}{2} (a_n^2 + b_n^2)^{\frac{1}{2}} \qquad (3\text{-}7)$$

and the phase angle of F(n) as a function of n by θ_n, that is

$$\theta_n = \tan^{-1} (- \frac{b_n}{a_n}) \qquad (3\text{-}8)$$

The absolute value of F(n), given by (3-7) as a function of the harmonic order n, is the amplitude spectrum of f(t), and the phase function (3-8) is the phase spectrum of f(t).

The IBM 360 subroutine FORIT was used to calculate the Fourier coefficients a_n and b_n, n= 0, 1, 2, 3, ... for the curve. Fig. 72 is the amplitude spectrum of var - iation of intensity in Central America from 300 BC to 1960 AD, the points plotted are amplitude (oersted) vs frequency (Cycles/2260 years). The period (years) corresponds to the frequency also shown on the top of the figure. In Fig. 73 the points plotted are amplitude vs period, instead of amplitude vs frequency as in Fig. 72. They show that the dominant peak is on the harmonic order three (n=3), the corresponding period is 753 years, and the amplitude is approximately 0.042 oersted. The other two peaks are on the harmonic order six (n=6) and the harmonic order nine (n=9). The corresponding periods are 377 years and 251 years, respectively. The amplitudes of these two peaks are 0.0104 oersted and 0.0055 oersted respectively.

A dominant period of approximate 700 years is suggested by a visual inspection of Fig.71.

Results from Norht America

Sixty-eight specimens from twenty-one samples which were collected from the Southwest United States (as shown in Fig. 68) have been measured in this study. Table 10 in the appendix shows the results of these measurements. The Fig. 74 shows the reliable intensity ratio F/F_o of the geomagnetic field in the Southwest United States during the past 2,000 years. Owing to the scarcity of reliable samples, it is impossible, as yet, to make a field intensity variation curve for this area. However, since the Southwest United States is not far from Mexico and the patterns of geomagnetic intensity for similar latitudes in Mexico and the Southwest are about the same (as shown in Fig. 75), the field intensity variation curve for Central America is plotted with the results from the Southwest United States (as shown in Fig. 76) and data are comparable. Some points not in agreement may be due to dating errors of the samples from either area. These results suggest the possibility that the secular variation curves of the field intensity for Mexico and the Southwest may be similar for the past 2,000 years.

Results from South America

Thirty-two specimens from fourteen samples, which were collected from Peru and Bolivia, as shown in Fig. 70 have been measured in this study. Table 11 in the appendix shows the results of these measurements. The intensity ratio F/F_o of the geomagnetic total force in Peru and Bolivia for the past 3,000 years is shown

in Fig. 77. The results suggest that the intensity in approximately 500 AD may have been almost twice as large as the present one. The ancient field intensity between 900 BC and 200 BC is represented by two data points only but they suggest that it was stronger than that now. By comparing these results with those on the Central American curve, which was obtained from this study, it is possible to suggest that a minimum field intensity may be between 300 BC and 200 BC. The most significant results of these studies of ancient intensity in Peru-Bolivia are that one half of the reliable samples indicate that the F/F_o values are between 1.5 to 2.0 and the other half gave values between 1.1 to 1.5. None of the results suggest that the field intensity in the past 3,000 years has been lower than the present field intensity (0.25-0.32 oersted). These data can be explained by the fact that Peru and Bolivia are almost in the center of a present low geomagnetic total field intensity area as shown in Fig. 75. It also follows that current values of geomagnetic field intensity are anomalous when considered with the data representing the past 3,000 years.

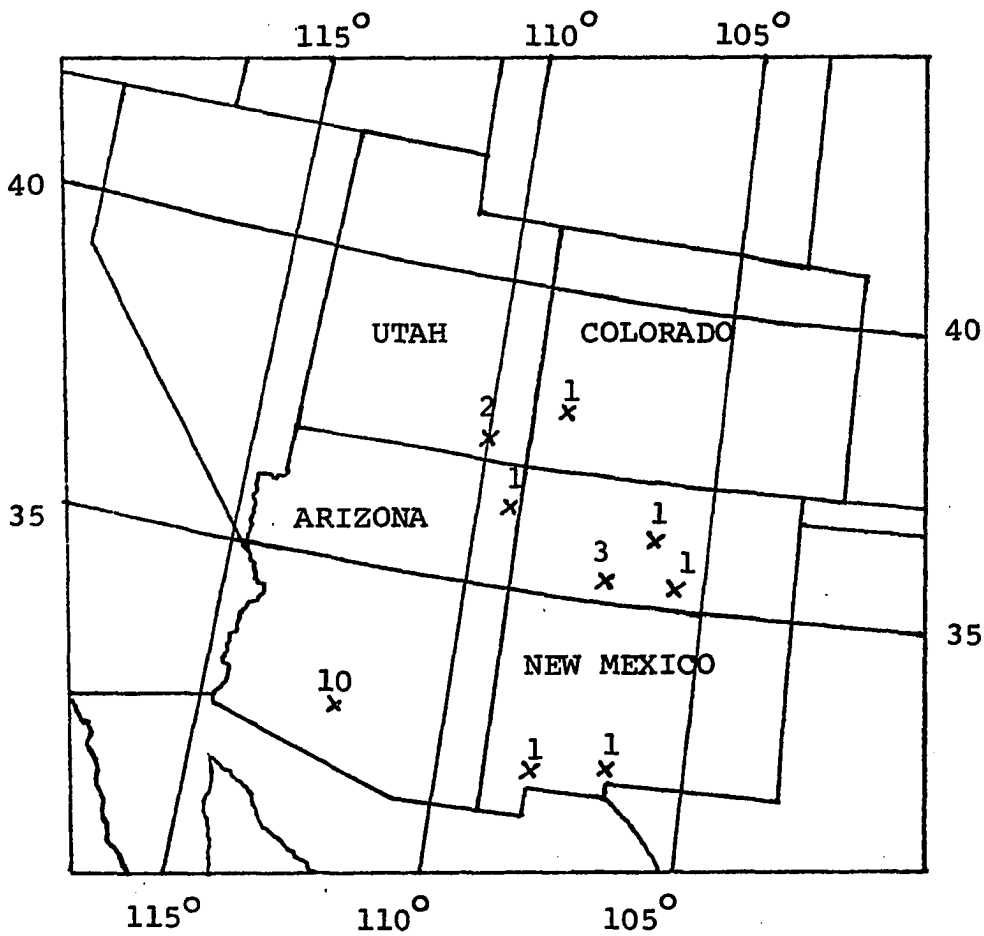

Fig. 68 Sampling site localities in Southwest United States (number above the site indicates the number of samples from the site).

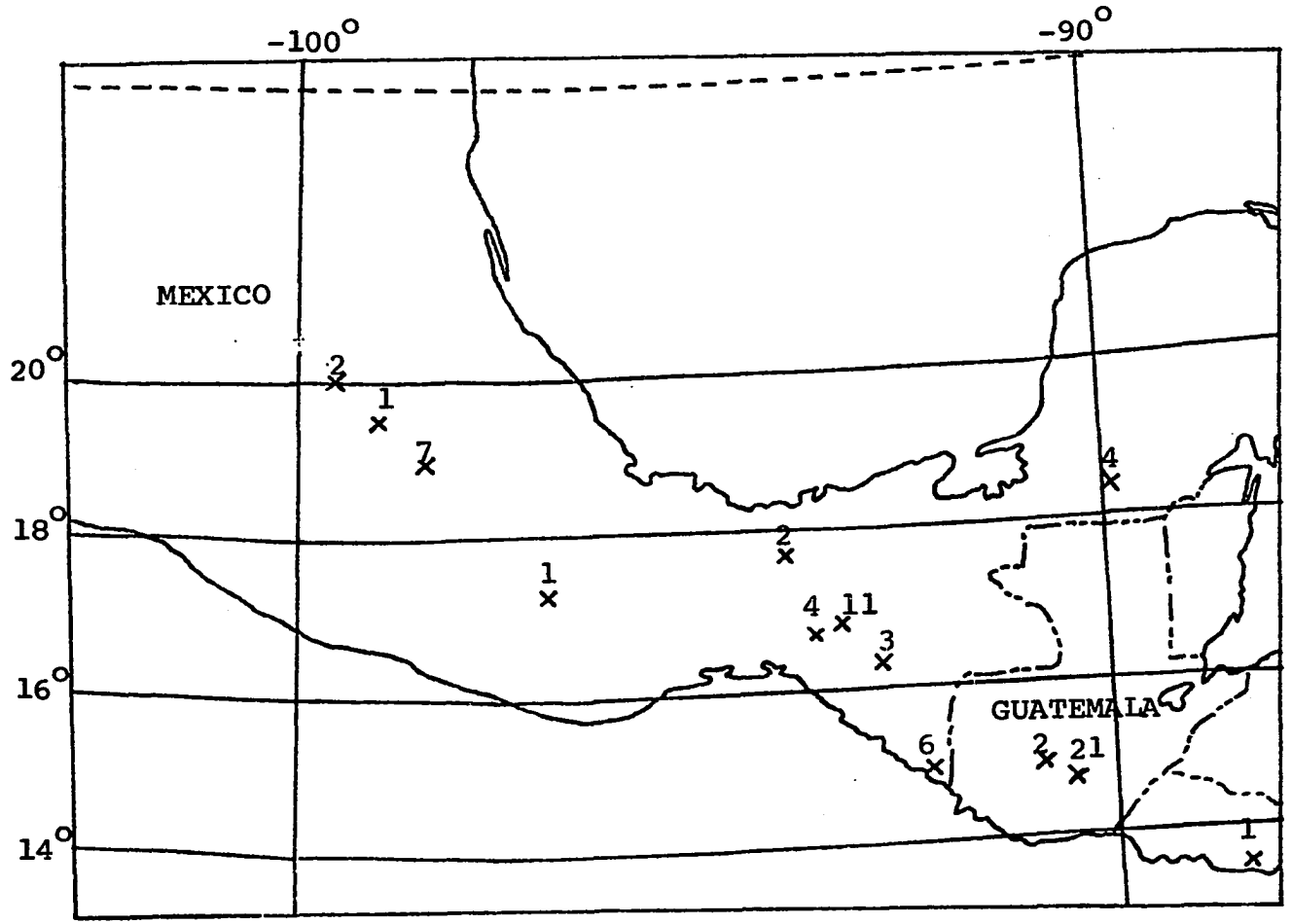

Fig. 69 Sampling site localities in Mexico and Guatemala (number above the site indicates the number of samples from the site).

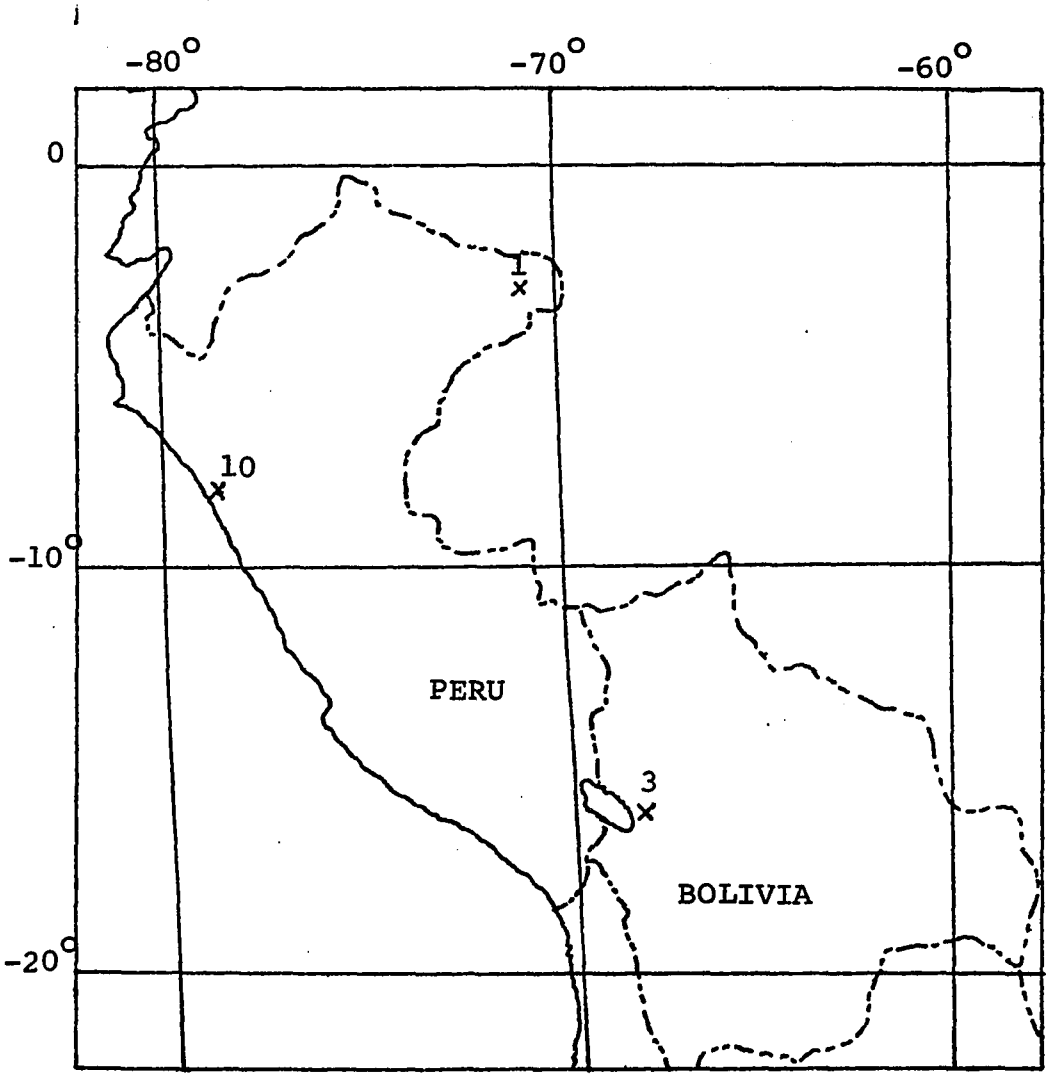

Fig. 70 Sampling site localities in Peru and Bolivia (Number above the site indicates the number of samples from the site).

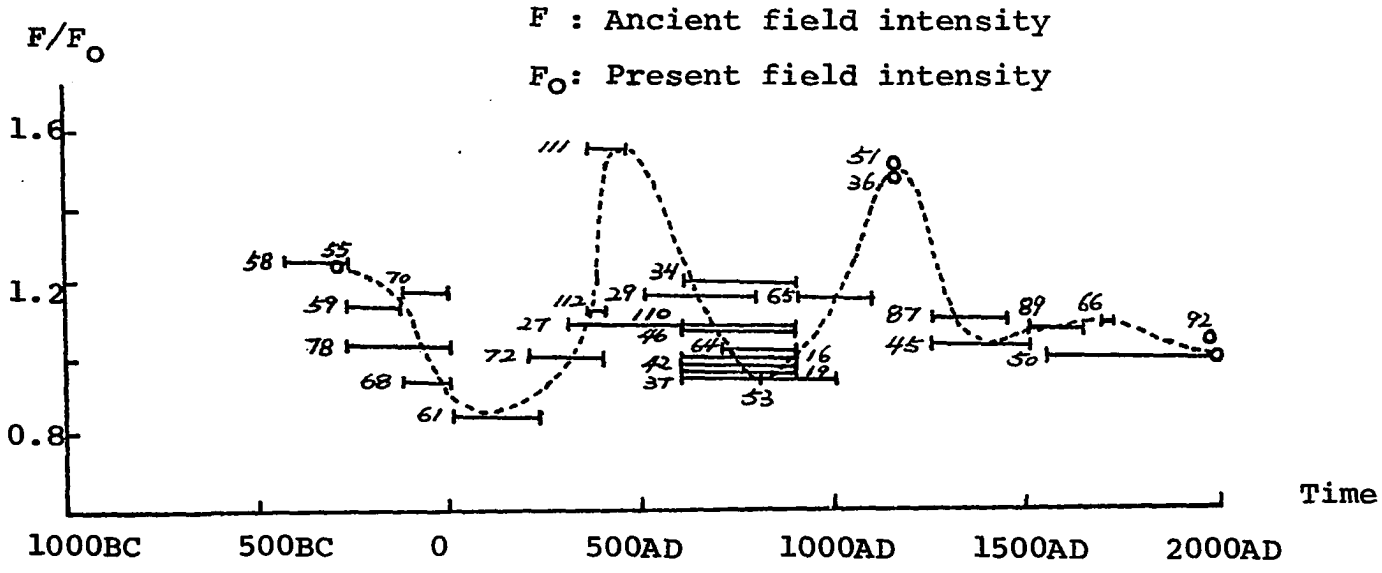

Fig. 71 Secular variation of the intensity of Geomagnetic Field in Mexico and Guatemala (The numbers along the curve indicate sample unmbers).

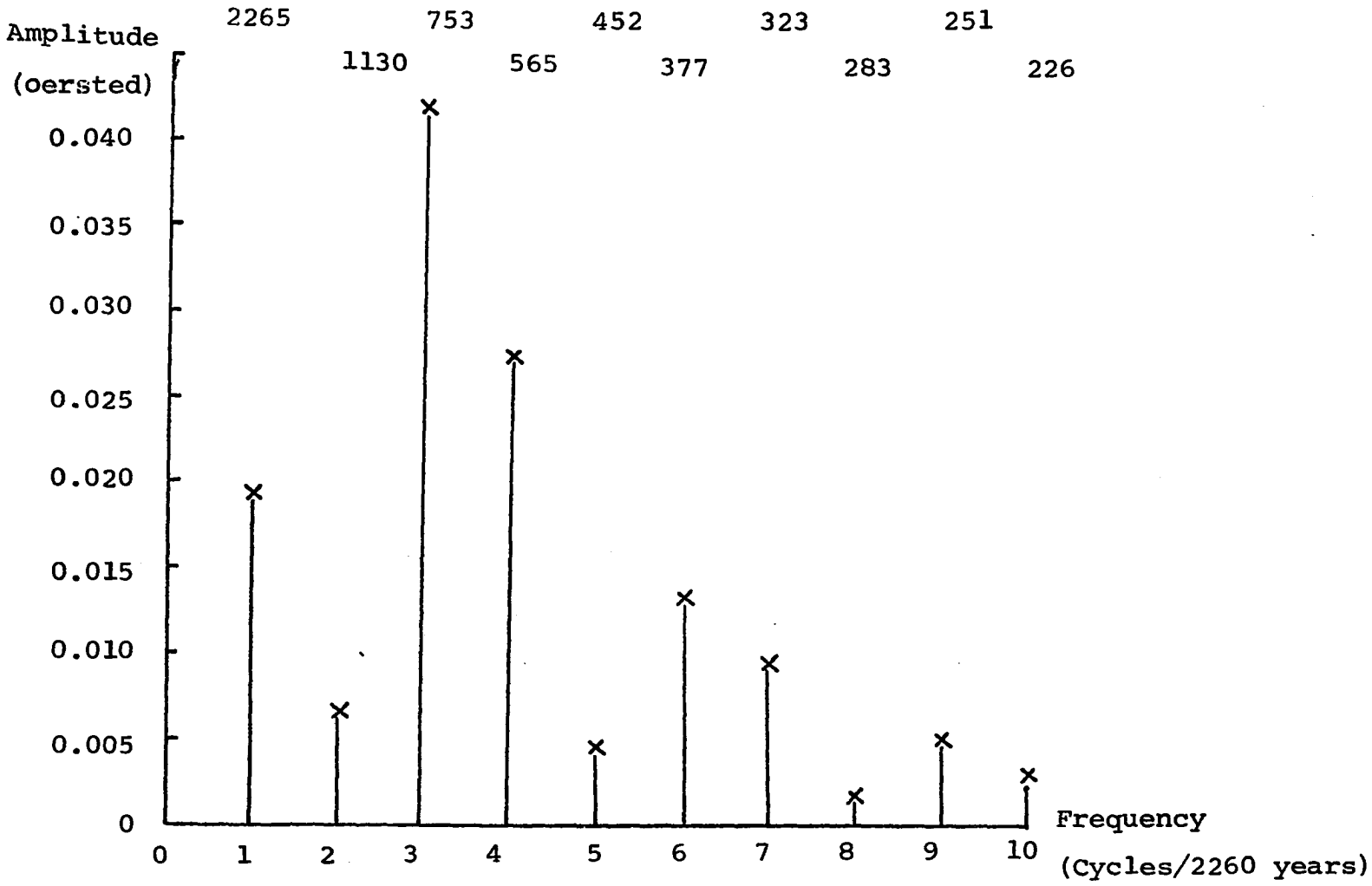

Fig. 72 Amplitude spectrum of variation of geomagnetic field intensity in Central America during the past 2260 years.

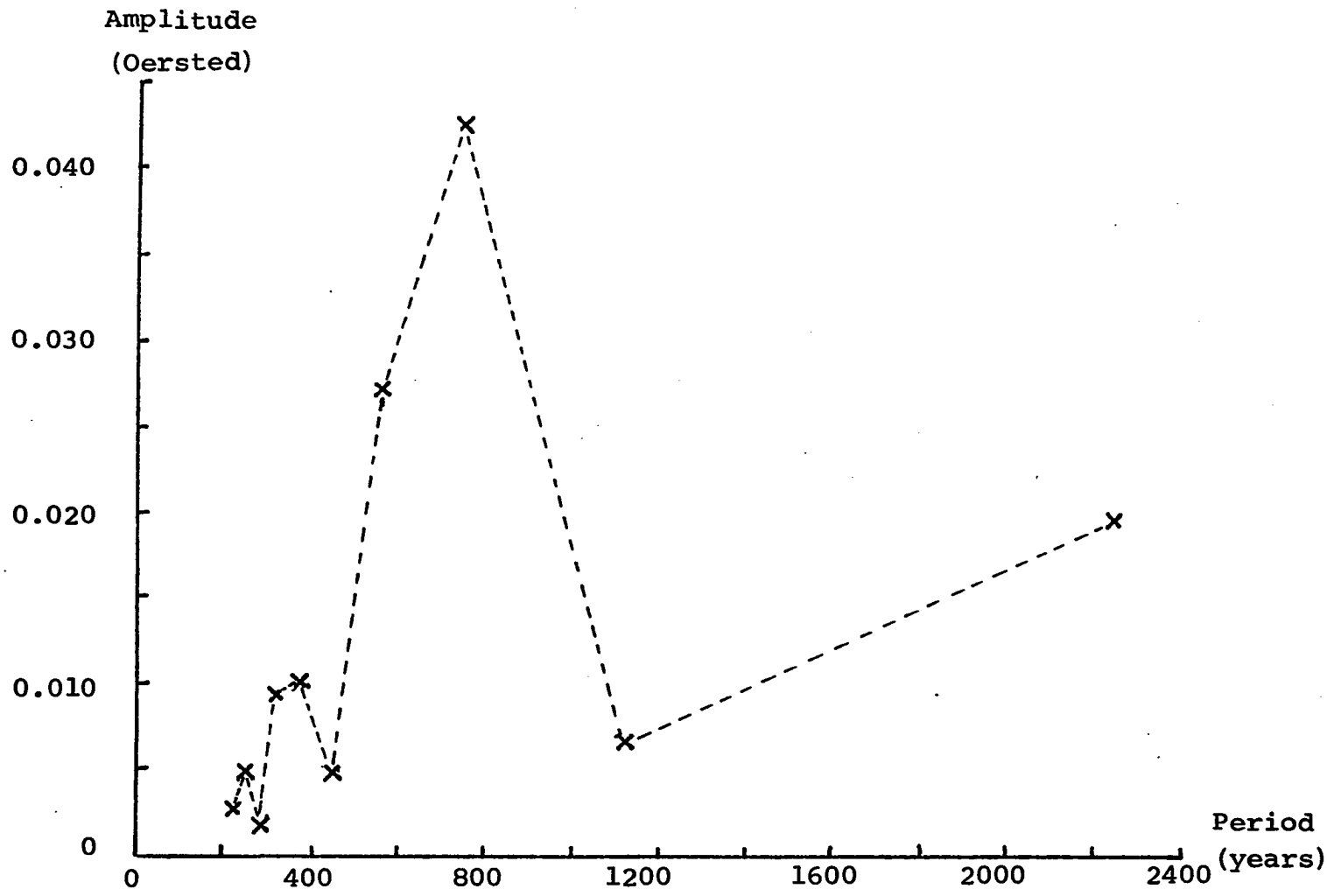

Fig. 73 Amplitude spectrum (amplitude vs period) of variation of geomagnetic field intensity in Central America during the past 2260 years.

F : Ancient field intensity

F_o : Present field intensity

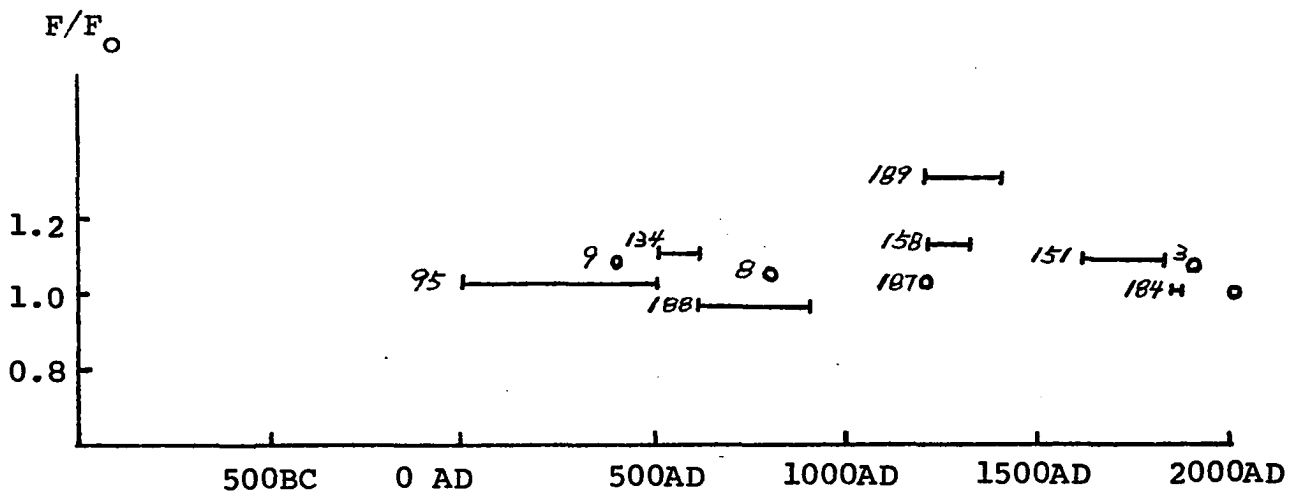

Fig. 74 Secular variation of geomagnetic field intensity in the Southwest United States (The numbers indicate sample numbers).

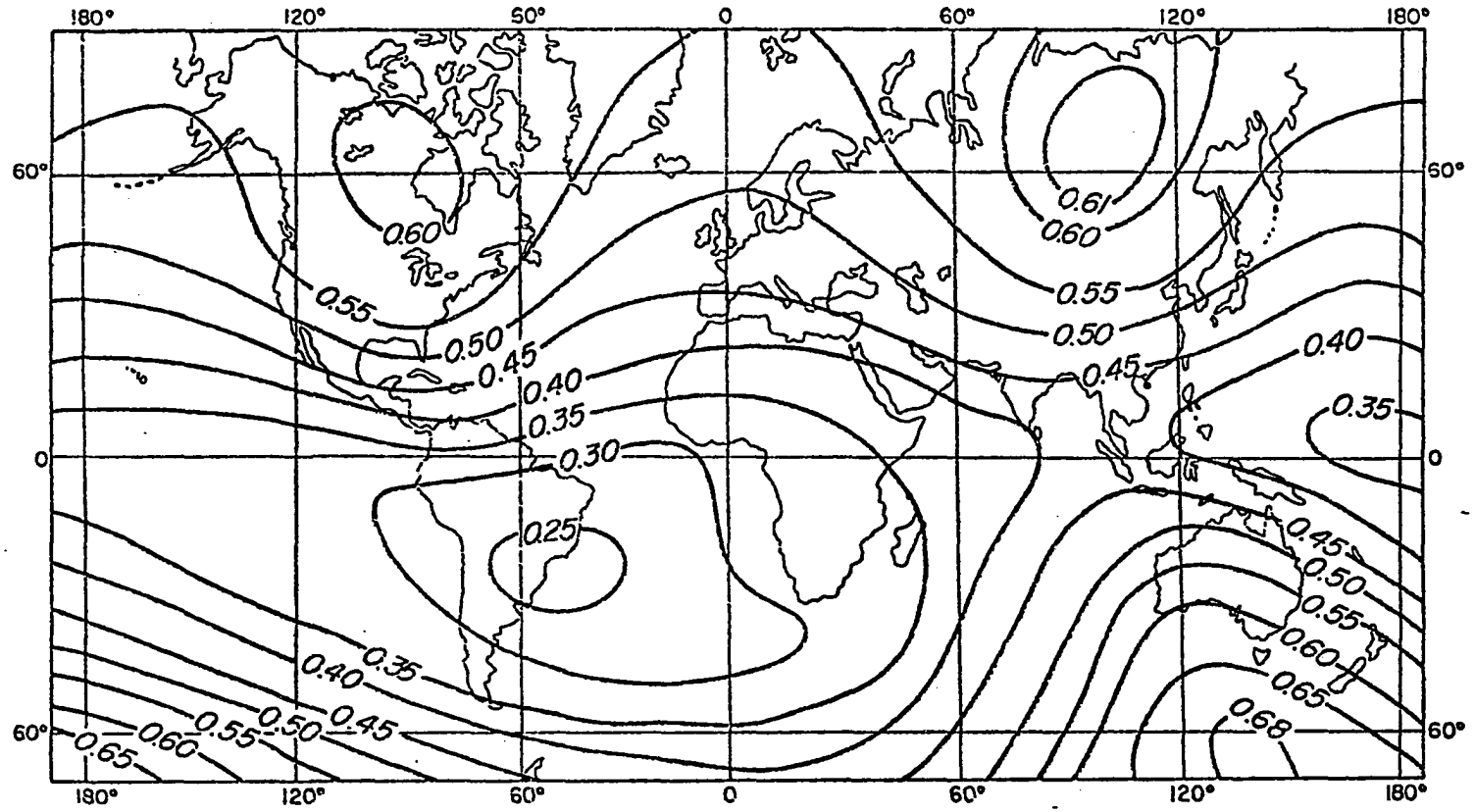

Fig. 75 Total intensity of the 1965 magnetic field.

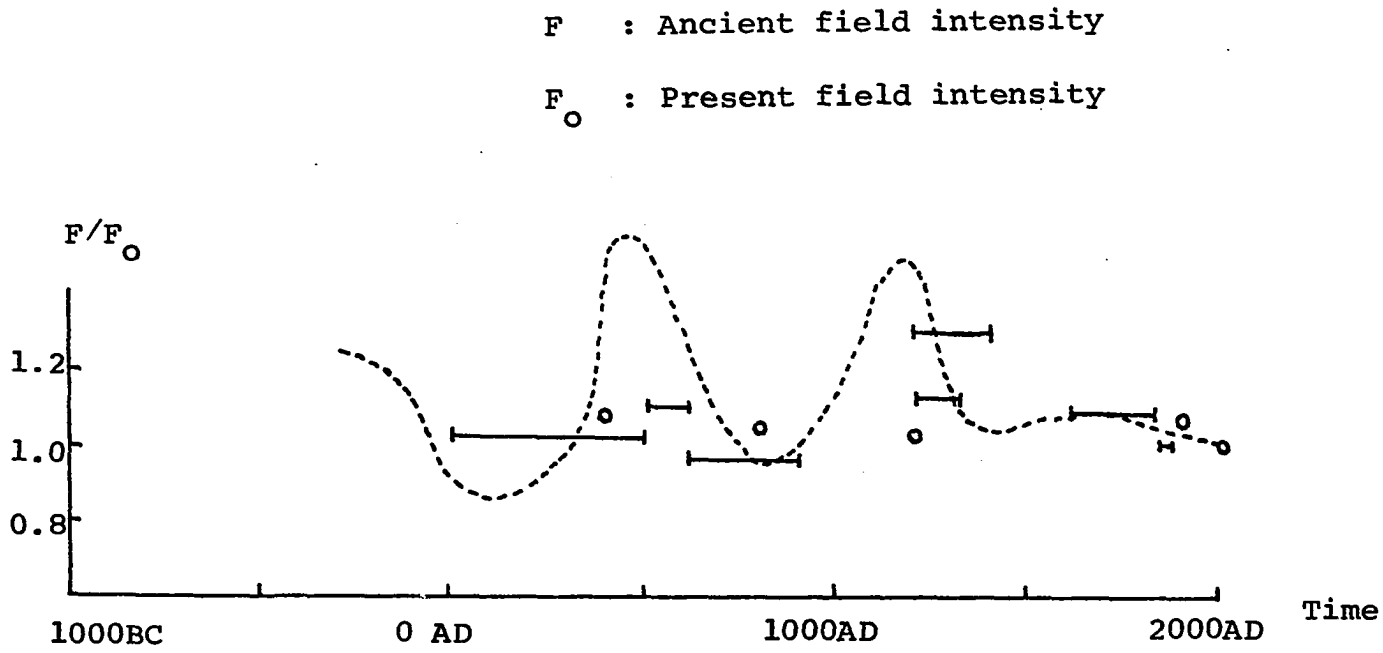

Fig. 76 Field intensity variation curve from Central America plotted with values of field intensity from Fig. 74

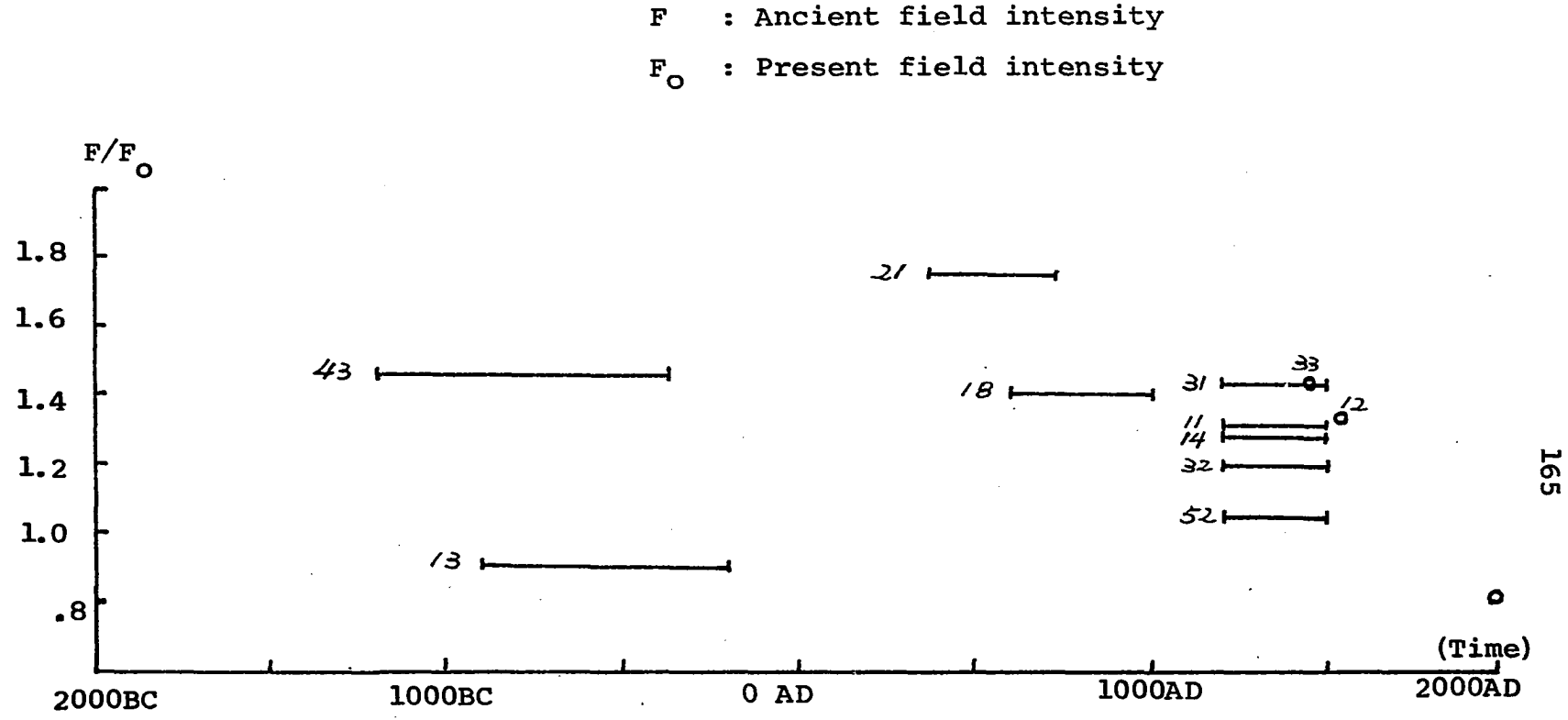

Fig. 77 Secular variation of the intensity of the geomagnetic field in Peru and Bolivia(The number indicate sample unmbers).

CHAPTER IV

CONCLUSIONS

The basic conclusions which can be drawn from this study are as follows :

(1) Theoretical calculations, test experiments, and actual measurements show that the results from Thelliers' Method are much more reliable than those from other methods presently used in archeomagnetic field intensity measurements. The reason for this is that magnetization of each specimen is imparted, step by step, from room temperature up to the Curie temperature in Thelliers' Method, whereas a thermal magnetization of each specimen is imparted only once in the other methods.

(2) The AF Demagnetization Method and ARM Method have some advantages for special samples, i.e., samples that been struck by lightning or fragile samples. On the other hand, if the sample is measured only by the AF Method or ARM Method, then it may give very poor or incorrect results.

(3) The best procedure to determine archeomagnetic intensity is to measure at least four specimens for each sample by Thelliers' Method (Method A) and at

least two specimens by either the AF Method or the ARM Method. The reliability of the results from either the AF Method or the ARM Method is less than that from the Thelliers' Method, but the AF or ARM Method can provide additional information of the characteristics of the NRM of the sample.

(4) Among the 100 samples, used in these studies 56 samples are pottery, 35 samples are baked clays, 7 samples are bricks and only 2 samples are lavas. Among the 56 pottery, only 24 samples (43 %) give reliable results. 25 samples (71 %) give reliable results among the 35 baked clays. Only 3 samples (43 %) give reliable results among the 7 bricks. Only 2 lava samples have been measured in this study, and one (50 %) gives reliable results. The results of these numbers suggest that the probability of having a reliable result from baked clay samples is almost 1.6 times that obtained from pottery or brick samples. This conclusion may be related to the fact that most of the pottery or bricks have been used by human beings in various ways after their original firing, but most baked clays have not been reused.

(5) The test experiment for Thelliers' Method indicates that the maximum deviation between the measured field intensity and the actual field intensity is 2.76 percent for the baked clay samples and 5.77 percent for the pottery samples. These results support the conclusion that baked clays are the better samples for archeomagnetic intensity studies.

(6) An examination of Thelliers' Method (A), (B), (C), and (D) shows that the use of a more precise apparatus and better methods (see chapter II) produces more reliable results from Thelliers' Method.

(7) Maximum field intensity at approximately 450 AD is indicated not only by the Central American results but is suggested by the South American results in this study. The absence of a similar peak in the Southwest United States may be due to the small number of samples measured.

(8) The Central American and North American results show that the F/F_o values of almost four-fifths of the measured samples are larger than one. The South American results indicate that half of the F/F_o values determined are between 1.5 to 2.0 and the other half between 1.1 and 1.5.

(9) A dominant peak in the Fourier analysis of the intensity variation curve from Central America shows a period of 753 years. This is due to the fact that peaks of the curve are at 440 AD and 1168 AD, respectively and 753 is a more or less average value between the two real values.

(10) All the archeomagnetic field intensity results for North, Central, and South America are in agreement with the idea that the intensities at 0 AD are nearly equal to the present intensities, but suffi cient data are locking as yet, implies that if westward drift of the non-dipole field is dominant secular variation, then the period or multiple of it for westward

drift is approximately 2,000 years. This conclusion is consistent with the results calculated by other authors (Yukutake, Nagata, etc.).

(11) The magnetic moment of the dipole field has not steadly decreased during the past 3,000 years.

(12) The field intensity secular variation curves for Central America and the Southwest United States could be similar and more data are needed to support this suggestion. Some data on the intensity secular variation for South America have been presented and it will be interesting to compare then to that from Central America when more results are available.

(13) The archeomagnetic field intensity curve for Central America may be a new basis for an archeological chronology in this area which may also be developed for Southwest United States and South America.

BIBLIOGRAPHY

Banerjee, S. K. and J. P. Mellema, A new method for the determination of paleointensity from the A. R. M. properties of rocks, Earth Planet. Sci. Let., 23, 177-184, 1974.

Banerjee, S. K. and J. P. Mellema, Lunar paleointensity from three Apollo 15 crystalline rocks using an A. R. M. method, Earth Planet. Sci. let., 23, 185-188 , 1974.

Bol'shakov, A. S. and G. M. Solodovnikov, Evaluation of the influence of chemical magnetization on the determination of the intensity of the ancient geomagnetic field, Earth Physics, 2, 92-94, 1972.

Braginskiy, S. I. and S. P. Burlatskaya, Comparison of archeomagnetic data with the analytical representation of the geomagnetic field for the last 350 years, Earth Physics, 1, 95-99, 1972.

Bucha, V., Archeomagnetic and paleomagnetic study of the magnetic field of the earth in the past 600,000 years , Nature, 213, 1005-1007, 1967.

Bucha, V. R. E. Taylor, R. Berger and E. W. Haury, Geomagnetic intensity: change during the past 3,000 years years in the western hemisphere, Science, 168, 111-114, 1970.

Burlatskaya, S. P. and G. N. Petrova, Reconstruction of the picture of the change in the magnetic field of the earth in the past with the aid of archeomagnetic method, Geomagnetizm i Aeronomiya, 1, 426-431,1961.

Chapman, S. and J. Bartel, Geomagnetism, Oxford Univ. Press. 1940.

Coe, R. S., The determination of paleo-intensities of the earth's magnetic field with emphasis on mechanisms which could cause non-ideal behavior in Thellier's method, J. Geomag. Geoelectr., 19, 157-179, 1967.

Coe, R. S., A comparison of three methods of determining geomagnetic paleointensities, J. Geomag. Geoelectr., 25, 415-435, 1973.

Cox, A., Analysis of present geomagnetic field for comparison with paleomagnetic results, J. Geomag. Geoelectr., 13, 101-112, 1962.

Cox, A. and R.R. Doell, long period variations of the geomagnetic field, Bull. Seism. Soc. AM., 54, 2243-2270, 1964.

Doell, R.R. and P.J. Smith, On the use of magnetic cleaning in paleointensity studies, J. Geomag. Geoelectr., 23, 579-594, 1969.

Dubois, R.L. and N. Watanabe, Preliminary results of investigations made to study the use of Indian pottery to determine the paleointensity of the geomagnetic field for the United States 600-1400 A.D., J. Geomag. Geoelectr., 17, 417-423, 1965.

Gauss, C. F. Allgemeine theorie des erdmagnetismus, in resultate magnetische verein, 1838.

Gellibrand, H., A discourse mathematical on the variation of the magnetical needle, London, 1635.

Gilbert, W., De magneticisque corporibus, et de magno magnete tellure physiologia nova, 1600. (English translation) Dover, New York, 1958.

Gough, D.I., A study of the paleomagnetism of the pilansberg dykes, Mon. Not. Roy. Astr. Soc. Geophys. Supp., 7, 196-213, 1956.

Graham, K.W. T., The re-magnetization of a surface outcrop by lightning currents, Geophys. J., 6, 149-161, 1961.

Hailwood, E.A. and L. Molyneux, Anhysteretic remanent magnetization due to asymmetrical alternating fields, Geophys. J. R. astro. Soc., 39, 421-434, 1974.

Hallimond, A. F. and E. F. Herroum, Laboratory determination of the magnetic properties of certain igneous rocks, Proc. Roy. Soc. London, 141, 302-314, 1933

Irving, E., Paleomagnetism, John Wiley & Sons, Inc., New York, 1964.

Jacobs, J. A., The Earth's Core and Geomagnetism, The MacMillan Co., New York, 1963.

Kitazawa, K. and K. Kobayashi, Intensity variation of the geomagnetic field during the past 4000 years in South America, J. Geomag. Geoelectr., 20, 7-19, 1968.

Kitazawa, K., Intensity of the geomagnetic field in Japan for the past 10,000 years, J. Geophys. Res., 75, 7403-7411, 1970.

Kobayashi, K., Chemical remanent magnetization of ferromagnetic minerals and its application to rock magnetism, J. Geomag. Geoelectr., 10, 99-117, 1959.

Kobayashi, K., An interpretation of the archeomagnetic field intensity, J. Geomag. Geoelectr., 21, 775-780, 1969.

Kovacheva, M., Upon the intensity of the ancient magnetic field during the last 2000 years in South-eastern Europe, Earth Planet. Sci. Let., 17, 199-206, 1972.

Mood, A. M. and F. A. Graybill, Introduction to the Theory of Statistics, McGraw-Hill Book Co., New York, 1963.

Nagata, T., Rock Magnetism, Maruzen Co., Tokyo, 1961.

Nagata, T., K. Kobayashi and E. J. Schwarz, Archeomagnetic intensity studies of South and Central America, Univ. of Pitt. Press, 1962.

Nataga, T., Y. Arai and K. Momose, Secular variation of the geomagnetic total force during the last 5000 years, J. Geophys. Res., 68, 5277-5281, 1963.

Rikitake, T., Electromagnetism and the Earth's Interior, Elsevier Publishing Co., Amsterdam, 1966.

Roquet, J., Ann. Geophys., 10, 226-282

Rusakov, O. M. and G. F. Zagniy, Intensity of the geomagnetic field in the Ukraine and Meldavia during the past 6000 years, Archaeometry, 15, 275-285, 1973.

Sasajima, S. and K. Maenaka, Intensity studies of the archeo-secular variation in West Japan with special reference to the hypothesis of the dipole axis rotation, Mem. College Sci., Univ. Kyoto, ser B33, 53, 1966.

Shashkanov, V. A. and V. V. Metallova, Violation of Thellier's law for partial thermoremanent magnetization, Earth Physics, 3, 80-86, 1972.

Shaw, J., A new method of determining the magnitude of the paleomagnetic field - application to five historic lavas and five archeological samples, Geophys. J. R. astro. Soc., 39, 133-141, 1974.

Smith, P. J., The intensity of the ancient geomagnetic field: a review and analysis, Geophys. J. R. astro. Soc., 12, 321-362, 1967.

Smith, P. J., Magnetic declination in mediaeval China, Nature, 214, 1213-1214, 1967.

Stephenson, A. and D. W. Collinson, Lunar magnetic field paleointensities determined by an anhysteretic remanent magnetization method, Earth Planet. Sci. Let., 23, 220-228, 1974.

Strangway, D. W. and B. E. McMahon, Magnetic paleointensity studies on a recent basalt from Flagstaff, Arizona, J. Geophys. Res., 73, 7031-7037, 1968.

Thellier, E. and O Thellier, Sur I'intensité du champ magnetique terrestre dans le passé historique, et géologique, Ann. Geophys., 15, 285-376, 1959.

van Zijl, J. S. V., K. W. T. Graham and A. L. Hales, The palaeomagnetism of the Stormberg Lava, II. The behavior of the magnetic field during a reversal, Geophys. J. R. astro. Soc., 7, 169-182, 1962.

Weaver, G. H., Some temperature related errors in paleomagnetic intensity measurements, Archaeometry, 12, 87-95, 1970.

Wilson, R. L., Paleomagnetism in northern Ireland: Part I. The thermal demagnetization of natural magnetic moments of rocks, Geophys. J. R. astro. Soc., 45-58, 1961.

York, D., Least-squares fitting of a straight line, Canadian J. of Physics, 44, 1079-1086, 1966.

York, D., The best isochron, Earth Planet. Sci. Let., 2, 479-482, 1967.

APPENDIX

Table 9 Results of samples from Central America.

Sample No.	Spec. No.	Material	Site Location			Age	Method of measurement	F_o Oe	F Oe	Reliability	F/F_o
			Site	Lat.	Long.						
15	1	Baked	Kaminal	14.70	-90.50	600AD-	Th(C)	0.42		P	
	2	clay	-juyu,			900AD	Th(C)			P	
			Guatema								
			-la								
16	1	Pottery	Kaminal	14.70	-90.50	600AD-	Th(C)	0.42	0.41	R	0.98
	2		-juyu,			900AD	Th(C)		0.41	R	0.98
			Guatema				Average		0.41		0.98
			-la								
17	1	Pottery	Kaminal	14.70	-90.50	600AD-	Th(C)	0.42		P	
	2		-juyu,			900AD	Th(C)			P	
			Guatema								
			-la								
19	1	Pottery	Kaminal	14.70	-90.50	600AD-	Th(C)	0.42	0.419	R	1.00
	2		-juyu ,			900AD	Th(C)			P	
	3		Guatema				Th(C)			P	
	4		-la				Th(C)		0.388	R	0.92
	5						W			P	
							Average		0.404		0.96

Symbols and abbreviations see the text

Table 9 (Continued)

Sample No.	Spec. No.	Material	Site Location			Age	Method of measurement	F_o Oe	F Oe	Reliability	F/F_o
			Site	Lat.	Long.						
22	1	Pottery	Kaminal-juyu, Guatemala	14.70	-90.50	200BC-300AD	Th(C)	0.42		P	
	2						Th(C)			P	
27	1	Baked clay	Kaminal-juyu, Guatemala	14.70	-90.50	300AD-600AD	Th(C)	0.42	0.39	R	
	2						Th(C)		0.45	R	
	3						Th(A)		0.43	VR	1.04
	4						Th(A)		0.45	VR	1.07
	5						Th(A)		0.42	VR	1.02
	6						Th(A)		0.49	VR	1.17
							Average				1.08
28	1	Baked clay	Kaminal-juyu, Guatemala	14.70	-90.50	600AD	Th(C)	0.42		P	
	2						Th(C)			P	
29	1	Baked clay	Kaminal-juyu, Guatemala	14.70	-90.50	500AD-800AD	Th(C)	0.42	0.41	R	
	2						Th(C)		0.46	R	
	3						Th(A)		0.52	VR	1.24

Table 9 (Continued)

Sample No.	Spec. No.	Material	Site Location			Age	Method of measure-ment	F_o Oe	F Oe	Relia-bility	F/F_o
			Site	Lat.	Long.						
	4						Th(A)		0.52	VR	1.24
	5						Th(A)		0.49	VR	1.18
	6						Th(A)		0.44	VR	1.06
							Average				1.16
34	1	Baked	Kaminal	14.70	-90.50	600AD-	Th(C)	0.42	0.49	R	1.17
	2	clay	-juyu,			900AD	Th(C)		0.51	R	1.21
			Guatema				Average				1.19
			-la								
36	1	Baked	Tula,	20.00	-99.30	1168AD	Th(C)	0.435	0.57	R	
	2	clay	Mexico				Th(C)		0.61	R	
	3						Th(A)		0.64	VR	1.47
	4						Th(A)		0.65	VR	1.50
	5						Th(A)		0.63	VR	1.45
	6						Th(A)		0.63	VR	1.45
							Average				1.47
37	1	Baked	Kaminal	14.70	-90.50	600AD-	Th(C)	0.42	0.39	R	0.93
	2	clay	-juyu,			800AD	Th(C)		0.41	R	0.98
			Guatema				Average				0.95
			-la								

Table 9 (Continued)

Sample No.	Spec. No.	Material	Site Location			Age	Method of measurement	F_o Oe	F Oe	Reliability	F/F_o
			Site	Lat.	Long.						
38	1	Pottery	Kaminal-juyu, Guatema-la	14.70	-90.50	200BC	Th(C)	0.42		P	
	2					300AD	Th(C)			P	
39	1	Pottery	Kaminal-juyu, Guatema-la	14.70	-90.50	200BC-300AD	Th(C)	0.42		P	
	2						Th(C)			P	
	3						Th(C)			P	
	4						Th(C)			P	
40	1	Pottery	Kaminal-juyu, Guatema-la	14.70	-90.50	600AD-900AD	Th(C)	0.42		P	
	2						Th(C)			P	
41	1	Pottery	Kaminal-juyu, Guatema-la	14.70	-90.50	200BC-300AD	Th(C)	0.42		P	
	2						Th(C)			P	
42	1	Pottery	Kamina	14.70	- 90.50	600AD-	Th(C)	0.42	0.42	P	

Table 9 (Continued)

Sample No.	Spec. No.	Material	Site Location			Age	Method of measurement	F_o Oe	F Oe	Reliability	F/F_o
			Site	Lat.	Long.						
	2		-juyu, Guatemala			900AD	Th(C)		0.42	R	1.00
							Average				1.00
44	1	Pottery	Kaminal	14.70	-90.50	600AD-	Th(C)	0.42		P	
	2		-juyu. Guatemala			900AD	Th(C)			P	
45	1	Pottery	Kaminal	14.70	-90.50	1250AD-	Th(C)	0.42	0.50	P	
	2		-juyu, Guatemala			1520AD	Th(C)		0.43	P	
	3						Th(B)			P	
	4						Th(B)			P	
	5						Th(A)		0.47	P	
	6						Th(A)		0.43	R	1.04
	7						Th(A)		0.42	R	1.02
	8						Th(A)		0.43	R	1.03
							Average				1.03
46	1	Pottery	Kaminal	14.70	-90.50	600AD-	Th(C)		0.45	R	1.07
	2		-juyu,			900AD	Th(C)		0.45	R	1.07

Table 9 (Continued)

Sample No.	Spec. No.	Material	Site Location			Age	Method of measurement	F_o Oe	F Oe	Relia-bility	F/F_o
			Site	Lat.	Long.						
			Guatema-la				Average				1.07
50	1	Baked	Huitzo,	17.30	-96.80	Historic	Th(C)			P	
	2	clay	Mexico			1550AD-	Th(C)	0.43	0.42	R	0.98
	3						Th(C)		0.44	R	1.02
	4					1971AD	Th(C)			P	
							Average				1.00
51	1	Baked	Tula ,	20.00	-99.30	1168AD-	Th(A)	0.445	0.69	R	1.58
	2	clay	Mexico				Th(A)		0.61	R	1.40
	3						Th(A)		0.63	R	1.45
	4						Th(A)		0.68	R	1.56
	6						AF		0.82	P	
	7						AF		o.88	P	
							Average				1.50
53	1	Baked	Chachi,	16.40	-92.70	800AD-	Th(C)	0.43		P	
	2	clay	Mexico			1000AD	Th(C)			P	
	3						Th(B)			P	
	4						Th(B)			P	
	5						Th(A)		0.51	P	

Table 9 (Continued)

Sample No.	Spec. No.	Material	Site Location			Age	Method of measurement	F_o Oe	F Oe	Reliability	F/F_o
			Site	Lat.	Long.						
	6						Th(A)		0.40	VR	0.94
	7						Th(A)		0.38	P	
	8						Th(A)		0.41	VR	0.96
	9						AF		0.39	P	
	10						AF		0.30	P	
							Average				0.95
54	1	Baked	Chachi	16.40	-92.70	800AD-	Th(C)	0.43	0.45	P	
	2	clay	Mexico			1000AD	Th(C)		0.46	P	
55	1	Lava	Cuicui-	19.60	-99.30	300BC	Th(C)	0.445		P	
	2		lco,				Th(C)		0.55	R	1.24
			Mexico				Average				1.24
56	1	Lava	Cuicui-	19.60	-99.30	300BC	Th(C)	0.445		P	
	2		lco,				Th(C)			P	
			Mexico								
57	1	Pottery	Panteon	16.40	-92.70	275BC-	Th(C)	0.43		P	
	2		of			1 AD	Th(C)			P	
			Chachi,								
			Mexico								

Table 9 (Continued)

Sample No.	Spec. No.	Material	Site Location			Age	Method of measurement	F_o Oe	F Oe	Reliability	F/F_o
			Site	Lat.	Long.						
58	1	Pottery	Chiapa	16.70	-93.20	425BC-	Th(C)	0.43		P	
	2		de Corzo			275BC	Th(C)			P	
	3		Mexico				Th(A)		0.54	R	1.26
	4						Th(A)		0.46	R	1.07
	5						Th(A)		0.55	R	1.30
	6						Th(A)		0.58	R	1.35
							Average				1.25
59	1	Pottery	Mirador	16.60	-93.50	275BC-	Th(C)	0.43		P	
	2		Mexico			125BC	Th(C)			P	
	3						Th(A)		0.50	R	1.18
	4						Th(A)		0.47	R	1.10
	5						Th(A)		0.48	R	1.12
	6						Th(A)		0.48	R	1.12
							Average				1.13
60	1	Pottery	Chiapa	16.70	-93.20	125BC-	Th(C)	0.43		P	
	2		de Corzo			1 AD	Th(C)			P	
			Mexico								
61	1	Pottery	Chiapa	16.70	-93.20	1 AD-	Th(C)	0.43		P	
	2		de			225AD	Th(C)			P	

Table 9 (Continued)

Sample No.	Spec. No.	Material	Site Location			Age	Method of measurement	F_o Oe	F Oe	Reliability	F/F_o
			Site	Lat.	Long.						
	3		Corzo,				Th(A)		0.36	R	0.84
	4		Mexico				Th(A)		0.36	R	0.84
	5						Th(A)		0.37	R	0.86
	6						Th(A)		0.35	R	0.81
	7						AF		0.31	P	
	8						AF		0.24	P	
	9						W		0.38	P	
	10						W		0.39	P	
							Average				0.84
62	1	Pottery	Chiapa	16.70	-93.20	225AD-	Th(C)	0.43		P	
	2		de Corzo,			450AD	Th(C)			P	
			Mexico								
63	1	Brick	Comal-	17.80	-93.80	400AD-	Th(C)	0.43		P	
	2		calco,			800AD	Th(C)			P	
	3		Mexico				Th(B)			P	
	4						Th(B)			P	
64	1	Pottery	Izapa,	15.00	-92.20	700AD-	Th(C)	0.42	0.45	R	1.07
	2		Mexico			900AD	Th(C)		0.41	R	0.96
							Average				1.02

Table 9 (Continued)

Sample No.	Spec. No.	Material	Site Location			Age	Method of measurement	F_o Oe	F Oe	Reliability	F/F_o
			Site	Lat.	Long.						
65	1	Pottery	Izapa,	15.00	[illegible]	900AD-	Th(C)	0.42	0.49	R	1.17
	2		Mexico			[illegible]00AD	Th(C)		0.48	R	1.14
							Average				1.15
66	1	Brick	Rec[illegible]				Th(C)	0.45			
	2		co[illegible]				Th(C)				
	3		Gu[illegible]				Th(A)		0.46	VR	1.13
	4		-1[illegible]				Th(A)		0.45	VR	1.10
	5						Th(A)		0.42	VR	1.03
	6						Th(A)		0.45	VR	1.10
	7						AF		0.46	R	
	8						AF		0.50	P	
	9						AF		0.47	R	
	10						W		0.49	P	
							Average				1.09
68	1	Pottery	Chiapa	16.70	-93.20	125BC-	Th(C)	0.43	0.405	R	0.94
	2		de Corzo, Mexico			1 AD	Th(C)		0.39	R	0.91
							Average				0.93
69	1	Pottery	Chiapa,	16.70	-93.20	125BC-	Th(B)	0.43		P	

Table 9 (Continued)

Sample No.	Spec. No.	Material	Site Location			Age	Method of measurement	F_o Oe	F Oe	Reliability	F/F_o
			Site	Lat.	Long.						
	2		de Corzo, Mexico			1 AD				P	
70	1	Pottery	Chiapa	16.70	-93.20	125BC-	Th(C)	0.43	0.50	R	1.17
	2		de Corzo			1 AD	Th(C)		0.50	R	1.17
			Mexico				Average				1.17
71	1	Pottery	Izapa,	15.00	-92.20	600AD-	Th(C)	0.42		P	
	2		Mexico			700AD	Th(C)			P	
	3						Th(B)			P	
	4						Th(B)			P	
	5						Th(A)		0.47	P	
	6						Th(A)		0.44	P	
	7						Th(A)		0.52	P	
	8						Th(A)		0.39	P	
72	1	Pottery	Izapa,	15.00	-92.20	200AD-	Th(C)	0.42	0.43	R	1.02
	2		Mexico			400AD	Th(C)		0.41	R	0.98
							Average				1.00

Table 9 (Continued)

Sample No.	Spec. No.	Material	Site Location			Age	Method of measurement	F_o Oe	F Oe	Reliability	F/F_o
			Site	Lat.	Long.						
65	1	Pottery	Izapa,	15.00	-92.20	900AD-	Th(C)	0.42	0.49	R	1.17
	2		Mexico			1100AD	Th(C)		0.48	R	1.14
							Average				1.15
66	1	Brick	Recole-	15.00	-91.00	1700AD-	Th(C)	0.45			
	2		coion ,			1715AD	Th(C)				
	3		Guatema				Th(A)		0.46	VR	1.13
	4		-la				Th(A)		0.45	VR	1.10
	5						Th(A)		0.42	VR	1.03
	6						Th(A)		0.45	VR	1.10
	7						AF		0.46	R	
	8						AF		0.50	P	
	9						AF		0.47	R	
	10						W		0.49	P	
							Average				1.09
68	1	Pottery	Chiapa	16.70	-93.20	125BC-	Th(C)	0.43	0.405	R	0.94
	2		de Corzo,			1 AD	Th(C)		0.39	R	0.91
			Mexico				Average				0.93
69	1	Pottery	Chiapa,	16.70	-93.20	125BC-	Th(B)	0.43		P	

Table 9 (Continued)

Sample No.	Spec. No.	Material	Site Location			Age	Method of measurement	F_o Oe	F Oe	Reliability	F/F_o
			Site	Lat.	Long.						
	2		de Corzo, Mexico			1 AD				P	
70	1	Pottery	Chiapa	16.70	-93.20	125BC-	Th(C)	0.43	0.50	R	1.17
	2		de Corzo Mexico			1 AD	Th(C)		0.50	R	1.17
							Average				1.17
71	1	Pottery	Izapa,	15.00	-92.20	600AD-	Th(C)	0.42		P	
	2		Mexico			700AD	Th(C)			P	
	3						Th(B)			P	
	4						Th(B)			P	
	5						Th(A)		0.47	P	
	6						Th(A)		0.44	P	
	7						Th(A)		0.52	P	
	8						Th(A)		0.39	P	
72	1	Pottery	Izapa,	15.00	-92.20	200AD-	Th(C)	0.42	0.43	R	1.02
	2		Mexico			400AD	Th(C)		0.41	R	0.98
							Average				1.00
73	1	Pottery	Izapa,	15.00	-92.20	600AD-	Th(C)	0.42		P	
	2		Mexico			700AD	Th(C)			P	

Table 9 (Continued)

Sample No.	Spec. No.	Material	Site Location			Age	Method of measurement	F_o Oe	F Oe	Reliability	F/F_o
			Site	Lat.	Long.						
74	1	Pottery	Izapa, Mexico	15.00	-92.20	700AD-900AD	Th(C)	0.42		P	
	2						Th(C)			P	
75	1	Pottery	Mirador, Mexico	16.60	-93.50	275BC-125BC	Th(C)	0.43		P	
	2						Th(C)			P	
	3						Th(C)			P	
	4						Th(C)			P	
76	1	Pottery	Chiapa de Corzo Mexico	16.70	-93.20	275BC-125BC	Th(B)	0.43		P	
	2						Th(B)			P	
77	1	Pottery	Chiapa de Corzo Mexico	16.70	-93.20	275BC-125BC	Th(C)	0.43		P	
	2						Th(C)			P	
78	1	Pottery	Puente-Las Flores Mexico	16.60	-93.50	275BC-125BC	Th(C)	0.43	0.44	R	1.03
	2						Th(C)		0.43	R	1.02
							Average				1.03

Table 9 (Continued)

Sample No.	Spec. No.	Material	Site Location			Age	Method of measurement	F_o Oe	F Oe	Reliability	F/F_o
			Site	Lat.	Long.						
79	1	Pottery	Media	16.70	-93.20	275BC-	Th(C)	0.43		P	
	2		Luna,			125BC	Th(C)			P	
	3		Mexico				Th(C)			P	
	4						Th(C)		0.461	R	1.07
							Average				1.07
80	1	Pottery	Becan,	18.50	-89.80	300BC-	Th(C)	0.44		P	
	2		Mexico			450BC	Th(C)			P	
84	1	Pottery	Becan,	18.50	-89.80	800AD-	Th(C)			P	
	2		Mexico			950AD	Th(C)			P	
85	1	Pottery	Becan,	18.50	-89.80	800AD-	Th(C)	0.44		P	
	2		Mexico			950AD	Th(C)			P	
86	1	Pottery	Becan,	18.50	-89.80	800AD-	Th(C)	0.44	0.36	P	
	2		Mexico			950AD	Th(C)		0.35	P	
87	1	Pottery	Cholula	19.00	-98.30	1250AD-	Th(C)	0.44	0.48	R	1.09
	2		Mexico			1450AD	Th(C)		0.49	R	1.12
							Average				1.10

Table 9 (Continued)

Sample No.	Spec. No.	Material	Site Location			Age	Method of measurement	F_o Oe	F Oe	Reliability	F/F_o
			Site	Lat.	Long.						
88	1	Pottery	Cholula, Mexico	19.00	-98.30	1500AD-1650AD	Th(C)	0.44		P	
	2						Th(C)			P	
89	1	Baked clay	Cholula Mexico	19.00	-98.30	1500AD-1650AD	Th(C)	0.44	0.46	VR	1.05
	2						Th(C)		0.48	VR	1.09
	3						Th(C)		0.46	VR	1.05
	4						Th(C)		0.48	VR	1.09
							Average				1.07
90	1	Pottery	Cholula, Mexico	19.00	-98.30	1500AD-1650AD	Th(C)	0.44		P	
	2						Th(C)			P	
	3						Th(B)			P	
	4						Th(B)			P	
91	1	Pottery	Mal Paso Salvage, Mexico	19.00	-98.30	700AD-1200AD	Th(C)	0.43		P	
	2						Th(C)			P	
92	1	Brick	Cholula, Mexico	19.00	-98.30	1971AD	Th(C)	0.44	0.42	R	
	2						Th(C)		0.44	R	
	3						Th(A)		0.45	R	1.04

Table 9 (Continued)

Sample No.	Spec. No.	Material	Site Location			Age	Method of measurement	F_o Oe	F Oe	Reliability	F/F_o
			Site	Lat.	Long.						
	4						Th(A)		0.48	R	1.09
	5						Th(A)		0.47	R	1.07
	6						Th(A)		0.47	R	1.07
							Average				1.07
93	1	Brick	Cholula	19.00	-98.30	1971AD	Th(C)	0.44		P	
	2		Mexico				Th(C)			P	
	3						Th(B)			P	
	4						Th(B)			P	
97	1	Brick	Comal-	17.80	-93.80	400AD-	Th(B)	0.44		P	
	2		calco			800AD	Th(B)			P	
			Mexico								
110	1	Baked	Kaminal	14.70	-90.50	600AD-	Th(B)			P	
	2	clay	-juyu,			900AD	Th(B)			P	
	3		Guatema				Th(A)	0.42	0.43	R	1.04
	4		-la				Th(A)		0.45	R	1.08
	5						Th(A)		0.46	R	1.10
	6						Th(A)		0.46	R	1.10
							Average				1.08

Table 9 (Continued)

Sample No.	Spec. No.	Material	Site Location			Age	Method of measurement	F_o Oe	F Oe	Reliability	F/F_o
			Site	Lat.	Long.						
111	1	Baked clay	Kaminal-juyu, Guatemala	14.70	-90.50	450AD-500AD	Th(B)				
	2						Th(B)				
	3						Th(A)			P	
	4						Th(A)			P	
	5						Th(A)		0.64	R	1.54
	6						Th(A)			P	
	7						AF		0.66	R	
							Average				1.54
112	1	Baked clay	Teotihuacan Mexico	19.70	-98.80	350AD-	Th(B)	0.44		P	
	2						Th(B)			P	
	3						Th(A)		0.55	R	
	4						Th(A)		0.49	VR	1.11
	5						Th(A)		0.54	R	
	6						Th(A)		0.49	VR	1.11
							Average				1.12
113	1	Baked clay	Valle San Juan El Salvador	13.30	-88.60	1 AD-	Th(B)	0.41		P	
	2						Th(B)			P	

Table 9 (Continued)

Sample No.	Spec. No.	Material	Site Location			Age	Method of measurement	F_o Oe	F Oe	Reliability	F/F_o
			Site	Lat.	Long.						
114	1	Brick	Sento Domingo Convent Antigua Guatema-la	15.00	-91.00	1600AD	Th(B)	0.415		P	
	2						Th(B)			P	
115	1	Baked clay	Kamina-juyu, Guatema-la	14.70	-90.50	550AD	Th(B)	0.42		P	
	2						Th(B)			P	

Table 10 Results of samples from North America.

Sample No.	Spec. No.	Material	Site Location			Age	Method of measurement	F_o Oe	F Oe	Reliability	F/F_o
			Site	Lat.	Long.						
1	1	Pottery	Snake-	33.20	-112.00	1000AD	Th(D)	0.51		P	
	2		town				Th(D)			P	
	3		Arizona				Th(D)			P	
	4						Th(C)			P	
	5						Th(C)			P	
	6						W			P	
	7						W			P	
2	1	Pottery	Snake-	33.20	-112.00	600AD	Th(D)	0.51		P	
	2		town				Th(D)			P	
	3		Arizona				Th(D)			P	
	5						Th(C)			P	
	6						Th(C)			P	
3	1	Pottery	Snake-	33.20	-112.00	1900AD	Th(D)	0.51	0.54	R	1.06
	2		town				Th(D)		0.53	R	1.04
	3		Arizona				Th(D)		0.53	R	1.04
	4						Th(C)		0.57	R	1.12
	9						Th(C)		0.55	R	1.09
	7						W		0.79	P	
	8						W		0.60	P	
	6						W		0.65	P	

Table 10 (Continued)

Sample No.	Spec. No.	Material	Site Location			Age	Method of measurement	F_o Oe	F Oe	Reliability	F/F_o
			Site	Lat.	Long.						
4	4	Pottery	Snake-	33.20	-112.00	200BC	Th(C)	0.51	0.46	P	
	6		town				Th(C)		0.37	P	
			Arizona								
5	1	Pottery	Snake-	33.20	-112.00	200BC	Th(C)	0.51	0.43	P	
	2		town				Th(C)		0.45	P	
			Arizona								
6	1	Pottery	Snake-	33.20	-112.00	1 BC	Th(C)	0.51	0.42	P	
	3		town				Th(C)		0.38	P	
			Arizona								
7	1	Pottery	Snake-	33.20	-112.00	1400AD	Th(C)	0.51	0.42	P	
	4		town				Th(C)		0.23	P	
8	1	Pottery	Snake-	33.20	-112.00	800AD	Th(C)	0.51	0.51	R	1.01
	2		town				Th(C)		0.55	R	1.10
			Arizona				Average				1.05
9	4	Pottery	Snake-	33.20	-112.00	400AD	Th(C)	0.51	0.59	R	1.16
	5		town				Th(C)		0.50	R	1.00

Table 10 (Continued)

Sample No.	Spec. No.	Material	Site Location			Age	Method of measurement	F_o Oe	F Oe	Reliability	F/F_o
			Site	Lat.	Long.						
			Arizona				Average				1.08
10	3	Pottery	Snake-	33.20	-112.00	200AD	Th(C)	0.51	0.37	P	
	4		town				Th(C)		0.51	P	
			Arizona								
95	1	Pottery	Winn	32.90	-108.60	0 AD-	Th(A)	0.515	0.53	R	1.03
	2		Canyon			500AD	Th(A)		0.51	R	0.99
	3		New				Th(A)		0.52	R	1.02
	4		Mexico				AF		0.52	R	
							Average				1.02
134	1	Baked	Gillilar	37.50	-108.70	500AD-	Th(A)	0.54	0.64	P	1.18
	2	clay	Colorado				Th(A)		0.60	R	1.12
	3						Th(A)		0.55	R	1.03
							Average				1.08
151	1	Pottery	Pecos	35.70	-105.70	1621AD	Th(A)	0.535	0.59	R	1.11
	2		Convent				Th(A)		0.51	R	0.97
	3		New				Th(A)		0.54	R	1.02
	4		Mexico				AF			P	
							Average				1.04

Table 10 (Continued)

Sample No.	Spec. No.	Material	Site Location			Age	Method of measurement	F_o Oe	F Oe	Reliability	F/F_o
			Site	Lat.	Long.						
156	1	Baked	Cochiti	35.70	-106.30	1700AD	Th(A)	0.535	0.69	P	
	2	clay	New				Th(A)		0.65	P	
	3		Mexico				Th(A)		0.68	P	
158	1	Baked	Cochiti	35.70	-106.30	1700AD-	Th(A)	0.535	0.59	R	1.11
	2	clay	New			1750AD	Th(A)		0.59	R	1.12
	3		Mexico				Th(A)		0.60	R	1.13
							Average				1.12
184	1	Baked	Fort	32.30	-106.80	1851AD	Th(A)	0.515	0.50	R	0.97
	2	clay	Filmore			1861AD	Th(A)		0.51	R	0.99
	3						Th(A)		0.52	R	1.01
							Average				1.00
185	1	Baked	Norman	35.40	- 97.70	1974AD	AF	0.539	0.55	P	
	2	clay	Oklahoma				AF		0.56	P	
186	1	Baked	Canyon	36.20	-109.40	780AD	Th(A)		0.68	P	
	2	clay	de Chelly				Th(A)		0.69	P	

Table 10 (Continued)

Sample No.	Spec. No.	Material	Site Location			Age	Method of measure-ment	F_o Oe	F Oe	Relia-bility	F/F_o
			Site	Lat.	Long.						
187	1	Baked	Cedar	37.50	-109.70	1200AD	Th(A)	0.540	0.54	R	1.06
	2	clay	Mesa,				Th(A)		0.44	P	
	3		Utah				Th(A)		0.54	R	1.01
							Average				1.02
188	1	Baked	Cedar	37.50	-109.70	600AD-	Th(A)	0.540	0.54	R	1.00
	2	clay	Mesa,				Th(A)		0.49	R	0.91
	3		Utah				Th(A)		0.52	R	0.96
							Average				0.96
189	1	Baked	Nambe	35.80	-105.90	1200AD-	Th(A)	0.537	0.82	P	
	2	clay	Falls,			1400AD	Th(A)		1.25	P	
	3		New				Th(A)		0.69	R	1.30
							Average				1.30

Table 11 Results of samples from South America.

Sample No.	Spec. No.	Material	Site Location			Age	Method of measurement	F_o Oe	F Oe	Reliability	F/F_o
			Site	Lat.	Long.						
11	1	Baked	Chan-	-8.00	-79.00	1200AD	Th(C)	0.300	0.50	R	
	2	clay	chan			1500AD	Th(C)		0.45	VR	1.50
							Average				1.50
12	1	Baked	Chin-	-3.70	-71.30	1537AD	Th(C)	0.310	0.47	VR	1.52
	2	clay	cheros				Th(C)		0.55	R	
			Peru				Average				1.52
13	1	Baked	Moche	-8.00	-79.00	900BC	Th(C)	0.300	0.34	VR	1.13
	2	clay	Vally			200BC	Th(C)		0.32	VR	1.07
			Peru				Average				1.10
14	1	Baked	Chan-	-8.00	-79.00	1200AD-	Th(C)	0.300	0.44	R	1.47
	2	clay	chan			1500AD	Th(C)		0.44	R	1.47
							Average				1.47
18	1	Pottery	Wari	-8.00	-79.00	600AD-	Th(C)	0.30	0.48	VR	1.60
	2		Peru				Th(C)		0.48	VR	1.60
	3						W		0.75	P	
							Average				1.60

Table 11 (Continued)

Sample No.	Spec. No.	Material	Site Location			Age	Method of measurement	F_o Oe	F Oe	Reliability	F/F_o
			Site	Lat.	Long.						
20	1	Pottery	Tiahuanaco Bolivia	-16.70	-68.30	374AD-	Th(C)	0.265		P	
21	1	Pottery	Tiahuanaco Bolivia	-16.70	-68.30	374AD-	Th(C)	0.265	0.53	R	1.99
	2						Th(C)		0.49	R	1.90
							Average				1.94
26	1	Baked clay	Chanchan Peru	-8.00	-79.00	1450AD-	Th(C)	0.300		P	
	2						Th(C)			P	
30	1	Baked clay	Chanchan Peru	-8.00	-79.00	1400AD	Th(C)	0.300		P	
	2					1500AD	Th(C)			P	
31	1	Baked clay	Chanchan Peru	-8.00	-79.00	1200AD-	Th(C)	0.300	0.47	R	1.59
	2					1500AD	Th(C)		0.49	R	1.63
	3						Th(B)		0.49	R	1.63
	4						Th(B)		0.40	R	1.63
							Average				1.62

Table 11 (Continued)

Sample No.	Spec. No.	Material	Site Location			Age	Method of measurement	F_o Oe	F Oe	Reliability	F/F_o
			Site	Lat.	Long.						
32	1	Baked	Chan-	-8.00	-79.00	1200AD-	Th(C)	0.300	0.42	R	1.43
	2	clay	chan,				Th(C)		0.43	R	1.44
	3		Peru				Th(B)		0.38	R	1.27
	4						Th(B)		0.40	R	1.39
							Average				1.37
33	1	Baked	Chan-	- 8.00	-79.00	600AD-	Th(C)	0.300	0.47	R	1.59
	2	clay	chan ,			900AD	Th(C)		0.49	R	1.64
			Peru				Average				1.62
43	1	Pottery	Tiahu-	-16.70	-68.30	1200BC-	Th(C)	0.265	0.44	R	1.66
			anaco,				Average				1.66
			Bolovia								
52	1	Baked	Chan-	-8.00	-79.00	1200AD	Th(C)	0.300	0.37	R	1.28
	2	clay	chan,			1500AD	Th(C)		0.36	R	1.20
			Peru				Average				1.24